

Engineering *Saccharomyces cerevisiae* toward n-butanol production

A thesis submitted to the University of Manchester for the degree of Doctor of
Philosophy in the Faculty of Life Sciences.

2015

Reem Swidah

Contents

List of figures.....	6
List of tables.....	9
List of abbreviations.....	10
Abstract.....	12
Declaration.....	13
Copyright statement.....	13
Communications.....	14
Acknowledgements.....	15
1. Introduction.....	16
1.1 General introduction.....	16
1.2 Types and properties of biofuels	17
1.2.1 First generation biofuels	17
1.2.1.1 Biodiesel.....	17
1.2.2 Second generation biofuels	18
1.2.2.1 Bioethanol.....	18
1.2.2.2 Butanol.....	20
1.2.3 Third generation biofuels.....	20
1.3 Properties of butanol	21
1.4 Biobutanol production.....	23
1.4.1 Enzymes involved in butanol production.....	23
1.4.1.1 Extracellular enzymes involved in hydrolysis of carbohydrates from biomass ..	23
1.4.1.2 Intracellular enzymes involved in biobutanol synthesis	24
1.4.1.3 Co-factors involved in the butanol synthetic pathway	26
1.5 Microorganisms involved in butanol production.....	28
1.5.1 Microorganisms which produce butanol naturally.....	28
1.5.2 Metabolically engineered microorganisms.....	29
1.5.2.1 Bacteria	31
1.5.2.2 Yeasts	32
1.6 Metabolic engineering strategies used to produce butanol and Iso-Butanol	33
1.6.1 Butanol production	33
1.6.2 Isobutanol production	34
1.7 Carbon metabolism in yeast	36

1.7.1 Overview	36
1.7.2 Monosaccharide derived from Lignocellulosic biomass	38
1.7.3 Glycolysis pathway	39
1.7.4 Ethanol metabolism in yeast.....	42
1.7.5 Acetyl-CoA biosynthesis.....	43
1.7.5.1 Pyruvate dehydrogenase	43
1.7.5.2 Pyruvate by-pass pathway	43
1.7.5.3 Ethanol as a carbon source after the diauxic shift.....	44
1.8 Butanol tolerance.....	45
1.8.1 Overview	45
1.8.2 Butanol toxicity	45
1.8.3 Strategies used to increase biofuel (solvent) tolerance	46
1.9 Protein synthesis.....	48
1.9.1 Overview of eukaryotic gene expression and protein synthesis	48
1.9.2 Translation initiation.....	50
1.10 Guanine nucleotide exchange factor (eIF2B).....	51
1.10.1 Overview	51
1.10.2 Role of eIF2B in translation initiation	52
1.10.3 The localisation of eIF2 and eIF2B	55
1.10.4 Alcohols, eIF2B regulation and the eIF2B body	55
1.11 Aims of butanol project	56
2. Materials and Methods.....	57
2.1 Culture conditions.....	57
2.1.1 Yeast strains and growth conditions.....	57
2.1.2 Bacterial strains and growth conditions	57
2.1.3 Antibiotic supplemented to selective media	58
2.2 DNA manipulation and analysis	58
2.2.1 Isolation of plasmid DNA from bacterial cells.....	58
2.2.2 Genomic DNA extraction of yeast cells.....	58
2.2.3 DNA amplification by polymerase chain reaction (PCR).....	59
2.2.4 Agarose gel electrophoresis.....	60
2.2.5 Restriction digest of PCR product or plasmid DNA.....	60
2.2.6 Ligation of vector and insert	60
2.2.7 Phenol-chloroform DNA purification	61

2.2.8 Yeast transformation with PCR product or Plasmid DNA	61
2.2.9 Bacterial transformation with plasmid DNA	62
2.2.10 Determination of DNA concentration.....	62
2.3 Protein analysis	62
2.3.1 Preparation of yeast whole cell extracts using trichloroacetic acid (TCA).....	62
2.3.2 SDS-Polyacrylamide gel electrophoresis (PAGE).....	63
2.3.3 Western Blot Analysis	63
2.3.4 Coomassie staining of protein gels	64
2.4 Strain construction.....	64
2.4.1 Cross-mating yeast strains	64
2.4.2 Tetrad dissection.....	64
2.4.3 Mating type assay	65
2.5 Gene integration, deletion and mutation	65
2.5.1 Single gene integration strategy	65
2.5.2 <i>ALD6</i> , <i>ACS2</i> and <i>ALD2</i> , <i>ACS2</i> integration strategy.....	66
2.5.3 Gene deletion strategy	66
2.5.4 Site directed mutagenesis at a genomic locus.....	67
2.5.5 Excision of <i>NATnt2</i> from the genome	68
2.6 Sucrose density gradient analysis	68
2.6.1 Extract preparation	68
2.6.2 Preparation of sucrose density gradients	69
2.6.3 Sedimentation of extracts in polysome gradients	69
2.7 Alcoholic fermentation analysis.....	70
2.7.1 Measurements of butanol and ethanol and standard operating procedure	70
2.7.2 Glucose Measurements	71
3. Construction strains of <i>Saccharomyces cerevisiae</i> harbouring five butanol synthetic genes	81
3.1 Introduction	81
3.2 The Integration strategy for introducing codon optimised butanol synthetic genes into <i>Saccharomyces cerevisiae</i>	82
3.3 Restriction digests for all plasmid templates.....	84
3.4 Generation of a strain with the five genes involved in butanol production exogenously integrated at high expression sites	86
3.5 Factors changed to increase the efficiency of <i>crt</i> and <i>ccr</i> cassettes integration within the genome	89

3.5.1 Re-design of the insertion primers	89
3.5.2 Restriction digests of pRS313- <i>ccr</i> and pRS314- <i>crt</i> plasmid templates	89
3.5.3 Plasmid template dilutions	91
3.6 Transformation and validation of the <i>ccr</i> and <i>crt</i> cassettes	91
3.7 Back-crossing to obtain multiple integrated genes in the same strain	95
3.8 Validation and phenotypic characterisation of the progeny obtained from the final cross	97
3.9 Verification PCR to confirm five butanol synthetic genes (<i>crt</i> , <i>ccr</i> , <i>adhe2</i> , <i>hbd</i> and <i>ERG10</i>) are presented in <i>GCD1</i> -S180 (B ^S) and <i>GCD1</i> -P180 (B ^R) strains	99
3.10 Protein expression of the enzymes involved in the butanol synthetic pathway.....	99
3.11 Quantifying butanol and ethanol production by gas chromatography	102
3.12 Discussion.....	104
4. Development of n-butanol production from <i>Saccharomyces Cerevisiae</i> via the application of various metabolic engineering strategies	106
4.1 Introduction	106
4.2 Deleting major alcohol dehydrogenase <i>ADH1</i> from the constructed strains.....	109
4.3 Construction of various mutants with <i>ADH1</i> deleted.....	109
4.4 Expressing of the <i>ALD6</i> and <i>ACS2</i> genes with a view to improving butanol production in the various constructed strains of <i>Saccharomyces cerevisiae</i>	116
4.5 Detecting protein expression for all the constructed strains that over-express the <i>ALD6 ACS2</i> cassette	120
4.6 Quantification of fermentation products from the <i>ALD6 ACS2</i> expressing strains	122
4.7 Construction of strains expressing <i>ALD2 ACS2</i> as an alternative to <i>ALD6 ACS2</i>	126
4.8 Ald2p and Acs2p protein detection in the various constructed strains.	130
4.9 Quantifying butanol and ethanol yield from <i>ALD2 ACS2</i> strains	132
4.10 Construction various mutants carrying a single deletion of <i>GPD1</i> or <i>GPD2</i>	134
4.11 Quantifying butanol and ethanol yield from the constructed strains lacking either <i>GPD1</i> or <i>GPD2</i> genes.....	138
4.12 Discussion.....	140
5. Optimizing the fermentation conditions for butanol production	144
5.1 Introduction	144
5.2 butanol production under aerobic and semi-anaerobic conditions	144
5.3 The impact of using 0.05 and 0.1 starting ODs on butanol production.....	147
5.4 The impact of using different glucose concentrations on butanol and ethanol production	149
5.5 The impact of using alternative carbon sources on butanol and ethanol production ...	153

5.6 Detect the influence of using different temperature 25, 30 and 37 °C on butanol and ethanol yield	158
5.7 The effect of scaling up the volume of the batch culture on production of butanol and ethanol	160
5.8 Discussion.....	162
6. Improve butanol tolerance with a view to higher butanol yields	165
6.1 Introduction	165
6.2 Validation of butanol production in B^R versus B^S strains	166
6.3 Construction strategy to generate a 'super' resistant strain in the butanol production background.	168
6.4 Introducing <i>loxp-natNT2-loxp</i> upstream of <i>GCD2</i> in WT (B^R)	170
6.5 Second phase in the mutation of <i>GCD2-S131</i> to encode either alanine or aspartic acid.	172
6.6 Growth analysis of the <i>GCD2</i> mutants.....	175
6.7 Polysome analysis of the mutated and unmutated strains	177
6.8 The impact of using <i>loxp-natNT2-loxp::GCD2</i> mutants on growth, ethanol and butanol production.....	180
6.9 Excision of the <i>loxp-natNT2-loxp</i> marker from the <i>GCD2</i> mutants	182
6.10 Analysis of Gcd2p expression levels for the <i>GCD2</i> mutants.	184
6.11 Assessment of butanol levels in the <i>GCD2</i> mutants lacking the <i>natNT2</i> marker.	186
6.12 Discussion.....	188
7. General Discussion	191
7.1 The ABE pathway and butanol production in <i>S. cerevisiae</i>	192
7.2 Improved carbon flux toward acetyl-CoA production promotes butanol production. ..	193
7.3 Targeted deletion of redox active enzymes in competing pathways	194
7.4 The best conditions for butanol production were detected	195
7.5 A butanol resistant strain generates higher levels of butanol.....	195
7.6 Overall Summary.....	198
8. Bibliography.....	199
9. Appendix.....	209

Word count: 58,760 words

List of figures

Figure 1.1 Comparison of petroleum with first and second generation biofuels.....	20
Figure 1.2 A simplified overview of biofuel production.....	24
Figure 1.3 The biosynthetic pathway for n-butanol production from <i>C.beijerinckii</i>	26
Figure 1.4 Development of metabolic engineering.	30
Figure 1.5 Sugar metabolism and glycolysis in yeast.....	41
Figure 1.6 Ethanol metabolisms in yeast	42
Figure 1.7 Translation initiation pathway in eukaryotic	54
Figure 3.1 A schematic representation of the Integration strategy for introducing codon optimised butanol synthetic genes into <i>Saccharomyces cerevisiae</i>	83
Figure 3.2 Restriction digests of the plasmid integration constructs.	85
Figure 3.3 Schematic representation of the pRS 315- <i>hbd</i> and pRS 316- <i>adhe2</i> vector carrying the integration cassette.	87
Figure 3.4 Verification of successful cassette integration at a specific location in the genome.	88
Figure 3.5 Restriction digests with <i>ScaI</i> and <i>BsmBI</i> for pRS313- <i>ccr</i> and pRS314- <i>crt</i> constructs	90
Figure 3.6. Dilutions of the digested construct.....	93
Figure 3.7 Verification of successful cassette integration of <i>crt</i> and <i>ccr</i> at a desired location in the yeast genome	94
Figure 3.8 Overall strategy to construct a strain of <i>Saccharomyces cerevisiae</i> bearing five butanol synthetic pathway genes.	96
Figure 3.9 Verification of <i>GCD1-S180</i> (B^S) and <i>GCD1-P180</i> (B^R) genotype.....	98
Figure 3.10 Verification PCR to confirm five butanol synthetic genes (<i>crt</i> , <i>ccr</i> , <i>adhe2</i> , <i>hbd</i> , <i>ERG10</i>) are presented in <i>GCD1-S180</i> (B^S) and <i>GCD1-P180</i> (B^R) strains.....	100
Figure 3.11 Protein expression from the single integrant and strains bearing all five genes..	101
Figure 3.12 Ethanol and butanol quantitation in media taken from strains bearing the five butanol production genes over a 21 day semi-anaerobic fermentation.....	103
Figure 4.1 The metabolic engineering strategy used to direct the carbon flux from glycolysis to the butanol production pathway in <i>Saccharomyces cerevisiae</i>	108
Figure 4.2 Construction and verification of the <i>ADH1</i> deletion from wild type strains (B^R) and strains bearing the butanol synthetic pathway (B^R +5g).	111
Figure 4.3 Ethanol and butanol levels in <i>adh1Δ</i> mutant strains and strains bearing the butanol synthesis pathway.....	114
Figure 4.4 The effect of <i>ADH1</i> deletion on growth and ethanol or butanol production from the constructed strains under semi-anaerobic conditions.	115
Figure 4.5 Strategy for improving butanol production by combining <i>ADH1</i> deletion with <i>ALD6</i> <i>ACS2</i> over-expression.	118
Figure 4.6 Integrating <i>ALD6</i> and <i>ACS2</i> cassette in <i>TRP1</i> locus.....	119
Figure 4.7 Protein expression of the Ald6 and Acs2 enzymes.	121
Figure 4.8 Improving butanol production by integration of an <i>ALD6 ACS2</i> expression cassette.	124

Figure 4.9 Integration of the <i>ALD6 ACS2 cassette</i> without <i>ADH1</i> deletion does not improve butanol production in the strain bearing ABE pathway.	125
Figure 4.10 Strategy used to replace <i>ALD6</i> with <i>ALD2</i> in the expression cassette.....	128
Figure 4.11 Integrating <i>ALD2</i> and <i>ACS2</i> cassette in <i>TRP1</i> locus.....	129
Figure 4.12 Protein expression of the Ald2 and Acs2 enzymes.	131
Figure 4.13 The impact of <i>ALD2</i> and <i>ALD6</i> over-expression on butanol production compared to <i>ALD6</i> and <i>ACS2</i> over-expression.	133
Figure 4.14 Generating anew constructed strains with <i>GPD1</i> and <i>GPD2</i> deletion using <i>B^R adh1Δ ALD2 ACS2+5g</i> strain.	136
Figure 4.15 PCR analysis to confirm the successful deletion for <i>GPD1</i> and <i>GPD2</i> in the different constructed strains.	137
Figure 4.16 Alcoholic fermentation experiment to assess the impact of <i>GPD1</i> and <i>GPD2</i> deletions on butanol production.	139
Figure 5.1 Impact of aerobic versus semi-anaerobic growth conditions on butanol production	146
Figure 5.2 The effect of using starting OD ₆₀₀ on butanol production under semi-anaerobic conditions.....	148
Figure 5.3 The impact of using different glucose concentrations on butanol and ethanol production under semi-anaerobic conditions.	151
Figure 5.4 Analysis of ethanol, butanol and glucose consumption in the production strain at day 13 using different starting glucose concentrations.	152
Figure 5.5 Metabolism of disaccharide and monosaccharide sugars in yeast.	156
Figure 5.6 The impact of using various feedstock carbon sources on ethanol and butanol production under semi-anaerobic conditions.	157
Figure 5.7 The impact of growth at various temperature on butanol and ethanol production under semi-anaerobic conditions.	159
Figure 5.8 The effect of scaling up the volume of the batch culture on butanol and ethanol production under semi-anaerobic conditions.	161
Figure 6.1 Validation of the difference in butanol production between <i>B^R</i> and <i>B^S</i> strains.....	167
Figure 6.2 Overall strategy used to construct the <i>GCD2-S131A</i> and <i>GCD2-S131D</i> mutant strains.	169
Figure 6.3 Integration of <i>loxP-natNT2-loxP</i> upstream of <i>GCD2</i>	171
Figure 6.4 Further strategy to generate <i>GCD2</i> mutations in the butanol production strain....	173
Figure 6.5 DNA sequence analysis of <i>GCD2</i> PCR products derived from the potential <i>GCD2</i> mutants.	174
Figure 6.6 Mutation of eIF2Bδ serine 131 alters butanol tolerance.....	176
Figure 6.7 Polysome analysis reveals that the <i>GCD2-S131A</i> mutant has increased tolerance to butanol, while the <i>GCD2-S131D</i> mutant is more sensitive to butanol.....	179
Figure 6.8 Detecting the impact of <i>GCD2</i> mutation on butanol, ethanol and growth rate.....	181
Figure 6.9 Excising strategy to take off <i>natNT2</i> from the genome.	183
Figure 6.10 Investigation of the expression of Gcd2p in the <i>GCD2</i> mutant and control strains.	185

Figure 6.11 Assessing the impact of <i>GCD2</i> mutation after marker removal on butanol, ethanol and growth rate.	187
---	-----

List of tables

Table 1.1 Comparison of butanol isomers.....	22
Table 1.2 Taxonomy of <i>S. cerevisiae</i>	32
Table 2.1 Yeast strain used in this study.....	72
Table 2.2 Plasmid used in this study.....	75
Table 2.3 Oligonucleotides used in this study.....	76
Table 2.4 Antibody used in this study.....	80
Table 2.5 Optimal conditions for restriction enzymes.....	80

List of abbreviations

Abbreviation	Meaning
4E-BP	eIF4E-binding protein
α	Alpha
Δ	Delta (delete)
μ	Micro (prefix)
A	Absorbency
AA	Amino acids
ABE	Acetone-Butanol-Ethanol
Adhe2	butanol dehydrogenase
ATP	Adenosine triphosphate
ATP	Adenosine triphosphate
bp	Base pairs
bp	Base pair
B^R	butanol Resistant Strains
B^R	butanol Sensitive Strains
C	Carbon
Ccr	butyryl-CoA dehydrogenase
cDNA	Complementary DNA
Crt	Crotonase
DEPC	Diethylpyrocarbonate
DNA	Deoxyribonucleic acid
dNTP	Deoxyribonucleotide
DTT	Dithiothreitol
EDTA	Ethylenediaminetetraacetic acid
eIF	Eukaryotic initiation factor
eIF2B	Eukaryotic initiation factor-2B
eRF	Eukaryotic release factor
Erg10	Thiolase enzyme
FFA	Free Fatty Acids
FFA	Free fatty acids
FRAP analysis	Fluorescence recovery after photo bleaching
GCD1	γ subunit of eIF2B
GCD2	δ subunit of eIF2B
GC-MS	Gas chromatography–mass spectroscopy
GDP	Guanosine diphosphate
GRAS	Generally regarded as safe
GTP	Guanosine triphosphate
Hbd	3-hydroxybutyryl-CoA dehydrogenase
HFR	Homology flanking region
K	Kilo (prefix)
kDa	Kilo Dalton
L	Litre(s)
LB	Luria-Bertani media
m	Milli (prefix)
M	Molar
Met-tRNAi	Initiator methionyl tRNA
MFC	Multi-factor complex
mRNA	Messenger RNA
NADH	Reduced form of nicotinamide adenine dinucleotide
NADPH	Nicotinamide adenine dinucleotide phosphate (reduced)
OD	Optical density
ORF	Open reading frame

p	Promoter
P-bodies	Processing bodies
PCR	Polymerase chain reaction
PDH	Pyruvate dehydrogenase
PEG	Polyethylene glycol
PH	A numeric scale used to specify the acidity or alkalinity of an aqueous solution
PIC	Pre-initiation complex
Poly(A)	Polyadenosine
Pre-mRNA	Precursor mRNA
RNA	Ribonucleic acid
rpm	Revolutions per minute
SC	Synthetic complete media lacking glucose
SCD	Synthetic complete media
SDS	Sodium dodecyl sulphate
SDS-PAGE	Sodium Dodecyl sulphate Polyacrylamide Gel Electrophoresis
Ser	Serine
SOP	Standard operating procedure
T	Temperature
t	Terminator
TAE	Tris base, acetic acid, EDTA
TAG	Triacylglycerol
TAGs	Transesterification of triacylglycerols
TBP	TATA box binding protein
TC	Ternary complex
TCA	Tricarboxylic acid
TDH3	Glyceraldehydes-3-phosphate dehydrogenase
TFIIB	Transcription initiation factor IIB
Tm	Melting temperature
tRNA	Transfer RNA
U	Unit
UTR	Untranslated region
v/v	Volume per volume
VHG	Very High Gravity fermentation
w/v	Weight per volume
YP	Yeast extract, peptone media
YPD	Yeast extract, peptone, glucose media

Abstract

Doctor of Philosophy in the Faculty of Life Sciences. 2015

Engineering of *Saccharomyces cerevisiae* toward n-butanol production

Reem Swidah

The University of Manchester, Faculty of Life Sciences, Manchester, M13 9PT, United Kingdom

Biobutanol represents a second generation biofuel, which can be produced from renewable resources by microorganisms. A *Saccharomyces cerevisiae* strain bearing the five butanol synthetic genes (*hbd*, *adhe2*, *crt*, *ccr* and *ERG10*) was constructed, where the *hbd*, *adhe2*, *crt* and *ccr* genes are derived from *Clostridium beijerinckii*, while *ERG10* is a yeast gene. The genes were transformed individually on single cassettes, which integrated into specific chromosomal sites. The single integrant strains were back-crossed to create a strain bearing all five butanol synthetic genes. The butanol synthetic enzymes appeared to be highly expressed in the cytosol, however, very little butanol was obtained (<10 ppm). Therefore, additional genetic manipulations were made with a view to restoring any redox imbalance channelling the carbon flux toward the butanol pathway. Deletion of the *ADH1* gene in strains with the butanol pathway improved production to ~250 ppm (203 mg/L) butanol. Further improvement to 360 ppm (292 mg/L) was gained by overexpressing the *ALD6* and *ACS2* genes, that are involved in synthesis of acetyl-CoA; the precursor for butanol biosynthesis. However, the replacement of *ALD6* with *ALD2*, which produces NADH instead of NADPH, didn't improve butanol yields. In addition, no significant improvement of butanol yield was obtained when dehydrogenase enzymes from the glycerol biosynthetic pathway were deleted. An initial assessment of the best conditions for butanol production were semi-anaerobic growth at 30°C in 2% glucose with a starting OD₆₀₀ of 0.1.

In this project, another key question was addressed: does the sensitivity of cells to short chain alcohols like butanol affect butanol production? Previous work in the Ashe lab has identified specific point mutations in the translation initiation factor, eIF2B, which generate resistance or sensitive phenotypes to exogenously added butanol. Here a comparison of butanol production in sensitive and resistant backgrounds showed that the butanol yield was 1.5-2 fold higher in a butanol resistant strain compared to the sensitive mutant. Generating a 'super' butanol resistant strain bearing a *GCD2-S131A* mutation in eIF2B promoted a higher butanol yield per cell. However, another consequence of this mutation was reduced growth. So the combination of these effects meant that the overall butanol concentration in media was similar to the control. Overall this work highlights that *S. cerevisiae* can produce butanol but that further optimisation both at the level of the strain and process engineering would be necessary before this would be of interest to the commercial sector.

Declaration

No portion of the work referred to in the thesis has been submitted in support of an application for another degree or qualification of this or any other university or other institute of learning

Copyright statement

- I. The author of this thesis (including any appendices and/ or schedules to this thesis) owns certain copyright or related rights in it (the “Copyright”) and/ he has given The University of Manchester certain rights to use such Copyright, including for administrative purposes.
- II. Copies of this thesis, either in full or in extracts and whether in hard or electronic copy, may be made only in accordance with the Copyright, Designs and Patents Act 1988 (as amended) and regulations issued under it or, where appropriate, in accordance with licensing agreements which the University has from time to time. This page must form part of any such copies made.
- III. The ownership of certain Copyright, patents, designs, trademarks and other intellectual property (the “Intellectual Property”) and any reproductions of copyright works in the thesis, for example graphs and tables (“Reproductions”), which may be described in this thesis, may not be owned by the author and may be owned by third parties. Such Intellectual Property and Reproductions cannot and must not be made available for use without the prior written permission of the owner(s) of the relevant Intellectual Property and/ or Reproductions.
- IV. Further information on the conditions under which disclosure, publication and commercialisation of this thesis, the Copyright and any Intellectual.
- V. Property and/ or Reproductions described in it may take place is available in the University IP Policy (see <http://www.campus.manchester.ac.uk/medialibrary/policies/intellectualproperty.pdf>), in any relevant Thesis restriction declarations deposited in the University Library, The University Library’s regulations (see <http://www.manchester.ac.uk/library/aboutus/regulations>) and in The University’s policy on presentation of Theses.

Communications

Oral presentations

- I. Reem Swidah, Chris Grant and Mark Ashe. **Biotechnology of yeast biofuels production**. Industrial Biotechnology & Synthetic Biology PhD & Postdoc Seminar Series, Manchester University, UK 2015.
- II. Reem Swidah, Chris Grant and Mark Ashe. **Biotechnology of yeast biofuels production**. University of Manchester Faculty of Life Sciences PhD conference, Manchester, UK 2015.
- III. Reem Swidah, Chris Grant and Mark Ashe. **Biotechnology of yeast biofuels production**. University of Manchester Faculty of Life Sciences PhD conference, Manchester, UK 2014.
- IV. Reem Swidah, Chris Grant and Mark Ashe. **Biotechnology of yeast biofuels production**. University of Manchester Faculty of Life Sciences, First Seminar Presentation Manchester, UK 2013.

Poster presentations

- I. Reem Swidah, Hui Wang, Peter Reid, Hassan Ahmed, Krishna Persaud, Chris Grant and Mark Ashe. **Biotechnology of yeast biofuels production**. British Yeast Group Meeting, Manchester, UK 2015
- II. Reem Swidah, Hui Wang, Chris Grant and Mark Ashe. **Biotechnology of yeast biofuels production**. University of Manchester, Faculty research symposium, Manchester, UK 2013.

Publications

- i. Swidah, R., H. Wang, P. J. Reid, H. Z. Ahmed, A. M. Pisanelli, K. C. Persaud, C. M. Grant, and M. P. Ashe. 2015. 'Butanol production in *S. cerevisiae* via a synthetic ABE pathway is enhanced by specific metabolic engineering and butanol resistance', *Biotechnol Biofuels*, 8: 97-105.

Reprints are included in the Appendix.

Acknowledgements

I would like to show my gratitude to my great supervisors Dr Mark Ashe and Professor Chris Grant who gave me the opportunity to participate in the biofuel project and do something I always like, as this thesis would not have been possible without the support, guidance, encouragement you have given me over the years which enabled me to study science.

I would sincerely thank you Mark once more for your nobility and generosity with me from initial to the final level; you have been amazing.

I would like also to thank Professor Graham Pavitt for positive advices during lab meetings and also for generous donation of reagents and antibodies as well as I would like to thank my colleagues. In particular: Jen for a great support and advice for writing, Rojerio, Kazz, Karin, Lydia, Chris, Martin, Hassan, Nkechi, Arunkumar, Rihanna, Alan, Paraskevi, Shaun, Vicky, Tawni, Henry, Sara, Benga, Norfadilah, Norhydaya for your friendship. I also would like to extend my acknowledgment to my great friends especially Aline and Rojerio for their support, friendship and company. I would like to thank British council for its support during my study.

Finally I would like to express my sincere appreciation to my family especially my great mum, dad and my amazing husband Jihad for the endless support, constant encouragement, love, confidence and strength you given me throughout the years, you have been amazing.

1. Introduction

1.1 General introduction

During the last decade the demand for chemical materials and fuel production from renewable resources has increased. This has been caused by a combination of factors including: rising concerns about climate change and global warming as well as an ever-decreasing supply of crude oil and consequent increase in price. In addition, there are a large number of legislations that restrict the use of non-renewable energy sources. The generation of biofuels (bioethanol, biodiesel and biobutanol) may form part of a solution that plugs a potential gap in future fuel availability while minimising the deleterious effects on the environment

Production of butanol was first reported by Louis Pasteur in 1861 through microbial fermentation (Gabriel *et al.* 1930). After that, Albert Fitz obtained butanol from glycerol by using a mixture of two bacteria. At the beginning of the 20th century, researchers focused mainly on producing different types of alcohol (butanol and amyl alcohol) and acetone for use in the rubber industry (Gabriel *et al.* 1930; Gabriel 1928). Professor Perkin and his assistant the chemist, Weizmann, from Manchester University, and Professor Fernbach and his assistant Schoen from the Pasteur Institute worked at the same time to produce butanol from different substrates. In 1911, Fernbach isolated a culture, which enabled him to generate butanol from potato starch. After this, Weizmann successfully isolated a bacterium called *Clostridium acetobutylicum*, which was used to produce high quantities of butanol from starch (Jones *et al.* 1986) .

During the First World War, acetone was the desired product, while butanol was just considered as a secondary product and was simply stored in bottles (Gabriel 1928). After that period, the development of the automobile industry created a demand for solvents, which were able to dry quickly for use in car painting. For that purpose, butanol and butyl acetate exhibited high quality as solvents. Butanol became the main product for this purpose and many companies tried to develop butanol production (Gabriel *et al.* 1930; Gabriel 1928). However, the yield of butanol varied due to differences in fermentation conditions such as strains used (bacteria and yeast),

substrates, pH, temperature, nutrients and the presence or absence of O₂ (Verónica García 2011) Furthermore, four important factors were found to be important when trying to produce butanol through the microbial industry: 1. the different locations of intracellular enzymes involved in butanol synthesis pathways, 2. the activities of these enzymes, 3. the balance of cofactors and 4. secondary product formation (Antoni *et al.* 2007).

1.2 Types and properties of biofuels

1.2.1 First generation biofuels

First generation or the early biofuels such as bioethanol and biodiesel have been produced directly from agricultural products through conventional fermentation technology (Hein *et al.* 2012). Feedstocks for bioethanol production are sugarcane, wheat and corn while, soybean, palm oil and animal fat are extensively used for biodiesel production (Balat *et al.* 2009).

1.2.1.1 Biodiesel

At the beginning of the 19th century, Rudolph Diesel proposed that plant oils could be used as a fuel for automobile engines. This type of fuel has better physicochemical properties due to its density and viscosity. Generally, biodiesel includes a mixture of methyl and/ or ethyl esters of fatty acids. These are produced through transesterification of triacylglycerols (TAGs) using chemical or enzymatic methods (Mirosztawa Szczesna Antczak 2009). Chemical methods, such as the addition of catalysts e.g, NaOH or KOH, are often used to accelerate the reaction in industry. However, these methods have some drawbacks, such as the production of glycerol as a main by-product and secondary by-products like monoglycerols and diacylglycerols. These methods also generate soap and pigments leading to increased costs of purification (Meher *et al.* 2006). In contrast, biodiesel can be produced in one step by using an enzymatic strategy. For instance, lipase enzymes (E.C 3.1.1.3) convert fats that contain TAG and free fatty acids (FFA) directly into biodiesel. To achieve this, both

tranesterification and esterification reactions occur at the same time. Additionally, such enzymatic methods can be carried out either in organic solvent systems or in a solvent free system (Shimada *et al.* 2002). In organic solvent systems, alcohol is added both at the beginning of the process and during the conversion of oil to alkyl ester by lipase. While in solvent-free systems, alcohol is added gradually in small amounts during the process in order to maintain a low concentration (Shimada *et al.* 2002).

Currently, biodiesel is being produced from various feedstocks. For instance, in South America, it is produced from sunflower or vegetable oil, while in European countries it is particularly produced from rape seed oil as a raw material. Many countries have strongly recommended the manufacture and use of first generation biofuels in order to decrease CO₂ emissions and limit climate change. However, the production of this kind of biofuel can be associated with serious problems. For example, increasing food prices and depletion of phosphorus (P), which is essential for crop production (Cordell *et al.* 2009). In addition, there are some restrictions on the use of biodiesel in the industrial sector because it cannot be transported or stored using the same infrastructure as gasoline.

1.2.2 Second generation biofuels

Second generation biofuels are also known as advanced biofuels and are manufactured from different sources of organic carbon (biomass). The biomass for second generation biofuels can be derived from different plant parts, such as stems, leaves and also plant waste material left after industrial food processing (Cobucci-Ponzano *et al.* 2015).

1.2.2.1 Bioethanol

Bioethanol is mainly produced from feedstocks using conventional fermentation. This includes several steps; production of lignocellulose materials, hydrolysis of cellulose and hemicelluloses, generating hexoses and pentoses, fermentation and finally the distillation step (Carere *et al.* 2008). About 10% of the

available sugar forms secondary products such as glycerol and succinic acid (Wheals *et al.* 1999). Glycerol synthesis also increases when there is a response to osmotic stress. The main process for bioethanol production is very high gravity (VHG) fermentation using highly concentrated media containing sugar, cane molasses and starch or grains. Usually, the productivity of ethanol is over 15% v/v and this has the advantage of decreasing the costs of distillation (Mussatto *et al.* 2010)

There are many countries that produce bioethanol in large quantities. This includes the United States, Brazil, Europe and China, which were found to produce 61%, 26.4%, 6.1% and 2% as a proportion of global bioethanol production in 2014, respectively as reported by ('Alternative Fuels Data Center' 2014). Moreover, according to this website, about 14 million gallons of bioethanol were produced in the US in 2014 and these numbers are likely to increase.

The main advantage of using bioethanol as a second generation biofuel instead of gasoline is to increase the power output, because it has a high vapour pressure as well as high boiling and evaporating point (Zaldivar *et al.* 2001). Therefore, second generation biofuels have been developed to overcome the limitations of first generation biofuels by using non-food crops as feedstocks. Bioethanol is highly water soluble which creates a need to distil it from fermentation broths (Singhania *et al.* 2013). As a result, bioethanol can be classified into different categories based on the type of feedstock that was used for its production. So, it is considered as a first generation biofuel when using food-crops for production. Whereas, it is considered as a second biofuel generation when lignocellulosic material is used for its production (Singhania *et al.* 2013). Figure 1 below summarises the differences between petroleum, first and second generation biofuels.

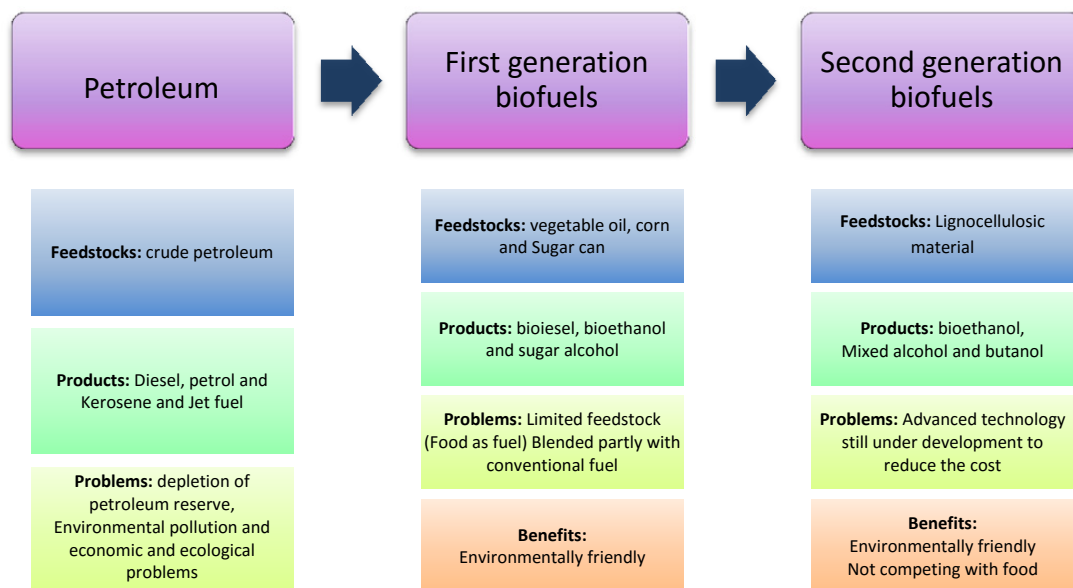


Figure 1.1 Comparison of petroleum with first and second generation biofuels.

The diagrams show a comparison of the different feedstocks used for biofuel production, along with the associated problems and benefits (Adapted from (Naik *et al.* 2010))

1.2.2.2 Butanol

Butanol is a non-polar molecule that contains four carbon atoms. It is much more similar to gasoline than bioethanol because it has 29.2 MJ/L energy density, whilst gasoline has 32 MJ/L energy density. Generally butanol is produced from fossil oil as a petro-chemical product or by fermentation processes; however, butanol from both of these sources has the same chemical properties. Butanol production will be discussed in detail in the following sections.

1.2.3 Third generation biofuels

The term “third generation biofuel” has only recently been given its own classification, as previously it was included in the second generation biofuels. However, when it became apparent that higher biofuel yields might be obtained from algae than other feedstocks and these could be associated with lower resource inputs,

the term was introduced (Behera *et al.* 2014). Algae have a range of advantageous characteristics compared to plants as a source of carbon including vast growth, minimal growth requirements (just water, sunlight and CO₂) and higher energy content per unit area (around 30% more than first and second generation biofuels according to the U.S. Department of energy (Behera *et al.* 2014). In addition, algae are deemed environmentally friendly: they have the capacity to grow effectively in wastewater or water contaminated with fertilizers, even after the water has been treated with digestive bacteria to break down toxic elements or nutrients derived from farming. They consume large amounts of carbon dioxide (CO₂): a major factor in climate change. Algae also produce oil that can be easily refined into diesel or other components of gasoline. Algae can be genetically modified to produce a wide range of biofuels such as: ethanol, biodiesel, butanol and even gasoline (Behera *et al.* 2014). However, there are still some major disadvantages to algae as a source of biofuel. Biomass production is still very expensive from an industry point of view, as it costs around 8£/Kg biomass. Researchers are still testing a variety of methods to grow and harvest algae in an attempt to decrease costs and the quantity of water required for cultivation. Other disadvantages include the potential for contamination by native algal species, the high risk of viral infection, the relatively high costs of using sterile CO₂ for biomass production, and the electricity requirement to power water pumps when using closed loop systems (Huang, Chen, *et al.* 2010; McGinn *et al.* 2011; Demirbas *et al.* 2011).


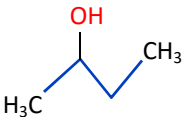
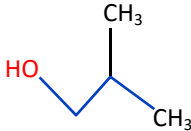
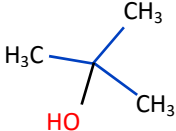
1.3 Properties of butanol

Butanol has two more carbon atoms than ethanol and is considered as a viable alternative to ethanol because it has a higher energy content (about 40% higher); it exhibits lower solubility in water (hygroscopicity); lower corrosivity and hence could be transported through standard pre-existing pipe lines. Therefore, there is no need to modify the infrastructure. Generally, butanol mixes with gasoline at any ratio and it can also be used as a fuel in conventional engines. However, butanol is much more toxic than ethanol and it also has a higher boiling point; thus, it requires higher energy levels for distillation from the fermentation media than ethanol (Fortman *et al.* 2008) .

There are four different types of butanol (Table 1.1): n-butanol, sec-butanol, isobutanol and tert-butanol. n-butanol and sec-butanol have long carbon chains and the position of the hydroxyl group is located at carbon 1 or 2 while, isobutanol and tert-butanol have branched carbon chains up to two or three respectively. These branched structures confer a higher octane number (Wallner *et al.* 2009). For example, *tert*-butanol has a higher octane number than isobutanol. However, the melting temperature of *tert*-butanol is about 25°C; much higher than the melting temperature of isobutanol which is about -108°C (Hong *et al.* 2012).

One route for butanol production that has been widely considered is the production of iso-butanol is from the amino acid valine (Colon *et al.* 2011). However, yields are generally low, as this requires a massive diversion of carbon towards valine metabolism (Park *et al.* 2014). A much simpler approach is to engineer organisms to produce n-butanol via the natural Clostridial pathway directly from intermediates in the major carbon flux pathway, glycolysis. Therefore, n-butanol, which also has a very favourable octane value, has also been intensively studied as an alternative to petroleum based fuels.

Table 1.1 Comparison of butanol isomers

	n-butanol	sec-butanol	iso-butanol	tert-butanol
Research octane number (RON)	78	32	84	89
Melting T °C	-89.5	-114.7	-108	25.7
Boiling T °C	117.7	99.5	108	82.4
				

1.4 Biobutanol production

1.4.1 Enzymes involved in butanol production

Biobutanol has been produced historically using the genus of *Clostridia* in one of the oldest industrial fermentation processes: the acetone-butanol-ethanol (ABE) fermentation (Lee *et al.* 2008). However, the toxicity of butanol affects the fermentation capacity of the microorganisms converting the sugar to the desired product (Huang, Liu, *et al.* 2010). The butanol biosynthesis pathway in these organisms includes both extracellular and intracellular enzymes.

1.4.1.1 Extracellular enzymes involved in hydrolysis of carbohydrates from biomass

Clostridia can produce extracellular enzymes that hydrolyze the biomass present in a feedstock into fermentable compounds. For example, biomass can include carbohydrates as a major component with celluloses, hemicelluloses and lignins comprising 75% of the dry weight (Balat *et al.* 2009). This genus of *Clostridia* can secrete different enzymes to facilitate carbohydrate hydrolysis into monomers. These monomers can then be used as a substrate for butanol production (Ezeji *et al.* 2007). For instance, to break-down starch α -amylase, β -amylase, pullulanase, glucoamylase and α -glucosidase are required, whereas for cellulose hydrolysis, cellulase and β -glucosidase are necessary for glucose production. Hemicellulase is used to breakdown chains of hemicelluloses, to produce xylose and arabinose as well as glucose. Maximal breakdown of these simple sugars is essential for an efficient fermentation process (Huang *et al.* 2010). Figure 3 below provides a simplified view of biofuel production.

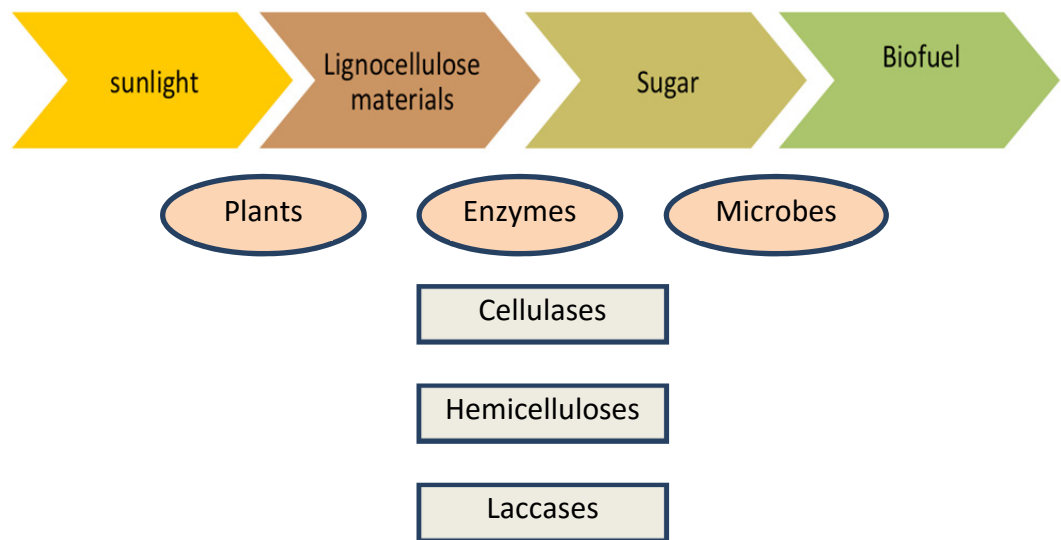


Figure 1.2 A simplified overview of biofuel production.

A biofuel production process includes different stages: production of lignocellulosic material via breaking down the complex polymers by hydrolysis enzymes (cellulases, hemicelluloses and laccases), producing monosaccharide and converting the substrate into the desired product by fermentation.

1.4.1.2 Intracellular enzymes involved in biobutanol synthesis

The various monosaccharide sugars are transported into the cell using specific membrane-bound transport systems that are highly active in micro-organisms like bacteria and yeast. This followed by metabolic processes including glycolysis and the pentose phosphate pathway. In *Clostridia*, the ABE fermentation process can be differentiated into two distinct phases: acidogenesis and solventogenesis. The main products of acidogenesis are lactate, acetate and butyrate. On the other hand, the main products of solventogenesis are ethanol, acetone and butanol in the ratio 6:1:3 (Tummala *et al.* 2003). Acetate and butyrate accumulate during the growth phase leading to a decrease in the pH. These acidic conditions, which are generated by the time stationary phase is reached, alter the metabolism towards solvent production (Jones *et al.* 1986).

In the butanol synthetic pathway five enzymes are required to convert acetyl-CoA into butanol including thiolase (Thl), 3-hydroxybutyryl-CoA dehydrogenase (Hbd), crotonase (Crt), butyryl-CoA dehydrogenase (Ccr), butyraldehyde dehydrogenase

(Adhe2) and butanol dehydrogenase (Adhe2) (Fig. 1.3). Thl plays an important role as it commits Acetyl-CoA to an anabolic pathway. It catalyses the condensation of two molecules of Acetyl-CoA into one molecule Acetoacetyl-CoA, which is then ultimately converted into butanol (Huang *et al.* 2010). The Butanol pathway is associated with the oxidation of NAD(P)H and release of CoA. Butanol dehydrogenases enzymes can have two different coenzyme requirements with the NADH-dependent enzyme active at lower pH (acidic) and the NADPH-dependent active in more basic conditions.

The yeast *S. cerevisiae* has a thiolase enzyme Erg10 but lacks direct homologues of the other butanol pathway enzymes (Hiser *et al.* 1994). Although, it should be noted that other yeast enzymes may exhibit pleiotropic substrate specificities and therefore may be able to perform the reactions involved. Interestingly, in yeast an alternative pathway of butanol production involving threonine metabolism has recently been suggested based on results using *adh1Δ* mutant strains (Si *et al.* 2014).

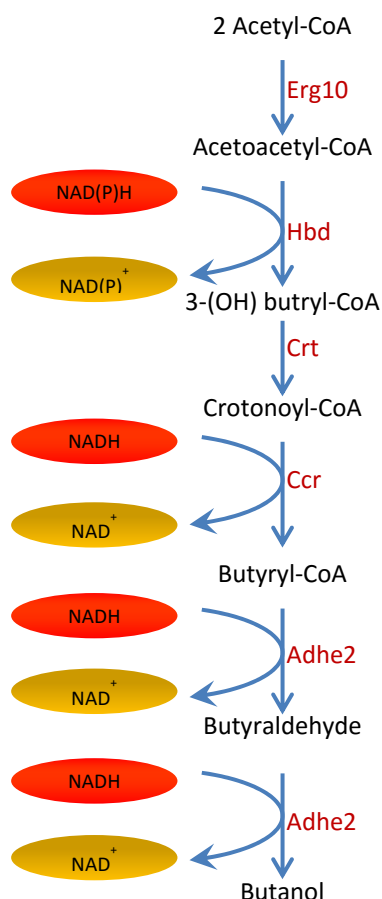


Figure 1.3 The biosynthetic pathway for n-butanol production from *C.beijerinckii*.

Enzymes which are used in the n-butanol pathway: thiolase (Thl), 3-hydroxybutyryl-CoA dehydrogenase (Hbd), crotonase (Crt), butyryl-CoA dehydrogenase (Ccr) and butanol dehydrogenase (Adhe2). Oxidation association with nicotine adenine dinucleotide (NADH) and nicotine adenine and disphosphonucleotide (NADPH).

1.4.1.3 Co-factors involved in the butanol synthetic pathway

The balance of energy and co-factor requirements is an important parameter in strain optimisation for the production of target molecules via metabolic engineering (Atsumi *et al.* 2008). To produce 1 mole of n-butanol from acetyl-CoA, 4 moles of NAD(P)H are required. Hence, the balance of NAD(P)H seems likely to be a key factor in the improvement of 1-butanol production. In addition, the 1-butanol production pathway has four intermediary metabolites that carry Co-A. These metabolites must be well balanced otherwise there will be a depletion of free Co-A (Astumi *et al.* 2008).

The maintenance of a redox balance for living cells is crucial in order to sustain the regular metabolic activities and enable growth. The pyridine nucleotides NADH and NADPH are critical in this regard. NADPH is produced by the oxidative part of the pentose phosphate pathway in many organisms. The oxidation of cytosolic NADPH can be performed by specific NADPH dehydrogenases: in some eukaryotes these are located externally on the mitochondria as part of a respiratory chain. However, such enzymes are absent from *S. cerevisiae* (de Vries *et al.* 1988; Marres *et al.* 1991; Small *et al.* 1998), so yeast cannot directly oxidize surplus cytosolic NADPH. Instead, in *S. cerevisiae* NADPH is oxidised by anabolic reactions as part of biochemical synthesis pathways (Gonzalez Siso *et al.* 1996).

There are a number of systems involved in oxidising NADH. For instance, under respiratory conditions both cytosolic and mitochondrial NADH can be oxidised by the respiratory chain. In eukaryotes such as yeast, cytosolic NADH can be transported into mitochondria by virtue of NADH/ NAD⁺ redox shuttles such as the malate aspartate NADH shuttle and the glycerol phosphate shuttle (Larsson *et al.* 1998; Bakker *et al.* 2001). Mitochondrial NADH dehydrogenases are involved in the oxidation of mitochondrial NADH as a first step in the respiratory chain (de Vries *et al.* 1988; Marres *et al.* 1991). There are two NADH dehydrogenase iso-enzymes both present on the inner mitochondrial membrane, one facing the matrix with the other facing the inter-membrane space (Luttik *et al.* 1998; Small *et al.* 1998). The reduction of cytosolic NAD⁺ to NADH occurs during glycolysis via the glyceraldehyde-3-phosphate dehydrogenase (GAPDH) enzyme, while in eukaryotes the reduction of the mitochondrial NAD⁺ predominantly occurs via the pyruvate dehydrogenase complex and the dehydrogenases of the TCA cycle in the mitochondrial matrix. When fermentable carbon is replete in yeast, NADH in the cytoplasm is largely oxidised via alcohol dehydrogenases leading to the production of ethanol from acetaldehyde (van Dijken *et al.* 1986). NADH can be oxidized in the mitochondria via a respiratory chain acceptor (de Vries *et al.* 1988; Luttik *et al.* 1998; Overkamp *et al.* 2000; Bakker *et al.* 2001). In *S. cerevisiae* under aerobic conditions where fermentable carbon is limited, there are two main systems involved in the oxidation of any excess cytosolic NADH: the external NADH dehydrogenase and the glycerol 3-phosphate shuttle, which is particularly active

under starvation conditions or at low growth rates when the availability of energy is limited (Bakker *et al.* 2001; Gonzalez Siso *et al.* 1996).

1.5 Microorganisms involved in butanol production

There are two different kinds of microorganisms that have been used for butanol production:

- Microorganisms which produce butanol naturally.
- Metabolically engineered microorganisms.

1.5.1 Microorganisms which produce butanol naturally

Historically, butanol has been produced exclusively by the genus *Clostridia* including *C. acetobutylicum*, *C. beijerinckii*, *C. saccharoperbutylacetonicum*, *C. saccharoacetobutylicum*, *C. aurantibutyricum*, *C. pasteurianum*, *C. sporogenes*, *C. cadaveris*, and *C. tetanomorphum* (Keis *et al.* 1995). However, the genus of *Clostridia* is not an ideal organism for the optimisation of butanol production. Genetic methodology and genomic information is less highly developed than for other systems. Growth rates of *Clostridia* can be quite low and *Clostridia* cannot tolerate butanol concentrations over 1-2% in fermentation media. Moreover, *Clostridia* produce various by-products such as, butyrate, acetone and ethanol (Huang *et al.* 2010). Finally, industrial Clostridial fermentations are prone to contamination both by other organisms and by bacteriophages (Zheng *et al.* 2009). Even so the major advantage of Clostridial species is the high yields that are attainable at lab scale. For instance, butanol levels from *Clostridium beijerinckii* BA101 were measured at about 11.9-14.3 g/L (van Maris *et al.* 2006). As a result of the potential drawbacks mentioned above, scientists have taken metabolic engineering strategies to generate non-native microorganisms, such as *Escherichia coli* and *Saccharomyces cerevisiae* that produce butanol.

1.5.2 Metabolically engineered microorganisms

In the early 1970s, the advent of genetic engineering meant that it became possible to produce compounds, which are not normally produced in microbes. This includes compounds such as insulin, human growth hormone and biofuels (Hong *et al.* 2012). Such processes offer potential benefits in terms of environmental and economic factors compared to traditional methods (Hong *et al.* 2012). As a result, industry has attempted to exploit these developments in biotechnology to produce important commercially viable compounds (Nielsen 2001; Tyo *et al.* 2007). Synthetic biology represents an evolution of metabolic engineering, which is reliant upon 'omics technologies, where whole pathways or systems are added to organisms with the goal of developing useful traits (Fig. 1.4) (Bro *et al.* 2004; Hermann 2004).

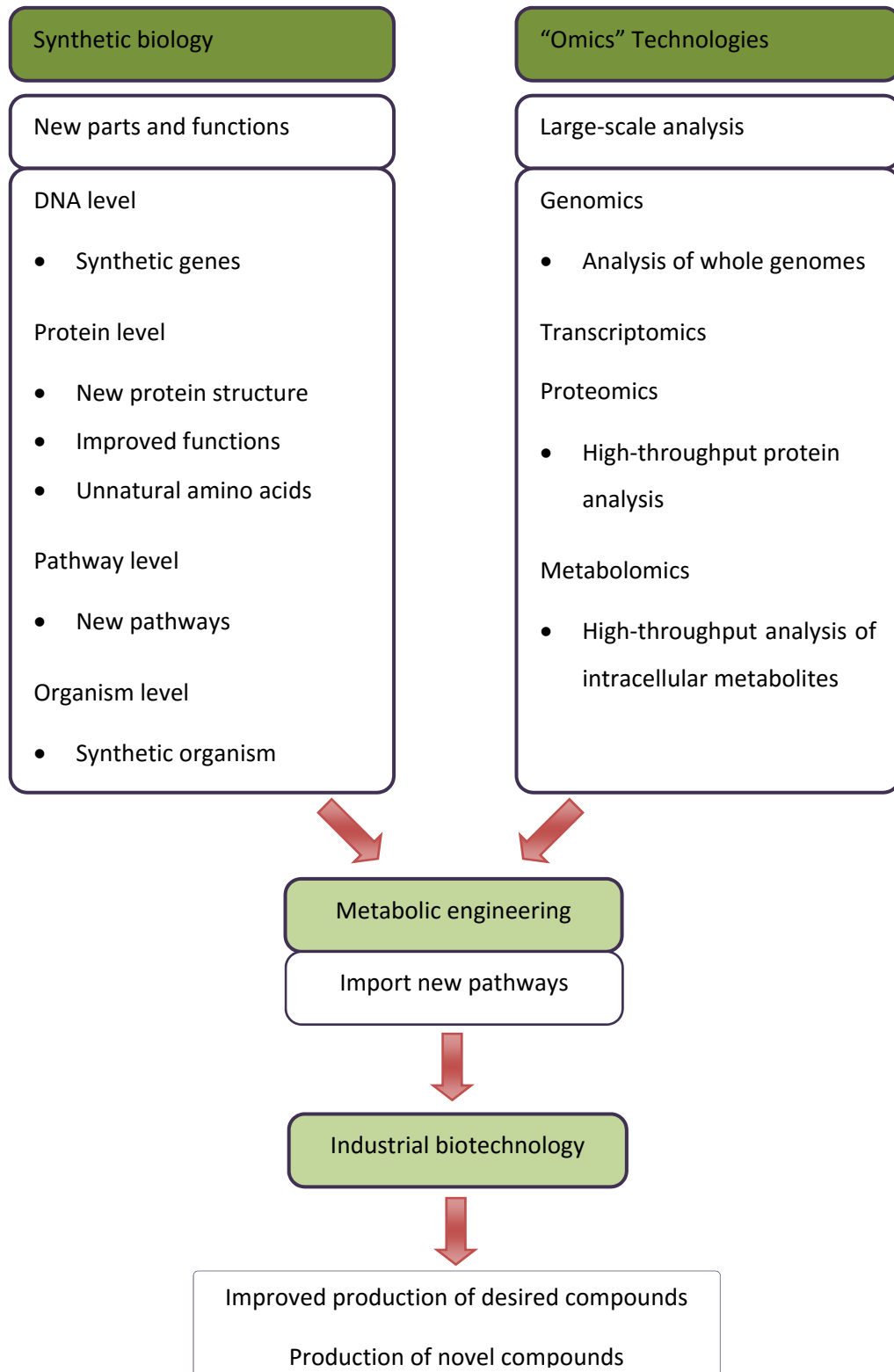


Figure 1.4 Development of metabolic engineering.

The improved production of desired products associated with the development of synthetic biology and 'omics' technologies (Tyo *et al.* 2007).

Synthetic biology can be used to redesign and reconstruct biological pathways in order to create new pathways or design novel regulatory systems (Martin *et al.* 2009). It provides the capability to assemble multiple enzymes from different microorganisms into a heterologous host to achieve a synthetic pathway and produce desired products (Krivoruchko *et al.* 2011). However, a challenge that could be associated with the insertion of heterologous genes into microorganisms is the possibility of effects on the expression of endogenous genes, which could alter the 'native' metabolism of the host cell. Furthermore, constructing new synthetic pathways in organisms could also lead to imbalances in gene expression, co-factors and metabolites that might affect the yield of a target compound (Atsumi *et al.* 2008).

1.5.2.1 Bacteria

Escherichia coli (*E. coli*) is an attractive micro-organism for use in biotechnological applications because it grows very rapidly and it is relatively straightforward to engineer genetic modifications. In one study the essential genes for 1-butanol production (*thl*, *hbd*, *crt*, *ccr* and *adhe2*) from *Clostridium acetobutylicum* were expressed using two different plasmid vectors (Atsumi *et al.* 2008). The resulting strains were tested under both anaerobic and aerobic conditions. Under anaerobic conditions, the strains produced 13.9 mg/L of 1-butanol. Hence, the authors speculated that NADH, which was produced in anaerobic conditions was limiting for 1-butanol production. 1-butanol yields under aerobic conditions were minimal, most likely because acetyl-CoA and NADH were consumed in the tricarboxylic acid cycle (TCA). In contrast, another study attempted to improve butanol production by deleting some *E. coli* native genes (Causey *et al.* 2004) Genes such as *ldha*, *adhe* and *frdPC* were selected as they encode components of potentially competing pathways. As a result, the production of butanol was increased two-fold due to decreases in the generation of by-products such as lactate, ethanol and succinate (Causey *et al.* 2004).

1.5.2.2 Yeasts

Yeasts are widely studied microorganisms across science, industry and medicine. Some species are used in fermentation to produce beverages and pharmaceutical products. However, some species can also cause disease or are involved in food spoilage. Nowadays, the budding yeast *Saccharomyces cerevisiae*, the fission yeast *Schizosaccharomyces pombe* and the methylotrophic yeast *Pichia Pastoris* have become model eukaryotic cells, which are used in both the academic and biotechnological sectors. Species of yeast are viewed as preferable to bacteria for some industrial applications for various reasons. Yeast are not infected by phage and generally tolerate altering osmotic and pH conditions. For example, yeast tolerate high sugar concentrations in the culture media at lower pH (Hong *et al.* 2012). By far the most widely used yeast species in biotechnology is *Saccharomyces cerevisiae*, although for recombinant protein production *Pichia Pastoris* is a common choice of microorganism. The taxonomy of *S. cerevisiae* which has been used in this thesis is detailed in Table 1.2.

Table 1.2 Taxonomy of *S. cerevisiae*

Taxonomic category	Example
Subdivision	<i>Ascomycotina</i>
Family	<i>Saccharomycetaceae</i>
Subfamily	<i>Saccharomycetoideae</i>
Genera	<i>Saccharomyces</i>
Species	<i>cerevisiae</i>

Saccharomyces cerevisiae (*S. cerevisiae*) has been used in traditional applications such as brewing and bread making. More recently, it has been used

extensively in different fundamental studies as a eukaryotic model cell, as well as in the industrial biotechnology sector to produce important heterologous products using different gene manipulation techniques (Luo *et al.* 1999). This is because it is extremely well characterized genetically, biochemically and physiologically. In addition, it was the first microorganism, which had its genome fully sequenced (Snyder *et al.* 2009) and in general it is regarded as a safe or 'GRAS' microorganism. Furthermore, a significant advantage of using *S. cerevisiae* over other expression systems is the ease with which gene insertions and deletions can be generated via homologous recombination. Moreover, yeast has the ability to tolerate many stress conditions and hence grows robustly in a wide spectrum of scenarios (Petranovic *et al.* 2010). However, *S. cerevisiae* has a serious limitation for biofuel production due to its inability to grow effectively on hemicelluloses. However, attempts to overcome this problem have been developed through metabolic engineering to enable *S. cerevisiae* to ferment xylose and arabinose, which are major monosaccharides derived from hemicellulose hydrolysis (Hahn-Hagerdal *et al.* 2007). Such studies have been aimed at increasing the fermentation efficiency to generate biofuels that are more economically competitive via increasing the percentage of raw material broken down from lignocellulosic feedstocks.

1.6 Metabolic engineering strategies used to produce butanol and Iso-Butanol

1.6.1 Butanol production

The first attempt to force an engineered strain of *S. cerevisiae* to produce 1-butanol used a plasmid vector system to overexpress the Clostridial ABE pathway (Steen *et al.* 2008); however, the productivity did not exceed 2.5 mg/L butanol, which is very low compared to Clostridial yields of ~20 g/L butanol. In a second study using plasmid vectors to express the pathway in *S. cerevisiae*, various engineering strategies were also taken to increase cytosolic acetyl-CoA. For example, the *ALD6*, *ACS2* and *ADH2* genes that encode components of the ethanol to acetyl-CoA pathway were overexpressed. In addition, the *CIT2* and *MLS1* genes were deleted, which encode components of the glyoxylate cycle: a metabolic cycle that normally depletes cytosolic

acetyl-CoA. In the resulting strains, the maximal butanol yield was measured at 16.3 mg/L (Krivoruchko *et al.* 2013). In a third study, an *adh1Δ* mutant of *S. cerevisiae* was observed to produce butanol even without the ABE, and it was proposed that deletion of *ADH1* activates an endogenous 1-butanol pathway involving threonine catabolism in the mitochondria (Si *et al.* 2014). The combination of the *ADH1* deletion with overexpressed enzymes of the leucine biosynthetic pathway, generated an engineered strain producing a maximal yield of 242.8 mg/L (Si *et al.* 2014). Other investigators have taken strategies towards boosting the level of cytosolic acetyl-CoA (Lian *et al.* 2014). Here ethanol and glycerol biosynthesis were restricted in *S. cerevisiae* using a combined deletion of the *ADH1*, *ADH4*, *GPD1* and *GPD2* genes in strains bearing the ABE pathway. This system was reliant on plasmid based vectors for the ABE pathway genes, and the resulting engineered strain produced less than 10 mg/L butanol. A second improvement in butanol yield was obtained when a pyruvate dehydrogenase bypass pathway was introduced to this system and here butanol production was greater than 100 mg/L (Lian *et al.* 2014). Finally, in a strain bearing plasmid derived ABE genes with the glycerol production pathway eliminated, replacement of the Clostridial *hbd* gene with the *ter* enzyme from *Treponema denticola* results in enhanced 1-butanol production with maximal yields of 14.1 mg/L (Sakuragi *et al.* 2015).

1.6.2 Isobutanol production

As well as n-butanol (1-butanol), isobutanol (2-methylpropan-1-ol) is also considered a superior liquid fuel to ethanol, and many researchers have been investigating possible routes for the production of isobutanol. A number of investigators have studied glycine metabolism through glyoxylate to α -ketovalerate and α -isoketovalerate, which in turn can be converted n-butanol and isobutanol, respectively (Branduardi *et al.* 2013). Using glycine as an external substrate, n-butanol and isobutanol accumulated in the fermentation medium to 92 and 58 mg/L, respectively. However, questions remain about the applicability of this approach, as glycine is not generally considered an industrial feedstock.

Other investigators have engineered strains of *S. cerevisiae* to produce isobutanol by overexpressing an α -keto acid decarboxylase gene (taken from a *Lactobacillus lactis* strain) in combination with combined overexpression of genes for the mitochondrial valine biosynthetic enzymes. Using this strategy isobutanol levels reached 93 mg/L when glucose was used as sole carbon source (Lee *et al.* 2012).

Other studies have produced isobutanol by overexpressing genes for valine metabolism e.g. *ILV2*, *ILV3*, and *ILV5*, as well as *BAT2*, a cytosolic branched-chain amino acid (BCAA) aminotransferase (Colon *et al.* 2011). This strategy led to isobutanol production up to 0.94 mg/g per glucose (which is roughly = 37.6 mg isobutanol/L) with glucose as the carbon source in minimal media under anaerobic conditions. Improvements in yield were attained when external amino acids were supplied in the culture media under aerobic conditions resulting in isobutanol yields of 2.4 mg/g per glucose (which is roughly = 40 mg isobutanol/L) (Chen *et al.* 2011).

Other studies have used alternative strategies to optimise isobutanol production in metabolically engineered strains of *S. cerevisiae*. For instance, isobutanol production was increased in by overexpressing the genes for both the valine pathway and leucine biosynthetic pathways, resulting in 376.9 mg/L of isobutanol from media containing high levels of glucose (100 g/L) (Park *et al.* 2014).

Overall, while progress has been made in engineering yeast strains to produce butanol and isobutanol, the yields that are currently being attained are well below those obtained from Clostridial fermentations. As a result there is plenty of scope for optimisation and improvement in these yields.

1.7 Carbon metabolism in yeast

1.7.1 Overview

Carbohydrate metabolism encompasses the processes by which complex sugars are broken down to intermediates and end product metabolites; as well as the pathways by which simple sugars, oligosaccharides, and polysaccharides are synthesized. Sugars represent the primary sources of energy for most cell types, indeed the yeast *Saccharomyce cerevsiae* has evolved to make preferential use of highly fermentable sugars like glucose and fructose. Simple monosaccharides can be transported across cell membranes in order to enter a variety of metabolic pathways. Hexose sugars such as glucose, in particular, are catabolised via the glycolytic pathway to generate small amounts of ATP. Products of the glycolytic pathway can either be further catabolised in mitochondria during respiration or they can be converted to end-product metabolites during fermentation: ethanol in yeast or lactic acid in certain mammalian cells. In metabolic engineering strategies, it is important to predict the carbon flux through these pathways in order to generate maximal yields of desired products. In addition, as lignocellulosic hydrolysates contain a range of different sugars it is important to consider the performance of production strains on a range of different sugars as carbon sources.

Although many yeast species are able to ferment sugars to ethanol, *S. cerevisiae* is the major microorganism that has been used historically in the production of alcoholic beverages. This relies upon its ability to rapidly consume sugars and convert them to high levels of ethanol (Rodrigues *et al.* 2006). Indeed, *S. cerevisiae* ferments glucose to ethanol even under aerobic conditions where it would be energetically more efficient to metabolise sugars via respiration. This phenomenon is known as the Crabtree effect (Pronk *et al.* 1996) and is contrary to the situation in most organisms where fermentation and the glycolytic flux are repressed when oxygen is available (Pasteur effect) (Rodrigues *et al.* 2006). In most eukaryotic organisms, pyruvate, the end product of glycolysis, is transported into mitochondria where via the pyruvate dehydrogenase complex, the citric acid cycle, the electron transport system and oxidative phosphorylation, ATP is efficiently generated. In contrast, in yeast, pyruvate is converted in the cytoplasm into acetaldehyde and CO₂ by pyruvate

decarboxylase, and then alcohol dehydrogenase enzymes convert the acetaldehyde to ethanol. It is thought that yeast has evolved this metabolic strategy to compete with other microorganisms: they rapidly deplete glucose and produce ethanol which is toxic to many of their competitors.

The metabolism of many sugars starts with the need for the sugar to be transported into yeast. This occurs either by facilitated diffusion or by a range of specific sugar transporters or permeases. For instance, *S. cerevisiae* has a wide range of glucose transporters that have various affinities for glucose (Flores *et al.* 2000). Some of these transporters will also transport fructose and mannose into yeast. Like glucose; fructose and mannose are phosphorylated by hexokinase to fructose-6-phosphate and mannose-6-phosphate, respectively. Fructose-6-phosphate is a glycolytic intermediate and mannose-6-phosphate can be converted to fructose-6-phosphate via a specific isomerase enzyme.

Disaccharide and trisaccharide sugars need to be hydrolysed into their constituent monosaccharides before entering the glycolytic pathway. Hydrolysis can occur outside the plasma membrane or inside the cell, after the sugar has been transported. For instance, sucrose is hydrolysed externally via invertase that is secreted by yeast (Flores *et al.* 2000). In contrast, maltose is transported into cells where the maltase enzyme breaks it down into two molecules of glucose (Drewke *et al.* 1988; Day *et al.* 2002).

1.7.2 Monosaccharide derived from Lignocellulosic biomass

Lignocellulose biomass is the most abundant material on the earth and it is considered a potential feedstock for biofuel production as it participates in reducing the price for the end product. Lignocellulose consists mainly of cellulose, hemicellulose and lignin as aromatic polymers. Cellulose is a polysaccharide consisting of a linear chain of β (1 \rightarrow 4) linked D-glucose units (Updegraff 1969) while, hemicellulose is a polysaccharide and includes xylan, glucuronoxylan, arabinoxylan, glucomannan and xyloglucan. These polysaccharides contain various monomer sugars: xylose, mannose, arabinose and galactose (Brannvall *et al.* 2007). The small units of sugar could be hexose sugars (6C) like: glucose, mannose, galactose or pentose sugars (5C): such as, xylose and arabinose. In this thesis, glucose has been used as a main substrate for butanol production and other fermentable sugars were also tested such as sucrose and mannose. In contrast to other fungi, *S. cerevisiae* is not able to ferment xylose naturally, as some metabolic enzymes involved in xylose and arabinose metabolism are absent or inactive compared to other fungus (Richard *et al.* 2003). Xylose is the most abundant hemicellulosic sugar and in order to be used as a carbon source, xylose needs to be transported into the cell through a specific carrier and then converted into intermediates of the glycolysis pathway. For instance, inside cells xylose can be converted into xylulose by xylose isomerase and then it can be phosphorylated by xylulokinase to xylulose-5-phosphate. Xylulose-5-Phosphate can enter the pentose phosphate pathway by which it can be converted into fructose-6-phosphate to enter glycolysis (Tanaka *et al.* 2002). Arabinose follows a similar metabolic route to xylose metabolism, as it can be converted to ribulose, ribulose-5-phosphate and then xylulose-5-phosphate (Richard *et al.* 2003) (Fig. 1.5).

Galactose is a monosaccharide that is transported into yeast via a specific permease; then inside the cell the Leloir pathway ultimately converts it to the glycolytic intermediate glucose-6-phosphate in a series of reactions (Sellick *et al.* 2008). Previous chemostat studies have found that during glucose to galactose transitions under anaerobic conditions, galactose is not consumed by yeast possibly because the energy status of the cell is reduced to such an extent that the transcriptional induction of genes for the Leloir enzymes and permease is prohibited (Van den Brink, 2009).

Another carbohydrate that is worth assessing in yeast strains that produce compounds for industry is glycerol. There are specific marine species of algae such as *Dunaliella salina* that produce high concentrations of glycerol in order to combat high osmotic pressure and these have been considered as a source of feedstock for fermentations (Liu *et al.* 2013). Glycerol is also a major by-product of biodiesel production (Ruhul *et al.* 2011). Therefore strategies where microorganisms are grown on glycerol to generate useful products are being actively sought (da Silva *et al.* 2009). In yeast glycerol is phosphorylated to glycerol-3-phosphate in the cytosol and then oxidised to dihydroxy-acetone-phosphate in mitochondria (Nevoigt *et al.* 1997). It is possible that this mitochondrial reaction would be deficient under anaerobic conditions such that glycerol use would require aeration.

1.7.3 Glycolysis pathway

Glycolysis is a central pathway by which glucose is oxidised to two molecules of pyruvate with the generation of a small amount of ATP (Madsen *et al.* 2005). Intracellular glucose is phosphorylated by hexokinase enzymes to glucose-6-phosphate and then isomerized to fructose-6-phosphate by phosphoglucose isomerase. The phosphofructokinase enzyme phosphorylates fructose-6-phosphate to fructose 1,6-bisphosphate. The two kinase reactions required to reach this stage use ATP as a source of phosphate and energy. Fructose 1,6-bisphosphate is then converted via a series of metabolites to pyruvate using various enzymes: aldolase, triosephosphate isomerase, glyceraldehyde 3-phosphate dehydrogenase, phosphoglycerate kinase, phosphoglycerate mutase, enolase and pyruvate kinase (Fig. 1.5). ATP is generated at the pyruvate kinase and phosphoglycerate kinase steps and NADH is generated at the glyceraldehyde 3-phosphate dehydrogenase step.

Generally in eukaryotes, about 50% of glucose-6-phosphate is metabolised via glycolysis and a large proportion of the rest of the carbon goes into the pentose phosphate pathway as fructose-6-phosphate (Vaseghi *et al.* 1999). The pentose phosphate pathway is required for the production of NADPH and ribose/ deoxyribose sugars (Vaseghi *et al.* 1999). The NADPH is used in anabolic reactions, and the ribose/

deoxyribose sugars are required for nucleotide metabolism. However in *S. cerevisiae*, which is a Crabtree positive yeast, there is a much lower carbon flux toward the pentose phosphate pathway and greater metabolism of carbohydrate through glycolysis (Blank *et al.* 2004).

Pyruvate represents a branch point metabolite that depending on environmental conditions or the yeast species can be converted into a range of different metabolites (Pronk *et al.* 1996). In most yeast species growing in an aerobic environment, pyruvate is oxidized to CO₂ via respiratory pathways in the mitochondria. Under anaerobic conditions, most pyruvate is converted into ethanol; or as described above for Crabtree positive yeast, pyruvate is converted to ethanol even in aerobic conditions (Pronk *et al.* 1996). Pyruvate can also be converted into many other metabolites including oxaloacetate and aspartic acid, alanine, the hydrophobic amino acids and 2,3-butanediol via acetoin (Ng *et al.* 2012).

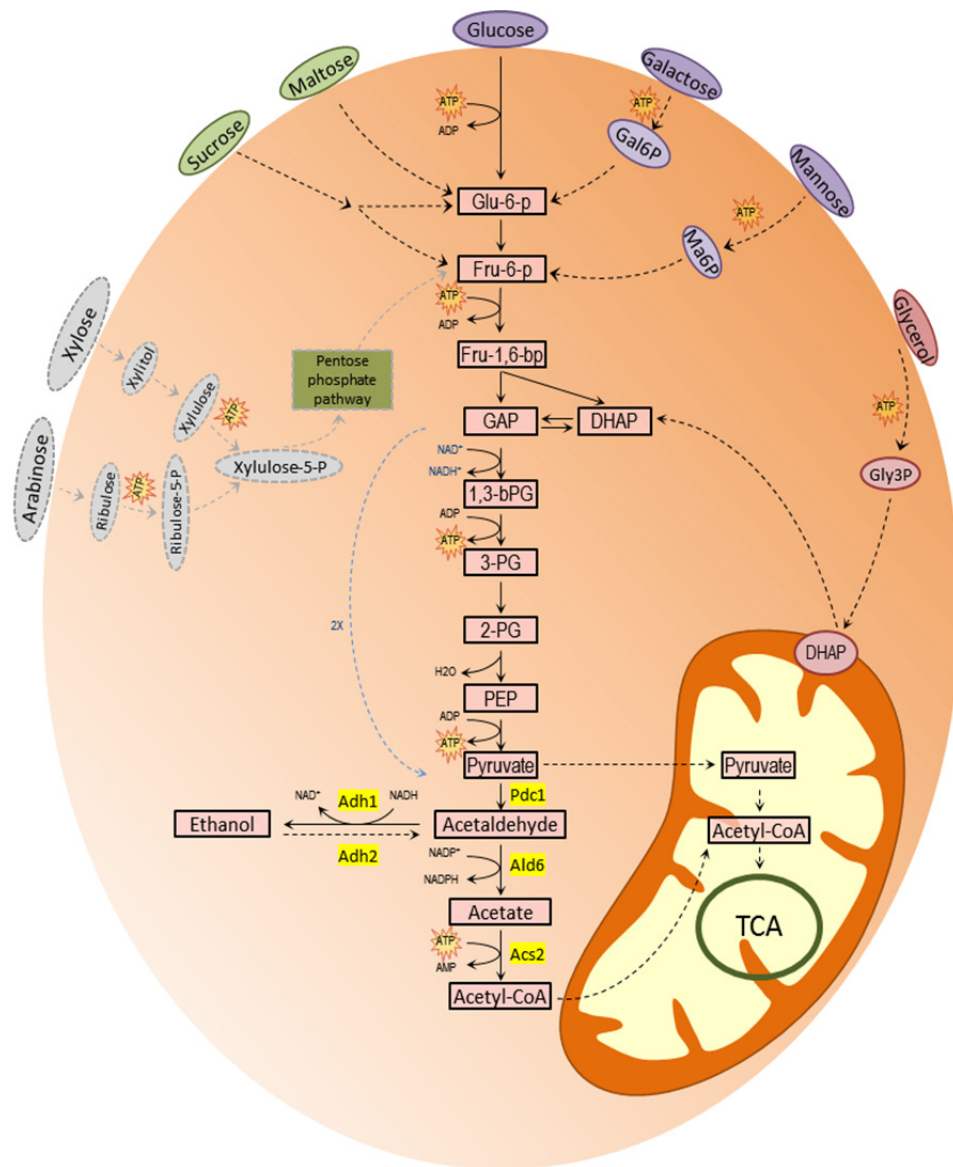


Figure 1.5 Sugar metabolism and glycolysis in yeast

Scheme shows how various sugars enter the glycolysis pathway through converting to intermediates which are involved in the glycolytic pathway and enable them to be metabolized, including monosaccharide sugars: glucose, fructose, mannose, galactose (in purple) and the sugar alcohol glycerol (in pink), disaccharide sugars: sucrose and maltose (in green) and non-fermentable sugars (in grey).

G6P glucos-6-phosphate
F6P fructose-6-phosphate
F1, 6 bP fructose1, 6-bi-phosphate
DHAP Dihydroxyacetone phosphate
GAP glyceraldehyd-3-phosphate
1,3bPG 1,3-bisphosphoglycerate

3PG 3-phosphoglycerate
2PG 2-phosphoglycerate
PEP phosphoenolpyruvate
Ma6P mannose-6-phosphate
Gal6P galactose-6-phosphate
Gly3P glycerol-3-phosphate

1.7.4 Ethanol metabolism in yeast

S. cerevisiae is able to consume all of the available glucose from the media very efficiently in order to convert it into ethanol to restore the NAD^+ used in glycolysis. The accumulation of ethanol is thought to be advantageous to yeast as it inhibits competing microbes via ethanol toxicity. Once glucose is depleted from the media, the glucose de-repression pathway is activated. This pathway releases a host of genes from a transcriptional repression pathway. These genes have many functions in respiration and alternative carbon source usage. For instance, *S. cerevisiae* activates the *ADH2* gene, which converts ethanol to acetaldehyde, which can subsequently be converted into acetyl-CoA (Pronk *et al.* 1996) (Fig. 1.6).

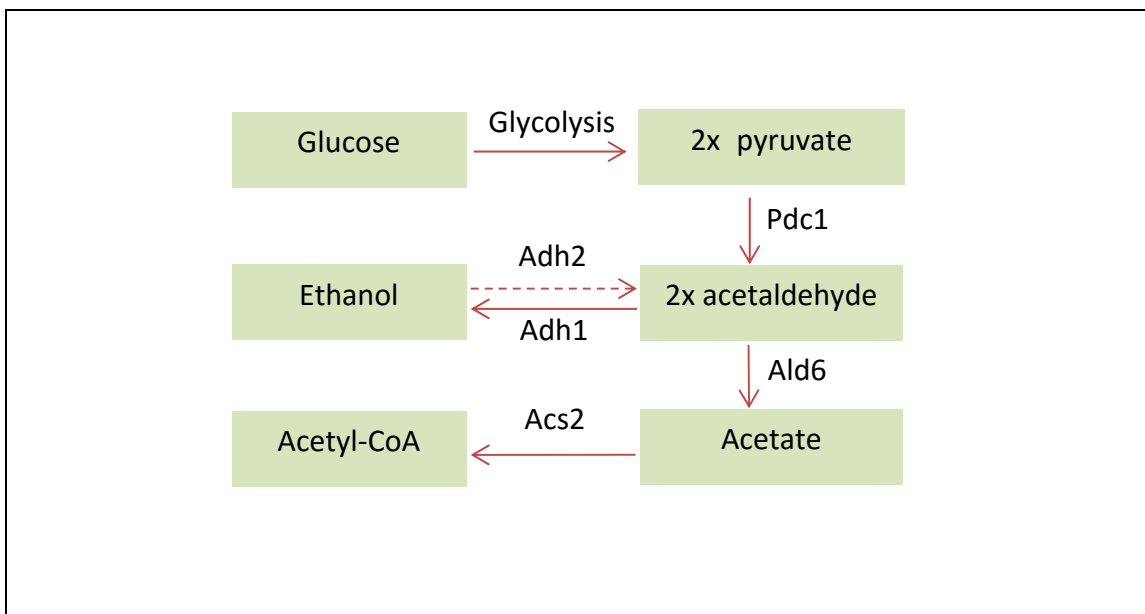


Figure 1.6 Ethanol metabolisms in yeast

The figure shows that most glucose is converted to ethanol at high glucose concentrations. Depletion of glucose from the media causes changes in gene expression that lead to the activation of the *ADH2* gene, which can convert ethanol back to acetaldehyde, so that yeast can consume it as a carbon source.

1.7.5 Acetyl-CoA biosynthesis

Acetyl-Co-enzyme A (Co-A) is a precursor for many biotechnologically relevant compounds produced by *S. cerevisiae* such as n-butanol, isoprenoids, lipids and flavonoids (Dyer *et al.* 2002; Steen *et al.* 2008; Shiba *et al.* 2007). Many of these pathways require multiple acetyl-CoA molecules in their synthesis, therefore the mechanism of acetyl-CoA production is an important consideration where production of these metabolites is the goal. Acetyl-CoA in yeast can be derived from the mitochondrial pyruvate dehydrogenase system, from the cytosolic pyruvate by-pass pathway or from the conversion of ethanol in a post-diauxic phase (Werner-Washburne *et al.* 1993).

1.7.5.1 Pyruvate dehydrogenase

Pyruvate is oxidized to CO₂ and acetyl-CoA via the citric acid cycle by the mitochondrial multi-enzyme complex pyruvate dehydrogenase (PDH) which consists of: pyruvate dehydrogenase (E1), dihydrolipoamide acetyl transferase (E2) and dihydrolipoamide dehydrogenase (E3). After being transported into the mitochondria via a specific carrier called the mitochondrial pyruvate carrier (Pronk *et al.* 1996; Flores *et al.* 2000), pyruvate undergoes an oxidative decarboxylation reaction with the acetyl group being transferred across three different enzyme bound cofactors thiamine pyrophosphate (TPP), lipoate and Co-enzyme A (Ciszak *et al.* 2003). The resulting acetyl-CoA can enter the citric acid cycle to undergo further oxidation to CO₂.

1.7.5.2 Pyruvate by-pass pathway

Alternatively, pyruvate can be converted to acetyl-CoA in the cytosol via the pyruvate by-pass pathway. This pathway requires the activity of the three enzymes: 1) pyruvate decarboxylase (Pdc), which converts pyruvate to acetaldehyde; 2) acetaldehyde dehydrogenase (Ald), which converts acetaldehyde to acetate; and 3) acetyl-CoA synthetase (Acs), which converts acetate to cytosolic acetyl-CoA. Acetyl-CoA can then be transported into the mitochondria. There are several genes that

encode pyruvate decarboxylase. *PDC1* is the main gene and responsible for about 80% of the enzyme activity. *S. cerevisiae* also has the *PDC5* and *PDC6* genes. Interestingly, pyruvate decarboxylase activity increases when glucose concentration is increased due to enhanced transcription of *PDC5* and *PDC6* (Jordan *et al.* 1997). There are five yeast genes that encode acetaldehyde dehydrogenase enzymes: *ALD1*, *ALD2*, *ALD3*, *ALD4*, *ALD5* and *ALD6*. The Ald2, Ald3 and Ald6 proteins are cytosolic enzymes with Ald6 using NADP⁺ as a cofactor, whereas Ald2 and Ald3 use NAD⁺. In contrast, Ald4p and Ald5p are mitochondrial enzymes that use either NAD⁺ or NADP⁺ as cofactors (Wang *et al.* 1998). Ald6 is constitutively expressed in the cytosol and an *ALD6* null mutant exhibits phenotypes that suggest it is likely to be the major enzyme (Meaden *et al.* 1997).

Yeast has two isoforms of the acetyl-CoA synthetase; Acs1 and Acs2. These enzymes are required for the production of acetyl-CoA from acetaldehyde. The *ACS1* and *ACS2* genes are required for growth on glucose and expressed under anaerobic conditions, suggesting that the production of cytosolic acetyl-CoA is important under these circumstances (van den Berg *et al.* 1996).

1.7.5.3 Ethanol as a carbon source after the diauxic shift.

When yeast switch their metabolism to ethanol consumption during the diauxic shift, the Adh2 enzyme that converts ethanol to acetaldehyde is induced. Under these circumstances the aldehyde dehydrogenase and acetyl-CoA synthetases described above can convert the acetaldehyde to acetyl-CoA (Pronk *et al.* 1996). Carnitine Acetyl transporters allow transport into the mitochondria for the purpose of energy generation. During growth on ethanol (or acetate) cytosolic acetyl-CoA can be built into larger four carbon compounds such as oxaloacetate via the glyoxylate pathway, which occurs in the cytosol and peroxisome of fungi and plants (de Jong-Gubbels *et al.* 1995).

Overall, while the metabolism of an organism like *S. cerevisiae* may seem superficially straightforward, a more detailed analysis suggests this is not the case. This

makes strategies that aim to hijack yeast metabolism towards the production of a specific desired metabolite far from trivial to design and optimise.

1.8 Butanol tolerance

1.8.1 Overview

One of the most important challenges facing researchers aiming to force micro-organisms to produce desirable chemicals, such as biofuels, is the potential for toxic effects. For the biofuel butanol, the toxic effects can include increased cell membrane fluidity and more specific effects on intracellular processes like protein synthesis. Solvent stress has been extensively studied where solvents are added exogenously, however the effects of intracellular solvent production are much less widely considered. Even so a number of strategies to combat the various toxic effects of biofuels like butanol have been taken.

1.8.2 Butanol toxicity

The antimicrobial effects of many compounds are intrinsically linked to their hydrophobicity, which determines the amount of the compound that accumulates in the cytoplasmic membrane. An accumulation of solvent in the membrane can cause various consequences for the cell. Solvents can affect cell viability by damaging the cell membrane leading to increased permeability, such that essential molecules such as ATP, mRNA, NADH, ions, phospholipids and soluble proteins can leak from the cell (Dunlop *et al.* 2011). These effects can also diminish energy transduction by disrupting proton motive forces. Generally longer chain alcohols are more toxic than shorter ones as the increased number of carbon atoms amplifies solvent hydrophobicity. As well as impacting directly on the membrane lipid bilayer, solvents can inhibit the function of membrane proteins, which can interfere with various essential physiological process, such as nutrient transport (Dunlop 2011).

The impact of various alcohols on protein synthesis at the level of translation initiation has been well characterised by the Ashe lab (Ashe *et al.* 2001). Fusel alcohols inhibit

the activity of eIF2B, which regulates the function of another translation initiation factor, eIF2. eIF2 forms part of a ternary complex that is critical for translation initiation, and in response to fusel alcohols, the levels of this ternary complex are reduced leading to an inhibition of protein synthesis (Taylor *et al.* 2010).

Recently, great efforts have been made to overcome the limitations of butanol toxicity (Dunlop 2011). A variety of strains have been engineered to be more tolerant to butanol and this could be a promising step toward improving biofuel production. In addition, it has been shown that increasing the tolerance to other solvents can increase solvent production; hence, a solvent tolerant micro-organism would appear to represent a more competent host for biofuel production (Alper *et al.* 2006; Tomas *et al.* 2003).

1.8.3 Strategies used to increase biofuel (solvent) tolerance

There are a wide range of mechanisms that have been used to increase tolerance to alcohols like butanol. Some of these are listed below.

- i. Heat shock proteins or chaperones are up regulated under alcohol stress. These proteins are involved in protein synthesis, transport, folding and degradation. Under stress conditions chaperones prevent protein aggregation and assist in protein refolding. A recent study in *Clostridia* has shown that overexpression of the heat shock genes *groESL* reduces butanol toxicity by up to 85% and improves butanol yields by 40% (Tomas *et al.* 2003).
- ii. Five mutations in genes which encode proteins with functions ranging from efflux pumps to cysteine degradation enzymes have been identified that improve isobutanol tolerance in *E. coli* strains. However, isobutanol production does not really improve in these mutant strains (Atsumi *et al.* 2010).
- iii. Mutation of the transcription factor Spt15 (Belotserkovskaya *et al.* 2000) in *S. cerevisiae* leads to increased ethanol tolerance and improves the capacity of the strain to consume glucose and efficiently convert it to ethanol (Alper *et al.* 2006).
- iv. Efflux pumps from an array of bacterial species have been introduced into *E. coli* in order to reduce biofuel toxicity (Dunlop *et al.* 2011). The efflux pumps are

membrane transporters that recognise the toxic compounds within the cell and pump them out using a proton motive force. Interestingly, for the engineered strains the heterologous efflux pumps restore growth on all of the biofuels tested except n-butanol and isopentanol. It seems the pumps work efficiently for long chain alcohols like hexanol, heptanol, octanol and nonanol but they are not efficient for shorter chain alcohols like butanol.

- v. Levels of butanol tolerance have been increased by combining butanol tolerance with other metabolic engineering approaches. For instance, overexpression of the heat shock protein Hsp42 and the up-regulation of *GPP2*, and *GLO1* in *S. cerevisiae* increases butanol tolerance up to 3% (v/v) (Ghiaci *et al.* 2013). It is possible that excess *GPP2* increases the capacity for NADH oxidation (Pahlman *et al.* 2001), as *GPP2* is involved in a final NADH-dependent step of glycerol biosynthesis. Glo1 is a glyoxylase involved in the breakdown of methylglyoxal; a toxic product of glycolysis (Aguilera *et al.* 2004), and *HSP42* encodes a cytosolic small heat shock protein that can prevent unfolded substrate proteins from irreversibly forming large protein aggregates (Wotton *et al.* 1996). Even though the resulting strain is more tolerant to butanol, the butanol yield does not appear to improve significantly. It is possible that the increased glycerol biosynthesis and respiration levels lead to decreased carbon flux toward butanol production (Ghiaci *et al.* 2013).
- vi. Other studies have screened various species of *S. cerevisiae* in a series of genetic crosses to measure the fermentation performance of progeny in the presence of butanol. Significant variation was detected between strains using a phenotypic microarray assay system (Zaki *et al.* 2014). However, one unifying discovery was that all of the butanol resistant strains exhibited an up-regulation of the *RPN4* gene (Xie *et al.* 2001). *RRN4* encodes a transcription factor that regulates the expression of the proteasome genes. The sequence of the *RPN4* gene is altered in the majority of resistant strains such that at the amino acid level, leucine 444 is altered to histidine (L444H) (Zaki *et al.* 2014). Other previously published work has demonstrated the presence of mutated alleles of *RPN4* in butanol resistant strains suggesting that the L444H mutation can somehow protect yeast from butanol stress (Gonzalez-Ramos *et al.* 2013).

- vii. Mutations in the *GCD1*, *GCN3* and *GCD6* genes encoding the γ , α and ε respectively of the translation initiation factor eIF2B (Ashe *et al.* 2001; Taylor *et al.* 2010) are associated with increased resistance in *S. cerevisiae* to butanol. In addition, recent and unpublished data from the Ashe lab has identified a specific mutation in the eIF2B δ gene (S131A) which leads to greater resistance to butanol. This work highlights the connection between the regulation of translation initiation and butanol tolerance.

The examples above show how complicated biofuel tolerance can be. Therefore, it is incredibly challenging to predict the implication of modifying a particular gene on butanol production. Furthermore, the degree to which general and other stress conditions alter biofuel production is currently unknown (Dunlop *et al.* 2011). In addition, for many of the examples of butanol tolerance it remains to be seen whether the tolerance leads to higher yields in a butanol production setting.

1.9 Protein synthesis

Butanol and other alcohols (excluding ethanol) target protein synthesis in a process that may form part of a nutrient signalling pathway (Dickinson 1996). Fusel alcohols derive from amino acids where the amine group has been utilised as a source of nitrogen (Lampitt 1919; Dickinson 1996). Therefore, it has been suggested that fusel alcohols signal nitrogen starvation, to impact on a range of physiological processes; for instance, they can induce pseudohyphal growth. So the regulation of protein synthesis described above may form part of this physiological starvation response.

1.9.1 Overview of eukaryotic gene expression and protein synthesis

The conversion of genetic information into protein sequence in eukaryotes relies upon transcription of the DNA sequence of a gene into mRNA in the nucleus followed by translation of the mRNA into protein in the cytoplasm. Transcription is

carried out by RNA polymerases to produce complementary RNA strands called primary transcripts. Transcription starts when transcription initiation factors (e.g. the TATA box binding protein (TBP) and transcription initiation factor IIB (TFIIB)) bind to a region of DNA (usually upstream of the gene) called the promoter to facilitate recruitment of RNA polymerase II (Rowlands *et al.* 1994; Hahn *et al.* 2011). The primary transcript is processed co-transcriptionally: the 5' end of the transcript has an unusual 7-methyl guanosine added called the mRNA cap structure; introns are removed in a process termed splicing and a polyadenylate (polyA) tail is added at the 3' end (Guthrie 1991). The combination of polyA tail addition and the linked process of transcription termination release the mRNA from the transcription machinery (Vinciguerra *et al.* 2004). The mRNA is then exported into the cytoplasm through the nuclear pore complex.

Once in the cytoplasm there is an exchange of nuclear for cytoplasmic RNA binding proteins which effectively select mRNAs for translation into protein. Generally, translation can be divided into three different stages: initiation, elongation and termination. The process is highly conserved and regulated across eukaryotes. The mRNA 5' cap and 3' poly (A) not only protect the mRNA from degradation, but they also facilitate its recognition via translation factors (Hinnebusch 2011). This recruits the ribonucleoprotein machine responsible for the translation of mRNA sequence into protein 'the ribosome'. The ribosome translates mRNAs with the help of adaptor RNA molecules called tRNAs: one end of the tRNA structure base pairs with the mRNA, while the other end is covalently bound to an amino acid (aminoacyl tRNA).

The ribosome consists of two subunits, the small (40S) and large (60S) subunits which are recruited independently to the mRNA during the initiation phase. The ribosome has three tRNA binding sites; A (acceptor), P (peptidyl transferase) and E (exit). Aminoacyl-tRNAs bind at the A site while, peptidyl tRNAs (covalently linked to the growing protein chain) bind at the P site and the exiting tRNAs are released from the E site. The mRNA is decoded by complementary base-pairing between the anticodon on the aminoacyl-tRNA and the codon on the mRNA in the A site of the ribosome. The amino acid located on the tRNA in the A site then forms a peptide bond with the amino acid at the end of the protein chain bound to the tRNA in the P site.

Repeated iterations of this process lead to the decoding of the sequence of an mRNA into a specific polypeptide chain. Translation termination occurs when the ribosome encounters one of three stop codons and involves two eukaryotic release factors, eRF1 and eRF3. The ribosome and protein chain are released from the mRNA and the ribosome can be recycled for further rounds of translation (Ziegler *et al.* 2011).

1.9.2 Translation initiation

Translation initiation is the process that is targeted by alcohols in yeast and it is defined as the assembly of a ribosome on an mRNA AUG codon with the initiator methionyl-tRNA (Met-tRNA_i^{Met}) present in the P-site. This process involves numerous translation initiation factors (eIFs), which are associated with either the Met-tRNA_i^{Met}, the ribosomal subunits or the mRNA. The process is extremely complicated and highly regulated in eukaryotic cells.

The translation initiation factors eIF3 and eIF1A associate with the 40S small ribosomal subunit facilitating its dissociation from the 60S ribosomal subunit. The guanine nucleotide exchange factor eIF2B exchanges the GDP-bound eIF2 from an inactive form into the translationally active GTP-bound form. This guanine nucleotide exchange reaction represents one of the fundamental, conserved and highly-regulated steps in the translation initiation pathway. The GTP bound form of eIF2 mediates bind to the Met-tRNA_i^{Met} to form a ternary complex (Kapp *et al.* 2004). With the aid of eIF1 and eIF5, the ternary complex interacts with the 40S small ribosomal subunit to form the 43S pre-initiation complex (PIC) (Asano *et al.* 2000).

The mRNA is also selected and prepared for translation. The 5' cap and poly (A) tail of the mRNA are recognised by the cap-binding complex (eIF4F) and the poly (A) binding protein (Pab1p in yeast) in the cytoplasm to enable the subsequent association of the mRNA with the ribosome. The cap-binding complex (eIF4F) consists of three initiation factors (eIF4E, eIF4G and eIF4A). eIF4E interacts directly with the 5' cap structure on the mRNA, while eIF4A, which is an ATP-dependent RNA helicase recruits, is thought to remove the secondary structure from 5' end of the mRNA (Svitkin *et al.* 2001). The removal of such secondary structures could either enhance binding of the

ribosome to the mRNA or it could allow easy passage of the mRNA along the 5'UTR. eIF4G serves as a scaffold protein; it binds to eIF4E, eIF4A and Pab1p and can direct the formation of a closed loop complex where the mRNA ends are joined via protein-RNA and protein-protein interactions (Wells *et al.* 1998; Tarun *et al.* 1996). While in higher eukaryotes eIF4G binds to eIF3 to bridge the interaction between the 43S complex and the mRNA to form a 48S complex, in yeast it seems eIF4G contacts eIF1 and eIF5 to achieve the same outcome (LeFebvre *et al.* 2006; Tarun *et al.* 1995). The preinitiation complex then scans along the mRNA 5'UTR in a 5' to 3' direction sampling each possible codon until a start codon (AUG) is recognised via base pairing with the anticodon part of the Met-tRNA_i^{Met}. Recognition of the start codon triggers GTP hydrolysis on eIF2 via the GTPase activating protein eIF5. This hydrolysis leads to global reorganisation of the preinitiation complex; aside from eIF1A most of translation initiation factors from the complex are released including eIF2-GDP bound to eIF5 (Unbehaun *et al.* 2004). With the aid of eIF5B-GTP, the 60S ribosomal subunit joins and when GTP hydrolysis takes place, eIF5B-GDP and eIF1A are released (Unbehaun *et al.* 2004). Thus, a functional 80S ribosome is formed at the AUG with the Met-tRNA_i^{Met} at the ribosomal P site.

Translation initiation in prokaryotes is much less complicated than in eukaryotes and involves smaller ribosomal subunits (30S and 50S) and there are only three initiation factors IF1, IF2 and IF3. The ribosome is recruited to the mRNA directly via the Shine Delgarno sequence, which is generally located around 8 bases upstream of the start codon AUG (Kozak 1999; Simonetti *et al.* 2011; Malys 2012). Following initiation in both prokaryotes and eukaryotes, translation moves to elongation via recruiting the next encoded tRNA to the ribosomal A site.

1.10 Guanine nucleotide exchange factor (eIF2B)

1.10.1 Overview

eIF2B is critical for the recycling of the eIF2-GDP produced after translation initiation is complete to eIF2-GTP, which is required for further rounds of translation initiation. eIF2B is a target for a whole range of stress pathways across eukaryotic

organisms. For instance, in yeast both amino acid starvation and fusel alcohols inhibit eIF2B activity to prevent guanine nucleotide exchange on eIF2 and lead to decreased levels of protein synthesis. In terms of biobutanol production in yeast, this inhibition of eIF2B and protein synthesis has obvious implications for possible production levels.

1.10.2 Role of eIF2B in translation initiation

Translation initiation in eukaryotic cells is highly regulated step and one of the key regulated processes is the eIF2B-dependent guanine nucleotide exchange reaction on eIF2 (Campbell *et al.* 2007). (Fig. 1.7). In the yeast *Saccharomyces cerevisiae*, eIF2B is encoded by the essential genes *GCD1* (eIF2B γ), *GCD2* (eIF2B δ), *GCD6* (eIF2B ϵ), *GCD7* (eIF2B β), and the nonessential gene *GCN3* (eIF2B α) (Hinnebusch *et al.* 2000). The eIF2B subunits form two sub-complexes, a regulatory complex containing eIF2B α , eIF2B β and eIF2B δ and catalytic subunits consists of eIF2B γ and eIF2B ϵ (Pavitt *et al.* 1998). The subunits in the regulatory complex are involved in the recognition of eIF2 α with phosphorylated Serine at position 51 (Pavitt *et al.* 1997). The affinity of eIF2B for this phopsho-eIF2 is 150 fold higher than for the non-phospho eIF2. As a result phopsho-eIF2 acts as a competitive inhibitor of eIF2B activity, because it binds and sequesters eIF2B rather than being released. This leads to a reduction in GTP-bound eIF2 and an accumulation of inactive eIF2-GDP with a consequent decrease in the rate of translation initiation (Rowlands *et al.* 1988). In contrast, the catalytic complex is unable to respond to phosphorylation, as it binds equally to either the phosphorylated or dephosphorylated form of eIF2 (Pavitt *et al.* 1998).

In yeast, there is only one eIF2 α kinase (Gcn2) that phosphorylates eIF2 α as its only substrate. This kinase is activated by stress conditions like amino acid starvation (Dever *et al.* 1992), which leads to the accumulation of non-amino-acylated tRNAs; these can bind and activate Gcn2 (Dong *et al.* 2000). The resulting induction of eIF2 α phosphorylation causes inhibition of eIF2B leading to lower ternary complex levels and reduced rates of translation initiation (Campbell *et al.* 2005). This regulatory system is highly conserved across eukaryotes; for instance, human cells have four eIF2 α kinases

that inhibit translation via the same mechanism but respond to different stimuli (Wang *et al.* 2001; Woods *et al.* 2001).

There are also mechanisms of translational regulation where eIF2B is directly targeted. In mammalian cells, eIF2B ϵ can be phosphorylated at Ser 525 and this modification can inhibit the guanine nucleotide exchange activity (Wang *et al.* 2008). In addition, fusel alcohols and volatile anaesthetics have been shown to target eIF2B in mechanisms that do not rely on the Gcn2p kinase or upon changes in eIF2 α phosphorylation (Ashe *et al.* 2001). Allelic variation in the *GCD1* (eIF2B γ) gene was found to explain differences in the tolerance of two W303-1A lab strains of *S. cerevisiae*, with Ser180 being associated with sensitivity and Pro180 being associated with higher levels of butanol resistance (Ashe *et al.* 2001). Butanol also leads to decreases in the level of ternary complex, which is more severe for the butanol sensitive strain than the resistant strain (Taylor *et al.* 2010). Subsequently, two mutations in *GCN3* (eIF2B α) were also found to give similarly high levels of butanol resistance (Taylor *et al.* 2010).

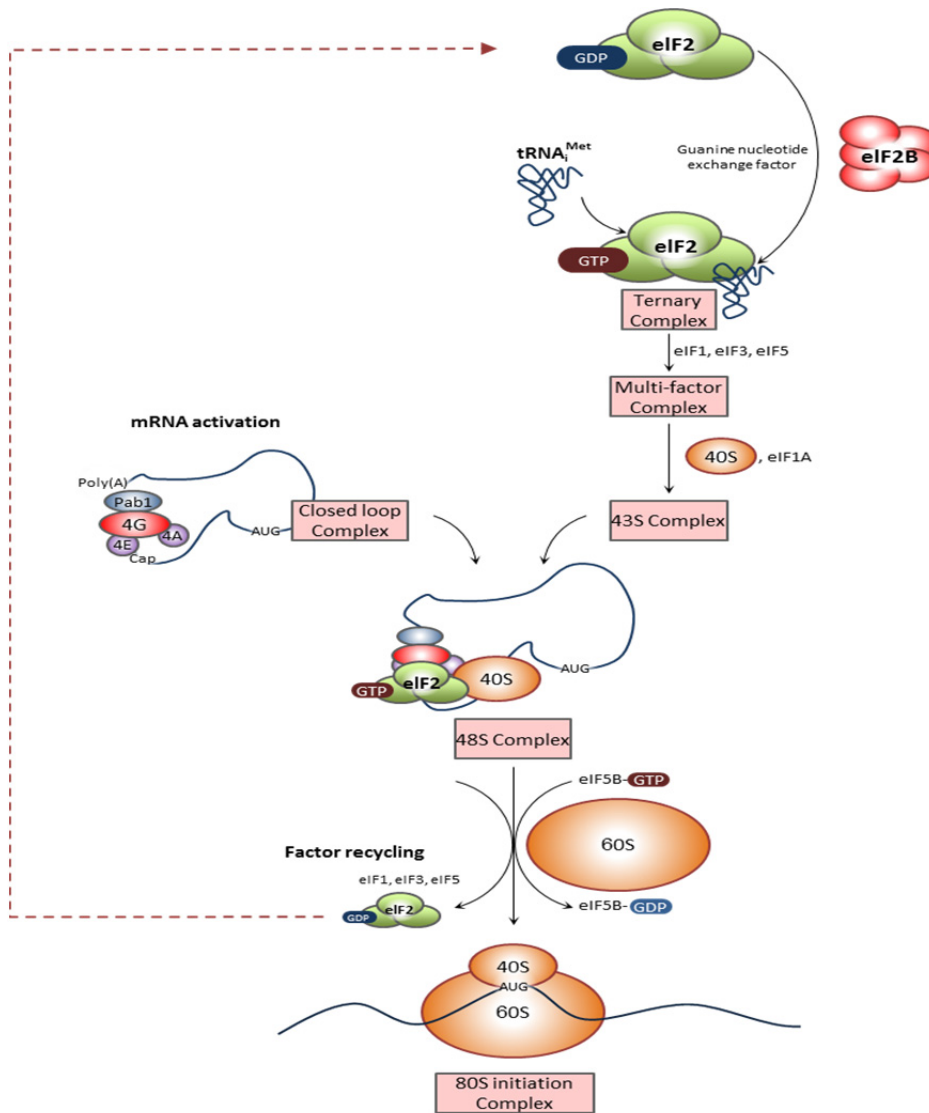


Figure 1.7 Translation initiation pathway in eukaryotic

The guanine nucleotide exchange factor, eIF2B, converts GDP-bound eIF2 into the GTP-bound eIF2. The GTP-bound eIF2 interacts with Met-tRNA_i^{Met} to form the ternary complex. Translation initiation factors eIF1, eIF3 and eIF5 join the ternary complex to form a multi-factor complex (MFC). eIF1A associates with recycled small ribosomal subunit 40S and joins the MFC. With the aid of eIF1 and eIF5, the interaction between 40S with ternary complex is induced to form 43S pre-initiation complex. mRNA selection for translation involves the formation of a closed loop complex. The eIF4F consisting of eIF4E, eIF4G and eIF4A binds to the mRNA cap and interacts with Pab1p bound to the poly A tail. Secondary structure is unwound by eIF4A facilitating interaction and scanning by the 43S preinitiation complex until the start codon is reached. Following AUG recognition, GTP hydrolysis occurs and the resulting eIF2-GDP and other factors (eIF1, eIF3, and eIF5) dissociate. Subsequently, the large 60S ribosomal subunit joins with the aid of eIF5B-GTP and following GTP hydrolysis, eIF5B-GDP and eIF1A are released.

1.10.3 The localisation of eIF2 and eIF2B

As well as being a hub for the control of translation initiation, eIF2B is also localised. GFP-tagging and immunolocalisation studies show that all five subunits of eIF2B localise to a large filament-like cytoplasmic body in *S. cerevisiae* and also in *C. albicans* (Egbe *et al.* 2015; Campbell *et al.* 2005). Furthermore, eIF2 is also co-localised to this body. Similar observations have been made in *Drosophila* where eIF2B filaments can be observed in the egg chamber (Noree *et al.* 2010). These filaments or bodies have been termed '2B bodies'

FRAP analysis (fluorescence recovery after photo bleaching) enables the study of the dynamics of fluorescent components inside living cells. Since photo bleaching of fluorescent proteins like GFP is irreversible but doesn't affect protein activity, the synthesis and movement of newly synthesized fluorescent protein can be studied (White *et al.* 1999). FRAP analysis of eIF2 and eIF2B within the yeast 2B body revealed that eIF2 shuttles rapidly between the foci and the cytoplasm, whereas eIF2B is a resident feature of the structure (Campbell *et al.* 2005).

FRAP analysis also reveals that the rate of recovery of fluorescence for eIF2 correlates precisely with the level of eIF2B-dependent guanine nucleotide exchange activity using mutants and a range of conditions with known alterations to this activity. (Campbell *et al.* 2005). These observations are suggestive that the 2B body represents a site of guanine nucleotide exchange where approximately 40% of the eIF2B in a cell is located (Campbell *et al.* 2005).

1.10.4 Alcohols, eIF2B regulation and the eIF2B body

Another striking observation relating to the 2B body is that the large filament moves rapidly around the cell. Further studies showed that the movement of 2B bodies has two phases: rapid movement within the cytosol and static tethering. Generally, 2B bodies move freely within the cytoplasm; they can transit around the vacuole and can also move into the developing daughter cell to rapidly return to the mother cells (Taylor *et al.* 2010). Intriguingly, fusel alcohols such as butanol have a great influence on the dynamics of the 2B body as they prevent the rapid diffusion of

the 2B body through the cytoplasm. This suggests that fusel alcohols stabilize the tethered form of the 2B body (Taylor *et al.* 2010). Interestingly, the levels of butanol required to inhibit the movement of 2B bodies vary according to the tolerance of the strains used: movement of the 2B body is inhibited at lower concentration in the butanol sensitive *GCD1-S180* than in the butanol resistant *GCD1-P180* strain background (Taylor *et al.* 2010).

1.11 Aims of butanol project

At the outset of this project, a key goal was to determine whether strains that are tolerant to butanol as a result of mutations in the eIF2B genes would actually generate higher levels of butanol than butanol sensitive strains. In order to realise this goal it was necessary generate a strain of yeast that produced substantial levels of butanol. Therefore, the initial goal of the project became the construction and characterisation of strains for the production of butanol.

With this in mind the five genes for butanol production from acetyl-CoA were overexpressed as well as those for the production of acetyl-CoA from acetaldehyde. In addition, competing pathways were deleted, such that in the final analysis, a strain with one gene deleted and seven genes over-expressed was constructed as the 'production strain' for butanol studies.

A secondary goal was to establish optimal conditions for butanol production investigating a variety of different growth parameters including different carbon sources, temperatures, pH, aerobicity and scale.

Finally, it became possible to test the initial theory that increasing butanol tolerance would lead to greater butanol production. This was achieved in two ways: using the original *GCD1-P180/ S180* strains and making a new butanol resistant mutation in the δ subunit of eIF2B.

2. Materials and Methods

2.1 Culture conditions

2.1.1 Yeast strains and growth conditions

All yeast strains used in this project are derived from W303-1A and strain genotypes are listed in Table 2.1. Strains were grown at 30°C on complete Yeast Extract Peptone Dextrose (YPD) media (2% [w/v] Bacto Peptone, 2% [w/v] glucose, 1% [w/v] Yeast extract) or on Synthetic Complete (SCD) media (0.17% [w/v] Yeast nitrogen base, 2% [w/v] glucose, 0.5% [w/v] ammonium sulphate). SCD media was supplemented with 0.02 mg/ml arginine, methionine, 0.06 mg/ml tyrosine, lysine and isoleucine, 0.05 mg/ml phenylalanine, 0.01 mg/ml glutamic acid and aspartic acid, 0.004 mg/ml serine, 0.0015 mg/ml valine and 0.002 mg/ml threonine. Media was also supplemented with 0.2% [w/v] tryptophan, histidine-HCl, adenine sulphate, uracil and 0.6% [w/v] leucine. When selection for a marker or plasmid was required the appropriate amino acid was excluded from the media. When strains were grown on solid media, the media was supplemented with 2% [w/v] agar (Melford).

Strains were induced to sporulate by either growth on sporulation media (1% (w/v) potassium acetate, 0.1% (w/v) Yeast extract and 0.5% (w/v) glucose) or on pre-sporulation media (10% (w/v) glucose, 1% (w/v) yeast extract, 0.5% (w/v) Bacto Peptone).

2.1.2 Bacterial strains and growth conditions

Escherichia coli bacteria (DH5α background strains bearing various plasmids) used in this study were incubated at 37°C in Luri-Bertani (LB) media (1% (w/v) Bacto Tryptone, 0.5% (w/v) Yeast extract, 10 mM sodium chloride). When strains were grown on solid media, LB was supplemented with 2% (v/w) agar.

2.1.3 Antibiotic supplemented to selective media

Antibiotic and drug stock solutions were stored at -20°C and those prepared in sterile distilled water were filter sterilised. Ampicillin (Sigma-Aldrich) was prepared as a 50 mg/ml stock solution and used in media at a concentration of 50 µg/ml. The drug G418 disulphide (Melford) was used at a final concentration of 400 µg/ml to select for strains expressing the *KanMX4* gene. ClonNAT (BioWerner) was used at a final concentration of 100 µg/ml. Phleomycin (Apollo Scientific Ltd) was supplemented into media at a final concentration of 20 µg/ml. Antimycin A (Sigma-Aldrich) was also used at a final concentration of 20 µg/ml. Cycloheximide (Calbiochem) was prepared as a 10 mg/ml stock in Diethylpyrocarbonate (DEPC) treated water and used at a final concentration of 100 µg/ml. Hygromycin B (Invitrogen) was used at a final concentration of 300 µg/ml.

2.2 DNA manipulation and analysis

2.2.1 Isolation of plasmid DNA from bacterial cells

Plasmid DNA was extracted from 5 ml of bacterial culture using a Qiagen Spin® miniprep alkaline lysis kit. Plasmid isolation was done as described by the manufacturer. Bacterial strains and plasmids used in this study are listed in Table 2.2.

2.2.2 Genomic DNA extraction of yeast cells

The genomic DNA extraction protocol was performed as described previously in (Hoffman *et al.* 1987). Yeast cultures were cultivated in 10 ml of YPD media overnight at 30°C with rotation at 180 rpm. Cells were harvested by centrifugation at 2500 rpm for 4 minutes in a Centra Thermo1EC centrifuge (Model CL3R). The cell pellet was washed with 500 µl of sterile distilled water and then re-suspended in 300 µl of genomic extraction solution (2% (v/v) Triton X-100, 1% (w/v) sodium dodecyl sulphate (SDS), 100 mM NaCl, 10 mM Tris-HCl pH 8.0 and 1 mM ethylenediaminetetraacetic acid (EDTA)). An equal volume of phenol: chloroform: isoamyl alcohol (25:24:1) and 200 µl of acid washed beads were added to the samples and vortexed for 45 seconds.

TE buffer (10 mM Tris-HCl pH 8.0, 1 mM EDTA) was added before centrifugation at 13000 rpm for 5 minutes. Samples were re-suspended in 1 ml of 100% ethanol and kept at -20°C for 30 minutes to precipitate DNA. Samples were centrifuged at 1000 rpm for 5 minutes and re-suspended in 400 µl of TE buffer containing 30 µg RNase A (Qiagen). Samples were incubated for 15 minutes at 37°C followed by the addition of 10 µl of 3 M sodium acetate pH5.2 and 1 ml of 100% ethanol. Samples were centrifuged at 1000 rpm for 10 minutes and the DNA pellet was allowed to dry. Finally, the DNA was washed with 70% [v/v] ethanol and re-suspended in 50 µl of sterile distilled water.

2.2.3 DNA amplification by polymerase chain reaction (PCR)

PCR reactions amplifying integration cassettes from the appropriate plasmid templates or genomic DNA were carried out using an Expand high fidelity kit (Roche). While verification of genomic integrations or deletions were carried out using a Taq polymerase kit (Bioline). Oligonucleotides used in this study are listed in Table 2.1.

Integration cassettes were generated by mixing 1 µl of the desired concentration of DNA template with 1X PCR buffer 2 (1.5 mM MgCl₂), 2.5 mM of each dNTP, 3.4 U of DNA Expand enzyme and sterile distilled water to a final volume of 50 µl. 0.2 µM of the appropriate oligonucleotides were added at 95 °C at the initial denaturation step. When the Taq polymerase kit was used, reactions were set up as described above however with 2.5U of Taq DNA polymerase and to a volume of 25 µl. PCR reactions were performed in a Biometra® T3 thermocycler and subjected to the following reaction conditions:

Initial denaturation at 95°C for 3 minutes

Denaturation at 95°C for 15 seconds

Annealing (at the appropriate temperature for the oligonucleotide primers)
for 30 seconds

Extension at 72°C for 30 seconds per kbp of product length

Denaturation, annealing and extension steps were repeated 30 times

Final extension at 72°C for 7 minutes with a final hold at 16°C

The annealing temperature was 5°C below the theoretical melting temperature (T_m) of oligonucleotides used. The T_m was estimated using the formula:

$$T_m = 2 [(A+T) + 2(G+C)]$$

Where A, T, G and C refer to the base composition of the oligonucleotide

2.2.4 Agarose gel electrophoresis

All PCR products were analysed by agarose gel electrophoresis. Samples were run on agarose gels consisting of 1% [w/v] agarose with 5 µg/ml SYBR® safe DNA gel stain (Invitrogen) in 1X TAE buffer (40 mM Tris-base, 1 mM EDTA pH8.0, 20 mM acetic acid). DNA samples were mixed with 5 µl loading dye buffer (25% [w/v] Ficoll, 2.5 µg/ml Orange G (Sigma-Aldrich), and 100 mM EDTA pH8.0). A molecular weight marker (hyperladder I, Bioline) was loaded to estimate the size of PCR products. DNA fragments were visualized using a 365 nm transilluminator (Bio-Rad) and the software Quantity One (Bio-Rad version 4.6).

2.2.5 Restriction digest of PCR product or plasmid DNA

Digestion of plasmid DNA was performed using 5 µg of DNA, 10 U of the appropriate restriction enzyme, 1X of the corresponding buffer, and sterile distilled water up to a final volume of 50 µl. 1X BSA was added to stabilise reactions if required. Reactions were incubated at the optimal temperature in a water bath for the appropriate amount of time. Optimal conditions for restriction enzymes are listed in Table 2.5

2.2.6 Ligation of vector and insert

Ligation reactions contained 1X ligase buffer (Roche), 1 µg of vector, 3µg of insert, 1 U of T4 DNA ligase (Roche) and sterile distilled water up to a final volume in 20 µl. Reactions were incubated for 1 hour at room temperature. Negative controls lacking insert, vector or DNA ligase were also used in each experiment.

2.2.7 Phenol-chloroform DNA purification

An equal volume of phenol-chloroform was added to tubes containing DNA samples and vortexed vigorously. The organic and aqueous phases were separated by centrifugation (Eppendorf, Model 5414D) at 13000 rpm for 10 minutes. The aqueous layer was then transferred to a fresh 1.5 ml microcentrifuge tube. Nucleic acids were precipitated by adding 1 ml of 100% ethanol and 40 µl of 3 M sodium acetate pH5.2 to the aqueous layer, subsequently DNA was pelleted by centrifugation at 13000 rpm for 15 minutes. The pellet was left to air dry and re-suspended in 20 µl of sterile distilled water.

2.2.8 Yeast transformation with PCR product or Plasmid DNA

Yeast strains were transformed using a high efficiency lithium acetate method (Schiestl *et al.* 1989). Yeast cultures were cultivated in 50 ml of YPD media and grown at 30°C to an OD₆₀₀ of 0.8. Cells were harvested by centrifugation at 5000 rpm for 5 minutes in a Centra, Thermo1EC centrifuge (Model CL3R). Pellet was washed in ½ the volume of sterile distilled water and re-suspended in 1 ml of 100 mM lithium acetate. Cells were pelleted at 13000 rpm for 15 seconds in a microcentrifuge and re-suspended in 400 µl of 100 mM Lithium acetate. Samples were then divided into 50 µl aliquots and 350 µl of transformation mixture, composed of 100 mM LiOAc, 38.0% [w/v] PEG and 125ng denatured salmon sperm DNA, was added. Approximately 10 µg of PCR product, 1µg of plasmid DNA or the equivalent volume of water (negative control) was added to the appropriate tubes. Cell suspensions were incubated at 30°C for 1 hour and then subjected to heat shock at 42°C for 40 minutes. Cells transformed with a PCR product were transferred to 3 ml of YPD and left at room temperature overnight. Successfully transformed cells were selected by streaking out onto the appropriate selective solid media and incubated for 2-4 days at 30°C.

2.2.9 Bacterial transformation with plasmid DNA

Plasmid DNA was transformed into XL10-Gold ultracompetent cells (Agilent) and performed as described by the manufacturer's instructions.

2.2.10 Determination of DNA concentration

DNA concentration was determined prior to each experiment using a Nano Drop 8000 Spectrophotometer (Thermo Scientific).

2.3 Protein analysis

2.3.1 Preparation of yeast whole cell extracts using trichloroacetic acid (TCA)

Yeast cultures were grown to an OD₆₀₀ of 1.0 in 10 ml of YPD media and collected by centrifugation at 8000 rpm for 4 minutes in a Centra, Thermo1EC centrifuge (Model CL3R). Cell pellets were re-suspended in 250µl of 20% TCA [v/v] and transferred to 1.5 ml lysis tubes (Sarstedt). Cells were pelleted by centrifugation at 16000 rpm for 5 minutes, TCA was aspirated off and pellets were frozen at -80°C. All subsequent steps were performed on ice unless noted otherwise. Samples were thawed and re-suspended in 250 µl of 20% [v/v] TCA. An equal volume of acid-washed glass beads (Sigma Aldrich) were added and cells were homogenised using a FastPrep®-24 instrument (MP Biomedical) for 20 seconds at 6.5 m/s speed, 3 times with 1 minute intervals on ice. The suspension was collected by piercing the bottom of the lysis tubes using a hot 22G needle, placing on top of a 1.5 ml microcentrifuge tube and subjecting to centrifugation at 6000 rpm at 4°C for 2 minutes. Beads were washed in 300µl of 5% TCA and collected as described above in the same tube as initial suspension. 700 µl of 5% [v/v] TCA was added to samples to make up to a final volume of 1.25 ml and were centrifuged at 14000 rpm at 4°C for 10 minutes. Pellet was washed with ½ the volume of 100% chilled ethanol and then finally re-suspended in 40 µl of 1 M Tris-HCl pH8.0. Samples were clarified by centrifugation at 14000 rpm for 5 minutes and supernatant transferred into a fresh 1.5 ml microcentrifuge tube.

2.3.2 SDS-Polyacrylamide gel electrophoresis (PAGE)

An equal volume of 2X SDS loading buffer (10% [v/v] glycerol, 3% [v/w] SDS, 5% [v/v] β -Mercaptoethanol, 62.5 mM Tris-HCl pH6.8, Bromophenol blue) was added to protein samples and boiled at 95°C for 5 minutes to denature proteins. Electrophoresis was performed on 10% polyacrylamide gels as previously described (Laemmli 1970), using the XCell SureLock® gel apparatus by Invitrogen. In general, a 4% stacking gel (4% [v/v] bisacrylamide/acrylamide, 125 mM Tris-HCl pH6.8, 0.1% [w/v] SDS) and a 10% bis-tris polyacrylamide resolving gel (10% [v/v] bisacrylamide/acrylamide (Sigma-Aldrich), 364 mM Tris-HCl pH8.8, 0.1% (w/v) SDS) was used. Polymerisation was promoted by adding 2.2 μ l/ml Tetramethylethylenediamine (TEMED, Sigma) and 0.06% (w/v) ammonium persulfate (APS) to gel solutions immediately before pouring.

Protein samples were loaded carefully and run at 150 V for 2.5 hour, or until the bromophenol blue dye reached the bottom of the gel, in 1X protein running buffer (0.19 M glycine, 1% [w/v] SDS, 25 mM Tris base). Protein markers (GH healthcare) were used to assess protein band sizes.

2.3.3 Western Blot Analysis

The SDS-PAGE resolving gel was removed from the cassette and rinsed in transfer buffer (20% [v/v] methanol, 192 mM glycine, 25 mM Tris base, 0.1% [w/v] SDS). Proteins were transferred onto a Hybond-ECL nitrocellulose membrane (Amersham) using an Xcell II™ blot module (Invitrogen) and carried out as described by the manufacturer. Transfer was performed at 30 V for 2 hours at room temperature. The membrane was removed and protein bands were visualized by staining in ponceau S solution (0.1% [w/v] Ponceau red in 1% acetic acid) for one minute. The membrane was then immersed in 1X PBS-Tween (137 mM sodium chloride, 2.7 mM potassium chloride, 10 mM sodium phosphate buffer pH7.4, 0.1% [v/v] Tween20) supplemented with 5% [w/v] skimmed milk, at 4°C on a rocking platform overnight. The required primary antibody was diluted to the desired concentration in 1X PBS-Tween 5% milk solution and applied to the membrane for 1 hour on a rocking platform at room temperature. The membrane was washed 3 times for 10 minutes in 1X PBS-Tween. An

appropriate secondary antibody was diluted in 1X PBS-Tween 5% milk solution and added to the membrane for 1 hour on rotation at room temperature. Dilutions of primary and secondary antibodies are specified in table 2.4.

Equal volumes of ECL reagents (GE Healthcare) were added directly to the membrane and then covered with saran wrap before exposure to x-ray film (Kodak). Film was developed using an x-ray film developer (Kodak BioMax MR Film).

2.3.4 Coomassie staining of protein gels

SDS-PAGE resolving gel was removed from the gel system and soaked in SimplyBlue safe stain (Invitrogen) for 1 hour and then washed in water.

2.4 Strain construction

2.4.1 Cross-mating yeast strains

MATa and *MATα* yeast strains were mated by inoculating a single colony from each strain into 5 ml of YPD and incubated overnight at 30°C. 1 ml of culture was centrifuged at 4000 rpm for 3 minutes (Eppendorf, Model 5414D), washed twice with sterile distilled water and then re-suspended in a final volume of 1 ml sterile distilled water. 50 µl was plated onto appropriate solid selective media for diploid cells and incubated overnight at 30°C.

2.4.2 Tetrad dissection

Diploid cells were sporulated using either solid or liquid sporulation media. Cells induced to sporulate on solid media cells were streaked onto sporulation plates and incubated at 30° C for 5 days. Whereas cells induced to sporulate in liquid media were initially streaked out onto pre-sporulation solid media and incubated at 30° C for 24 hours. Then cells from one colony were re-suspended in 2 ml of liquid sporulation media, with the appropriate auxotrophic amino acids at 0.2% [w/v]. Cells were

incubated at 25°C for five days, followed by incubation at 30°C for three days on rotation.

Cells from colonies grown either on solid sporulation media or 2 ml of cell grown in liquid sporulation media were re-suspended in 50 µl of tetrad dissection mix (1 M sorbitol, 1 mg/ml lyticase (Sigma-Aldrich)). Cell suspensions were incubated at 37°C for 10 minutes in a water bath, then 800 µl of sterile distilled water was added gently and mixed by inversion. 12 µl of cell suspension was added to a well on solid YPD media and allowed to dry. Tetrad dissection was performed using a Singer MSM System microscope to achieve haploidy (Guthrie and Fink, 1991). Dissected tetrads were incubated at 30°C for 2 days. Plates were replica plated using velveteen cloths onto appropriate selection media and assayed for their mating type. Desired homologous recombination was assessed by appropriate growth phenotype on selection media and genotype was verified by PCR as described above.

2.4.3 Mating type assay

Yeast mating type was assayed using two different tester strains; yMK50 (α tester) and yMK51 (a tester) (Guthrie and Fink, 1991). Tester strains were grown in liquid YPD media to logarithmic phase at 30°C. 150 µl of cells were spread onto YPD plates and allowed to dry. Tested strains were replica plated onto these plates and incubated at 30°C overnight. *MAT α* strains generate a small halo by inhibiting the growth of yMK51 on a tester plate. In contrast, *MAT a* strains generate a large halo by inhibiting the growth of yMK50 on tester plates. Growth of diploid cells are not inhibited by either tester strains and therefore do not generate a halo on either plate.

2.5 Gene integration, deletion and mutation

2.5.1 Single gene integration strategy

In order to introduce any of the *hbd*, *adhe2*, *crt*, *ccr* and *ERG10* genes into the W303-1A laboratory strain, integration cassettes harbouring; a *TDH3* promoter, the desired gene, FLAG tag, a *CYC1* terminator and an auxotrophic marker were generated.

Specific integration oligonucleotides, which are 20 bps homologous to either side of the integration cassette and 70-100 bps homologous to sites flanking the insertion locus in the yeast genome, were used to amplify out the cassette from plasmids detailed in Table 2.2. Successful recombination of the cassettes were selected by growth phenotype on appropriate selective media and subsequently verified by PCR using verification primers. A series of three different PCR reactions were performed to evaluate whether integration had occurred in the correct locus. The first PCR reaction establishes the upstream integration boundary, the second establishes the downstream boundary and the third spans the whole target gene locus. Oligonucleotides used in this method are listed in Table 2.3.

2.5.2 *ALD6*, *ACS2* and *ALD2*, *ACS2* integration strategy

In order to integrate *ALD6* and *ASC2* or *ALD2* and *ACS2* genes together, plasmids bearing a *TDH3* promoter, *ALD6* or *ALD2*, a FLAG tag and a *CYC1* terminator followed by a *TEF1* promoter, *ACS2*, a FLAG tag and *ADH1* terminator were used (see Table 2.2). A hygromycin resistance gene marker was located just downstream of the dual gene cassette and 200 bp flanking regions homologous to the *TRP1* locus were placed on either side of the whole cassette to direct integration via homologous recombination. *BspQI* type IIS restriction sites were placed outside the cassette such that their cleavage site would generate a cassette without leaving any unwanted linker sequences. The successful integration of the dual gene cassette was selected by growth phenotype on the appropriate selection media and verified by PCR using a similar strategy as described in section 2.5.1.

2.5.3 Gene deletion strategy

For deletion of particular genes, a strategy was devised whereby the corresponding gene was replaced with a marker cassette. In this study *ADH1* was replaced by *ADE2*, while *GPD1* or *GPD2* were replaced by the nourseothricin resistance gene *natNT2*. An *ADE2* gene cassette was amplified out of either the pBEVYGA vector

or directly from the genome. Whereas the *natNT2* gene, flanked by two loxP sites, was amplified out of the pZC2 vector (Carter and Delneri. 2010).

Oligonucleotides designed to amplify the deletion cassettes comprised of 60-70 bps homologous to flanking regions upstream and downstream of the target gene open reading frame and 20 bps homologous to either side of the *ADE2* or *natNT2* gene. Therefore the resulting deletion cassette could replace the target gene via homologous recombination. Successful deletion of the target gene was selected by growth phenotype on appropriate selection media and subsequently verified by PCR analysis using a similar strategy as described in section 2.5.1.

2.5.4 Site directed mutagenesis at a genomic locus

Site directed mutagenesis was performed in two steps similar to what has previously been described in (Storici *et al.* 2001). The first step involves insertion of the *natNT2* gene upstream of the gene of interest using primers bearing 80 bps homologous to flanking regions of the integration site located upstream of *GCD2* and 20 bps homologous to either side of the *natNT2* gene. Successful integration of the *natNT2* gene was selected on YPD solid media supplemented with the drug clonNAT and confirmed using a verification PCR strategy.

The second step was performed by generating a mutagenic cassette using specific oligonucleotides homologous to either side of the *natNT2-GCD2* gene generated in the previous step. However, the reverse oligonucleotide contains point mutations that would convert serine 131 to either alanine (*GCD2 S131A*) and generated a *Bss*HII restriction site or aspartic acid (*GCD2 S131D*) and generate a *Bam*HI restriction site. The resulting cassettes were transformed directly into *B^R adh1Δ ALD6 ACS2 +5g* strain and successful integration of the mutagenic cassette was selected by growth phenotype on YPD solid media supplemented with the drug clonNAT. To verify the incorporation of the point mutations, a PCR product was generated which included a small fragment of the *natNT2* gene and 150 bps downstream of the point mutation. The resulting PCR product was then digested by *Bss*HII and *Bam*HI to confirm whether alanine or aspartic acid mutation was incorporated into the genome, respectively.

2.5.5 Excision of *NATnt2* from the genome

Yeast cells bearing the nourseothricin resistance gene *natNT2* flanked by two loxP site were transformed with 0.25–0.5 µg of pSH-*ble* plasmid, using the high efficiency protocol as described in section 2.2.8. The pSH-*ble* plasmid carries a *cre*-recombinase gene under the control of a *GAL1* promoter and phleomycin marker. Strain bearing the pSH-*ble* plasmid were initially grown overnight in 10 ml of YP liquid media supplemented with 2% (w/v) raffinose. Expression of the *cre* recombinase was induced by growth in YP liquid media supplemented with 2% (w/v) galactose. Cells were grown to exponential phase before being plated on YPD solid media. Cells were incubated for 2 days at 30°C, single colonies were selected and re-streaked onto fresh YPD solid media. Successful deletion of the *natNT2* gene was identified by growth phenotype on YPD solid media and YPD solid media supplemented with the drug ClonNAT. The genotype was subsequently verified by PCR analysis using a strategy similar to that described in section 2.5.1.

2.6 Sucrose density gradient analysis

2.6.1 Extract preparation

Yeast strains were cultivated in 100 ml of YPD to an OD₆₀₀ of 0.6 at 30°C and divided into 50 ml aliquots. An appropriate concentration of butanol was added to cultures [v/v] and then incubated at 30°C for 10 minutes. Cultures were transferred into pre-chilled tubes containing 500 µl of 10 mg/ml cycloheximide (Calbiochem) and incubated on ice for 1 hour. Cells were pelleted by centrifugation at 5000 rpm for 5 minutes at 4°C. All subsequent steps were carried out at 4°C. Cell pellets were re-suspended in 25 ml of cold lysis buffer (20 mM HEPES pH7.4, 2 mM magnesium acetate, 100 mM potassium acetate, 100 µg/ml cycloheximide, 0.5 mM DTT). Samples were subjected to centrifugation at 5000 rpm for 5 minutes and re-suspended in 800 µl of lysis buffer. Cells were pelleted by centrifugation at 13000 rpm for 15 seconds (Eppendorf, Model 5414D) and re-suspended in a final volume of 200 µl of lysis buffer. Cells were lysed with 200 µl of pre-chilled mini glass beads (Sigma-Aldrich) and

vortexed for 20 seconds 6 times with a cooling interval of 40 seconds in iced water. Samples were centrifuged at 10000 rpm for 5 minutes and the supernatant was transferred into fresh 1.5 ml microcentrifuge tubes. Extracts were purified again by centrifugation at 10000 rpm for 15 minutes and the final lysate was transferred into fresh 1.5 ml microcentrifuge tubes. Samples were stored at -80°C to prevent degradation prior to use.

2.6.2 Preparation of sucrose density gradients

Sucrose solutions ranging between 15-50% were prepared from a 60% DEPC treated sucrose stock solution and 10x polysome buffer (100 mM Tris acetate pH7.4, 700 mM ammonium acetate, 40 mM magnesium acetate) as detailed in the table below. Solutions were carefully dispensed into SW41 polyallomer centrifuge tubes (Beckman Coulter) in 2.25 ml aliquots, 50% sucrose was added first and ending with 15% to generate a gradient. Layers were frozen immediately in liquid nitrogen before added the subsequent layer. Gradients were stored at -80°C and defrosted overnight at 4°C prior to use.

Sucrose solutions for gradient preparation

	50%	42%	33%	24%	15%
10X Polysome buffer (ml)	11.25	11.25	11.25	11.25	11.25
60% Sucrose solution (ml)	93.75	78.75	62.5	45	28.125
DEPC water (ml)	7.5	22.5	38.75	56.25	73.127

2.6.3 Sedimentation of extracts in polysome gradients

Extract concentration was determined using a NanoDrop 8000 Spectrophotometer (Thermo Scientific) and 2.5 A₂₆₀ units of extract were layered on top of the tube containing the sucrose gradient. Samples were subjected to centrifugation at 4000 rpm for 2.5 hours in a SW41 rotor (Beckman). The gradients

were then pumped through a flow-through UV spectrophotometer (OSCO, Model UA-6) using a peristaltic pump (ISCO) and the absorbance at 245 nm was continuously measured.

2.7 Alcoholic fermentation analysis

2.7.1 Measurements of butanol and ethanol and standard operating procedure

Batch cultures used for butanol and ethanol production were carried out in semi-anaerobic conditions. 45ml of fresh YPD media was aliquoted into semi-anaerobic fermentation vials and then were sealed with rubber stoppers and aluminium crimps (Supelco). Vials were autoclaved at 100°C for 120 min. Pre-culture were prepared by inoculating some colonies in 5ml of YPD media. These inocula were grown at 30°C at 180 rpm agitation for 3 days. Strains were inoculated from pre-cultures into the 45mls of sterile YPD media contained in the semi-anaerobic fermentation vials, to a starting OD₆₀₀ of 0.1. Strains were then grown over a 21 day period at 30°C in a static incubator. On days; 0, 4, 7, 9, 11, 13, 15, 17, and 21, 3ml samples were taken regularly using a 5ml syringe needle. 1ml of the extracted sample was used to measure the OD₆₀₀ using a spectrophotometer (Eppendorf Bio photometer plus). The remaining 2ml of sample was passed through a 0.22µm filter (Millex®-GP) into gas chromatography (GC) vials and analysed using an Agilent 6850A GC system with an Agilent 4513A automatic injector, sampler and controller (Agilent technologies Ltd, Stockport, UK). A J&W DB-WAX capillary column (30m× 0.25mm, 0.25µM, Agilent technologies Ltd) was used for chemical separation. Samples were quantified relative to standards of ethanol and butanol: the first standard contained 1% (v/v) ethanol, 100ppm (v/v) iso-butanol and 100ppm (v/v) butanol, while the second standard contained 0.1% (v/v) ethanol, 500ppm (v/v) iso-butanol and 100ppm (v/v) butanol. The significant difference between the mean of butanol production/OD₆₀₀ was analysed based on student t-test. Significant difference was considered when $p < 0.05$.

2.7.2 Glucose Measurements

Glucose concentration was measured using a glucose (GO) assay kit, (Sigma-Aldrich). The method used was as described by the manufacture.

Samples were collected regularly from alcoholic fermentation experiment on the days mentioned previously in section 2.7.1. Samples were passed through a 0.22 μm filter (Millex®-GP) and diluted with sterile distilled water to approximately 20-80 μg glucose/ml.

Table 2.1 Yeast strain used in this study

Strain	Abbreviation	Genotype	Source
yMK24	WT (B ^R)	<i>MATα GCD1-P180, ade2-1, his3-11,15, leu2-3,112, trp1-1, ura3-1</i>	Ashe strain collection
yMK36	WT (B ^S)	<i>MATα GCD1-S180, ade2-1, his3-11,15, leu2-3,112, trp1-1, ura3-1</i>	Ashe strain collection
yMK37	WT (B ^S)	<i>MATα GCD1-S180, ade2-1, his3-11,15, leu2-3,112, trp1-1, ura3-1</i>	Ashe strain collection
yMK50	yMK50	<i>MATα sst1</i>	Ashe strain collection
yMK51	yMK51	<i>MATα sst2</i>	Ashe strain collection
yMK1865	B ^S + <i>adhe2</i>	<i>MATα GCD1-S180, ade2-1, his3-11,15, leu2-3,112, trp1-1, ura3-1::TDH3p-adhe2-Flag2-CYC1t-URA3</i>	This study
yMK1866	B ^S + <i>hbd</i>	<i>MATα GCD1-S180, ade2-1, his3-11,15, leu2-3,112, trp1-1, ura3-1::TDH3p-hbd-Flag2-CYC1t-LEU2</i>	This study
yMK1874	B ^S + <i>ERG10</i>	<i>MATα GCD1-S180, ade2-1, his3-11,15, leu2-3,112, trp1-1, ura3-1::TDH3p-ERG10-Flag2-CYC1t- KanMX4</i>	This study
yMK1876	B ^S + <i>hbd, adhe2</i>	<i>GCD1-S180, ade2-1, his3-11,15, leu2-3,112, trp1-1, ura3-1::TDH3p-hbd-Flag2- LEU2-CYC1t, TDH3p-adhe2-Flag2-URA3-CYC1t</i>	This study
yMK1896	B ^R + <i>ccr</i>	<i>MATα GCD1-P180, ade2-1, his3-11,15, leu2-3,112, trp1-1, ura3-1::TDH3p-ccr-Flag2-CYC1t-HIS3</i>	This study
yMK1897	B ^R + <i>crt</i>	<i>MATα GCD1-P180, ade2-1, his3-11,15, leu2-3,112, trp1-1, ura3-1:: TDH3p-crt-Flag2-CYC1t-TRP1</i>	This study
yMK1898	B ^S + <i>hbd, adhe2, ERG10</i>	<i>MATα GCD1-S180, ade2-1, his3-11,15, leu2-3,112, trp1-1, ura3-1::TDH3p-hbd-Flag2-CYC1t-LEU2, TDH3p-adhe2-Flag2-CYC1t-URA3, TDH3p-ERG10-Flag2 -CYC1t-KanMX4</i>	This study
yMK2069	B ^R + <i>crt, ccr</i>	<i>MATα GCD1-P180, ade2-1, his3-11,15, leu2-3,112, trp1-1, ura3-1::TDH3p-crt-Flag2-CYC1t-TRP1, TDH3p-ccr-Flag2-CYC1t-HIS3</i>	This study
yMK2070	B ^R + <i>crt, ccr</i>	<i>MATα GCD1-P180, ade2-1, his3-11,15, leu2-3,112, trp1-1, ura3-1:: TDH3p-crt-Flag2-CYC1t-TRP1, TDH3p-ccr-Flag2-CYC1t-HIS3</i>	This study
yMK2071	B + <i>hbd, adhe2, ERG10, crt, ccr</i>	<i>ade2-1, his3-11,15, leu2-3,112, trp1-1, ura3-1,::TDH3p-hbd-Flag2-CYC1t-LEU2, TDH3p-adhe2-Flag2-CYC1t-URA3, TDH3p-ERG10-Flag2-CYC1t-KanMX4, TDH3p-crt-Flag2-CYC1t-TRP1, TDH3p-ccr-Flag2 -CYC1t-HIS3</i>	This study
yMK2074	B ^S +5g	<i>MATα GCD1-S180, ade2-1, his3-11,15, leu2-3,112, trp1-1, ura3-1::TDH3p-hbd-Flag2-CYC1t-LEU2, TDH3p-adhe2-Flag2-CYC1t-URA3, TDH3p-ERG10-Flag2-CYC1t-KanMX4, TDH3p-crt-Flag2 -CYC1t-TRP1, TDH3p-ccr-Flag2-CYC1t-HIS3</i>	This study
yMK2077	B ^R +5g	<i>MATα GCD1-P180, ade2-1, his3-11,15, leu2-3,112, trp1-1, ura3-1::TDH3p-hbd-Flag2-CYC1t-LEU2, TDH3p-adhe2-Flag2-CYC1t-URA3, TDH3p-ERG10-Flag2-CYC1t-KanMX4, TDH3p-crt-Flag2-CYC1t-TRP1, TDH3p-ccr-Flag2-CYC1t-HIS3</i>	This study

yMK2226	B ^R <i>adh1Δ</i> +5g	MATα GCD1-P180, <i>ade2-1</i> , <i>his3-11,15</i> , <i>leu2-3,112</i> , <i>trp1-1</i> , <i>ura3-1::TDH3p-hbd-Flag2-CYC1t-LEU2</i> , <i>TDH3p-adhe2-Flag2-CYC1t-URA3</i> , <i>TDH3p-ERG10-Flag2-CYC1t-KanMX4</i> , <i>TDH3p-crt-Flag2-CYC1t-TRP1</i> , <i>TDH3p-ccr-Flag2-CYC1t-HIS3</i> , <i>adh1Δ::ADE2</i>	This study
yMK2227	B ^R <i>adh1Δ</i> ALD6 ACS2 +5g	MATα GCD1-P180, <i>ade2-1</i> , <i>his3-11,15</i> , <i>leu2-3,112</i> , <i>trp1-1</i> , <i>ura3-1::TDH3p-hbd-Flag2-CYC1t-LEU2</i> , <i>TDH3p-adhe2-Flag2-CYC1t-URA3</i> , <i>TDH3p-ERG10-Flag2-CYC1t-KanMX4</i> , <i>TDH3p-crt-Flag2-CYC1t-TRP1</i> , <i>TDH3p-ccr-Flag2-CYC1t-HIS3</i> , <i>adh1Δ::ADE2</i> , <i>TDH3p-ALD6-Flag2-CYC1t-TEF1p-ACS2-Flag2 ADH1t-hph</i> , <i>adh1Δ::ADE2</i>	This study
yMK2228	B ^S <i>adh1Δ</i> +5g	MATα GCD1-S180, <i>ade2-1</i> , <i>his3-11,15</i> , <i>leu2-3,112</i> , <i>trp1-1</i> , <i>ura3-1::TDH3p-hbd-Flag2-CYC1t-LEU2</i> , <i>TDH3p-adhe2-Flag2-CYC1t-URA3</i> , <i>TDH3p-ERG10-Flag2-CYC1t-KanMX4</i> , <i>TDH3p-crt-Flag2-CYC1t-TRP1</i> , <i>TDH3p-ccr-Flag2-CYC1t-HIS3</i> , <i>adh1Δ::ADE2</i>	This study
yMK2232	B ^S ALD6 ACS2+5g	MATα GCD1-S180, <i>ade2-1</i> , <i>his3-11,15</i> , <i>leu2-3,112</i> , <i>trp1-1</i> , <i>ura3-1::TDH3p-hbd-Flag2-CYC1t-LEU2</i> , <i>TDH3p-adhe2-Flag2-CYC1t-URA3</i> , <i>TDH3p-ERG10-Flag2-CYC1t-KanMX4</i> , <i>TDH3p-crt-Flag2-CYC1t-TRP1</i> , <i>TDH3p-ccr-Flag2-CYC1t-HIS3</i> , <i>adh1Δ::ADE2</i> , <i>TDH3p-ALD6-Flag2-CYC1t-TEF1p-ACS2-Flag2-ADH1t-hph</i>	This study
yMK2234	B ^R + ALD6 ACS2	MATα GCD1-P180, <i>ade2-1</i> , <i>his3-11,15</i> , <i>leu2-3,112</i> , <i>trp1-1</i> , <i>ura3-1::TDH3p-ALD6-Flag2-CYC1t-TEF1p-ACS2-Flag2-ADH1t-hph</i>	This study
yMK2237	B ^S <i>adh1Δ</i> ALD6 ACS2+5g	MATα GCD1-S180, <i>ade2-1</i> , <i>his3-11,15</i> , <i>leu2-3,112</i> , <i>trp1-1</i> , <i>ura3-1::TDH3p-hbd-Flag2-CYC1t-LEU2</i> , <i>TDH3p-adhe2-Flag2-CYC1t-URA3</i> , <i>TDH3p-ERG10-Flag2-CYC1t-KanMX4</i> , <i>TDH3p-crt-Flag2-CYC1t-TRP1</i> , <i>TDH3p-ccr-Flag2-CYC1t-HIS3</i> , <i>adh1Δ::ADE2</i> , <i>TDH3p-ALD6-Flag2-CYC1t-TEF1p-ACS2-Flag2-ADH1t-hph</i> , <i>adh1Δ::ADE2</i>	This study
yMK2300	B ^R <i>loxp-natNT2-loxp::GCD2</i>	MATα GCD1-P180, <i>ade2-1</i> , <i>his3-11,15</i> , <i>leu2-3,112</i> , <i>trp1-1</i> , <i>ura3-1, loxp-natNT2-loxp::GCD2(S131)</i>	This study
yMK2301	B ^R <i>adh1Δ</i> ALD6 ACS2 +5g, <i>loxp-natNT2-loxp::GCD2 S131</i>	MATα GCD1-P180, <i>ade2-1</i> , <i>his3-11,15</i> , <i>leu2-3,112</i> , <i>trp1-1</i> , <i>ura3-1::TDH3p-hbd-Flag2-CYC1t-LEU2</i> , <i>TDH3p-adhe2-Flag2-CYC1t-URA3</i> , <i>TDH3p-ERG10-Flag2-CYC1t-KanMX4</i> , <i>TDH3p-crt-Flag2-CYC1t-TRP1</i> , <i>TDH3p-ccr-Flag2-CYC1t-HIS3</i> , <i>adh1Δ::ADE2</i> , <i>TDH3p-ALD6-Flag2-CYC1t-TEF1p-ACS2-Flag2 ADH1t-hph</i> , <i>adh1Δ::ADE2</i> , <i>loxp-natNT2-loxp::GCD2(S131)</i>	This study
yMK2302	B ^R <i>adh1Δ</i> ALD6 ACS2 +5g, <i>loxp-natNT2-loxp::GCD2 S131A</i>	MATα GCD1-P180, <i>ade2-1</i> , <i>his3-11,15</i> , <i>leu2-3,112</i> , <i>trp1-1</i> , <i>ura3-1::TDH3p-hbd-Flag2-CYC1t-LEU2</i> , <i>TDH3p-adhe2-Flag2-CYC1t-URA3</i> , <i>TDH3p-ERG10-Flag2-CYC1t-KanMX4</i> , <i>TDH3p-crt-Flag2-CYC1t-TRP1</i> , <i>TDH3p-ccr-Flag2-CYC1t-HIS3</i> , <i>adh1Δ::ADE2</i> , <i>TDH3p-ALD6-Flag2-CYC1t-TEF1p-ACS2-Flag2 ADH1t-hph</i> , <i>adh1Δ::ADE2</i> , <i>loxp-natNT2-loxp::GCD2(S131A)</i>	This study
yMK2304	B ^R <i>adh1Δ</i> ALD6 ACS2 +5g, <i>loxp-natNT2-loxp::GCD2 S131D</i>	MATα GCD1-P180, <i>ade2-1</i> , <i>his3-11,15</i> , <i>leu2-3,112</i> , <i>trp1-1</i> , <i>ura3-1::TDH3p-hbd-Flag2-CYC1t-LEU2</i> , <i>TDH3p-adhe2-Flag2-CYC1t-URA3</i> , <i>TDH3p-ERG10-Flag2-CYC1t-KanMX4</i> , <i>TDH3p-crt-Flag2-CYC1t-TRP1</i> , <i>TDH3p-ccr-Flag2-CYC1t-HIS3</i> , <i>adh1Δ::ADE2</i> , <i>TDH3p-ALD6-Flag2-CYC1t-TEF1p-ACS2-Flag2 ADH1t-hph</i> , <i>adh1Δ::ADE2</i> , <i>loxp-natNT2-loxp::GCD2(S131D)</i>	This study

yMK2307	B ^R <i>adh1Δ</i> ALD2 ACS2+5g	MATα GCD1-P180, <i>ade2-1</i> , <i>his3-11,15</i> , <i>leu2-3,112</i> , <i>trp1-1</i> , <i>ura3-1::TDH3p-hbd-Flag2-CYC1t-LEU2</i> , <i>TDH3p-adhe2-Flag2-CYC1t-URA3</i> , <i>TDH3p-ERG10-Flag2-CYC1t-KanMX4</i> , <i>TDH3p-crt-Flag2-CYC1t-TRP1</i> , <i>TDH3p-ccr-Flag2-CYC1t-HIS3</i> , <i>adh1Δ::ADE2</i> , <i>TDH3p-ALD2-Flag2-CYC1t-TEF1p-ACS2-Flag2</i> ADH1t-hph, <i>adh1Δ::ADE2</i>	This study
yMK2308	B ^S <i>adh1Δ</i> ALD2 ACS2+5g	MATα GCD1-P180, <i>ade2-1</i> , <i>his3-11,15</i> , <i>leu2-3,112</i> , <i>trp1-1</i> , <i>ura3-1::TDH3p-hbd-Flag2-CYC1t-LEU2</i> , <i>TDH3p-adhe2-Flag2-CYC1t-URA3</i> , <i>TDH3p-ERG10-Flag2-CYC1t-KanMX4</i> , <i>TDH3p-crt-Flag2-CYC1t-TRP1</i> , <i>TDH3p-ccr-Flag2-CYC1t-HIS3</i> , <i>adh1Δ::ADE2</i> , <i>TDH3p-ALD2-Flag2-CYC1t-TEF1p-ACS2-Flag2</i> ADH1t-hph, <i>adh1Δ::ADE2</i>	This study
yMK2328	B ^R <i>adh1Δ</i> ALD6 ACS2 +5g, <i>loxp::GCD2</i> <i>S131D</i>	MATα GCD1-P180, <i>ade2-1</i> , <i>his3-11,15</i> , <i>leu2-3,112</i> , <i>trp1-1</i> , <i>ura3-1::TDH3p-hbd-Flag2-CYC1t-LEU2</i> , <i>TDH3p-adhe2-Flag2-CYC1t-URA3</i> , <i>TDH3p-ERG10-Flag2-CYC1t-KanMX4</i> , <i>TDH3p-crt-Flag2-CYC1t-TRP1</i> , <i>TDH3p-ccr-Flag2-CYC1t-HIS3</i> , <i>adh1Δ::ADE2</i> , <i>TDH3p-ALD6-Flag2-CYC1t-TEF1p-ACS2-Flag2</i> ADH1t-hph, <i>adh1Δ::ADE2</i> , <i>loxp::GCD2(S131D)</i>	This study
yMK2432	BR <i>adh1Δ</i> ALD6 ACS2 +5g, <i>loxp::GCD2</i> <i>S131</i>	MATα GCD1-P180, <i>ade2-1</i> , <i>his3-11,15</i> , <i>leu2-3,112</i> , <i>trp1-1</i> , <i>ura3-1::TDH3p-hbd-Flag2-CYC1t-LEU2</i> , <i>TDH3p-adhe2-Flag2-CYC1t-URA3</i> , <i>TDH3p-ERG10-Flag2-CYC1t-KanMX4</i> , <i>TDH3p-crt-Flag2-CYC1t-TRP1</i> , <i>TDH3p-ccr-Flag2-CYC1t-HIS3</i> , <i>adh1Δ::ADE2</i> , <i>TDH3p-ALD6-Flag2-CYC1t-TEF1p-ACS2-Flag2</i> ADH1t-hph, <i>adh1Δ::ADE2</i> , <i>loxp::GCD2(S131)</i>	This study
yMK2435	BR <i>adh1Δ</i> ALD6 ACS2 +5g, <i>loxp::GCD2</i> <i>S131A</i>	MATα GCD1-P180, <i>ade2-1</i> , <i>his3-11,15</i> , <i>leu2-3,112</i> , <i>trp1-1</i> , <i>ura3-1::TDH3p-hbd-Flag2-CYC1t-LEU2</i> , <i>TDH3p-adhe2-Flag2-CYC1t-URA3</i> , <i>TDH3p-ERG10-Flag2-CYC1t-KanMX4</i> , <i>TDH3p-crt-Flag2-CYC1t-TRP1</i> , <i>TDH3p-ccr-Flag2-CYC1t-HIS3</i> , <i>adh1Δ::ADE2</i> , <i>TDH3p-ALD6-Flag2-CYC1t-TEF1p-ACS2-Flag2</i> ADH1t-hph, <i>adh1Δ::ADE2</i> , <i>loxp::GCD2(S131A)</i>	This study
yMK2438	B ^R <i>gpd2Δ adh1Δ</i> ALD2 ACS2+5g	MATα GCD1-P180, <i>ade2-1</i> , <i>his3-11,15</i> , <i>leu2-3,112</i> , <i>trp1-1</i> , <i>ura3-1::TDH3p-hbd-Flag2-CYC1t-LEU2</i> , <i>TDH3p-adhe2-Flag2-CYC1t-URA3</i> , <i>TDH3p-ERG10-Flag2-CYC1t-KanMX4</i> , <i>TDH3p-crt-Flag2-CYC1t-TRP1</i> , <i>TDH3p-ccr-Flag2-CYC1t-HIS3</i> , <i>adh1Δ::ADE2</i> , <i>TDH3p-ALD6-Flag2-CYC1t-TEF1p-ACS2-Flag2</i> ADH1t-hph, <i>adh1Δ::ADE2</i> , <i>gpd2Δ::loxp-natNT2-loxp</i>	This study
yMK2440	B ^R <i>gpd1Δ adh1Δ</i> ALD2 ACS2+5g	MATα GCD1-P180, <i>ade2-1</i> , <i>his3-11,15</i> , <i>leu2-3,112</i> , <i>trp1-1</i> , <i>ura3-1::TDH3p-hbd-Flag2-CYC1t-LEU2</i> , <i>TDH3p-adhe2-Flag2-CYC1t-URA3</i> , <i>TDH3p-ERG10-Flag2-CYC1t-KanMX4</i> , <i>TDH3p-crt-Flag2-CYC1t-TRP1</i> , <i>TDH3p-ccr-Flag2-CYC1t-HIS3</i> , <i>adh1Δ::ADE2</i> , <i>TDH3p-ALD6-Flag2-CYC1t-TEF1p-ACS2-Flag2</i> ADH1t-hph, <i>adh1Δ::ADE2</i> , <i>gpd1Δ::loxp-natNT2-loxp</i>	This study

Table 2.2 Plasmid used in this study

Plasmid	Main features	Bacteria name	Source
pRS316- <i>adhe2</i>	<i>TDH3p-adhe2-Flag2-CYC1t-URA3</i>	BMK633	Ashe collection
pRS315- <i>hbd</i>	<i>TDH3p-hbd-Flag2- LEU2- CYC1t-LEU2</i>	BMK627	Ashe collection
pRS313- <i>ccr</i>	<i>TDH3p-ccr-Flag2-CYC1t-HIS3</i>	BMK632	Ashe collection
pRS314- <i>crt</i>	<i>TDH3p-crt-Flag2-CYC1t-TRP1</i>	BMK626	Ashe collection
pYM30- <i>ERG10</i>	<i>TDH3p-ERG10-Flag2-CYC1t -KanMX4</i>	BMK637	Ashe collection
pBMH- <i>ALD6-ACS2-HYGR</i>	<i>TDH3p-ALD6-Flag2-CYC1t-TEF1p-ACS2-Flag2-ADH1t-hphNT1</i>	BMK671	Ashe collection
pBMH- <i>ALD2-ACS2-HYGR</i>	<i>TDH3p-ALD2-Flag2-CYC1t-TEF1p-ACS2-Flag2-ADH1t-hphNT1</i>	BMK630	This study
pBEVYGA	<i>ADE2</i>	BMK623	Ashe collection
pGAL1-Cre-Ble (pSH-ble)	Cre recombinase enzyme	BMK721	Ashe collection
pZC2	<i>loxp-natNT2-loxp</i>	BMK757	Delneri collection (Carter and Delneri, 2010)

Table 2.3 Oligonucleotides used in this study

ORS N°	Primer Name	Purpose	Primer Sequence
1	<i>GCD1</i> VF	Verification of B ^S /B ^R strains	TGCTGACCAAAAG
2	<i>GCD1</i> VR	Verification of B ^S /B ^R strains	AGCATTCAAGTT
3	<i>hbd</i> F-amp	Amplification of <i>hbd</i> integration cassette	AAAGAAAGAGATTAAATAAAGAATGATTTACAATCTA GTCGCAAAAACAAGTACAGTGCTGACGTCCCATCCTC GAGGAGTTTATCATTATC
4	<i>hbd</i> R-amp	Amplification of <i>hbd</i> integration cassette	CTGTTCTCTTATGTATTTTTAATCGTCCTTGTATGGAA GTATCAAAGGGGACGTTCTTCACCTCCTTGGAA GTTTCGTCTACCCTATGAACA5
5	<i>hbd</i> VF	Verification of <i>hbd</i> integration	ATTGTTACGCTTAGTATAGTT
6	<i>hbd</i> VR	Verification of <i>hbd</i> integration	GAGTAATCTTCATTGCGCTTA
7	<i>adhe2</i> F-amp	Amplification of <i>adhe2</i> integration cassette	CACAATAATACCGTGTAGAGTTCTGTATTGTTCTTCTT AGTGCTTGTATATGCTCATCCCGACCTTCCAT CTCGAGGAGTTTATCATTATC3
8	<i>adhe2</i> R-amp	Amplification of <i>adhe2</i> integration cassette	AAAGAAAACTAACACATTAATGTAGTTTTAAAATTC AAATCCGAACAACAGAGCATAGGGTTTCGCAAAGTA CTGAGAGTGCACCACGCT
9	<i>adhe2</i> VF	Verification of <i>adhe2</i> integration	AGTTACTTTCTTAACAACGTTA
10	<i>adhe2</i> VR	Verification of <i>adhe2</i> integration	AGACAGAAGTCCAAATCACGT
11	<i>crt</i> F-amp	Amplification of <i>crt</i> integration cassette	TCATAGACATTAATCATTGGTTGTATGATAAAAATATC GCAAGAATTATTCTAACGTTAGATTAGATTCCAGCC ACTCGAGGAGTTTATCATTATC
12	<i>crt</i> R-amp	Amplification of <i>crt</i> integration cassette	CAGAAAGTCTACAGCAACAGAAAGCTCAGTGAATCAT TAACTGTTGGAATAAGACTCAACTGCGATCTATCGAC TAGTACTTATAGTACCAGTATATTAGATTGTACTGAGA GTGCACCA
13	<i>crt</i> VF	Verification of <i>crt</i> integration	TTTAAAGTATGTGCTTGTCT
14	<i>crt</i> VR	Verification of <i>crt</i> integration	TAACGCTGCTTTTCAAATCACGA
15	<i>ccr</i> F-amp	Amplification of <i>ccr</i> integration cassette	TTCATTAGATTTGATGACTGTTTCTCAAACCTTTATGTC ATTTTCTTACACCGCATATGATTATATACTAGAAACAT GAATACTACTAAATAGATGATAACTCGAGGAGTTTAT CATTATC
16	<i>ccr</i> R-amp	Amplification primer of <i>ccr</i> integration cassette	TTGTAATAGGCCGGCATTTTTTTGGTTAATAACAATGC CAGATAACCGCGAAGATTATAATGGTTTATCGGTTG CATTTTCCATGAGTATAGAACTAGATTGTACTGAGA GTGCACCA
17	<i>ccr</i> VF	Verification of <i>ccr</i> integration	AGCTATAATGTAGGTATACAGT
18	<i>ccr</i> VR	Verification of <i>ccr</i> integration	GTACAGTTGGACCGTCTTCAT
19	Middle test primer to check all up VR	Internal forward primer targeting the vector sequence for	CTCCTTACGCATCTGTGCGG

		verification of <i>hbd</i> , <i>adhe2</i> , <i>crt</i> , <i>ccr</i> and <i>ERG10</i> integration cassettes	
20	Middle test primer to check all down VR	Internal reverse primer targeting the vector sequence for verification of <i>hbd</i> , <i>adhe2</i> , <i>crt</i> , <i>ccr</i> and <i>ERG10</i> integration cassettes	CGAATTGGAGCTCCACCGCG
21	<i>ALD6</i> , <i>ACS2</i> VF	Verification of <i>ALD6</i> <i>ACS2</i> integration	GAAAACGGAAGAGGAGTAGGG
22	<i>ALD6</i> , <i>ACS2</i> VR	Verification of <i>ALD6</i> <i>ACS2</i> integration	CGTCGAAACTAAGTTCTTGG
23	<i>ALD6 ACS2</i> VF-hygo	internal forward primer targeting hygromycin marker	GTTATGTTTATCGGCACTTG
24	<i>ALD6 ACS2</i> VR	External reverse primer for verification of <i>ALD6</i> <i>ACS2</i> Integration	CGAGGATACGGAGAGAGGTATG
25	<i>ALD2</i> F-amp	Amplification of <i>ALD2</i> with <i>Bam</i> HI site	TTCGACGGATCCATGCCTACCTGTATACTGATATCG
26	<i>ALD2</i> R-amp	Amplification of <i>ALD2</i> with <i>CYC1t+</i> <i>Ppu</i> MI site	TAAATAGGGACCTAGACTTCAGGTTGTCTAACTCCTTC TTAACGCGTACCAGTAATGTCCTTATCGTCATCGTCCT TGTAAGTACACAGTAATGTCCTTATCGTCATCGTCCTTG TAGTCACCGAAGCGGTGTTGTCCAAAGAGAGATTATG
27	<i>ALD2ACS2</i> VF	Verification of <i>ALD6</i> <i>ACS2</i> integration	GAAAACGGAAGAGGAGTAGGG
28	<i>ALD2 ACS2</i> VR	Verification of <i>ALD6</i> <i>ACS2</i> integration	CGTCGAAACTAAGTTCTTGG
29	<i>ALD2</i> VR	Internal primer for verification of <i>ALD2</i> integration	GTTTCGGCTATTTGTATTG
30	<i>GPD1</i> -FD	Amplification of <i>natNT2</i> deletion cassette for deletion of <i>GPD1</i>	CATAAGACATCAAGAAACAATTGTATATTGTACACCC CCCCCTCCACAAACACAAATATTGATAATATAAAGTT CGTACGCTGCAGGTCGAC
31	<i>GPD1</i> -RD	Amplification of <i>natNT2</i> deletion cassette for deletion of <i>GPD1</i>	GAATATGATATAGAAGAGCCTCGAAAAAAGTGGGGG AAAGTATGATATGTTATCTTTCTCCAATAAATCACTAT AGGGAGACCGGCAG

32	<i>GPD2</i> -FD	Amplification primer of <i>natNT2</i> deletion cassette for deletion of <i>GPD2</i>	GTTTATGTATTTTGGTAGATTCAATTCTTTCCCTTTCCTTTCTTCGCTCCCTTCTTATCATTCGTACGCTGCAGGTCGAC
33	<i>GPD2</i> -RD	Amplification of <i>natNT2</i> deletion cassette for deletion of <i>GPD2</i>	GGTTGGGGGAAAAAGAGGCAACAGGAAAGATCAGAGGGGAGGGGGGGGAGAGTGTCACTATAGGGAGACCGGCAG
34	<i>GCD2</i> Ramp -S131 A	Amplification of <i>GCD2</i> mutagenic cassette (S131A + <i>Bss</i> HII site)	GATTCGCGAAGTTTTTGGCGCGCTTACTGCACTGGTTAAAGC
35	<i>GCD2</i> Ramp For S131 D	Amplification of <i>GCD2</i> mutagenic cassette (S131D + <i>Bam</i> HI site)	GATTCGCGAAGTTTTTGGATCCGATACTGCACTGGTTAAAGC
36	<i>GCD2</i> -Re+ 528	Amplification of <i>GCD2</i> cassette	GATGCAGATACAGTAGACGAC
37	<i>natNT2</i> Famp	Amplification of loxP– <i>natNT2</i> -loxP from pZC2 vector with homology flanking region corresponding to chromosomal integration site upstream of <i>GCD2</i>	GAAAAAGAGGAAAAATAGTACCAAAACACCCCATAGGAAATATATAAAATAAACATACCTGTAAATACTAAAAAGTAGAATTCGTACGCTGCAGGTCGAC
38	<i>natNT2</i> Ramp	Amplification loxP– <i>natNT2</i> -loxP from pZC2 vector with homology flanking region corresponding to chromosomal integration site upstream of <i>GCD2</i>	GTGAAGAGATTCCCGGGTAAATATAAACATAATTAATACAATAATAGCAATATATGTGACGAACTGTGCACTATAGGGAGACCGGCAG
39	<i>GCD2</i> VF for <i>natNT2</i> integration	Verification of <i>natNT2</i> integration upstream of <i>GCD2</i>	GGCGCGGAATAAAGGACTTG
40	<i>GCD2</i> VR for <i>natNT2</i> integration	Verification of <i>natNT2</i> integration upstream of <i>GCD2</i>	GCAATTTGATTATCGACGCTT
41	<i>natNT2</i> VF	Internal forward primer for verification of <i>natNT2</i> integration	GGTCAGGTTGCTTTCTCAGG
42	<i>natNT2</i> VR	Internal reverse primer for verification of <i>natNT2</i> integration	GTACGAGACGACCACGAA

43	<i>GCD2</i> Ramp For S131 original	Amplification of the WT <i>GCD2</i> cassette	GATTCGCGAAGTTTTGGAGATGATACTGCACTGGTTAAAGC
44	<i>ERG10</i> VF	Verification for <i>ERG10</i> integration	GATTAATCTGATATCAAGTTA
45	<i>ERG10</i> VR	external verification for <i>ERG10</i> integration	TGGTGCCAGAGTCGTTGTCAC
46	<i>ADH1</i> F amp	Amplification of <i>ADE2</i> deletion cassette from the genome	CTACTCTCTAATGAGCAACG
47	<i>ADH1</i> R amp	Amplification of <i>ADE2</i> deletion cassette from the genome	GACCTCATGCTATACCTG
48	<i>ADH1</i> VF EX	External verification of <i>ADH1</i> deletion	CTCACCATATCCGCAATGAC
49	<i>ADE2</i> VR IN	Internal reverse primer for verification of <i>ADE2</i> integration	TCGTAGCCATGCAACAAGAG
50	<i>ADE2</i> VF IN	Internal forward primer for verification of <i>ADE2</i> integration	CATATGCTATTTCCGCAAGC
51	<i>ADH1</i> VR EX	External verification of <i>ADH1</i> deletion	ACTGAAGGCTAGGCTGTGGA
52	<i>GPD1</i> VF EX	External verification of <i>GPD1</i> deletion	CTGGCTTGGTATTGGCAGTT
53	<i>GPD1</i> VR EX	External verification of <i>GPD1</i> deletion integration	CCGACAGCCTCTGAATGAGT
54	<i>GPD2</i> VF EX	External verification of <i>GPD2</i> deletion	GCAGCTCTTCTCTACCCTGTC
55	<i>GPD2</i> VR EX	External verification of <i>GPD2</i> deletion	AAAAGCTCGAAGAAACAGCTT

ORSN[®]: Oligo Reem Swidah number

Table 2.4 Antibody used in this study

Target	Primary antibody		Secondary antibody		Source
	Name	Dilution	Name	Dilution	
Flag2	α flag	1:500	anti-mouse	1:10000	Sigma
Gcd2	GCD2 480 (IP)	1:500	coat-anti-mouse	1:5000	Odyssey
Gcd2	GCD2 483 (western)	1:500	coat-anti-mouse	1:5000	Odyssey
Protein A (Pab1)	α Pab1	1:500	coat-anti-rabbit	1:5000	Odyssey

Table 2.5 Optimal conditions for restriction enzymes

Enzyme	Temperature	Time	BSA
<i>Mnl</i> I	37°C	60 min	yes
<i>Xho</i> I	37°C	60 min	Yes
<i>Bam</i> HI	37°C	60 min	yes
<i>Eag</i> I	37°C	60 min	yes
<i>Bsm</i> BI	55°C	120min	no
<i>Sca</i> I	37°C	120min	no

3. Construction strains of *Saccharomyces cerevisiae* harbouring five butanol synthetic genes

3.1 Introduction

The yeast *Saccharomyces cerevisiae* is a robust microorganism that is widely used for traditional applications such as brewing and bread making. Recently it has been used extensively in the industrial biotechnology sector to produce various products using different gene manipulation techniques (Luo *et al.* 1999). One specific application has been the production of biofuels. There are a number of key factors that have stimulated the use of yeast in biotechnological applications. It is extremely well characterized biochemically, physiologically and genetically. It was the first microorganism to have its genome fully sequenced (Snyder *et al.* 2009). It is generally regarded as safe (GRAS) and can tolerate many stress conditions. Furthermore, a significant advantage of using *S. cerevisiae* over other expression systems for synthetic biology is the effectiveness of gene insertion/ deletion via homologous recombination (Petranovic *et al.* 2010).

Historically, butanol has been produced extensively from *Clostridia* species (Keis *et al.* 2001). However, such bacterial production can be associated with some drawbacks. For instance, the microorganisms are strictly anaerobic and only grow in a limited pH range. They are relatively intolerant to oxygen, alcohols and fermentation by-products. Furthermore, they achieve butanol production via a complex two phase fermentation: acidogenesis and solventogenesis which makes high yields difficult to achieve (Liu *et al.* 2012). A further disadvantage at the industrial scale is the level of fermentation spoilage via bacteriophage infection.

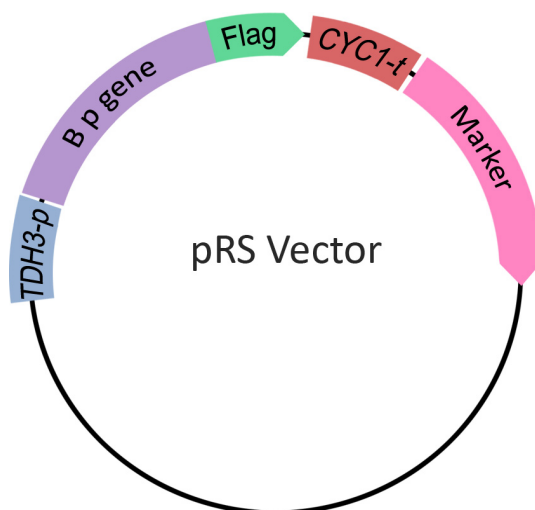
Therefore, in this project we have decided to investigate whether using *Saccharomyces cerevisiae* as an alternative host for butanol production could overcome any of the limitations associated with bacterial production strategies. In order to attempt to produce butanol, we constructed a strain of *S. cerevisiae* that carries a highly expressed butanol synthetic pathway consisting of the *ccr*, *crt*, *hbd*, *adhe2* and *ERG10* genes. *ccr*, *crt*, *hbd*, *adhe2* are heterologous genes: *crt*, *hbd*, *adhe2* were taken from *Clostridium beijerincki* and *ccr* was taken from *Streptomyces collinus* whereas *ERG10* is already present in *S. cerevisiae* but it is only poorly expressed (Hiser

et al. 1994). First of all, the *TDH3* promoter was cloned into five shuttle vectors pRS13, pRS14, pRS15, pRS16 and PBMH vector which each harbour a different marker. Five synthesised cassettes with codon optimised *ccr*, *crt*, *hbd*, *adhe2* and *ERG10* were cloned separately into these vectors. The integration cassettes were amplified and transformed into specific yeast genomic loci, which were selected as they had previously been identified as high expression sites (Flagfeldt *et al.* 2009) The single integrant strains were originally constructed in two wild type backgrounds (B^R and B^S) that vary at a single genetic locus according to butanol sensitivity (Ashe *et al.* 2001). Following the successful integration of these cassettes separately within the W303-1A laboratory strain, successive backcrosses were performed to obtain metabolically engineered strains of *S. cerevisiae* expressing the five butanol synthetic genes. Each synthetic gene was tagged at the C-terminus with the Flag epitope to enable detection of expressed proteins by western blotting. The construction of these strains allowed the levels of ethanol and butanol to be evaluated over the course of an extended semi-anaerobic fermentation.

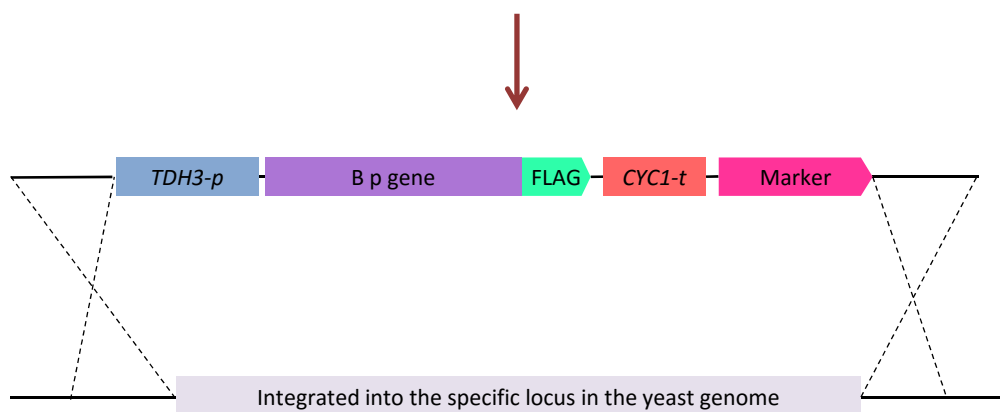
3.2 The Integration strategy for introducing codon optimised butanol synthetic genes into *Saccharomyces cerevisiae*.

In order to introduce the butanol synthetic pathway into *S. cerevisiae*, the first step was to generate integration cassettes using a PCR based strategy. The forward and reverse integration PCR primers were designed such that they would amplify a fragment from plasmids that had been previously designed and constructed in the Ashe lab. The cassette in the plasmid included a *TDH3* promoter, the gene of interest with a C-terminal Flag epitope, a terminator and an appropriate marker. The strategy for amplifying each integration cassette also added 5' and 3' homologous flanking regions to allow successful integration through homologous recombination at specific sites in the genome (Fig. 3.1 A). Each butanol integration cassette was targeted to high expressing chromosomal integration site in the yeast genome (Flagfeldt *et al.* 2009). A detailed summary listing the strains to be used, the chromosomal integration sites, the specific gene from the butanol synthetic pathway and the genetic marker to be used is presented in Fig. 3.1 C.

A



B



C

Host Strains		Chromosomal integration site	Gene	Marker
yMK 24	B^R	Chr VIII (529857-530389)	<i>crt</i>	<i>TRP1</i>
yMK 23	B^R	Chr XIII (481412-481926)	<i>ccr</i>	<i>HIS3</i>
yMK 37	B^S	Chr XVI (776494-777609)	<i>adhe2</i>	<i>URA3</i>
yMK 36	B^S	Chr XVI (881267-882041)	<i>hbd</i>	<i>LEU2</i>
yMK 36	B^S	Chr XIV (727312-727705)	<i>ERG10</i>	<i>G418</i>

Figure 3.1 A schematic representation of the integration strategy for introducing codon optimised butanol synthetic genes into *Saccharomyces cerevisiae*. A) Representative pRS vector carrying the integration cassette with the *TDH3* gene promoter, a butanol production gene (B p gene), the Flag epitope tag and the *CYC1* gene terminator. B) The integration cassette was generated by PCR, and used for homologous recombination at a specific locus in the yeast genome. C) A table summarizes properties of the strains used.

3.3 Restriction digests for all plasmid templates

In order to verify that the individual components were present in four of the integration cassette plasmids, restriction digests were performed with unique restriction enzymes *XhoI*, *BamHI* and *EagI* on the four plasmid templates pRS313-*ccr*, pRS314-*crt*, pRS315-*hbd* and pRS316-*adhe2* (Fig. 3.2 A). *XhoI* and *BamHI* should release the *TDH3* promoter, whereas *BamHI* and *EagI* should release the individual butanol synthetic gene and the *CYC1* terminator from these plasmids. Therefore, *XhoI*/ *BamHI* and *BamHI*/ *EagI* restriction digests on the plasmids were found to result in appropriately sized restriction products when separated on agarose gels (Fig. 3.2 B and 3.2 C) relative to the theoretical size of the products (Fig 3.2 D and 3.2 E). Hence, it was confirmed that the plasmids from the Ashe lab collection (constructed, sequenced and archived by Dr Hui Wang) contain the *TDH3* promoter, the functional gene with Flag and the *CYC1* terminator.

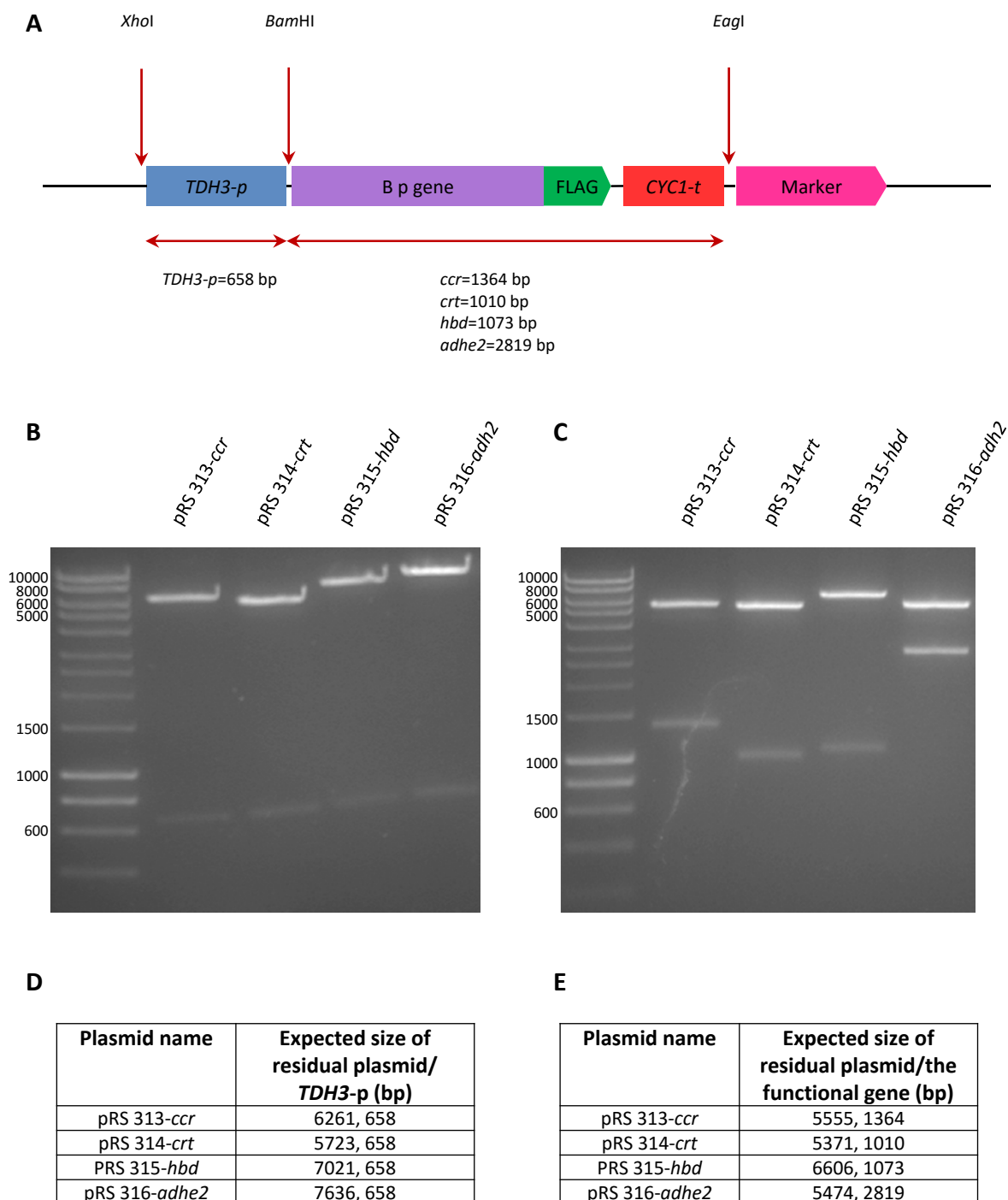


Figure 3.2 Restriction digests of the plasmid integration constructs.

A) Figure shows a schematic representation of the position of the restriction sites *XhoI*, *BamHI* and *EagI* on the integration cassette vectors. B) and C) Photographed gels of *XhoI/BamHI* digestion products and *BamHI/EagI* digestion products from each of the plasmid templates, respectively. A) The size of the products on the agarose gels closely matches the theoretical size of the *TDH3* promoter and functional gene. (D) and (E) Tables showing the expected sizes for the various digestion products.

3.4 Generation of a strain with the five genes involved in butanol production exogenously integrated at high expression sites

In order to introduce the *hbd* and *adhe2* genes separately into the W303-1A laboratory strain, the desired cassettes for the *hbd* and *adhe2* genes were PCR amplified using specific integration primers: P1=ORS3 and P2=ORS4 for *hbd* cassette and P1=ORS7 and P2=ORS8 for *adhe2* cassette (see Table 2.3). Bands consistent with the expected ~4.3kb and 5.4kb PCR products were obtained on agarose gels (Fig. 3.3 B). The *MAT α* W303-1A laboratory strain bearing a B^S allele of *GCD1-S180* (yMK37) was transformed with the *adhe2* cassette, whereas a *MAT α* version of this strain (yMK36) strain was transformed with the *hbd* cassette. Possible transformants were selected on appropriate dropout media, re-streaked and processed for the preparation of genomic DNA. PCR analysis on the resulting genomic DNA was used to confirm the successful integration of the *hbd* and *adhe2* cassettes at the specific loci in the yeast genome. A series of three different PCR reactions on this genomic DNA were performed to evaluate whether correct integration had occurred. The verification primers for the integration of *hbd* cassette are: P1=ORS5, P2=ORS20, P3=ORS19 and P4=ORS6 while, the verification primers for the integration of *adhe2* cassette are: P1=ORS9, P2=ORS20, P3=ORS19 and P4=ORS10. The first PCR product validates the upstream insertion site, the second PCR product validates the downstream chromosomal integration site and the third PCR product spans the whole cassette (Fig. 3.4 A). The PCR products obtained for the transformants relative to the controls for the non-transformed strain show that the *hbd* and *adhe2* cassettes had been successfully integrated at the correct locus in the genome of transformants (Fig. 3.4 B and 3.4 C).

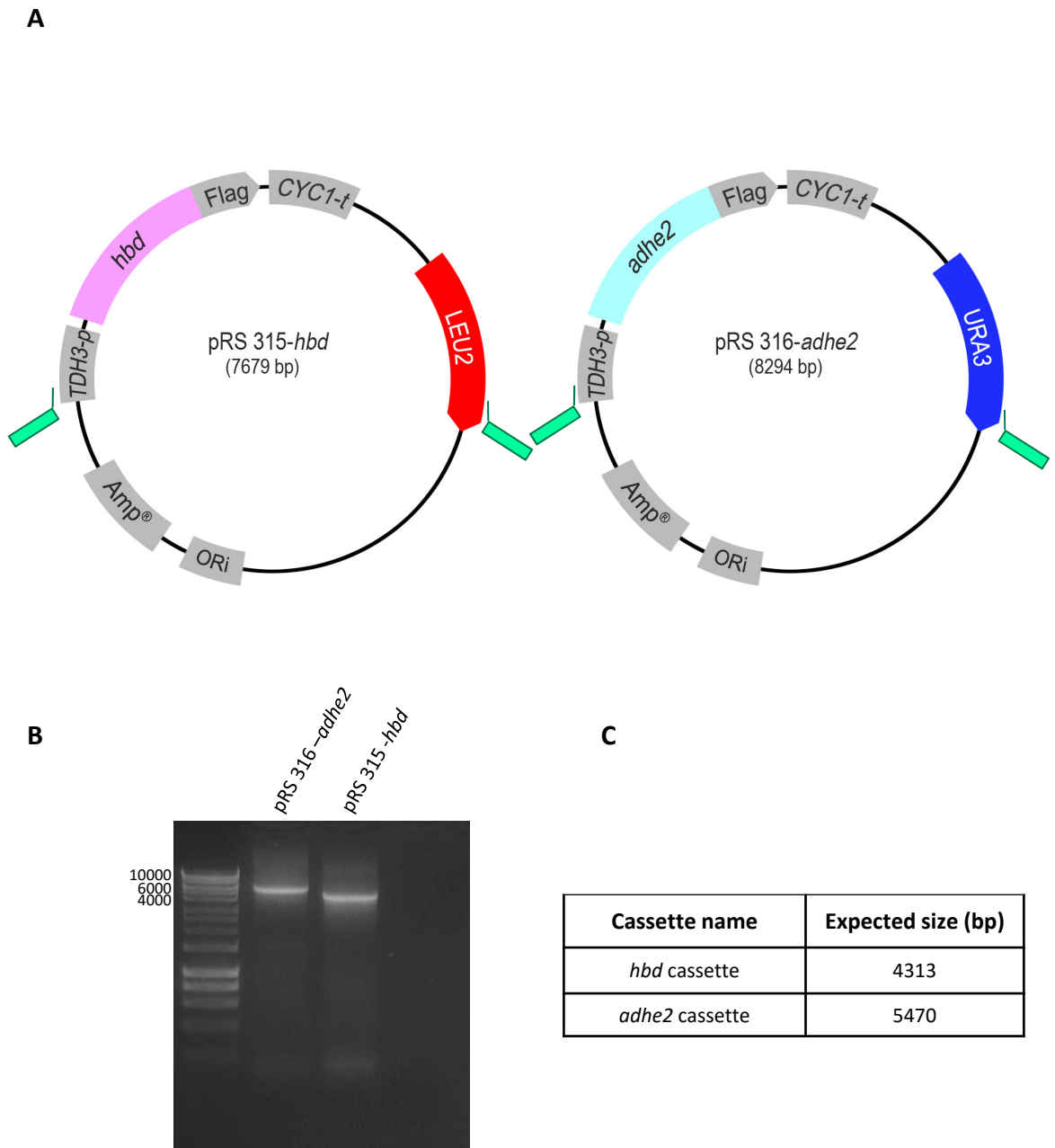
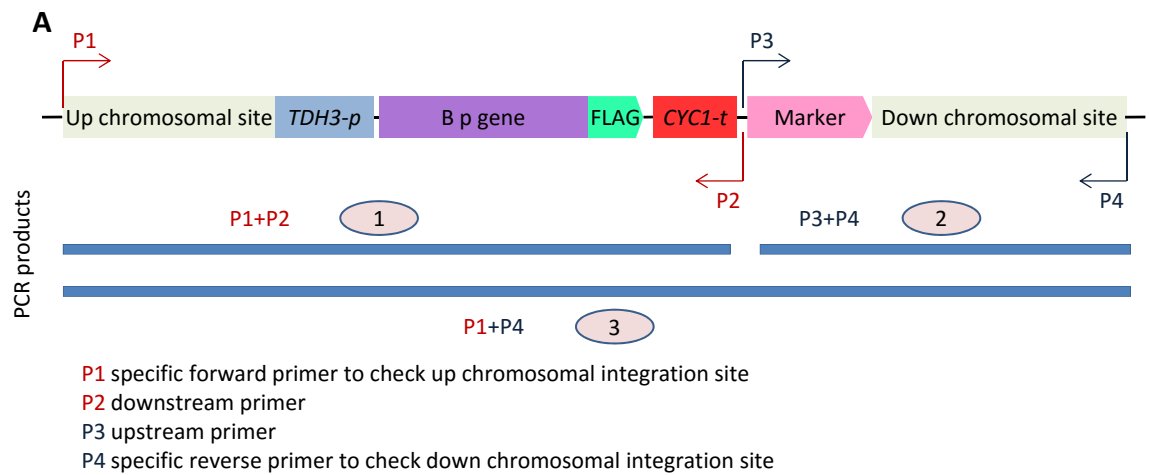
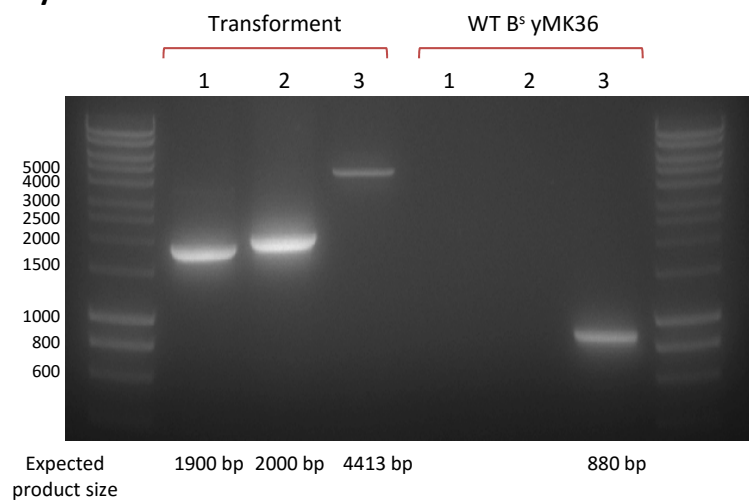


Figure 3.3 Schematic representation of the pRS 315-*hbd* and pRS 316-*adhe2* vector carrying the integration cassette. A) Schematic representation of the amplification sites for the forward and reverse primers (in green). B) Photographed gel showing the *hbd* and *adhe2* integration cassettes. C) A table showing the theoretical size of the integration cassettes.



B WT B^s yMK36 transformed with *hbd*



C WT B^s yMK37 transformed with *adhe2*

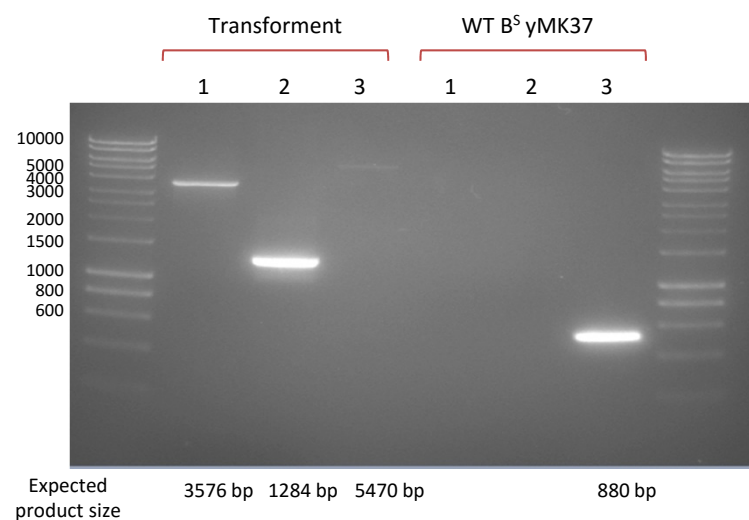


Figure 3.4 Verification of successful cassette integration at a specific location in the genome. A) Schematic representation of the PCR strategy used to confirm the correct integration of the appropriate cassette for each potential transformant. Three PCR reactions are set up using the appropriate primers listed in Table 2.3. B) and C) Depict agarose gels where the various PCR products derived from genomic DNA prepared from a transformant and wild type strain are separated.

3.5 Factors changed to increase the efficiency of *crt* and *ccr* cassettes integration within the genome

Even though the *adhe2* and *hbd* integrated strains were successfully generated, problems were encountered for the *crt* and *ccr* cassettes in that high levels of false positive transformants were obtained (data not shown). In order to achieve the correct cassette integration for *crt* and *ccr* a number of alterations were made to the standard method with a view to increasing the efficiency of correct integration.

3.5.1 Re-design of the insertion primers

In order to increase the efficiency of cassette integration into specific loci, the first factor altered was the length of the homology present on the insertion primers. Even though 35 bp as a length for the homology flanking region (HFR) can be sufficient (Manivasakam *et al.* 1995), the efficiency of homologous recombination is increased when the length of HFR is increased. Therefore, the HFR in the integration primers was increased to 100 bp instead of 70 bp. The amplification primers for the integration of *crt* cassette are: P1=ORS11 and P2=ORS12 while, the amplification primers for the integration of *ccr* cassette are: P1=ORS15 and P2=ORS16 and the sequences of these primers are listed in Table 2.3.

3.5.2 Restriction digests of pRS313-*ccr* and pRS314-*crt* plasmid templates

In order to decrease the chance of obtaining false positive transformants derived from the plasmid template for the integration cassette PCR, a strategy was devised to linearise the plasmid template prior to the PCR reaction. A digest using the restriction enzymes *ScaI* and *BsmBI* would likely significantly inhibit any plasmid replication in yeast, as the digest removes the majority of the yeast origin of DNA replication (Fig. 3.5 A). Therefore, a *ScaI*/ *BsmBI* digestion was performed and the expected digestion products were obtained respectively (Fig. 3.5 B and 3.5 C).

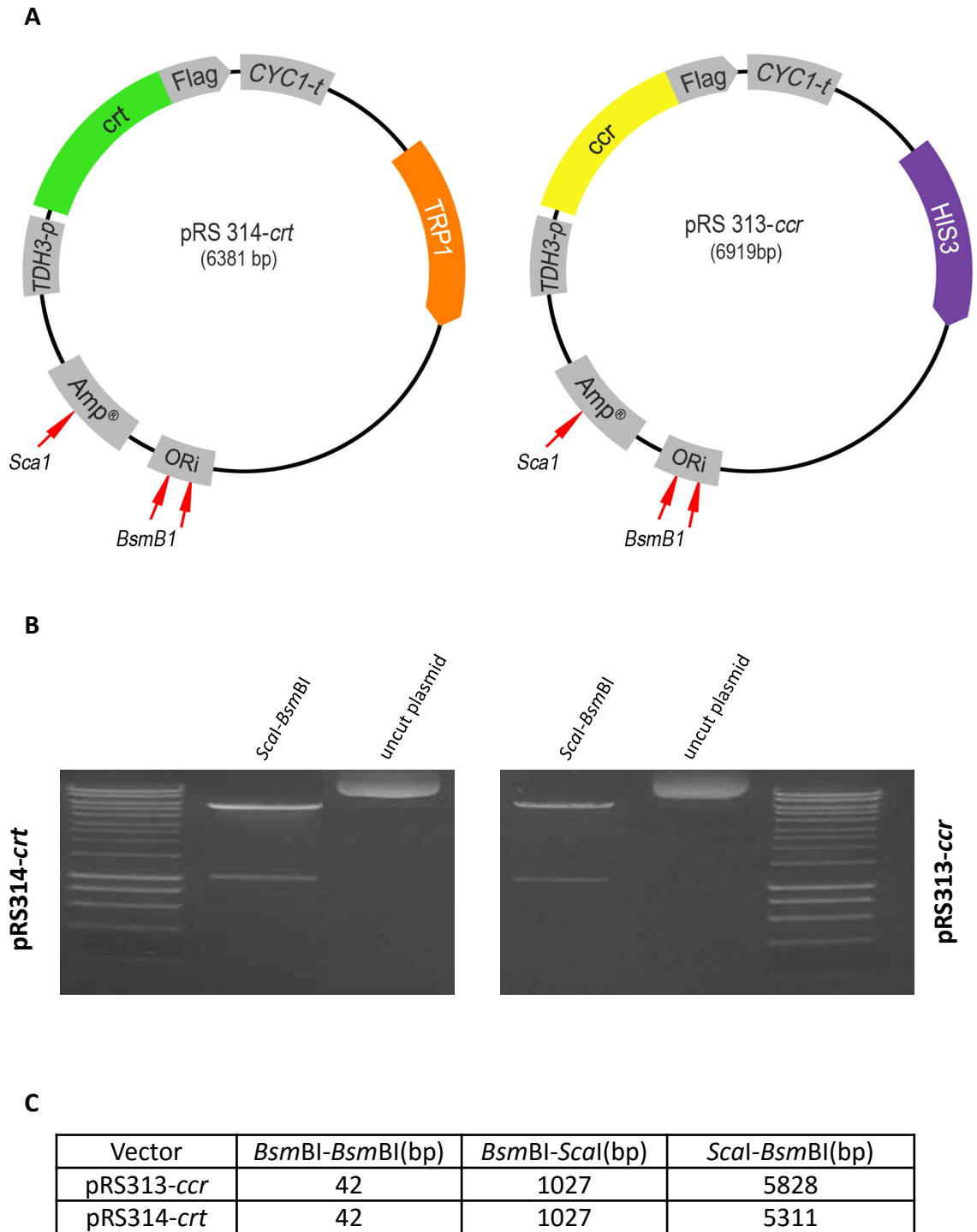


Figure 3.5 Restriction digests with *ScaI* and *BsmBI* for pRS313-*ccr* and pRS314-*crt* constructs. A) Schematic representation of the restriction sites for the enzymes on the plasmid templates. *ScaI* and *BsmBI* were used to linearise the plasmid construct. *ScaI* cuts in the ampicillin resistance gene, while *BsmBI* cuts twice at the origin of replication. B) Figure shows agarose gel separating *ScaI* and *BsmBI* digestion products compared to uncut DNA template. C) The expected digestion products are listed in the table.

3.5.3 Plasmid template dilutions

In order to get maximum levels of the integration cassette PCR product with the minimum amount of digested plasmid template, the template was titrated in the PCR reaction. Therefore, various dilutions were prepared at 1/100, 1/1000, 1/10000, 1/20000 and 1/50000 from each digested template and PCR reactions were set up using the new longer insertion primers. Clearly, the level of PCR product was reduced with increased template dilution (Fig. 3.6). The optimal template dilution for the generation of the *ccr* cassette was judged to be 1/2000, whereas for the *crt* cassette the 1/1000 dilution was selected. These dilutions represented the lowest level of template which gave maximal levels of product.

3.6 Transformation and validation of the *ccr* and *crt* cassettes

The aim at the outset of this project was to generate both B^R and B^S versions of strains bearing the butanol synthesis pathway. The B^S strain background has been used for the *adhe2* and *hbd* genes, so the B^R strain background was used here to allow a strategy of back-crossing to give the full pathway in both backgrounds. Therefore, yMK23 (*MATa* B^R) strain was transformed with the *ccr* PCR integration product, while yMK24 (*MATα* B^R) was transformed with the *crt* cassette. Transformants were selected on appropriate selective media and genomic DNA was prepared to enable the accuracy of integration for each cassette to be assessed. A similar validation strategy to that described above was used here and sizes of the 3 PCR products obtained relative to controls showed that successfully integrated transformants had been obtained (Fig. 3.7). The verification primers for the integration of *crt* cassette are: P1=ORS13, P2=ORS20, P3=ORS19 and P4=ORS14 while, the verification primers for the integration of *ccr* cassette are: P1=ORS17, P2=ORS20, P3=ORS19 and P4=ORS18. In addition to the four strains described above, a yMK36 strain transformed with an *ERG10* cassette was also constructed by Dr. Peter Reid in the Ashe lab. In this cassette, the *TDH3* promoter drives C-terminally flag tagged *ERG10* with a downstream *kanMX4* marker. Therefore

at this stage of the project, five single integration gene strains had been successfully obtained.

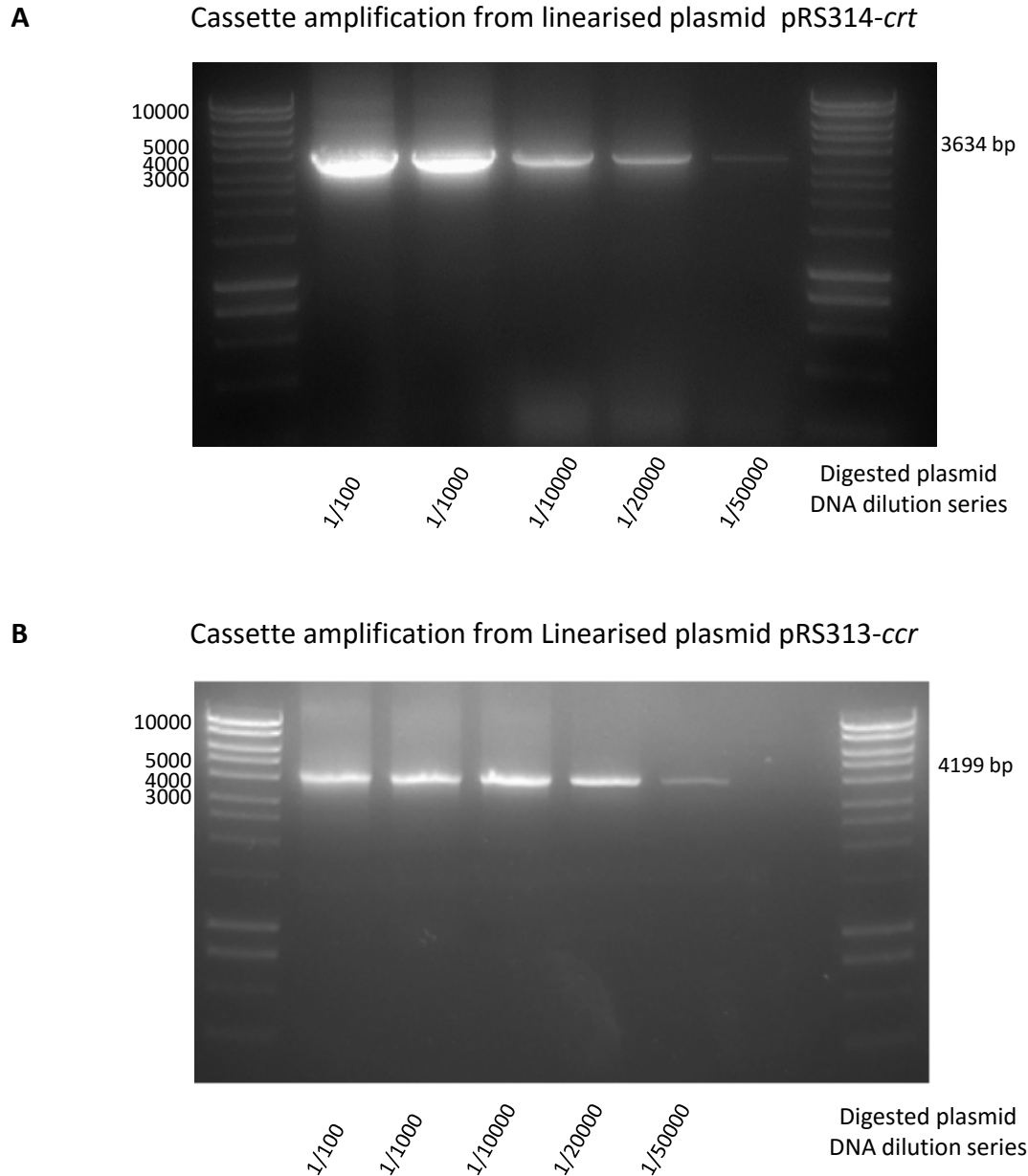


Figure 3.6 Dilutions of the digested construct. Figure shows agarose gels where amplified *ccr* and *crt* cassettes have both been detected at varying dilutions of digested plasmid DNA templates. The expected PCR product size and the dilution level for the linearised DNA plasmid template are labelled on the photo.

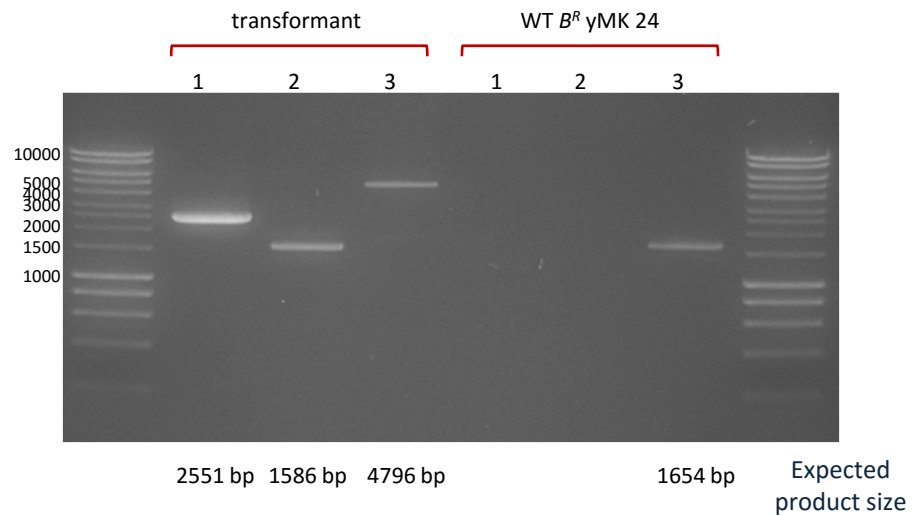
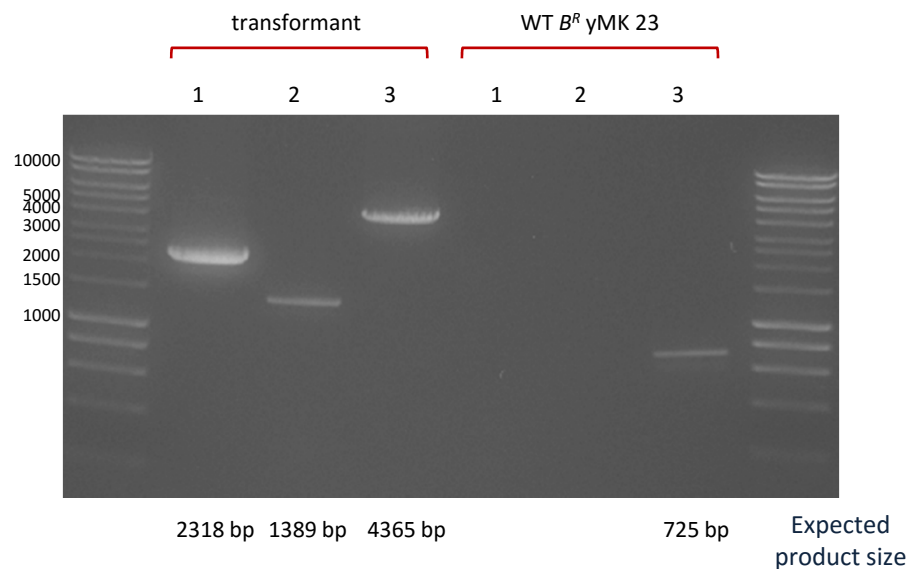
A**WT *B^R* yMK 24 transformed with *crt*****B****WT *B^R* yMK 23 transformed with *ccr***

Figure 3.7 Verification of successful cassette integration of *crt* and *ccr* at a desired location in the yeast genome. Agarose gels showing the three different PCR reactions that were used to amplify different parts of the integrated cassette from transformant and wild type genomic DNA. The expected PCR products sizes are labelled below the gel while the DNA markers are labelled on the left.

3.7 Back-crossing to obtain multiple integrated genes in the same strain

In order to generate a final strain bearing all butanol genes *hbd*, *adhe2*, *crt*, *ccr* and *ERG10*, genes, a strategy involving four different back-crosses was devised (Fig. 3.8). The first cross was performed to enable the production of a haploid strain bearing both the *hbd* and *adhe2* genes. The verified single integrant *hbd* and *adhe2* strains (yMK1866 and yMK1865) were mated together; diploid cells were selected and plated onto sporulation plates. The resulting tetrads were dissected and the genotype of haploid tetrads was ascertained to ensure that double integrant haploid strains had been obtained. The second backcross involved taking a *hbd adhe2* haploid strain (yMK1876) and crossing it to an *ERG10* strain (yMK1874) to generate a triple integrant strain. The third back-cross was performed to generate a haploid strain bearing both the *crt* and *ccr* genes from the single integrant *crt* and *ccr* strains (yM1897 and yMK1896). The final back-cross involved mating this *crt ccr* haploid strain to a strain carrying the *adhe2 hbd ERG10* genes. The production of this strain would allow the question as to whether strains bearing a codon-optimised butanol synthetic pathway are capable of producing substantial yields of butanol. The strategy used to generate the strains would also enable the pathway to be generated in both the B^R and B^S backgrounds to potentially test whether Butanol resistant strains produce more butanol.

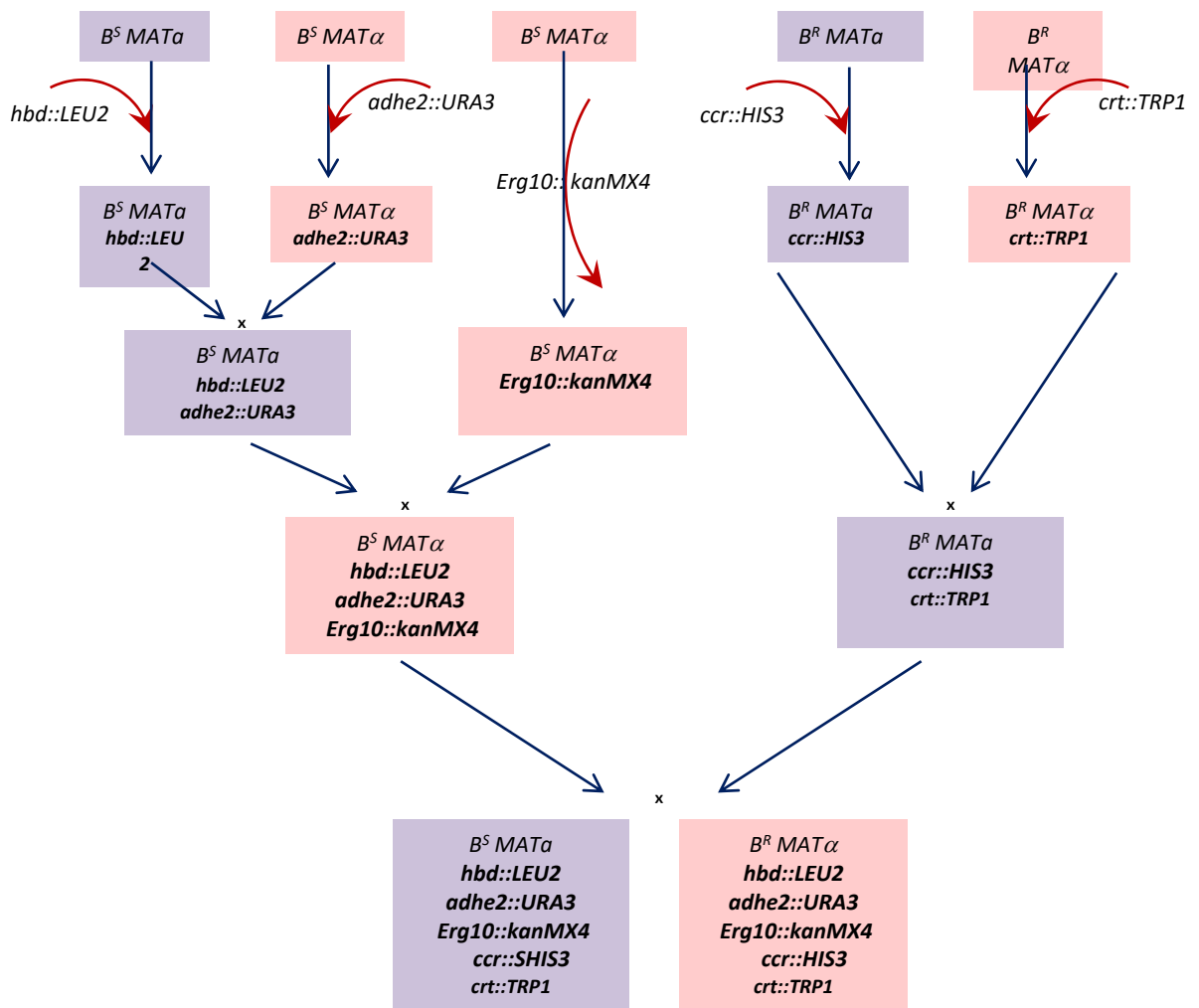


Figure 3.8 Overall strategy to construct a strain of *Saccharomyces cerevisiae* bearing five butanol synthetic pathway genes. Individual integration cassettes which carry a butanol synthetic gene with a different marker were generated and transformed into an individual strain of W303-1A either MAT α or MATa, B^R or B^S . Verified single integrant strains were obtained, and via a series of backcrosses a strain of *S.cerevisiae* bearing five butanol synthetic genes either in the B^R or B^S background were generated.

B^S = (GCD1-S180)

B^R = (GCD1-P180)

MAT α / MATa = yeast mating type

hbd, *adhe2*, *ERG10*, *ccr* and *crt* are butanol synthetic genes

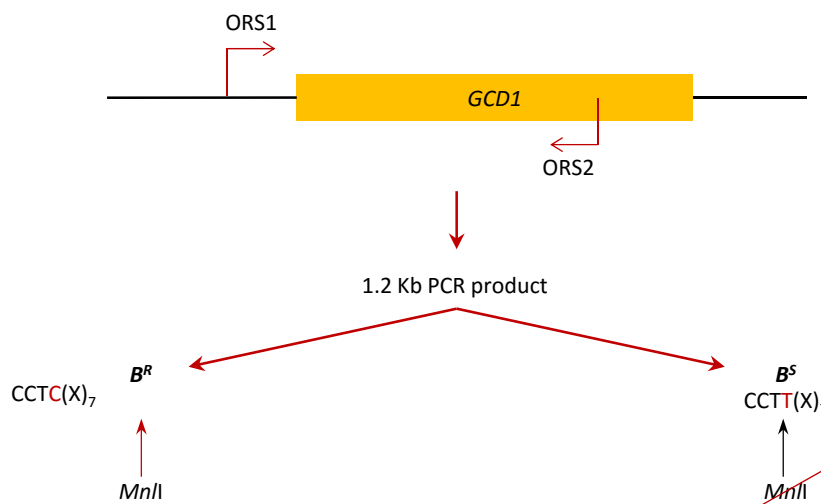
LEU2, *URA3*, *kanMX4*, *HIS3* and *TRP1* = markers used for selection

3.8 Validation and phenotypic characterisation of the progeny obtained from the final cross

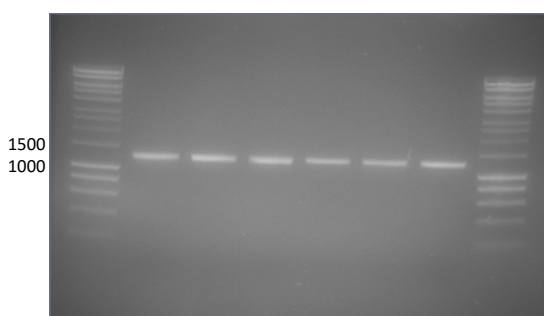
After the final back-cross, haploid strains were selected that potentially contain all five butanol pathway genes, as they grow on selective media lacking Leucine, Tryptophan, Uracil and Histidine but containing G418. In order to distinguish between butanol resistant and sensitive progeny a PCR based assay was used. The variant gene at this locus is *GCD1*, which encodes the γ subunit of eIF2B: the B^R strain harbours *GCD1-P180* and the B^S strain has *GCD1-S180*. The fragment pattern from an *MnII* restriction digestion of a specific *GCD1* PCR product amplified using the P1=ORS1 and P2=ORS2 primers on genomic DNA from the progeny distinguishes between these two forms. A 1200 bp PCR product was amplified from the genomic DNA samples using amplifying primers P1=ORS1 and P2=ORS2 (Listed in Table 2.3) (Fig. 3.9 B) and subsequent restriction digestion with *MnII* produced two basic patterns of digested products. A band of ~550 bp indicates a B^S strain, whereas a band of ~400 bp indicates a B^R strain (Fig. 3.9 C and D). Two of the strains exhibited B^R pattern (Fig. 3.9 C lanes 1 and 6) while the rest of the selected haploid strains exhibit the B^S pattern (Fig. 3.9 C lanes 2-5).

A further experiment was performed to investigate the mating types of all the strains used by using a lawn of mating type tester strains; yMK51/ yMK50 as described in Materials and Methods. This assay allows *MATa* and *MAT α* strains to be distinguished. Both B^R strains are *MAT α* while both mating types *MATa* and *MAT α* are present among the B^S strains (data not shown).

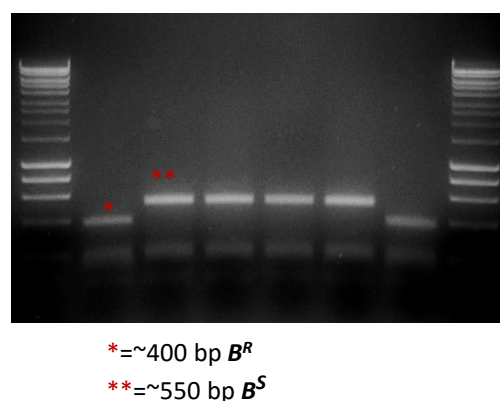
A



B Isolation of a *GCD1* fragment by PCR



C Digestion of the *GCD1* fragment with *MnlI*



D Expected *MnlI* digestion products (bp)

<i>B^R</i> +5g	<i>B^S</i> +5g
66	66
164	---
175	175
191	191
199	199
391	
---	555

Figure 3.9 Verification of *GCD1-S180* (*B^S*) and *GCD1-P180* (*B^R*) genotype. A) Figure shows schematic representation of a PCR strategy for amplification and validation of the *GCD1* fragment from putative *B^S* and *B^R* strains. B) Figure shows *GCD1* PCR products obtained from genomic DNA samples prepared from the progeny of the final cross in Figure 3.8 using the ORS1 and ORS2 primers (Listed in Table 2.3). C) The PCR products were digested with *MnlI* and the products were run on an agarose gel. The 550 bp versus 391 bp product is diagnostic for the mutation (red asterisks). D) A table depicting the theoretical digested band sizes for products derived from the *B^S*+5g and *B^R*+5g strain.

5g= five butanol synthetic genes

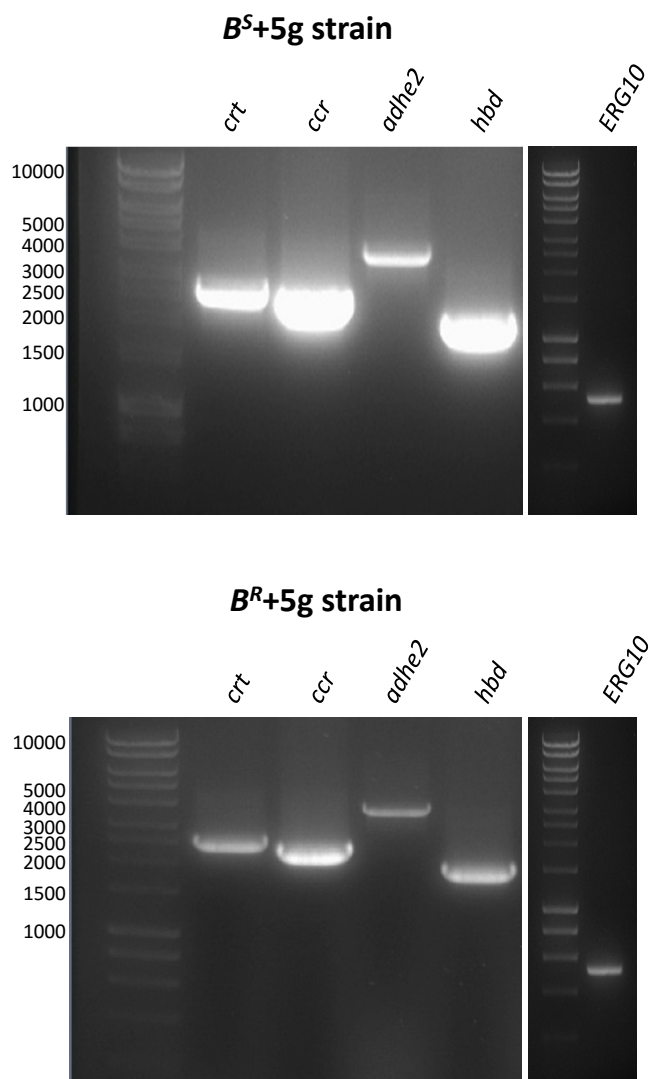
3.9 Verification PCR to confirm five butanol synthetic genes (*crt*, *ccr*, *adhe2*, *hbd* and *ERG10*) are presented in *GCD1-S180* (B^S) and *GCD1-P180* (B^R) strains

Finally, in order to confirm the presence of each integration cassette at the specific locus in the yeast genome in the constructed *GCD1-S180* (B^S) and *GCD1-P180* (B^R) strains, a diagnostic PCR reaction was performed for each of the loci. More specifically, a PCR reaction that generates a fragment from the boundary between the cassette and upstream of the chromosomal integration site was conducted by using appropriate checking primers: P1=ORS5, P2=ORS20 for *hbd* cassette, P1=ORS9, P2=ORS20 for *adhe2* cassette, P1=ORS13, P2=ORS20 for *crt* cassette, P1=ORS17, P2=ORS20 for *ccr* cassette and P1=ORS44, P2=ORS45 for *ERG10* cassette (all primer sequences are listed in Table 2.3). Five PCR products of appropriate sizes were generated for both the B^R and B^S strains (Fig. 3.10) and they indicate that both strains appear to carry the five butanol synthetic genes at the correct loci.

3.10 Protein expression of the enzymes involved in the butanol synthetic pathway

In order to both confirm the validity of the strains and demonstrate high level expression of the butanol synthetic enzymes (Crt, Ccr, Hbd, AdhE2 and Erg10), protein extracts were prepared and Western blotting was performed using anti-Flag antibodies. Protein bands of appropriate sizes were observed for all of the single integrant strains and these same bands were also observed in the strains carrying all five genes. Interestingly, the Crt, Hbd, AdhE2 and Erg10 were found to be more highly expressed than Ccr, where the signal was significantly reduced (Fig. 3.11). The precise reason why the expression of the Ccr enzyme was lower than that of the other enzymes is unknown. Possible explanations could relate to the precise site of integration, the stability of the expressed protein or the mRNA half-life. However, what is apparent from the western analysis is that all of the exogenously added genes are expressed into protein and that there is little difference between the B^S and B^R strains in terms of levels of these proteins.

A



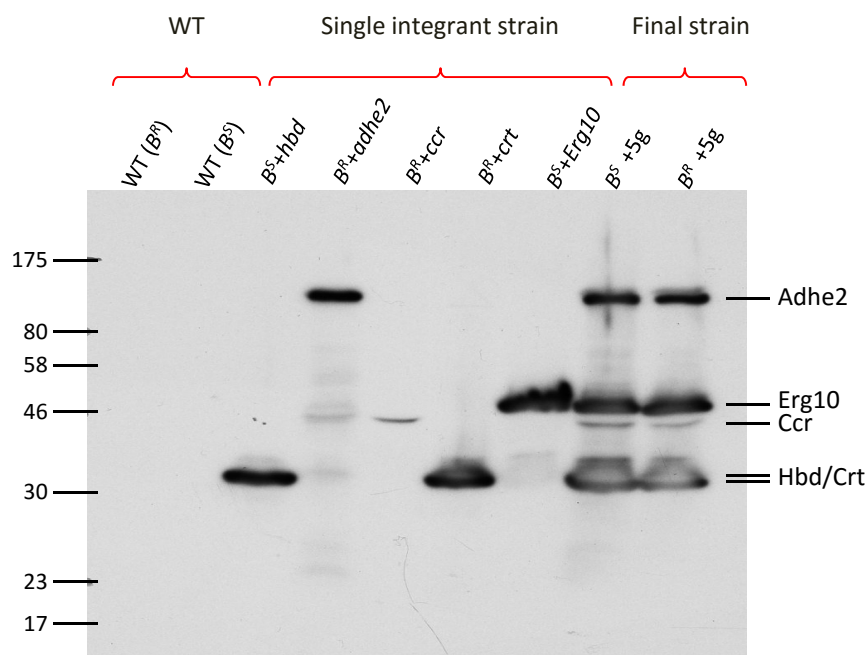
B

Table Expected product size

Gene	Expected band size
<i>crt</i>	2551
<i>ccr</i>	2318
<i>adhe2</i>	3576
<i>hbd</i>	1900
<i>Erg10</i>	199

Figure 3.10 Verification PCR to confirm five butanol synthetic genes (*crt*, *ccr*, *adhe2*, *hbd* and *ERG10*) are presented in *GCD1-S180* (*B^S*) and *GCD1-P180* (*B^R*) strains. A) Figure shows agarose gels of PCR products generated by amplifying a specific fragment from each gene *crt*, *ccr*, *adhe2*, *hbd* and *ERG10* by using the appropriate primers listed in Table 2.3. B) Table depicting the expected PCR product sizes.

A



B

Flag-tag-integrated protein for	Expected size (kDa)
Hbd	30.31
Adhe2	94.78
Ccr	40.04
Crt	28.17
Erg10	41.7

Figure 3.11 Protein expression from the single integrant and strains bearing all five genes. (A) Figure shows a western blot probed with anti-Flag antibodies where the protein samples were derived from the wild type, the single integrant strains and from the *GCD1-S180* (B^S) and *GCD1-P180* (B^R) strains that express all five butanol synthetic enzymes. The protein ladder sizes are depicted on the left and the proteins are labelled on the right, whereas the identity of the integrated gene and the type of strain are labelled above the blot. (B) A table of expected protein sizes for the Flag-tagged exogenous proteins.

3.11 Quantifying butanol and ethanol production by gas chromatography

The main aim of the project at this point was to quantify the fermentation products from the strains described above; particularly ethanol and butanol. In order to measure alcohol production during a 21 day semi-anaerobic fermentation, yeast strains were processed using a standard operating procedure (SOP) to minimise any differences across experiments (see Section 2.7). The yeast strains were inoculated in YPD media into small semi-anaerobic chambers at a starting OD₆₀₀ of 0.1 (at least 5 cultures per strain). Samples were collected over a 21 day period and the level of alcohols relative to standards was measured using GC-FID analysis (see Section 2.7).

Both the B^S and B^R strains carrying the full butanol synthetic pathway (B^R +5g and B^S +5g) produce a maximum of about 1.2% (v/v) ethanol after as little as 4 days. There was no significant difference between these two strains and the level of ethanol remained the same over the fermentation period. Both strains produce very small amounts of butanol: less than 10 ppm (Fig. 3.12). A result that is consistent with prior attempts to insert a butanol production pathway into yeast (Steen *et al.* 2008).

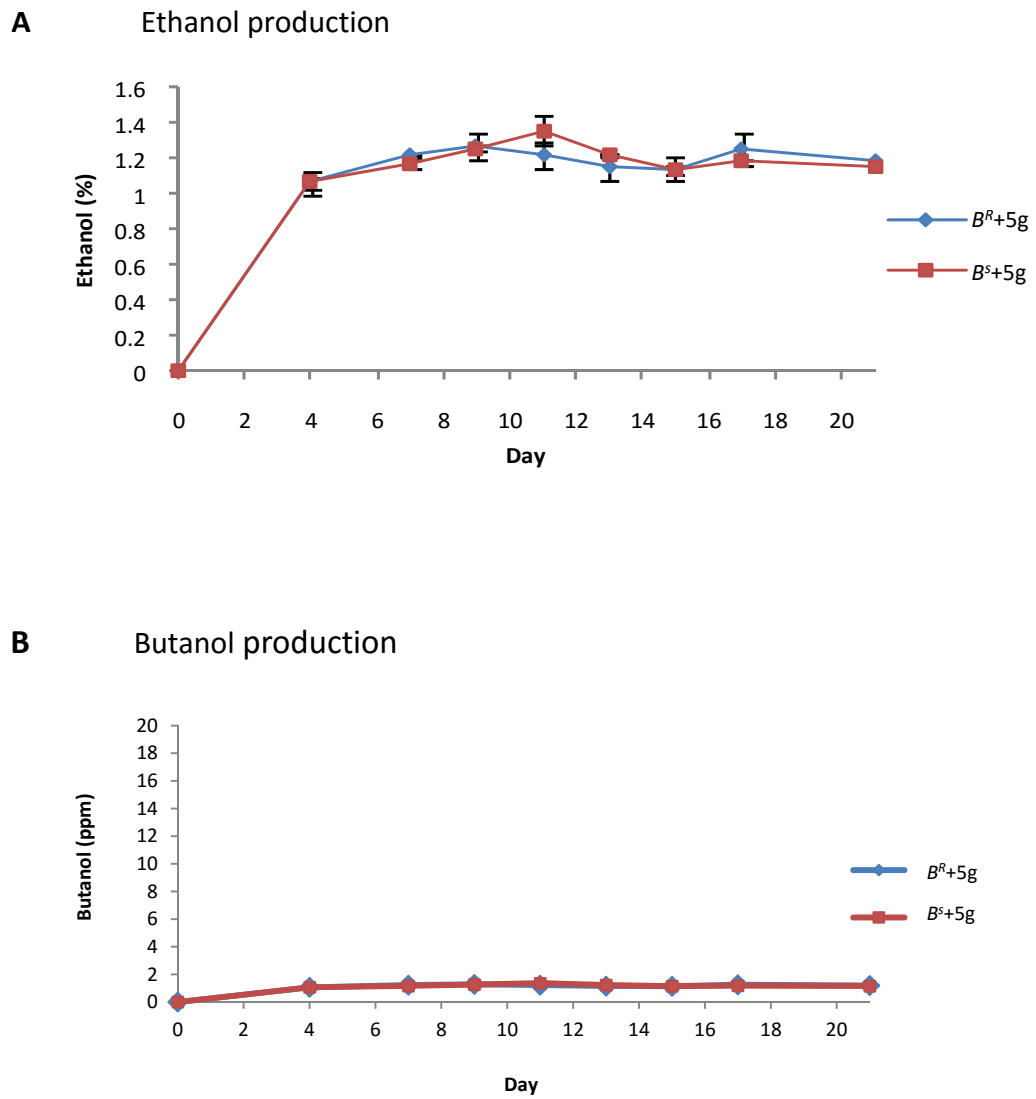


Figure 3.12 Ethanol and butanol quantitaion in media taken from strains bearing the five butanol production genes over a 21 day semi-anaerobic fermentation. The top graph represents the level of ethanol, while the graph underneath shows no significant production of butanol from either strain.

3.12 Discussion

The main aim of this project was to produce butanol from strains of *Saccharomyces cerevisiae*. Therefore a strategy was devised to generate a metabolically engineered strain of *Saccharomyces cerevisiae* bearing the five butanol synthesis genes (*hbd*, *adhe2*, *crt*, *ccr* and *ERG10*) all under the control of the *TDH3* promoter. Therefore, W303-1A was transformed individually with the five integration cassettes. The successful construction of these new single integration strains was validated using PCR analysis on genomic DNA from the transformants. A strategy was devised to generate a strain bearing all five integration cassettes via a series of backcrosses. As a result, the constructed strains, B^S+5g and B^R+5g, were successfully made.

All of the butanol synthetic genes were tagged with a Flag epitope, which enabled the protein expression levels to be assessed by western blotting. Crt, Hbd, AdhE2 and Erg10 are highly expressed in the single integrant strain and in the constructed strains, while the Ccr enzyme has a lower level of expression in both the single integrant strain and in the constructed strains. Ethanol and butanol levels were assessed for the constructed strains B^S+5g and B^R+5g strains by performing semi-anaerobic fermentation experiments. Both strains produce about 1.2% of ethanol and no significant levels of butanol. A number of possible explanations could account for the lack of butanol production. These include a lack of activity for one or more of the inserted genes, a lack of cytosolic acetyl-CoA to serve as a substrate for the pathway or a lack of reducing power to drive the pathway to completion.

To study these possibilities in more detail, a strategy will be undertaken to investigate whether metabolic engineering of key steps in the pathway will channel metabolites from glycolysis to the butanol synthetic pathway. Such strategies will not only provide more acetyl-CoA but they will provide the cells with greater reducing power.

A similar strategy to that described here has been used previously to attempt to produce butanol using *S. cerevisiae*. Here the *hbd*, *adhe2*, *crt*, *ccr* and *ERG10* genes were cloned into two shuttle vectors (Steen *et al.* 2008). This resulted in the production 2.5 mg/L of n-butanol when using 2% galactose as carbon source. *E. coli*

has also been used as a host for a similar butanol production pathway by introducing Clostridia genes *thl*, *hbd*, *crt*, *bcd*, *etfAB* and *adhe2* (Atsumi *et al.* 2008). This led to 139 mg/L under anaerobic conditions. Other studies have used *Clostridium saccharoperbutylacetomicum* and have enhanced butanol production by using lactic acid and pentose as co-substrates via fed-batch culture through ABE fermentation to give a maximum of 15.6 g/L butanol (Yoshida *et al.* 2012).

4. Development of n-butanol production from *Saccharomyces Cerevisiae* via the application of various metabolic engineering strategies

4.1 Introduction

In the previous chapter, a metabolically engineered strain of *S. cerevisiae* harbouring the heterologous ABE fermentation pathway in two wild type backgrounds (B^R and B^S) was generated. While these constructed strains produce similar levels of ethanol to the parental strains, they generate very little butanol (less than 10 ppm). Many factors could be contributing to the inability of these strains to produce butanol. For instance, the ABE pathway is mainly NADH dependent (Dong *et al.* 2015) and introduction of this heterologous pathway into yeast could potentially generate redox imbalance inside the cells. In addition, the supply of cytosolic acetyl-CoA, the precursor of the ABE pathway, could be limited. In contrast to many other eukaryotic cells, yeast produce acetyl-CoA in the cytoplasm during the metabolism of ethanol. However, the genes involved in this conversion are activated under glucose limiting/ respiratory conditions (Wu *et al.* 2004) In addition, the metabolism of yeast is geared towards the glycolytic conversion of glucose to ethanol, which competes with the ABE pathway through the consumption of most of the carbon source available.

Therefore, in this chapter a variety of metabolic engineering strategies to enhance the availability of acetyl-CoA will be explored. The first strategy that was undertaken was deletion of the major alcohol dehydrogenase *ADH1* (Leskovac *et al.* 2002), which is involved in ethanol production using NADH as a cofactor. *ADH1* deletion might lead to increased carbon flux from pyruvate toward butanol production via disruption of ethanol production and a resulting accumulation of acetaldehyde. This deletion should also improve NADH levels in the cytosol, as the alcohol dehydrogenase step is one of the major redox regulated reactions in yeast cells (Fig. 4.1). A second engineering strategy was designed as an attempt to improve butanol production further, by channelling the carbon flux towards the butanol synthetic pathway. A cassette was designed to constitutively express the *ALD6* and *ACS2* genes that encode enzymes involved in the conversion of acetaldehyde to acetyl-CoA. Ald6p is a cytosolic aldehyde dehydrogenase which uses $NADP^+$ as cofactor (Boubekeur *et al.*

2001) while, Acs2p is an acetyl-CoA synthase catalysing acetyl-CoA biosynthesis using ATP (Chen *et al.* 2012). The combination of the two strategies described above may have the added benefit that it would decrease the toxic impact of acetaldehyde accumulation in the *adh1Δ* mutant and as such lead to increased supplies of cytosolic acetyl-CoA. A further modification of this strategy would be a switch of the *ALD6* gene to *ALD2*. Ald2p is another cytosolic iso-enzyme of Ald6p which reduces acetaldehyde to acetate; however, Ald2p uses NAD⁺ as cofactor as opposed to NADP⁺. Therefore it is possible that this switch might not only channel carbon to the butanol pathway but also may provide greater NADH. Finally, a metabolic strategy was devised to explore the impact of deleting other competing pathways such as the glycerol biosynthetic pathway. Generally, the glycerol-3-phosphate dehydrogenases Gpd1p and Gpd2p are involved in glycerol production and use NADH as a cofactor (Albertyn *et al.* 1994). Previous studies have indicated that glycerol levels increase in strains lacking the *ADH1* gene (de Smidt *et al.* 2012). Therefore, deletion of the *GPD1* and *GPD2* genes might reduce the use of carbon in competing pathways, as well as increase levels of NADH for the butanol synthetic pathway.

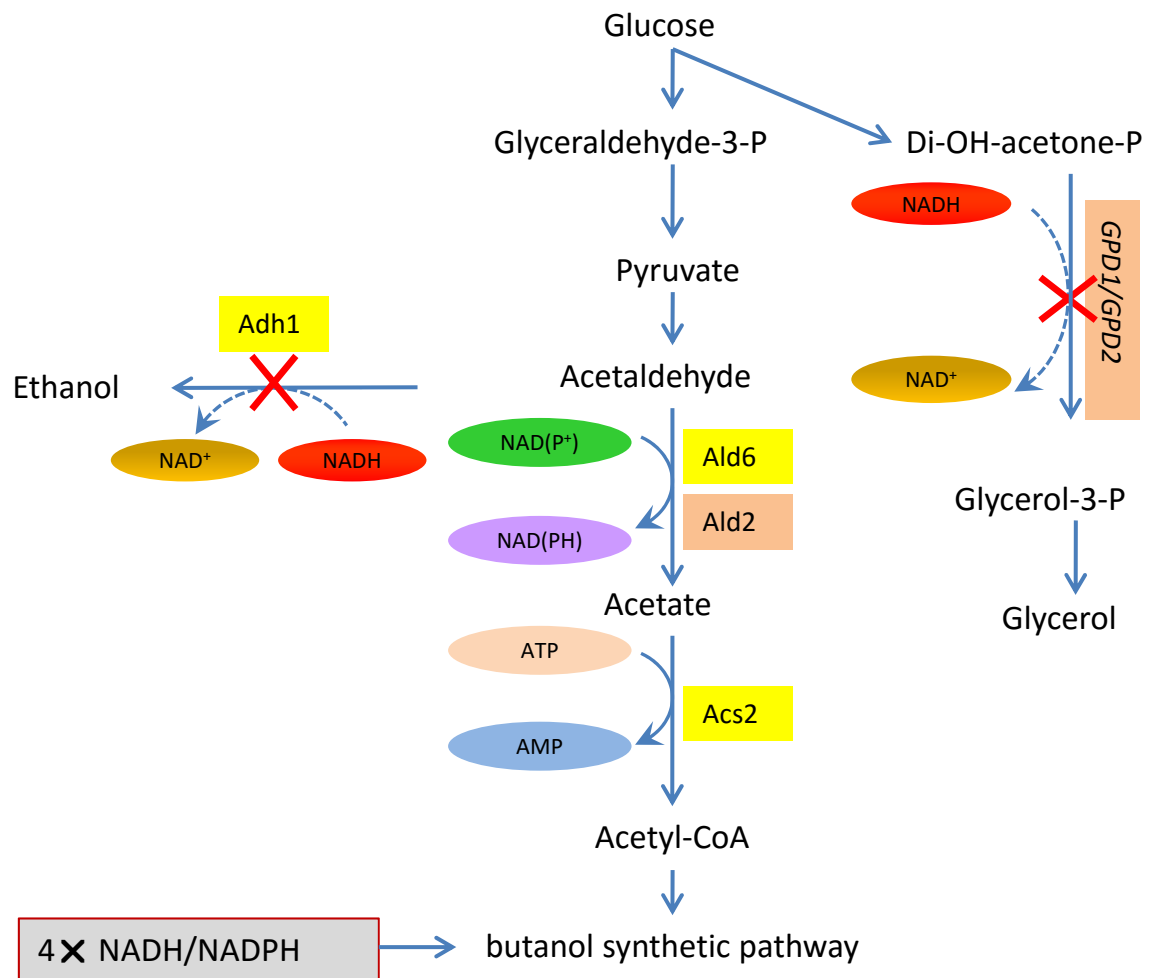


Figure 4.1 The metabolic engineering strategy used to direct the carbon flux from glycolysis to the butanol production pathway in *Saccharomyces cerevisiae*. Pyruvate is the end product of the glycolytic pathway and a variety of metabolites can be generated from it; such as, acetaldehyde, ethanol and acetyl-CoA. Acetyl-CoA is the precursor for butanol synthesis. Different strategies were employed in an attempt to improve metabolic flux to butanol, including:- *ADH1* deletion, *ALD6 ACS2* overexpression, *ALD2 ACS2* overexpression and *GPD1/GPD2* deletions.

4.2 Deleting major alcohol dehydrogenase *ADH1* from the constructed strains

One of the major limitations of introducing the ABE heterologous pathway into yeast is the potential for redox imbalance within the cell. As highlighted previously, the five added enzymes utilise 4 molecules of NAD(P)H to generate butanol and require a ready supply of acetyl-CoA. Therefore, the question as to whether the disruption of ethanol production by inactivation *ADH1* would lead to improve acetyl-CoA levels and ultimately increase n-butanol production was investigated.

Adh1p represents the major alcohol dehydrogenase in yeast (Leskovac *et al.* 2002) which plays an important role in the fermentation process (Fig. 4.2 A). Adh1p is involved in the reduction reaction of acetaldehyde to ethanol as a final step in glucose fermentation. While Adh1p is the major enzyme, the *S. cerevisiae* genome encodes four other alcohol dehydrogenases Adh2p, Adh3p, Adh4p and Adh5p. All of these enzymes apart from Adh2p are involved in ethanol metabolism via the reduction of acetaldehyde to ethanol, while Adh2p catalyzes the reverse reaction by oxidizing ethanol to acetaldehyde (Young *et al.* 1985; Bennetzen *et al.* 1982) and (Drewke *et al.* 1988).

4.3 Construction of various mutants with *ADH1* deleted

In order to target the *ADH1* gene for deletion, a strategy was devised whereby the *ADH1* gene was replaced with an *ADE2* marker cassette. The *ADE2* gene was amplified either from the pBEVYGA vector or directly from the genome from a strain yMK 1792 which has a functional *ADE2* gene. The deletion cassette was PCR amplified using specific integration primers P1=ORS46 and P2=ORS47, which are listed in Table 2.3. The resulting cassette was transformed into the yeast strains yMK2074 and yMK2076. Selection of the deletion mutants on selective SCD-ADE plates proved more complicated than anticipated, as many of the potential transformants were false positives in that they did not harbour the *ADE2* gene at the *ADH1* locus. It is possible that the high background of Ade⁺ colonies results from reversion of the auxotrophic *ade2-1* mutation at the genomic *ADE2* locus. Therefore, a secondary screen was devised during the course of the project and used to increase the likelihood of

obtaining a transformant lacking *ADH1* activity. More specifically, previous studies have shown that *adh1Δ* mutants are sensitive to the mitochondrial electron transport chain inhibitor, antimycin A (Paquin *et al.* 1986). Therefore, potential transformants were screened via a serial dilution analysis relative to the parent strains on Antimycin A plates. Any strains that exhibited sensitivity to Antimycin A also were white suggesting that they had a functional *ADE2* gene (Fig. 4.2 F). In order to further test whether the *ADH1* gene had been replaced by *ADE2* in the transformants, genomic DNA was prepared and a PCR based validation strategy was employed. Three different verification PCR reactions were performed by using the primers: P1=ORS48, P2=ORS49, P3=ORS50 and P4=ORS51 listed in Table 2.3. Figure 4.2 B provides a schematic representation of this PCR verification strategy where the first PCR product validates the upstream chromosomal insertion site, the second PCR product validates the downstream chromosomal integration site and the third PCR product spans the whole integrated cassette. The resulting PCR products from these reactions were separated on agarose gels (Fig. 4.2 C and 4.2 D). All of the PCR products for the mutants closely match the expected product sizes listed in table 4.2.E and are distinct from the pattern of products obtained for the parent strains bearing the wild type *ADH1* gene. From these results it was concluded that the *ADH1* gene had been successfully deleted from yeast strains both harbouring and lacking the exogenous ABE pathway genes. The single *adh1Δ* in the strain with the ABE pathway was done by Dr Hui Wang in the Ashe laboratory and all the rest of *adh1Δ* for other strains were made by Reem Swidah.

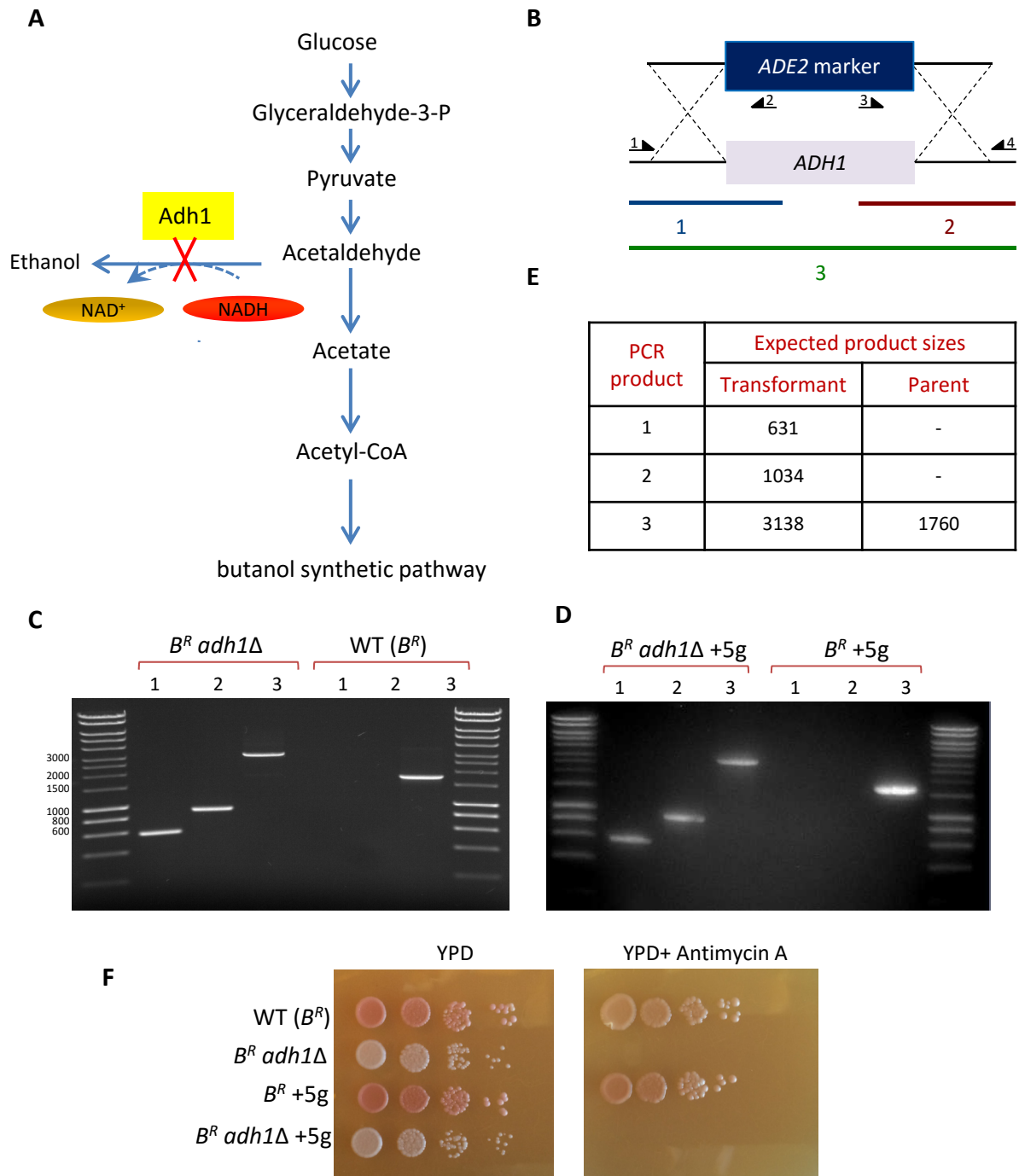


Figure 4.2 Construction and verification of the *ADH1* deletion from wild type strains (B^R) and strains bearing the butanol synthetic pathway (B^R+5g). A) Figure shows a schematic representation of how carbon flux might be channeled from the glycolytic pathway toward the butanol production pathway by *ADH1* deletion. The fact that *ADH1* deletion could also provide reducing power (NADH) that could drive the butanol synthetic pathway is highlighted. B) A schematic of the *ADH1* deletion strategy and the PCR-based strategy used to verify the genomic deletion of the *ADH1* gene using the verification primers (listed in Table 2.3). C) and D) Photographed agarose gels showing the electrophoresis of various PCR products generated from mutant and parental strain genomic DNAs. The PCR products closely match the theoretical sizes presented in the table (E). F) A serial dilution analysis of the parental and potential *adh1Δ* strains, shows that as would be anticipated for genuine *adh1Δ* strains, the generated mutants are sensitive to an inhibitor of respiration, Antimycin A.

At this stage of the project, a key question was whether deletion of the *ADH1* gene had any impact on butanol production for the constructed strains. Therefore, alcoholic fermentation experiments were performed. Pre-cultures were grown aerobically at 30 °C for one day and then diluted to a starting OD₆₀₀ of 0.1 in the semi-anaerobic vials for all the tested strains. At day 5 ethanol and butanol were measured relative to standards using GC. As described previously, both B^R and B^S strains bearing the ABE pathway (B^R +5g and B^S+5g) produce standard amounts of ethanol 1.2% relative to the wild type strains and very low levels of butanol less than 10 ppm (Fig. 4.3 A and B). Notably, the B^R*adh1Δ* strain has a massive reduction in ethanol production, the level of ethanol was less than 0.02% and surprisingly, this mutant was able to produce small amounts of butanol (40 ppm). This unexpected result was consistent with recently published observations showing that *S. cerevisiae* can produce butanol where *ADH1* is deleted via an endogenous threonine catabolic pathway in mitochondria (Si *et al.* 2014). However, deletion of the *ADH1* gene in the context of a strain bearing the exogenous ABE pathway (B^R*adh1Δ*+5g) achieved higher butanol production (200 ppm) and 0.4% ethanol levels compared to the strain lacking ABE exogenous pathway.

Another independent fermentation experiment was performed to confirm the impact of *ADH1* deletion on growth, ethanol and butanol production over 21 days under semi-anaerobic conditions. In terms of OD₆₀₀, the mutants lacking *ADH1* grow to low final OD₆₀₀ values under semi-anaerobic conditions when compared to the strains with *ADH1*. However, the presence of the exogenous ABE pathway in the B^R*adh1Δ*+5g strain does generate higher OD₆₀₀ than in the *adh1Δ* mutant lacking the ABE pathway (B^R*adh1Δ*) (Fig. 4.4 A). It is possible that the presence of the ABE pathway rescues growth to some extent by removing toxic intermediary metabolites such as acetaldehyde, pyruvate and acetic acid that accumulate in *adh1Δ* mutants. Alternatively, the exogenous *adhe2* gene from *Clostridium Beijerinckii* could at some low level complement the lack of *ADH1*.

The results for ethanol levels mirror what was observed for OD₆₀₀. So for the *adh1Δ* mutants, levels of ethanol varied depending upon whether the mutants harboured the ABE pathway. Specifically, the B^R*adh1Δ* strain produced less than 0.02%

ethanol, whereas the B^R *adh1Δ*+5g strain produces 0.4% ethanol (Fig. 4.4 B). It seems likely this difference stems from the improved growth characteristics of the strain.

In terms of butanol levels the repeat experiment over an extended time course paralleled the results described above over a 5 day fermentation. Hence, a very low yield of butanol was obtained for the B^R+5g strain, and the butanol level did not exceed 40 ppm for B^R*adh1Δ* strain. However, for the B^R *adh1Δ*+5g strain around 200 ppm of butanol was obtained (Fig. 4.4 C).

Noticeably therefore, the B^R *adh1Δ*+5g strain has grown better and produced more ethanol and butanol compared to the strain without the ABE pathway. However, when the butanol level was normalized to the OD₆₀₀ for both *ADH1* deletion strains, approximately the same level of butanol was produced per cell (Fig. 4.4 D). In conclusion, the deletion of *ADH1* has proved critical in improving butanol yields in the constructed strains, although it is unclear whether the improvement is due to activation of an endogenous pathway for butanol production or activation of this pathway combined with the ABE pathway.

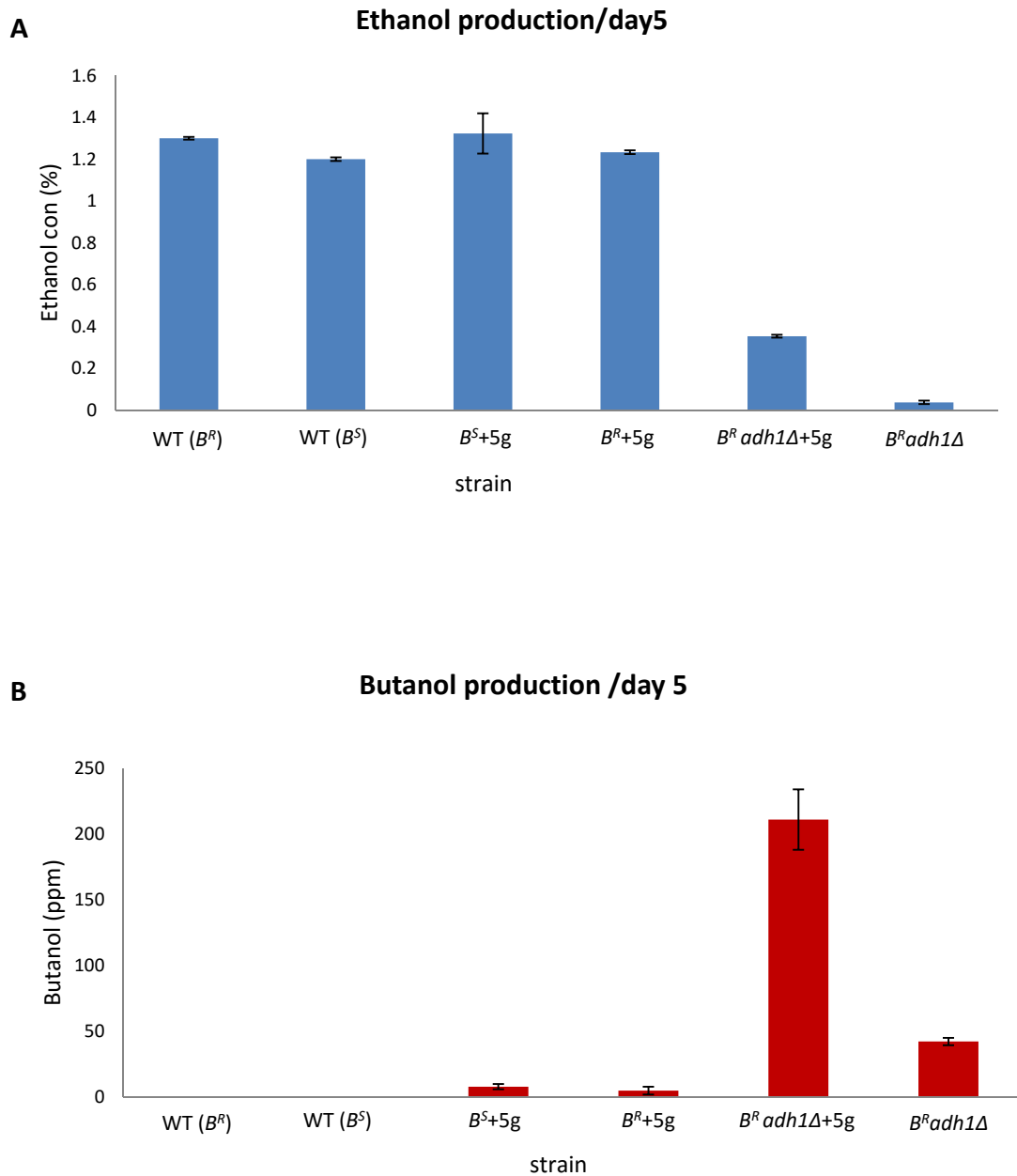


Figure 4.3 Ethanol and butanol levels in *adh1Δ* mutant strains and strains bearing the butanol synthesis pathway. A) Plot shows the level of ethanol produced in media collected from various strains growing semi-anaerobically for 5 days. B) Plot shows the butanol level in the media collected after 5 days. Columns and error bars correspond to the average value and standard deviations for three biological replicates for each strains

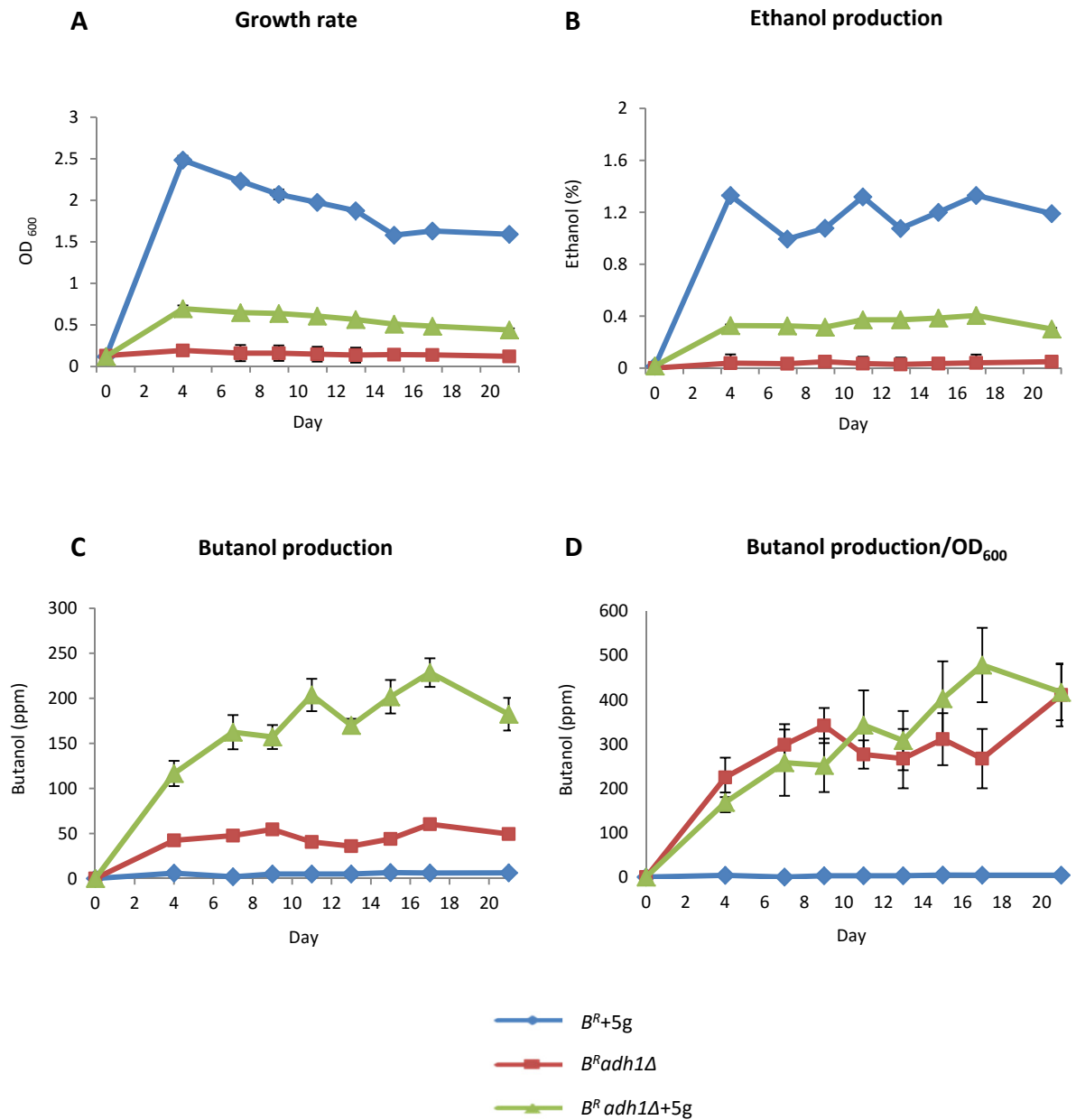


Figure 4.4 The effect of *ADH1* deletion on growth and ethanol or butanol production from the constructed strains under semi-anaerobic conditions. A) Diagram shows the OD₆₀₀ of the *adh1Δ* mutants and the parent strain with the exogenous ABE pathway. B), C) and D) Plots shows ethanol levels, butanol levels and butanol levels normalized to OD₆₀₀, respectively, in the parental and *adh1* mutant strains.

4.4 Expressing of the *ALD6* and *ACS2* genes with a view to improving butanol production in the various constructed strains of *Saccharomyces cerevisiae*

In order to attempt to improve butanol production further, a second approach was taken with the overall goal of increasing levels of cytosolic acetyl-CoA and hence channelling the metabolic carbon flux from the glycolytic pathway toward butanol production. This strategy was to over-express the aldehyde dehydrogenase and acetyl-CoA synthetase that between them catalyse the production of acetyl-CoA from acetaldehyde (Fig. 4.5 A). There are five yeast genes that encode the aldehyde dehydrogenase enzyme (*ALD2*, *ALD3*, *ALD4*, *ALD5* and *ALD6*) and two genes that encode the acetyl-CoA synthetase (*ACS1* and *ACS2*) (Chen *et al.* 2012). *ALD6* is recognised as a major cytosolic enzyme that uses NADP⁺ as a cofactor (Meaden *et al.* 1997; Navarro-Avino *et al.* 1999; Boubekour *et al.* 2001). The inability of *ALD6* null mutant strains to grow on ethanol or produce acetate during anaerobic growth suggests that this gene is a major source of the enzyme (Meaden *et al.* 1997). This phenotypic evidence combined with the fact that Ald6p is cytosolic and is thought to be constitutively expressed (Onodera *et al.* 2004; Meaden *et al.* 1997) provided the rationale for the selection of the *ALD6* gene here. For the acetyl-CoA synthetase, Acs2p is viewed as the active enzyme under anaerobic glucose fermentation (Takahashi *et al.* 2006; van den Berg *et al.* 1996) and the *ACS2* gene was therefore selected for over-expression.

Using a similar strategy to that taken for the genes of the ABE pathway, Peter Reid and Mark Ashe in the Ashe lab designed an *ALD6 ACS2* cassette. The *ALD6* gene with a flag epitope sequence was placed under the control of a *TDH3* promoter with the *CYC1* terminator sequence downstream of the gene, and the *ACS2* with the flag epitope sequence was placed under the control of the *TEF1* promoter with the *ADH1* terminator located downstream of the gene (Fig. 4.5 B). The gene cassettes were organised in tandem and placed upstream of a Hygromycin resistance gene marker. In addition, 200 bp flanking regions homologous to the *TRP1* locus were placed at either side of the whole cassette to direct integration via homologous recombination (Fig. 4.5 B). Finally, *BspQI* type IIS restriction sites were placed outside the cassette such that their cleavage site cleaved out the cassette without leaving any unwanted linker

sequences. The whole cassette was synthesized by Biomatik Corporation, Canada - Tradekey, the PBMH vector backbone to produce the plasmid pBMH-ALD6-ACS2--*hphNT1*

Therefore, I isolate the *ALD6 ACS2* cassette via restriction digestion of the pBMH-ALD6-ACS2-*hphNT1* using *BspQI* (Fig. 4.5 C). Even though the 329 bp band was only visible as a faint product, the digestion products correlated well with the theoretical band sizes (listed in table 4.5D). The whole digest was then used in a standard yeast transformation with the goal of directing the cassette to the *TRP1* locus via homologous recombination. Strains (both B^R and B^S versions) WT B^R lacking the ABE pathway and B^S bearing the ABE pathway B^S+5g or additionally carrying the *ADH1* deletion (B^S*adh1Δ*+5g and B^R*adh1Δ*+5g) were transformed with the cassette.

In order to confirm that the *ALD6 ACS2* cassette was integrated successfully at the *TRP1* locus, a confirmation PCR strategy was used (Fig. 4.6 A). The verification primers for the integration of *ALD6 ACS2* cassette are P1=ORS21, P2=ORS22, P3=ORS23 and P4=ORS24 listed in Table 2.3. Three different PCR reactions were performed: the first PCR product validates the upstream chromosomal integration site, the second validates the downstream chromosomal integration site, while the third PCR product spans the whole cassette. All PCR reactions were performed using genomic DNA from the potential *ALD6 ACS2* integrants relative to the parental strains (Fig. 4.6 B, C, D and E). The size of the fragments relative to the theoretical products (table 4.6F) indicates that the *ALD6 ACS2* cassette was integrated successfully in each of the strains.

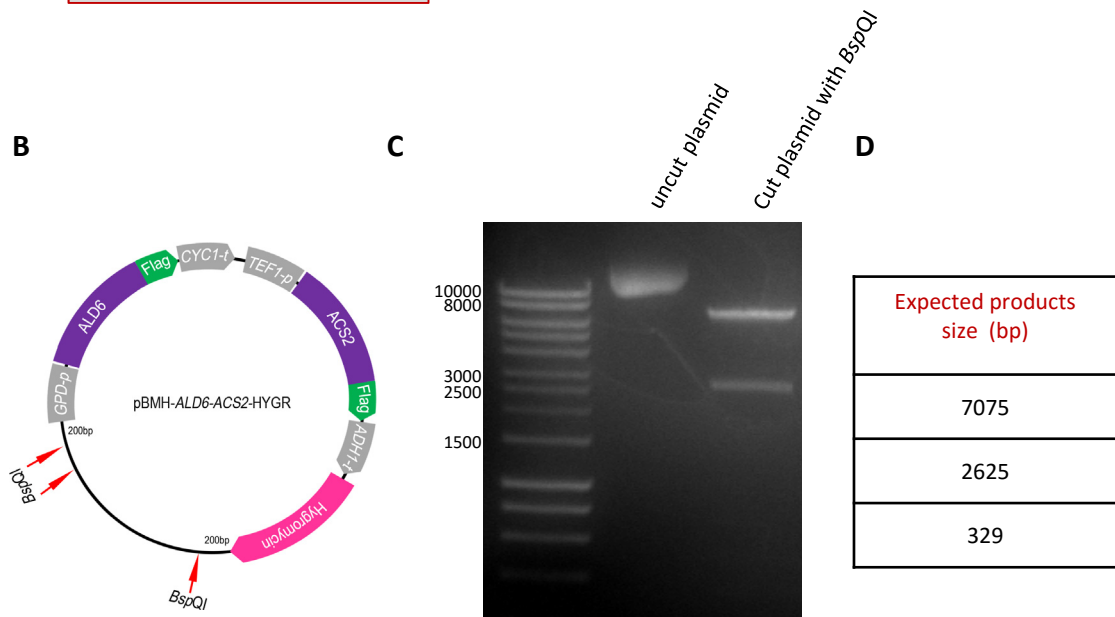
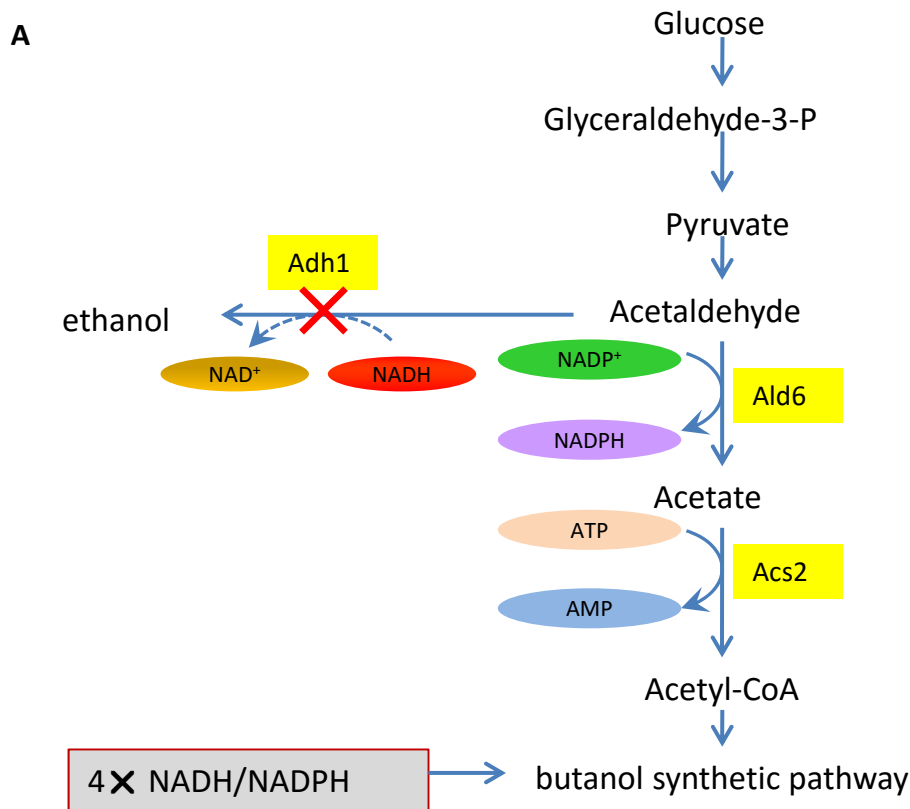


Figure 4.5 Strategy for improving butanol production by combining *ADH1* deletion with *ALD6 ACS2* over-expression. A) Figure shows a schematic representation of how cytosolic Acetyl-CoA could accumulate in the cell with over-expression *ALD6* and *ACS2*. The carbon flux is directed from glycolytic pathway toward butanol production pathway, Ald6p converts acetaldehyde to acetate while, Acs2p is involved in Acetyl-CoA synthesis. B) Schematic representation of the positions of *BspQI* restriction site used for generation the integration cassette containing the *ALD6* and *ACS2* genes. C) Photographed agarose gel showing *BspQI* digestion products of the plasmid pBMH-*ALD6-ACS2-HYGR*. The size of the digestion products on the agarose gels closely match the theoretical size. D) Table shows the expected digestion product sizes.

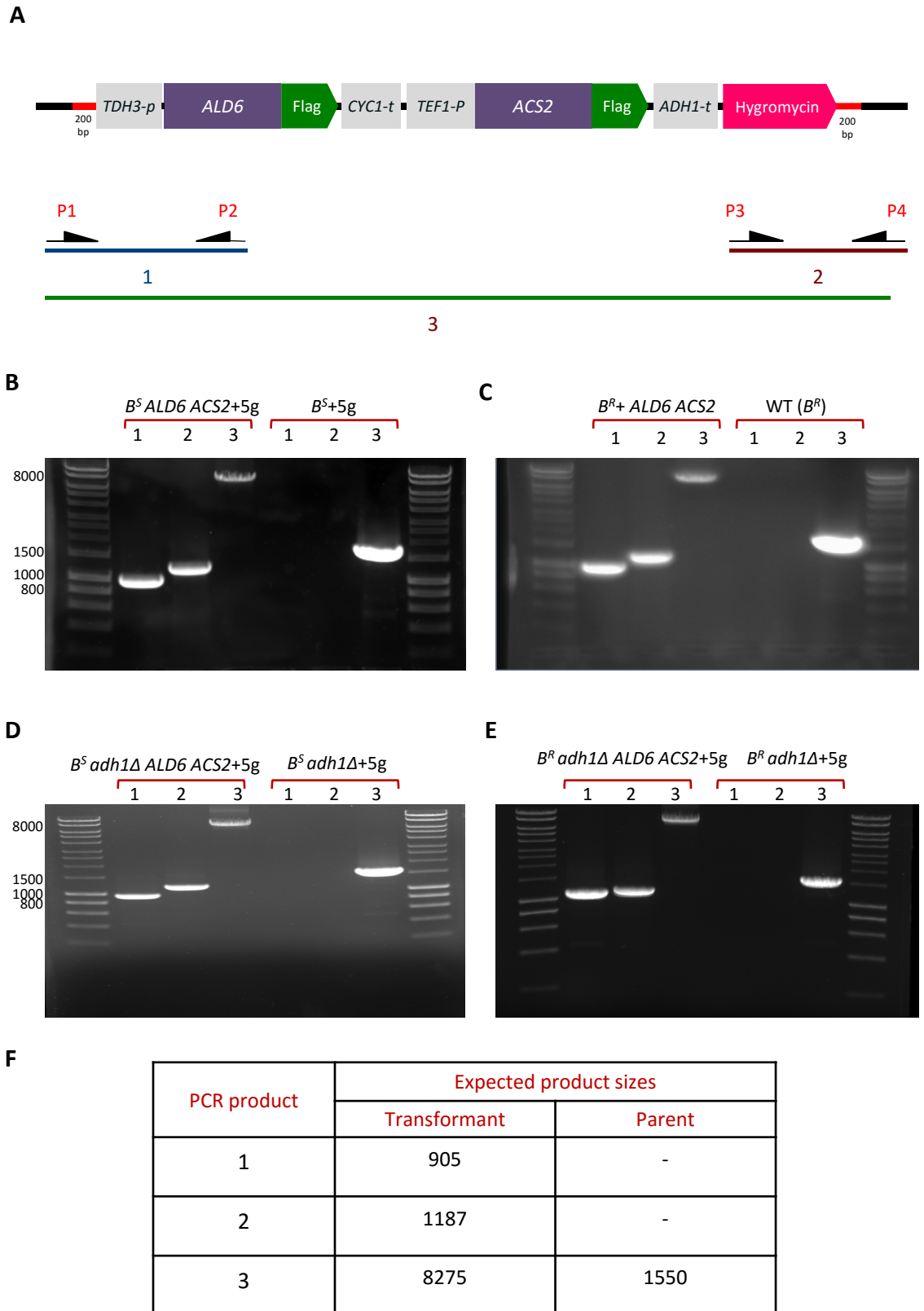
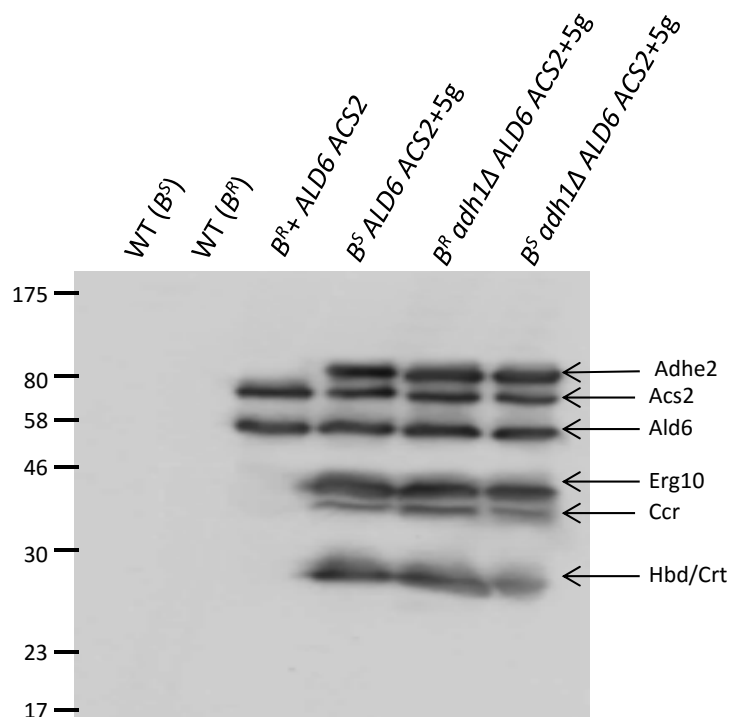


Figure 4.6 Integrating *ALD6* and *ACS2* cassette in *TRP1* locus. A) Schematic representation of the PCR strategy used to verify the successful genomic integration of *ALD6 ACS2* for each mutant using the verification primers listed in Table 2.3. B), C), D) and E) photographed gels showing the PCR products derived from genomic DNA prepared from *ALD6 ACS2* integrants and the parental strains. F) A table showing the theoretical sizes of the PCR products from these strains.

4.5 Detecting protein expression for all the constructed strains that over-express the *ALD6 ACS2* cassette

In order to assess whether proteins of an expected size for Ald6p and Acs2p are produced in the constructed strains, whole cell protein extracts were prepared from a host of strains. The single integrant strain ($B^R + ALD6 ACS2$) bearing just the *ALD6 ACS2* cassette was used as a control and other strains bearing the ABE pathway with the *ALD6 ACS2* cassette were tested (e.g. $B^S ALD6 ACS2+5g$, $B^S adh1\Delta ALD6 ACS2+5g$ and $adh1\Delta.ALD6 ACS2 B^R+5g$). An anti-flag antibody was used for immunoblotting as all of the integrated genes carry flag epitopes at their C-terminus to allow protein detection. Bands corresponding to the size of Ald6p and Acs2p were detected in all strains that carried the cassette. Indeed in the single integrant strains these were the only bands detected. No background was observed in the progenitor strains (WT (B^R) and WT (B^S)) (Fig. 4.7 A). In conclusion, bands corresponding to all of the integrated proteins Adhe2, Acs2p, Ald6p, Erg10p, and Crtp were detected. The band for Ccrp appeared less intense as mentioned previously (Fig. 3.11 A), therefore it is possible that the expression of this protein is lower than the others in the ABE pathway. All of the integrated proteins for the constructed strains closely match the expected protein sizes listed in (Fig. 4.7 B).

A



B

Flag-tag-integrated protein for	Predicted size (kDa)
Adhe2	95.9
Acs2	76.62
Ald6	55.62
Erg10	42.82
Ccr	41.16
Crt	29.29

Figure 4.7 Protein expression of the Ald6 and Acs2 enzymes. A) Figure shows a western blot probed with anti-Flag antibodies where protein samples were derived from the single integrant strains and the combined strains in both the *GCD1-S180* (B^S) and *GCD1-P180* (B^R) backgrounds. Protein marker sizes are depicted on the left and the proteins are labelled on the right of the blot. The identity of the strain used to generates the protein sample is labelled over the blot. B) A table of predicted protein sizes for the Flag-tagged exogenous proteins.

4.6 Quantification of fermentation products from the *ALD6 ACS2* expressing strains

Following the successful construction of various strains with highly expressed *ALD6 ACS2* genes, the focus turned to an investigation of the impact of these genes on butanol and ethanol production. Therefore, fermentations were carried out according to the SOP defined in section 2 Materials and Methods. Firstly, the capacity of *ALD6* and *ACS2* expression to improve butanol production in *adh1Δ* strains bearing the ABE pathway was assessed. Therefore, butanol production was compared in the B^R *adh1Δ*+5g strain and the new strain B^R *adh1Δ ALD6 ACS2*+5g harbouring the *ALD6 ACS2* cassette. No significant difference was observed in the growth between these two mutants that both lack *ADH1*, as both strains grow comparably to low OD₆₀₀ values relative to the parent strain B^R+5g (Fig. 4.8 A). Equally, only the parent strain B^R+5g produces high levels of ethanol (around 1.2-1.4% (v/v)), while as might be expected for *adh1Δ* strains, the B^R *adh1Δ*+5g and B^R *adh1Δ ALD6 ACS2*+5g strains only accumulate ethanol to about 0.3% (v/v) (Fig. 4.8 B). Interestingly, expression of the *ALD6 ACS2* cassette had a positive effect on butanol production: the level of butanol was increased ~80% in the B^R *adh1Δ ALD6 ACS2*+5g (butanol ~350 ppm) compared to the B^R *adh1Δ*+5g strain (~200 ppm butanol) over the fermentation period (Fig. 4.8 C). When the butanol levels were normalised to the OD₆₀₀, all the constructed strains gave similar patterns (Fig. 4.8 D). Therefore, *ALD6 ACS2* expression gives greater butanol production in the constructed strain bearing the ABE pathway and lacking *ADH1* activity. It is clear from the figure 4.8 the improved butanol is not a result of improved growth. Therefore, the impact of *ALD6 ACS2* on growth in *adh1Δ* strains may occur as a result of decreased accumulation of toxic intermediates such as acetaldehyde and acetate. If these are metabolised to cytosolic acetyl-CoA this could explain the improvement in butanol levels.

In order to assess whether *ALD6 ACS2* expression had any impact in an *ADH1* wild type strain bearing the ABE pathway, a B^S *ALD6 ACS2*+5g was used. As expected, this strain grows to a higher OD₆₀₀ and produces more ethanol than *adh1Δ* mutant strains (B^R *adh1Δ ALD6 ACS2*+5g and B^S *adh1Δ ALD6 ACS2*+5g) (Fig. 4.9 A and B). A comparison of butanol synthesis over the fermentation for the B^S *ALD6 ACS2*+5g and B^S *adh1Δ ALD6 ACS2*+5g strains showed that expression of the *ALD6 ACS2* cassette was

not sufficient to promote butanol synthesis, and that *ADH1* deletion was essential in this context (Fig. 4.9 C).

Intriguingly it was noted at this stage of the project that the butanol resistant strain (B^R *adh1Δ* *ALD6 ACS2*+5g) produced higher levels of butanol (1.5-2 fold) than the butanol sensitive strain (B^S *adh1Δ* *ALD6 ACS2*+5g). Moreover, the resistant mutant produced slightly lower levels of ethanol, especially at early points in the fermentation period. It is therefore possible that butanol resistant strains have greater capacity for butanol production and that this has knock-on effects in terms of carbon flux to ethanol. Previous studies from the Ashe lab have characterised the But^S (B^S) and But^R (B^R) phenotypes and shown that they are entirely dependent upon a specific allelic change in the *GCD1* gene (encoding the γ subunit of eIF2B). Proline at residue 180 gives a resistant phenotype whereas a serine at this position increases butanol sensitivity (Ashe *et al.* 2001; Taylor *et al.* 2010). This result and the question as to whether butanol resistant strains can produce more butanol is covered in much greater detail in Results Chapter 6.

Overall it appears that expression of *ALD6 ACS2* can help to improve butanol production in yeast bearing a butanol production pathway, but only when combined with an *ADH1* deletion.

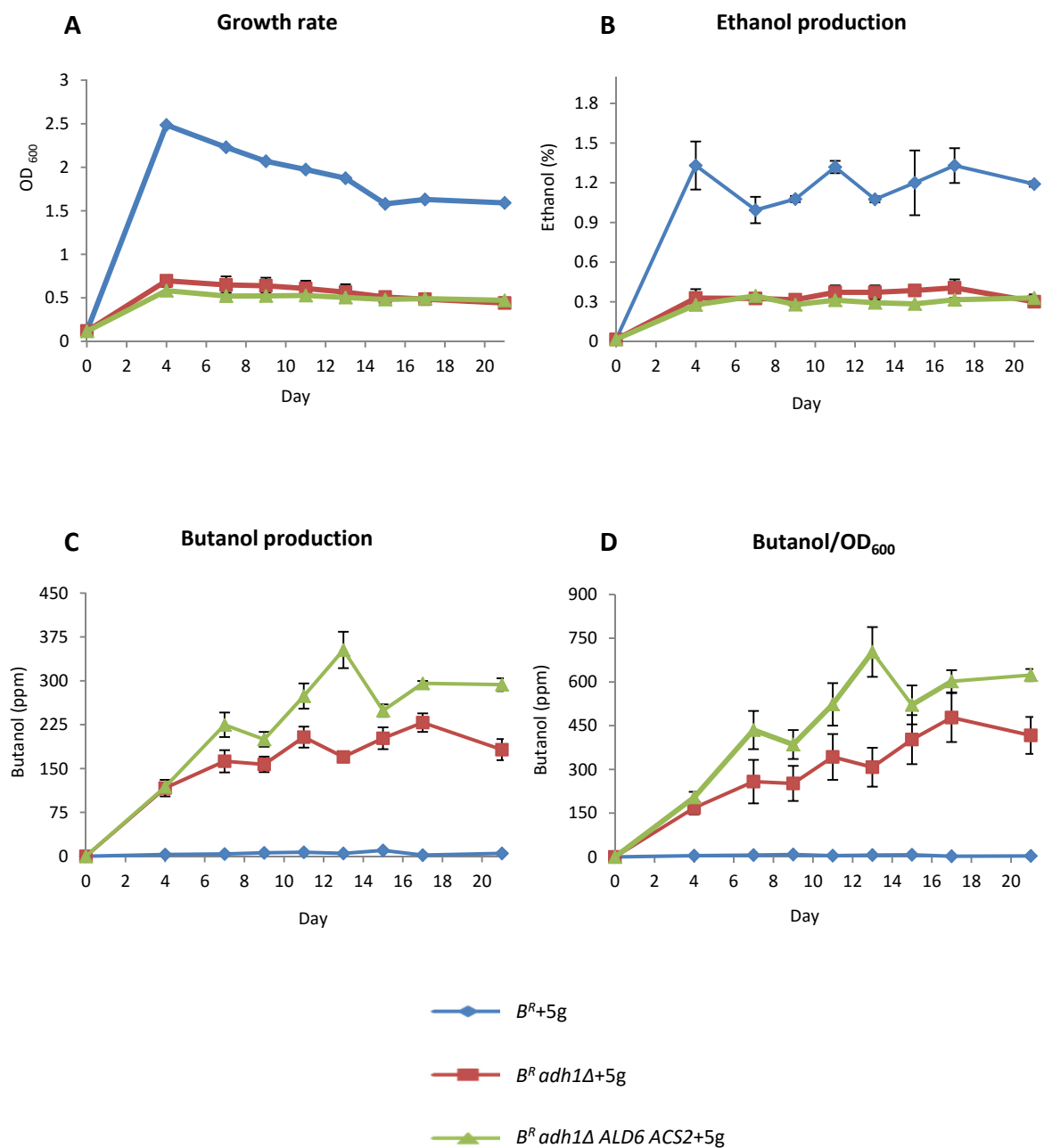


Figure 4.8 Improving butanol production by integration of an *ALD6 ACS2* expression cassette. Plots show measurement of various parameters for all constructed strains with/without the *ALD6 ACS2* expression cassette:- A) Growth rate, B) ethanol levels, C) butanol levels and D) butanol levels normalised to OD₆₀₀.

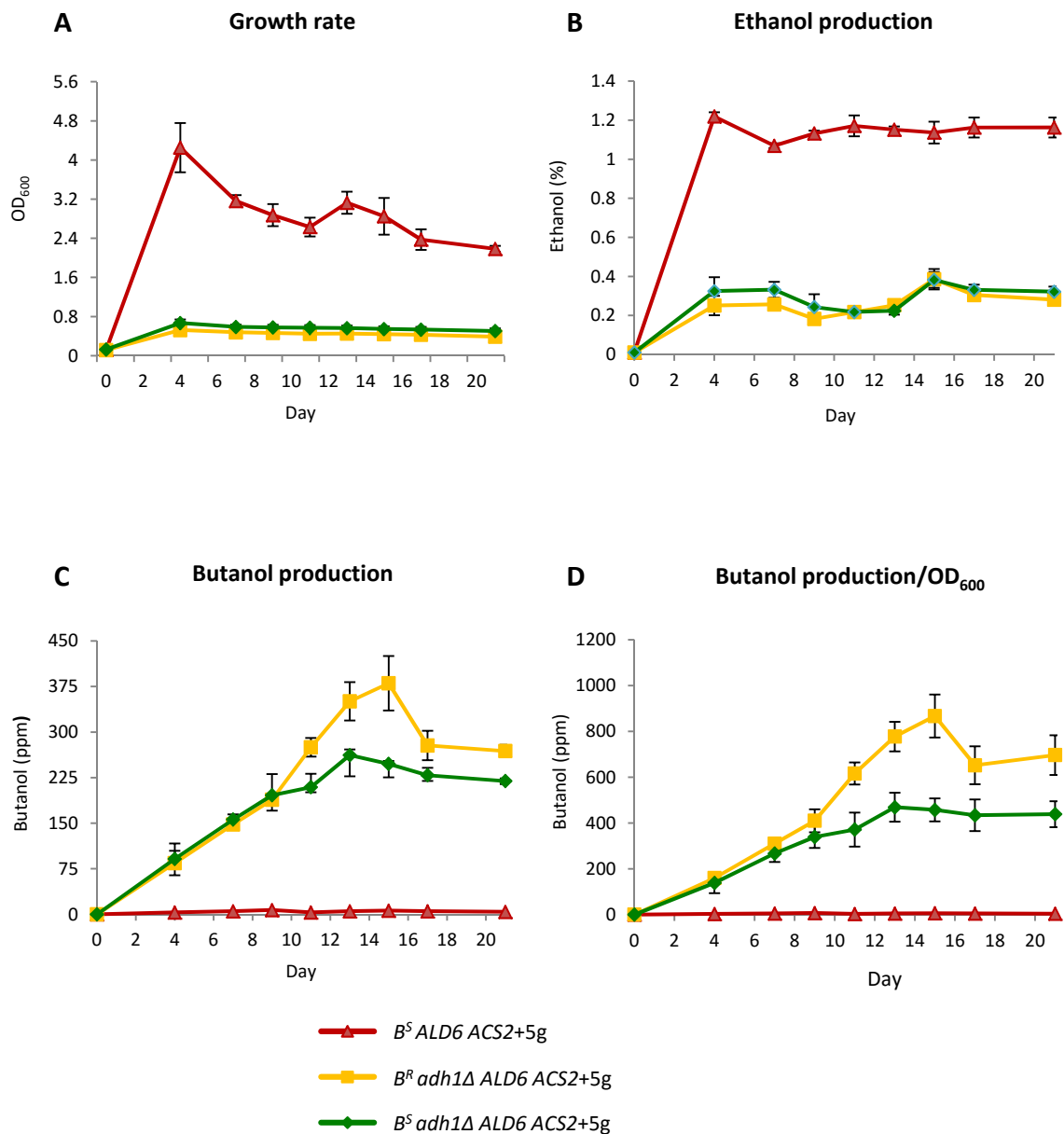


Figure 4.9 Integration of the *ALD6 ACS2* cassette without *ADH1* deletion does not improve butanol production in the strain bearing ABE pathway. Plots show measurement of various parameters for all constructed strains with/without the *ALD6 ACS2* expression cassette:- A) Growth rate, B) ethanol levels, C) butanol levels and D) butanol levels normalised to OD₆₀₀.

4.7 Construction of strains expressing *ALD2 ACS2* as an alternative to *ALD6 ACS2*.

At this stage of the project, the question was raised as to whether the Ald6p aldehyde reductase was the wisest choice of enzyme for the strategy described above. This enzyme uses NADP^+ as a cofactor to produce NADPH (Meaden *et al.* 1997), (Navarro-Avino *et al.* 1999), (Boubekeur *et al.* 2001), whereas the enzymes of the butanol pathway require NADH. Therefore, the decision was made to investigate whether replacement of Ald6p with Ald2p could increase butanol yield in the system. Ald2p catalyses the reduction of acetaldehyde to acetate using NAD^+ as cofactor (Aranda *et al.* 2003); therefore, as well as facilitating higher production of cytosolic acetyl-CoA, this enzyme could help to restore any redox imbalance in the cell that might be caused by butanol synthesis.

The plasmid bearing the *ALD2 ACS2* cassette was generated using a replacement strategy where *ALD6* was precisely switched for *ALD2* in the pBMH-*ALD6-ACS2-hphNT1* plasmid (Fig. 4.10). As such, *Bam*HI and *Ppu*MI restriction enzymes were used to remove *ALD6*: *Bam*HI cuts upstream of *ALD6*, while *Ppu*MI cuts within the *CYC1* terminator (Fig. 4.10 A). At the same time, any components removed from the vector by using these enzymes needed to be re-inserted at the same time as the *ALD2* coding sequence (i.e the Flag tag and the small part of the *CYC1* terminator). In order to achieve this specific primers were designed: the forward primer (ORS25) was precisely homologous to the upstream region of *ALD2* and carried a *Bam*HI site, whereas the reverse primer (ORS26) contained a section homologous to the downstream region of *ALD2* as well as a section to replace removed elements (the Flag and a small part of the *CYC1* terminator sequence) and a *Ppu*MI site was included (Fig. 4.10 B). The coding sequence of *ALD2* was PCR amplified with the primers described above using genomic DNA prepared from the W303-1A (B^R) strain (yMK23). This product was then sub-cloned into the pGEM-T Easy plasmid using the TA cloning method. Insert and vector for the *ALD6* replacement cloning were then generated using *Bam*HI and *Ppu*MI on the pGEM-Teasy *ALD2* and pBMH-*ALD6-ACS2-HYGR* constructs respectively (Fig. 4.10 C). The vector and insert were then gel purified and DNA ligation reactions were set up which were transformed into *E. coli*. Plasmid was prepared from potential transformants and screened by restriction digestion with

*Bsp*QI. Plasmids were selected where three digestion products that closely matched the theoretical sizes depicted in the table were evident (Fig. 4.10 F and H). To ensure that mutations had not been generated during the amplification/ sub-cloning procedure, the entire *ALD2* gene within the new plasmid template was sequenced and no errors were identified. The resulting plasmid was called pBMH-*ALD2*-ACS2-HYGR and bacteria carrying this plasmid were archived in the Ashe lab bacterial strain collection as BMK730.

The procedure for integration of the *ALD2 ACS2* cassette into the yeast genome is essentially identical to that used for the *ALD6 ACS2* cassette. In brief, *Bsp*QI digestion generates a cassette with 200 bp flanking regions homologous to part of the *TRP1* locus, such that the fragment can be integrated at this site. The digested cassette was transformed directly into the B^R *adh1Δ*+5g and B^S *adh1Δ*+5g strains. In order to verify the successful integration of the cassette into the *TRP1* locus in potential transformants, a standard confirmation PCR strategy using the verification primers on genomic DNA: P1=ORS27, P2=ORS22, P3=ORS23 and P4=ORS28 listed in Table 2.3 (Fig. 4.11 A). A comparison of the pattern of bands obtained from the three PCR reactions (Fig. 4.11 C and D) with the expected sizes (Fig. 4.11 B) shows that transformants, where successful integration has occurred, have been generated for each of the strains used.

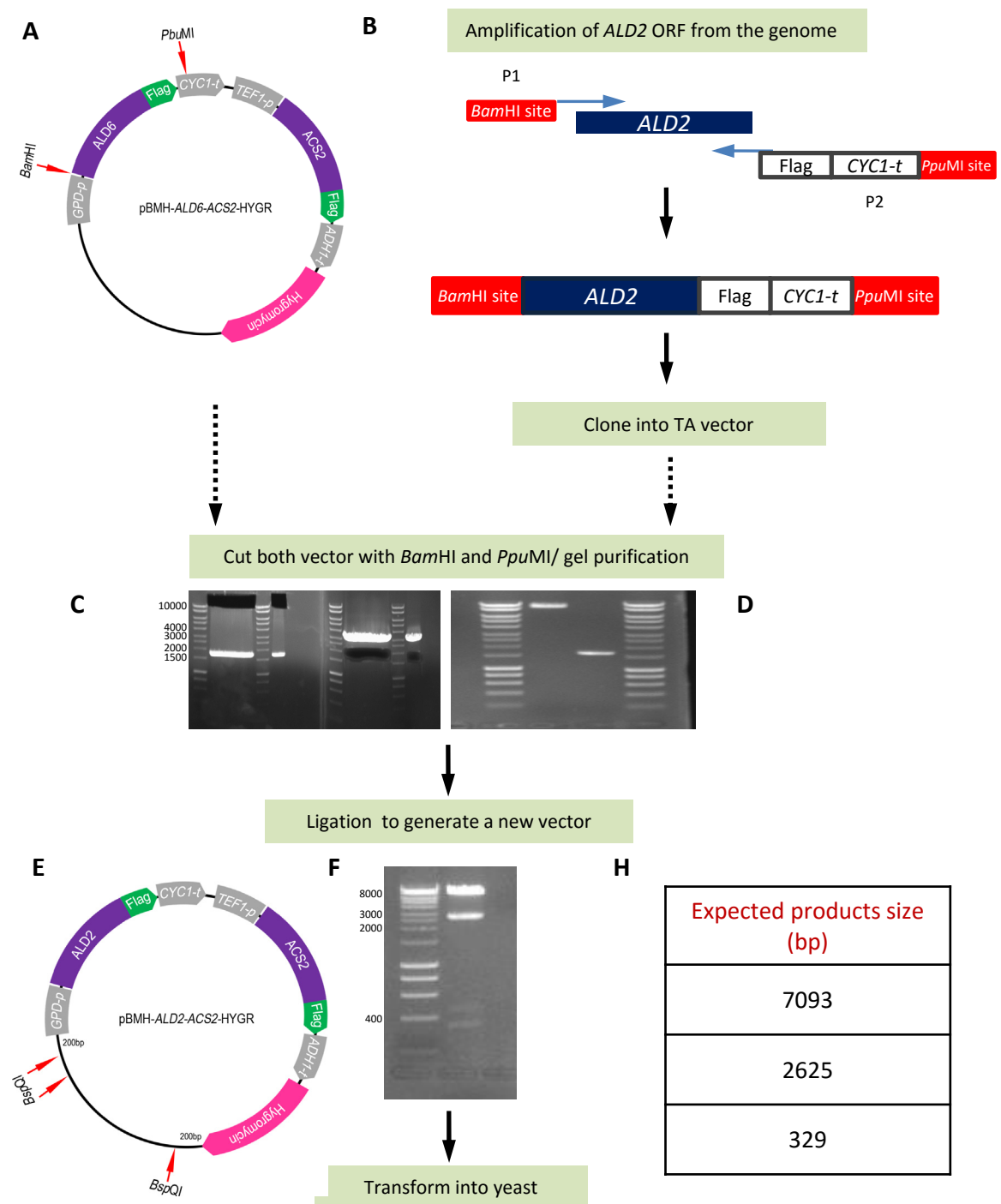


Figure 4.10 Strategy used to replace *ALD6* with *ALD2* in the expression cassette. A) Schematic representation of the restriction sites for the enzymes *Bam*HI and *Ppu*MI on the plasmid templates. B) Strategy used to generate a new construct bearing the *ALD2* gene in place of *ALD6*. The *ALD2* ORF was PCR amplified using primers designed to include the Flag and the restriction sites for *Bam*HI and *Ppu*MI flanking the ORF (see Table 2.3). The PCR product was sub-cloned into the pGEM-T Easy Vector. C) An agarose gel showing the digestion products for both the vector and insert with *Bam*HI and *Ppu*MI. D) Analysis of gel purified fragments where the gel shows the ratio between the vector and insert used in the ligation reaction. E) Schematic representation of the new construct and the restriction sites for *Bsp*QI. F) Agarose gel separating *Bsp*QI digestion products. H) The theoretical sizes of the digestion products.

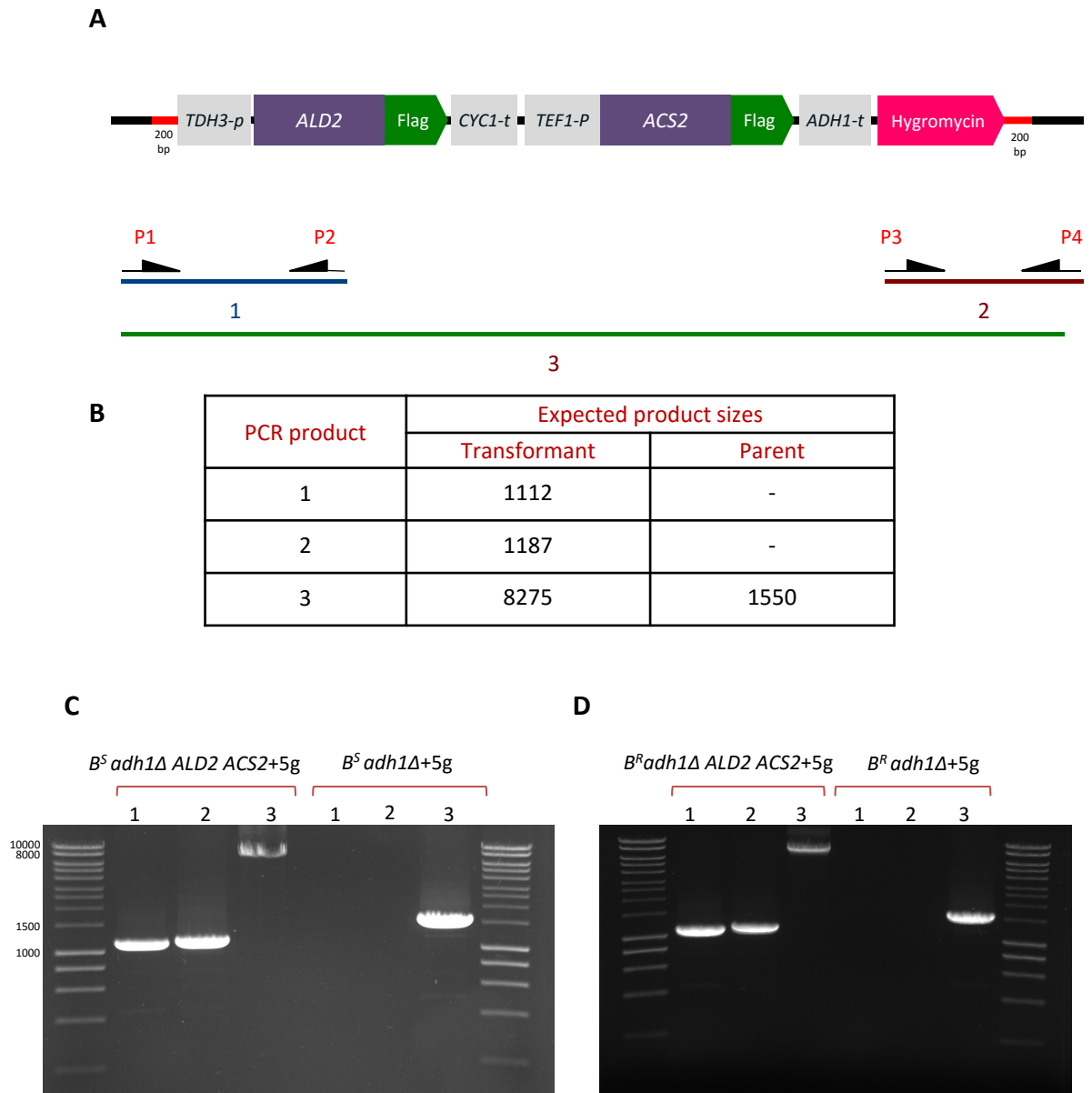
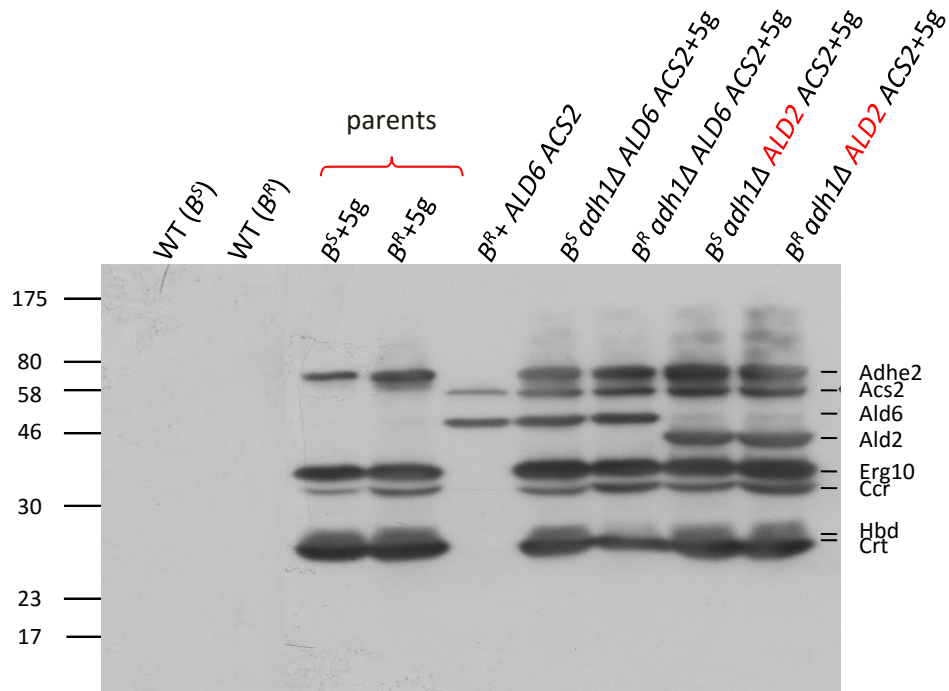


Figure 4.11 Integrating *ALD2 ACS2* cassette in *TRP1* locus. A) Schematic representation of PCR strategy used to confirm the successful integration of the *ALD2 ACS2* cassette into the *TRP1* locus using the verification primers listed in Table 2.3. B) A table showing the theoretical sizes of the PCR products from these strains. C) and D) Photographed gels showing the PCR products derived from genomic DNA prepared from *ALD6 ACS2* integrants and the parental strains.

4.8 Ald2p and Acs2p protein detection in the various constructed strains.

A further important experiment was to investigate whether the *ALD2 ACS2* cassette was directing expression of appropriately sized proteins in the new strains. In order to assess this, whole cell protein extracts were prepared from various strains bearing the cassette as well as the parental strains, and immunoblotting with anti-Flag antibodies was carried out. Proteins of appropriate size for all of the integrated genes that carry the C-terminal flag tags were observed (Fig. 4.12 A). Comparison to control strains and the expected sizes (Fig. 4.12 B) allowed the identification of these protein bands (see also Fig. 3.11 and 4.7). As described previously, the proteins of the ABE pathway, Adhe2p, Hbdp and Crtp and Erg10p appear equivalently expressed, whereas Ccrp protein expression seemed weaker. For the added yeast genes, protein levels for Acs2p, Ald6p, Ald2p seemed equivalent and high to the other added gene. One unusual observation was that Ald2p was expected to yield a similar sized band to Ald6p (Fig. 4.12 B). However, the blot clearly shows that Ald2p is migrating as if it were at least 1 kDa smaller than Ald6p (Fig. 4.12 A). One possible explanation for this would be that a mutation to the *ALD2* start codon was leading to expression from a downstream in-frame AUG codon to generate smaller protein product. In order to ensure that there is no such mutation across the entire *ALD2* gene, it was sequenced again after amplification from genomic DNA and compared to the sequence from the pBMH-*ALD2-ACS2-hphNT1* plasmid. No mutations were identified across the genomically integrated *ALD2* sequence, therefore it was assumed that the altered mobility might represent some subtle difference in the structure of Ald2p relative to Ald6p.

A



B

Flag-tag-integrated protein for	Expected size (kDa)
Adhe2	95.9
Acs2	76.62
Ald6	55.62
Ald2	56.32
Erg10	42.82
Ccr	41.16
Crt	29.29

Figure 4.12 Protein expression of the Ald2 and Acs2 enzymes. A) Figure shows a western blot probed with anti-Flag antibodies where protein samples were derived from the various integrant strains combined in both the *GCD1-S180* (B^S) and *GCD1-P180* (B^R) backgrounds. Protein marker sizes are depicted on the left and the proteins are labelled on the right of the blot. The identity of the strain used to generates the protein sample is labelled over the blot. B) A table of predicted protein sizes for the Flag-tagged exogenous proteins. The migration of Ald2 protein appears different to the theoretical value.

4.9 Quantifying butanol and ethanol yield from *ALD2 ACS2* strains

The next step was to compare butanol production in strains with the *ALD6 ACS2* cassette relative to those carrying *ALD2 ACS2*. The strains tested were either butanol resistant or sensitive; they carried the ABE pathway and they were deleted for *ADH1*.

Over the course of the standard semi-anaerobic fermentation, strains bearing *ALD2 ACS2* grow to similar OD₆₀₀ values and produce similar quantities of ethanol compared to strains carrying *ALD6 ACS2* (Fig. 4.13 A and B). When butanol levels were measured over the same fermentations, the situation was slightly more complex (Fig. 4.13 C). The B^R *adh1Δ ALD6 ACS2*+5g strain generated the highest butanol levels at about 350 ppm and as described above (e.g. see Fig. 4.9 C) the butanol yield was higher in the B^R strain relative to the B^S strain. For the matching strains carrying the *ALD2 ACS2* cassette no improvement in butanol production was observed; in fact the yield was slightly lower compared to the *ALD6 ACS2* strains. A small difference between the B^R and B^S strain was observed but this was not as substantial as the difference observed between B^R and B^S strains for the *ALD6 ACS2* strains. The differential production in B^R versus B^S strains will be explored in much greater detail in Results chapter6.

The fact that expression of Ald2p did not improve butanol yields could suggest that providing the butanol synthetic pathway with NADH molecules as opposed to NADPH was not important for improving flux towards butanol production in cells. Alternatively, Ald2p may be less active or somehow functionally compromised relative to the Ald6p enzyme. This is perhaps supported by the slightly reduced butanol levels from the *ALD2 ACS2* strains. However, when the OD₆₀₀ is taken into account it seems the *ALD2 ACS2* strain performs similar to the *ALD6 ACS2*; therefore, any differences in butanol yield could possibly be attributed to small differences in biomass accumulation during fermentation.

The overall conclusion from this section is that the exchange of *ALD2* for *ALD6* in the butanol production strains developed here resulted in minimal changes to butanol yields.

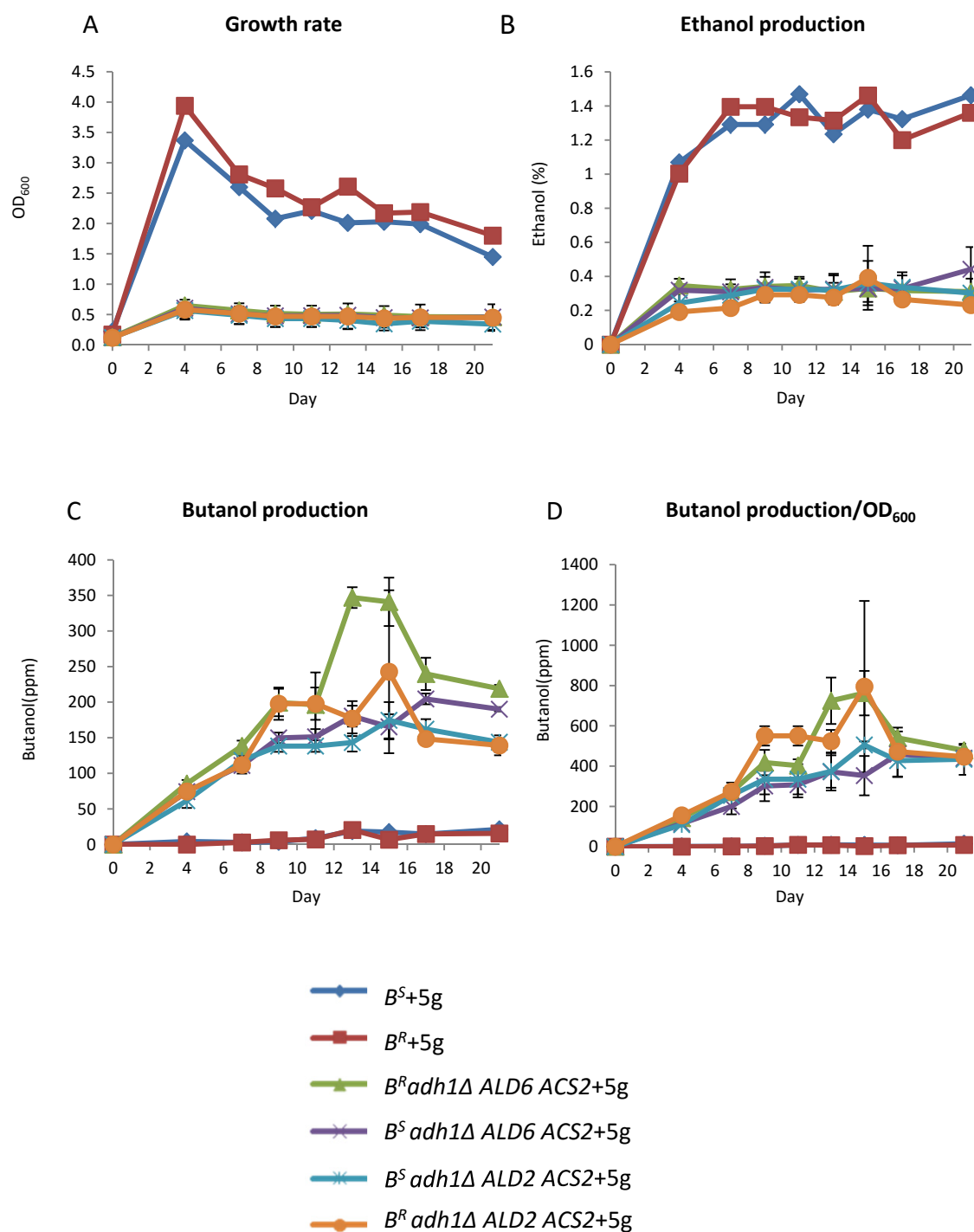


Figure 4.13 The impact of *ALD2* and *ALD6* over-expression on butanol production compared to *ALD6* and *ACS2* over-expression. Figure shows measurement of A) Growth rate, B) ethanol levels, C) butanol levels and D) butanol levels normalised to OD₆₀₀ for all constructed strains.

4.10 Construction various mutants carrying a single deletion of *GPD1* or *GPD2*

One of the main aims of this project was to investigate whether the impairment of competing pathways, such as ethanol and glycerol biosynthesis, could increase butanol production by both decreasing the level of by-products and providing the cells with more reducing power in the form of NADH. It is already apparent from the data presented above that reduced ethanol biosynthesis in the form *ADH1* deletion is critical for butanol biosynthesis providing validity to this approach.

In terms of glycerol biosynthesis, *GPD1* and *GPD2* encode NAD⁺ dependent glycerol-3-phosphate dehydrogenases involved in glycerol production (Albertyn *et al.* 1994). Therefore, a decision was made to explore the strategy of deleting the genes encoding these enzymes with a view to limiting carbon flux towards glycerol while at the same time increasing the pool of NADH (Fig. 4.14 A).

In order to generate strains bearing the single deletion of either *GPD1* or *GPD2*, a decision was made of using a cassette bearing the nourseothricin resistance gene (*natNT2*) surrounded by two *loxP* sites in the plasmid pZC2 (Carter and Delneri. 2010). Specific long primers were designed (The deletion primers for *GPD1* are P1=ORS30 and P2=ORS31 while, the deletion primers for are P1=ORS32 and P2=ORS33 listed in Table 2.3) such that they could be used to amplify the cassette from pZC2 then after transformation of the resulting PCR product into yeast, the sequence introduced with the primer would target the cassette to precisely delete the *GPD1* and *GPD2* genes (Fig. 4.14 B and C).

A decision was made at the time of the experiment to use the B^R *adh1Δ* *ALD2* *ACS2*+5g and B^S *adh1Δ* *ALD2* *ACS2*+5g strains. The reasoning was that if the goal was to improve NADH levels to a point where butanol synthesis became the major route of carbon flux, then using a strain carrying the *ALD2* NADH producing enzyme was the natural choice. With hindsight it may have been advisable to use the *ALD6* containing strain as this ultimately proved to generate slightly higher butanol yields.

Successful deletion of both the *GPD1* and *GPD2* genes was confirmed using a standard three PCR reaction verification strategy with specific primers: The verification primers for the deletion of *GPD1* are P1=ORS52, P2=ORS42, P3=ORS41 and P4=ORS53

while, the verification primers for the deletion of *GPD2* are P1=ORS54, P2=ORS42, P3=ORS41 and P4=ORS55 listed in Table 2.3. The first PCR product establishes the upstream deletion boundary, the second establishes the downstream boundary and the third spans the whole region of the genome (Fig. 4.15 A). The PCR products that were generated from genomic DNAs derived from specific transformants and the parents (Fig. 4.15 B and D) closely match the theoretical size depicted in the tables (Fig. 4.15 F and H). Therefore, the deletion strains have been successfully generated.

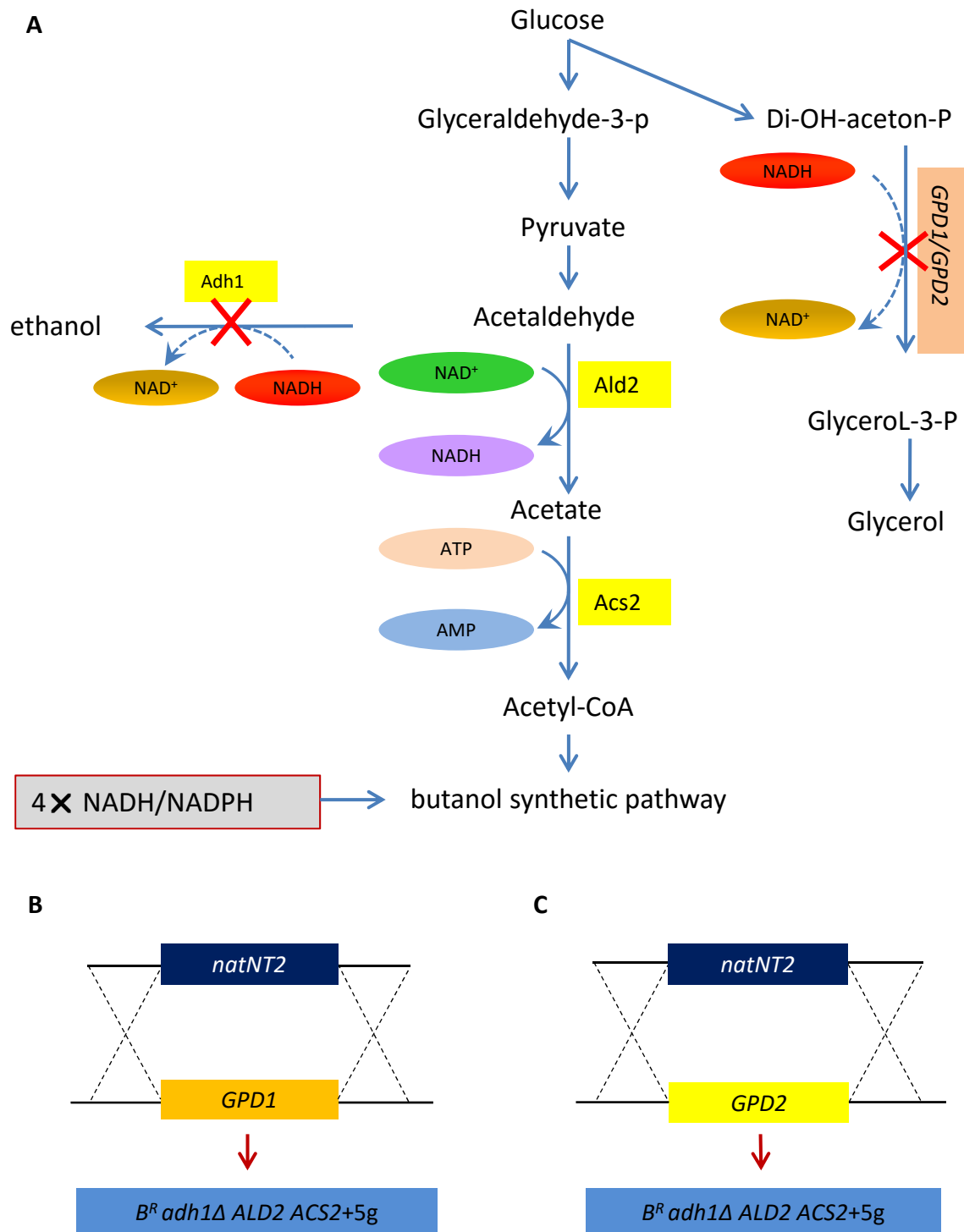


Figure 4.14 Generating new constructed strains with *GPD1* and *GPD2* deletion using $B^R adh1\Delta ALD2 ACS2+5g$ strain. A) Figure shows schematic representation of the glycerol side pathway and the fact that carbon flux could be channelled towards butanol production by deleting the genes *GPD1* and *GPD2*. These genes encode enzymes of glycerol biosynthesis that might compete with butanol production. B) and C) Figures show the deletion strategy for *GPD1* and *GPD2* using *natNT2* marker.

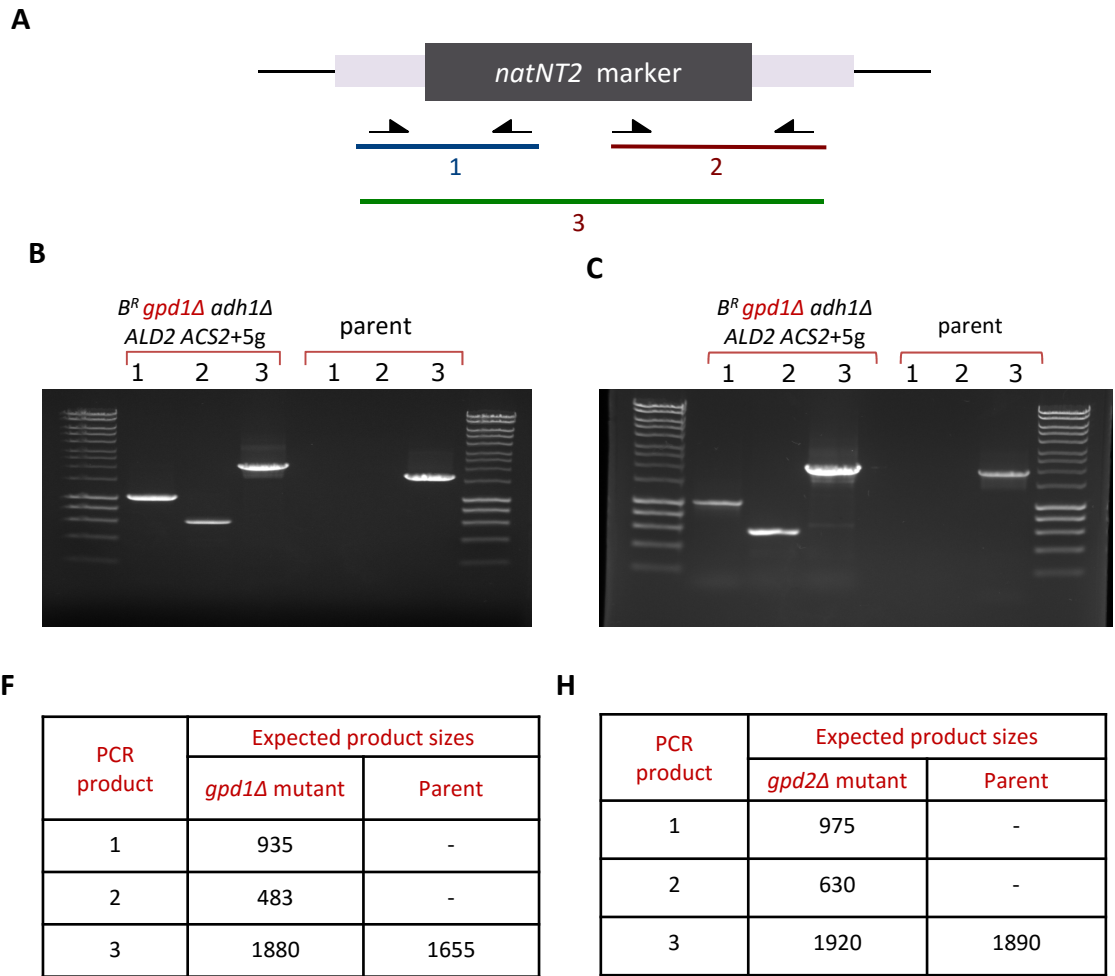


Figure 4.15 PCR analysis to confirm the successful deletion for *GPD1* and *GPD2* in the different constructed strains. A) Figure shows the verification PCR strategy and the three PCR products that would be generated from genomic DNA derived from the potential mutants. B) photographed gel shows the separation of PCR products for *GPD1* deletion. PCR products were generated from genomic DNA derived from the transformant and the wild type. C) Agarose gel showing the PCR analysis for *GPD2* deletion, three PCR products were generated from genomic DNA of the mutant and the wild type. F) and H) Tables showing the expected bands sizes. All PCR products closely match the appropriate size .

4.11 Quantifying butanol and ethanol yield from the constructed strains lacking either *GPD1* or *GPD2* genes

Over the course of standard semi-anaerobic fermentation experiments, the mutant lacking *GPD2* grew well (Fig. 4.16 A) and surprisingly produced much the same level of ethanol as strains bearing a wild type *ADH1* gene (compare with previous e.g. Figure 4.4 B). At this point, the strain was rechecked at the *ADH1* locus and it was confirmed that the *ADH1* gene was still deleted with *ADE2* in the *GPD2* mutant strain (data not shown). Therefore, this result suggests that deletion of *GPD2* somehow rescues ethanol production in an *adh1Δ* strain. One possibility that the expression of one of the other *ADH* genes is increased and that this compensates for the lack of *ADH1*. The obvious consequence of increasing carbon flux to ethanol is that for the *GPD2Δ* strains very little butanol is produced (Fig. 4.16 C).

In contrast to the *GPD2* mutant, the *GPD1* mutant is almost indistinguishable from the parent strain in terms of growth, ethanol production and butanol yields (Fig. 4.16 A, B and C). Therefore, attempts to limit glycerol production and improve NADH levels to allow greater butanol production via the deletion of the *GPD1* and *GPD2* genes have been largely unsuccessful. Deletion of *GPD1* has little effect, whereas deletion of *GPD2* rescues ethanol production instead of improving butanol levels.

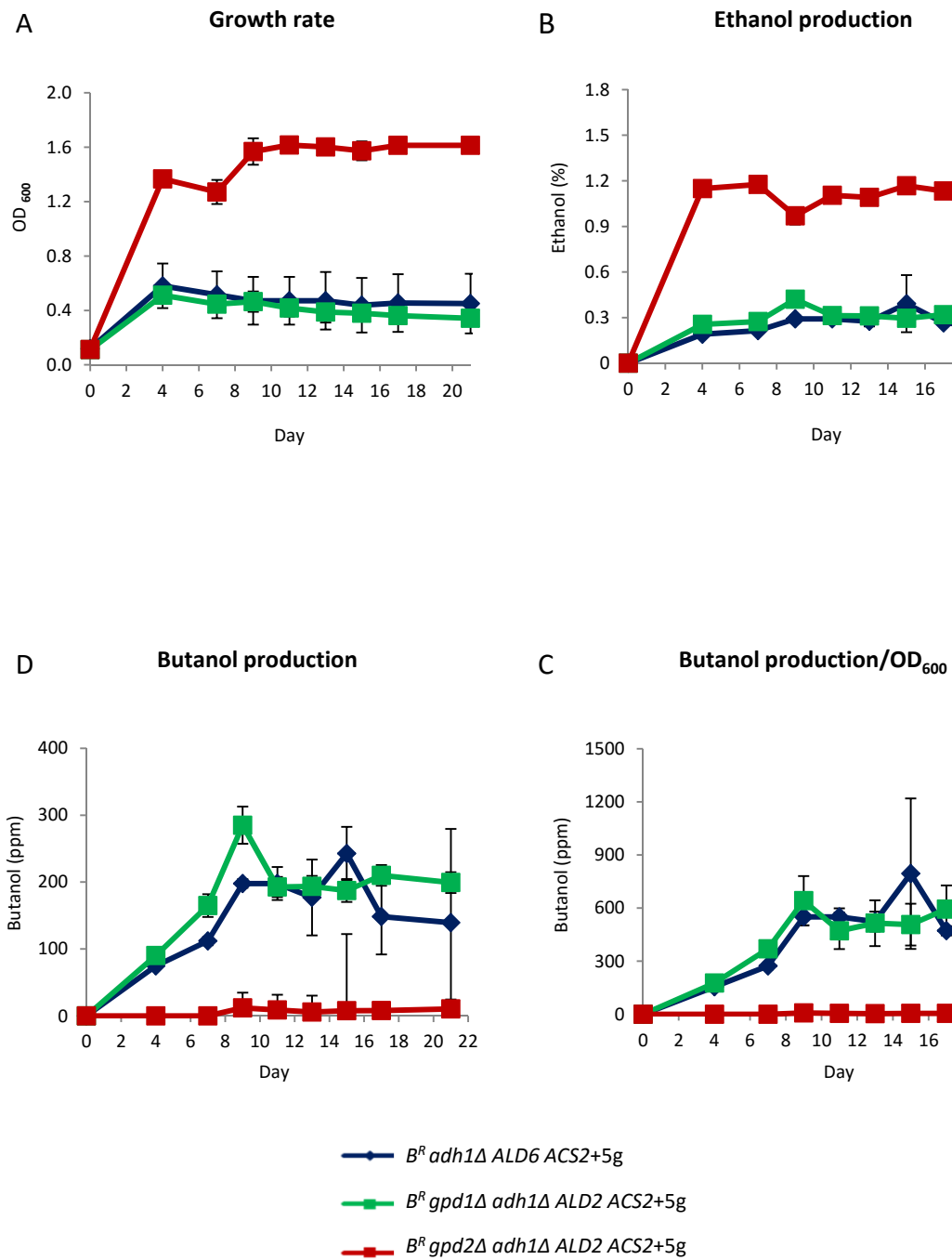


Figure 4.16 Alcoholic fermentation experiment to assess the impact of *GPD1* and *GPD2* deletions on butanol production. Figure shows measurement of A) Growth rate, B) ethanol levels, C) butanol levels and D) butanol levels normalised to OD₆₀₀ for the *gpd1Δ* and *gpd2Δ* mutant relative to the parent strain.

4.12 Discussion

Our results and those of others show that engineered yeast strains bearing the ABE pathway from *Clostridia* species produce very little butanol (Qureshi *et al.* 1999). Many factors might explain this low yield. Firstly, the ABE pathway is an NADH-dependent pathway, which, if active, could generate redox imbalance. In addition, it is possible that the main substrate for butanol production, cytosolic acetyl-CoA, is somehow limiting. Generally, cytosolic acetyl-CoA is readily used as an intermediate for the transfer of acetyl groups. Therefore, this pool of acetyl-CoA can serve as a precursor for fatty acid biosynthesis, isoprenoids and vitamins (Krivoruchko *et al.* 2015). Even metabolic pathways upstream of cytosolic acetyl-CoA could compete with butanol production such as the biosynthetic pathways culminating in ethanol and glycerol. Therefore, in this chapter a number of metabolic engineering strategies were taken in an attempt to overcome the potential problems associated with introducing the ABE pathway into yeast.

The first strategy taken was the deletion of the major yeast alcohol dehydrogenase gene *ADH1*. This improved butanol production significantly, presumably by reducing ethanol levels, increasing NADH levels and ultimately leading to the accumulation of cytosolic acetyl-CoA. Notably, all *ADH1* mutants grew poorly under semi-anaerobic conditions which may be linked to the toxic effects of acetaldehyde accumulation (Ng *et al.* 2012). Surprisingly and consistent with recently published observations (Si *et al.* 2014), an *adh1Δ* mutant was able to produce butanol even without the ABE pathway, although butanol levels were less than 40 mg/L. It has been proposed that deletion of *ADH1* activates an endogenous 1-butanol pathway involving threonine catabolism in mitochondria (Si *et al.* 2014). In contrast, strains deleted for *ADH1* that also carry the ABE pathway generate more butanol (162 mg/L) suggesting that a combination of the endogenous and exogenous pathways can lead to higher butanol yields.

A second metabolic engineering strategy to drive cytosolic acetyl-CoA production was explored. Ald6p, a cytosolic aldehyde dehydrogenase, and Acs2p, the acetyl-CoA synthase, are endogenous enzymes that are involved in the conversion of acetaldehyde to acetyl-CoA. These enzymes are expressed under stress conditions or

when cells use non-fermentable sugars as a carbon source (Aranda *et al.* 2003). Therefore, the *ALD6* and *ACS2* genes were placed in a high expression context, in that they were codon optimised, placed under the control of a strong constitutive promoter and given strong terminator regions. High level expression of the *ALD6* and *ACS2* genes in the *adh1Δ* mutant bearing the ABE pathway generated peak butanol levels of up to 308 mg/L. These results are consistent with other studies where the accumulation of cytosolic acetyl-CoA improves butanol production (Krivoruchko *et al.* 2013).

Prior to the studies described in this chapter, other investigators similarly explored butanol production via a series of metabolic engineering steps (Tucci *et al.* 2007; Krivoruchko *et al.* 2013). In these previous studies, plasmid vectors were used and it was viewed at the outset that our genomic integration strategy might enable more robust butanol production. However, in one such study, even though yields were much lower than those obtained in our experiments, the greatest improvement of butanol level (to 10.3 mg/L) was achieved when *ALD6* and *ACS2* were overexpressed (Tucci *et al.* 2007). This is consistent with our observations where the B^R *adh1Δ ALD6 ACS2*+5g strain that generates ~308 mg/L is the most robust butanol production strain that we have thus far generated. In another study where plasmid vectors were used to express the ABE pathway in yeast, various engineering strategies were taken to improve cytosolic acetyl-CoA (Krivoruchko *et al.* 2013). Progress in optimising the butanol yield was made by deleting the *CIT2* and *MLS1* enzymes of the glycosylate cycle: a metabolic cycle that depletes cytosolic acetyl-CoA. These authors also overexpressed the *ALD6*, *ACS2* and *ADH2* with maximal butanol yields reaching 16.3 mg/L. Interestingly, considerable clonal variation was observed when measuring butanol yields (Krivoruchko *et al.* 2013). The fact that the strains described in this thesis generate higher yields with less clonal variation highlights the advantages of genomic integration engineering strategies in synthetic biology applications. These higher yields may result from greater, more consistent expression of the trans-genes, as the sites of integration were selected on the basis of high expression (Flagfeldt *et al.* 2009).

In our study, we also explored strategies that ultimately did not lead to marked improvements in butanol yield. In the first of these we replaced *ALD6* with *ALD2* in our

butanol production strain. Given the fact that butanol production requires NADH and that Ald2p would generate NADH, whereas Ald6p generates NADPH, it was surprising that expression of Ald2p did not improve butanol yields. It is possible that the Ald2p enzyme is less active than Ald6p, or that components of the butanol synthetic pathway can make use of NADPH for reducing power. However, both of these potential explanations would require substantial further investigation.

The second strategy that did not improve butanol levels was the deletion of either the *GPD1* or *GPD2* gene to restrict glycerol biosynthesis. The underlying hypothesis for this experiment was that decreasing the level of glycerol could alter the carbon flux towards the ABE pathway and also might provide the cell with higher levels of NADH. Intriguingly, ethanol production and growth were rescued when *GPD2* was deleted from the production strain (bearing the ABE pathway, the *ALD2 ACS2* cassette and lacking *ADH1*). The underlying explanation for these observations is currently unknown but it is possible that *GPD2* deletion somehow activates another alcohol dehydrogenase in yeast, which leads to the production of 'normal' levels of ethanol. The improved flux towards ethanol biosynthesis most likely explains the complete lack of butanol production observed for this strain. Other investigators have taken similar strategies towards boosting cytosolic acetyl-CoA (Lian *et al.* 2014). In these studies, the authors investigated the impact of restricting ethanol and glycerol biosynthesis using a combined deletion of the *ADH1*, *ADH4*, *GPD1* and *GPD2* genes in strains bearing the ABE pathway. Once again, this system was reliant on plasmid based vectors for the ABE pathway, but consistent with the studies presented in this thesis, the resulting strain produced less than 10m g/L butanol. Subsequent improvement in butanol production was obtained by using a variety of strategies to increase cytosolic acetyl-CoA. For instance, significant increases in butanol were observed when a pyruvate dehydrogenase bypass pathway was introduced. The highest yield (more than 100 mg/L) was obtained using the most efficient way to generate cytosolic acetyl-CoA: over-expression of the *ALD6* and *ACS2* genes. Therefore, it is possible that a combined deletion of *GPD1* and *GPD2* could generate improvements in butanol synthesis in the system used in this thesis, although this has not yet been tested.

Another important observation made in this chapter is that a butanol resistant strain ($B^R adh1\Delta ALD6 ACS2+5g$) produces higher amounts of butanol (1.5-2 fold) than a butanol sensitive strain ($B^S adh1\Delta ALD6 ACS2+5g$) (Fig. 4.9). This is intriguing, as the difference in butanol sensitivity was established at concentrations above 10 g/L (Ashe *et al.* 2001). In contrast the strains developed here generate a maximum of 300-400 mg/L. One possible explanation for this discrepancy is that the effects of butanol added extracellularly versus the effects of butanol that is produced intracellularly are quite different. For instance, if transport of butanol across membranes were a limitation then the 'true' intracellular concentration of butanol could vary dramatically. The impact of improved butanol tolerance is further explored in chapter 6 of this thesis.

5. Optimizing the fermentation conditions for butanol production

5.1 Introduction

In the previous chapter, a variety of metabolic engineering strategies were taken in an attempt to enhance the availability of acetyl-CoA and ultimately improve butanol production. These experiments showed that in a yeast strain bearing the Clostridial ABE pathway, levels of butanol were increased significantly by a single deletion of the *ADH1* gene and a further small improvement was obtained via the expression of either the *ALD6 ACS2* or *ALD2 ACS2* combinations of genes.

One of the main challenges in biotechnology is to improve the efficiency of production from the organism in question. Optimisation of the fermentation conditions can play a critical role in improving the yield of desired products (Fischer *et al.* 2008). Therefore, a decision was made to select the B^R *adh1Δ ALD6 ACS2*+5g strain, as a reasonably robust butanol producer to study the impact of various fermentation parameters on the yield of alcohols. These parameters include aerobic and semi-anaerobic conditions, different size inoculums, different glucose concentrations, alternative carbon sources, different temperature and scale up.

5.2 butanol production under aerobic and semi-anaerobic conditions

In order to study whether aerobic or semi-anaerobic conditions during fermentation impact on butanol and ethanol production, early experiments were carried out over 5 days at 30°C. Ethanol levels from the control strain bearing just the ABE pathway, B^R+5g, reached approximately 1.2% (v/v) under semi-anaerobic conditions and less than 0.6% under aerobic conditions (Fig. 5.1 A). The reduced ethanol under aerobic conditions likely reflects the fact that a portion of the carbon has been metabolised via respiration providing more efficient biomass production compared to the semi-anaerobic fermentation. The production of ethanol even in the presence of oxygen is a well-established phenomenon in *S. cerevisiae*, being first noted by Herbert Grace Crabtree in the 1920s (Crabtree 1928) and thereafter termed the 'Crabtree Effect' (van Dijken *et al.* 1993).

In contrast, the B^R *adh1Δ* *ALD6* *ACS2*+5g strain produces much less ethanol; 0.3% under semi-anaerobic conditions while no-ethanol was detectable under aerobic conditions (Fig. 5.1 A). Lower ethanol levels were anticipated under semi-anaerobic conditions as a result of the deletion of the major alcohol dehydrogenase, *ADH1*. Under aerobic conditions it is possible that any ethanol produced is immediately consumed via respiration. In terms of butanol yields, for the B^R+5g control strain butanol was produced at very low levels (less than 10 ppm) under either semi-anaerobic or aerobic conditions. While as described in chapter 4, the B^R *adh1Δ* *ALD6* *ACS2*+5g strain under semi-anaerobic conditions produces a reasonable amount of butanol (160 ppm) (Fig. 5.1 B). In contrast, very little butanol was detected under aerobic conditions in this strain. Overall butanol is only really produced at any appreciable level when the selected butanol production strain is grown under semi-anaerobic conditions.

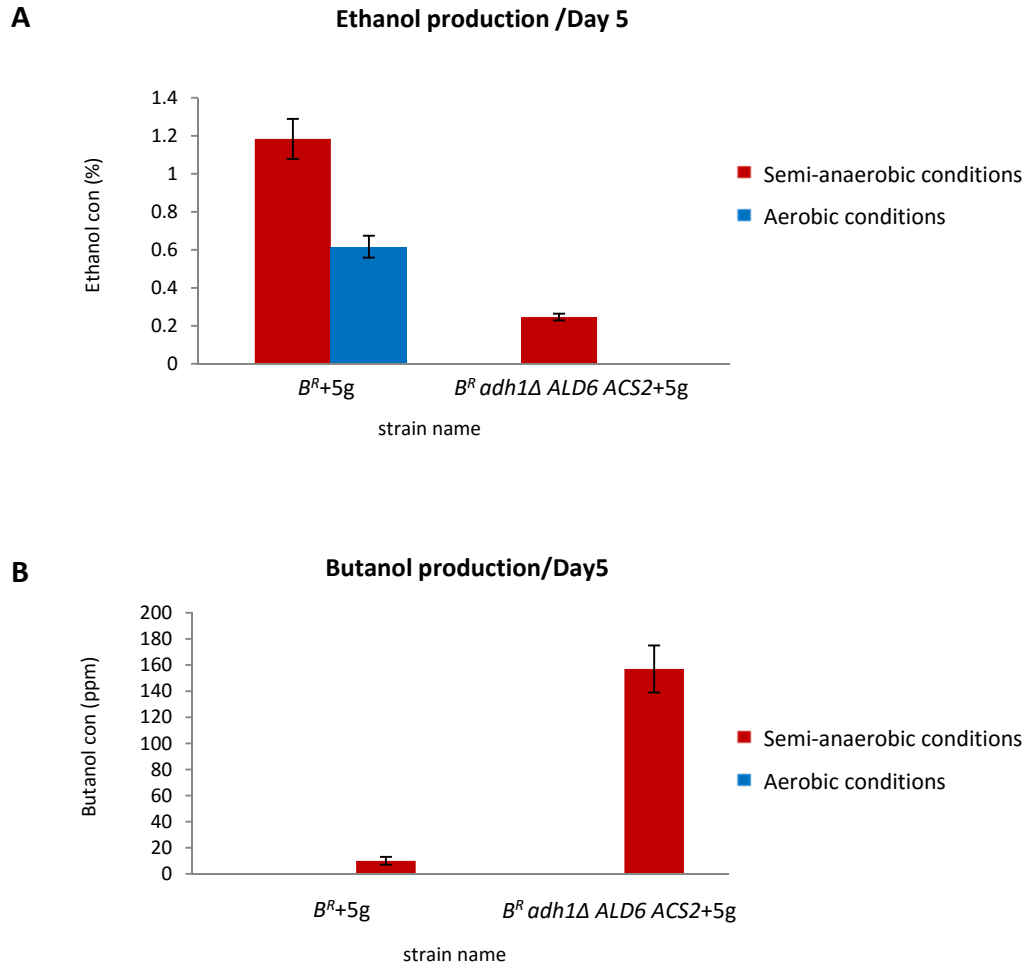


Figure 5.1 Impact of aerobic versus semi-anaerobic growth conditions on butanol production. A) Figure shows the levels of ethanol produced on day 5 of aerobic (blue bars) or semi-anaerobic (red bars) fermentations using a strain bearing just the ABE pathway (B^R+5g) or the butanol production strain ($B^R adh1\Delta ALD6 ACS2+5g$). B) As above except butanol levels were assessed. Butanol was only obtained from semi-anaerobic fermentations.

5.3 The impact of using 0.05 and 0.1 starting ODs on butanol production

In order to explore the effect of varying the starting inoculum on butanol production, two fermentation experiments were carried out using starting OD₆₀₀ values of 0.05 and 0.1. The standard operating procedure (defined in section 2 materials and methods) was used for these experiments apart from the variation in inoculum. The fermentations were allowed to run for 11 days at 30°C under semi-anaerobic conditions. The higher inoculum fermentations reached slightly higher culture densities compared to those with the lower inoculum (Fig. 5.2 A). In addition, apart from minor variation early in the fermentations, the levels of ethanol were slightly higher for the high starting inoculum (Fig. 5.2 B). In terms of butanol levels, no major difference was evident early in the fermentation, however, by the final day butanol levels were slightly higher around 260 ppm when a 0.1 OD₆₀₀ inoculum was used while only 180 ppm was obtained when a 0.05 OD₆₀₀ inoculum was used (Fig. 5.2 C). One possible explanation for this could be that by starting with a higher biomass the strain is more resistant to butanol toxicity and this eventually enables the strain to produce more ethanol and butanol. However, there is no significant difference for butanol production when butanol levels were normalized to OD₆₀₀ (Fig. 5.2 D). Therefore a tentative conclusion would be that starting with the higher OD₆₀₀ leads to slightly greater biomass and butanol yield over the time. However, to conclude this unambiguously a larger experiment would need to be performed over a more extended time frame with greater variation in the starting inoculum.

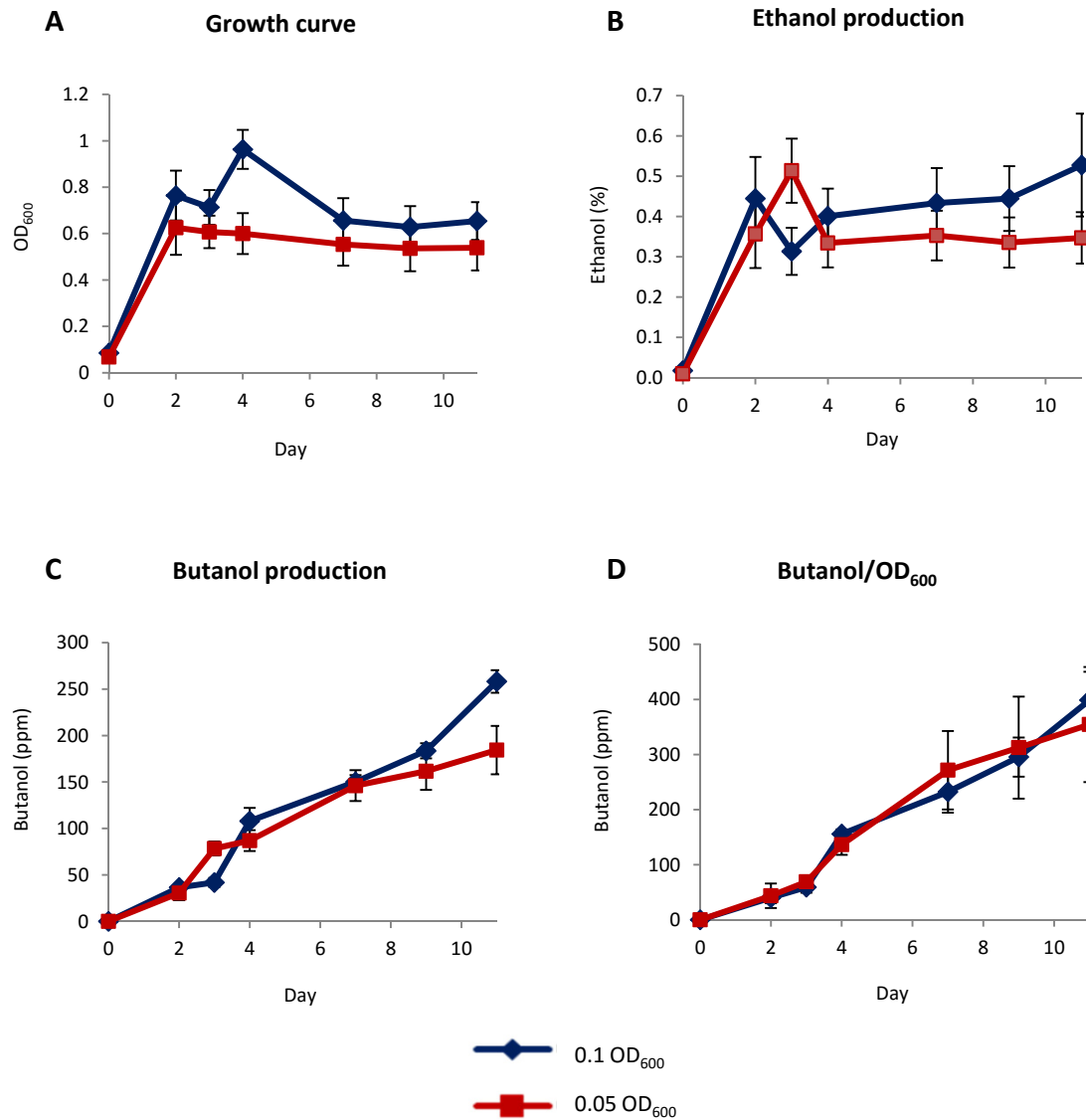


Figure 5.2 The effect of using starting OD₆₀₀ on butanol production under semi-anaerobic conditions. Plots show measurement of growth (A), ethanol levels (B), butanol levels (C) and butanol levels normalised to growth (D) for the butanol production strain (*B^R adh1Δ ALD6 ACS2+5g*) using starting OD₆₀₀ values of either 0.05 (red) or 0.1 (blue).

5.4 The impact of using different glucose concentrations on butanol and ethanol production

Previous studies have taken an approach where higher starting glucose concentrations were used, to force higher production of butanol. For instance, the levels of butanol and acetone yield were dramatically elevated from *Clostridium beijerinckii* BA101 grown in medium containing 6% glucose (Formanek *et al.* 1997). To test whether this is also apparent for the butanol production system used in this thesis, fermentations were run using the butanol production strain, B^R *adh1Δ* *ALD6* *ACS2+5g*, at different starting glucose concentrations (2, 4, 7, 10 and 20%). Surprisingly, no significant difference was noted in the cell density attained for the butanol production strain at the different glucose concentrations (Fig. 5.3 A). Equally, while the highest and lowest ethanol levels observed were in the 20% and 2% glucose fermentations respectively, the difference was not dramatic given the 10-fold difference in initial carbon level (Fig. 5.3 B). It is possible in this strain that the accumulation of toxic metabolites as a consequence of *ADH1* deletion is the key to growth rate and growth level such that varying carbon source levels does not have a particularly significant impact. Interestingly, the highest level of butanol obtained was in the 2% glucose fermentation, but overall as for growth and ethanol levels, varying the glucose concentration made very little difference to the quantity of butanol produced (Fig. 5.3 C). When the butanol levels were normalized to OD₆₀₀ the slight increase for the 2% glucose fermentation was more evident (Fig. 5.3 D).

A key question from these data was whether there is residual glucose left especially in fermentations with higher starting glucose levels. Figure 5.4 A and B summarize the differences in butanol and ethanol production on day 13 of the fermentations above, respectively. The trends described above are evident: increasing the glucose concentration led to a gradual increase in ethanol production (from 0.22% up to 0.42%) and the highest butanol value was obtained from the 2% glucose fermentation. Interestingly, the butanol production strain does not consume all of the glucose that is available in the media across these fermentations. For instance, in the 20% glucose fermentation, less than half of the starting glucose is consumed (Fig. 5.4 C). Overall, based upon these results, 2% glucose was selected as the starting

concentration for subsequent fermentations, as increasing the glucose concentration only led to increased ethanol production with very little improvement in butanol levels.

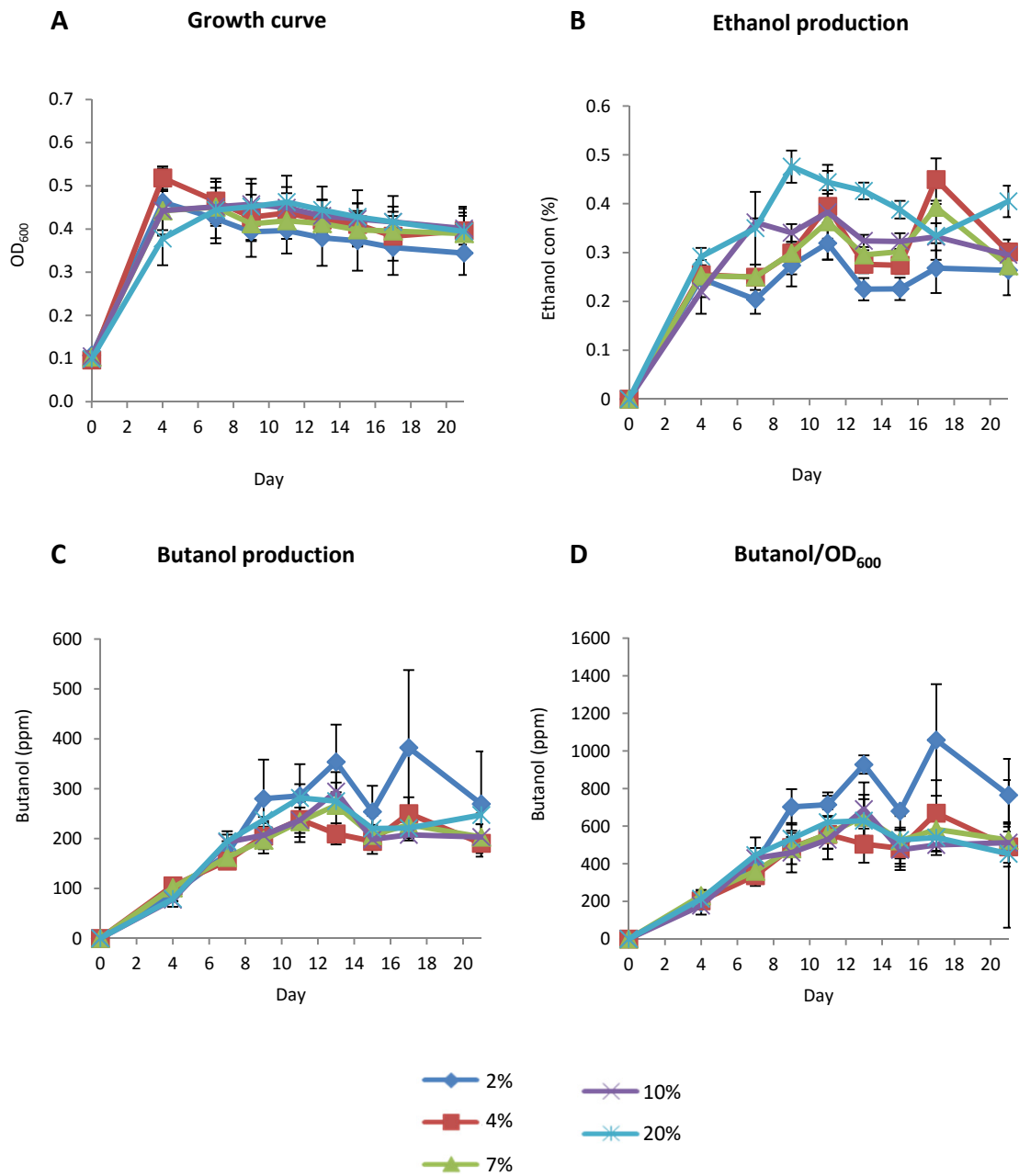


Figure 5.3 The impact of using different glucose concentrations on butanol and ethanol production under semi-anaerobic conditions. Figure shows measurement of growth (A), ethanol levels (B), butanol levels (C) and butanol levels normalised to OD₆₀₀ (D) for the butanol production strain (*B^R adh1Δ ALD6 ACS2+5g*) using different glucose concentrations (2% up to 20%) for 21 day semi-anaerobic fermentations.

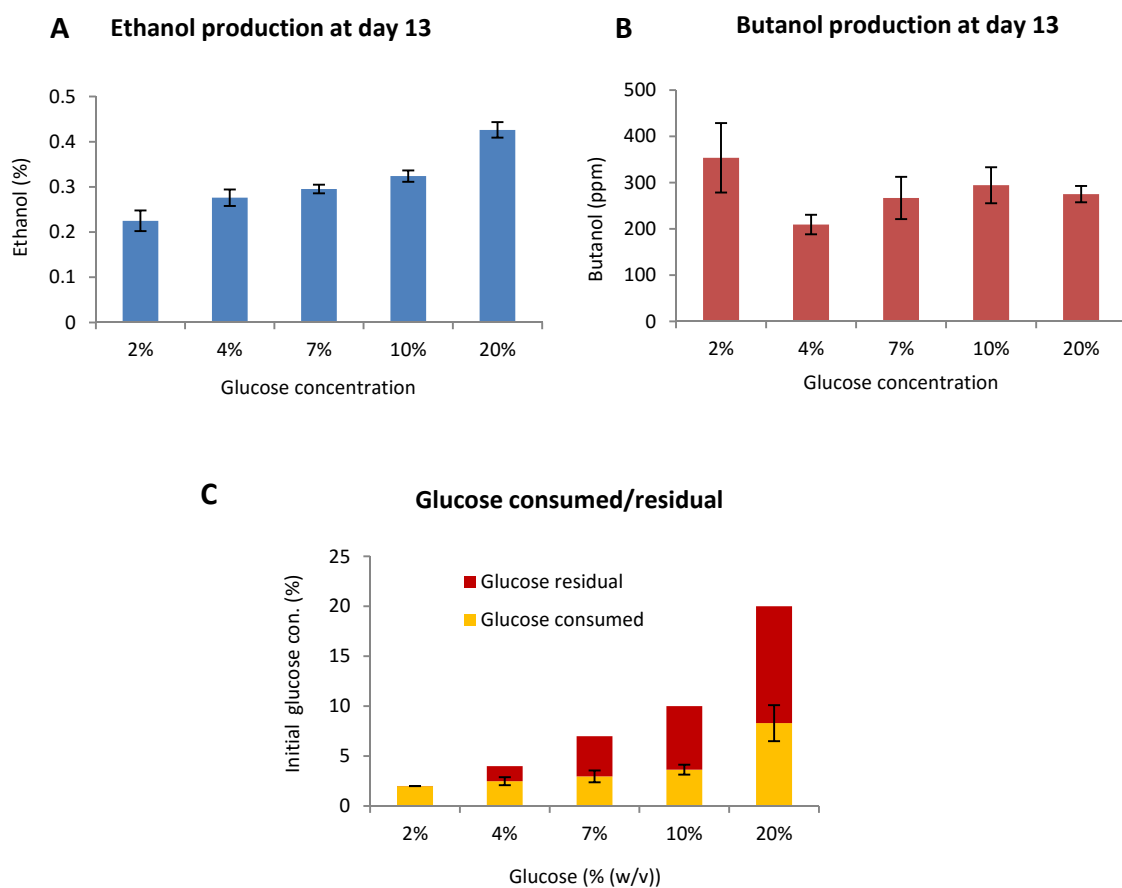


Figure 5.4 Analysis of ethanol, butanol and glucose consumption in the production strain at day 13 using different starting glucose concentrations. Figure shows the levels of ethanol (A), butanol (B) and glucose (consumed versus residual) (C) on day 13 of fermentation experiments in Figure 5.3.

5.5 The impact of using alternative carbon sources on butanol and ethanol production

One of the major challenges for butanol production is to produce butanol from a cheaper feedstock to enable butanol to compete with ethanol in the biofuel market. While *Saccharomyces cerevisiae* is somewhat limited in its capacity to use alternative carbon sources; for example it cannot ordinarily metabolise xylose and arabinose (Kim, Park *et al.* 2013), it was still considered of value to test whether butanol can be produced from other carbon sources that *S. cerevisiae* does grow on. Therefore, a panel of alternative carbon sources were assessed in fermentations under semi-anaerobic conditions for the butanol production strain (B^R *adh1Δ ALD6 ACS2+5g*). Different types of carbon sources were selected: disaccharide sugars represented by sucrose and maltose: monosaccharide sugars including the hexose sugars mannose, galactose and glucose: and finally glycerol which is a sugar alcohol. The disaccharides were selected as they represent industrially important sugar sources, although they do compete with food production. Glycerol is produced at high levels by specific species of algae and these have been touted as a potential feedstock for industrial fermentations. Glycerol cannot be metabolized by yeast under strict anaerobic conditions but it is unclear under whether it can be used under the semi-anaerobic conditions used in this thesis. Each carbon source needs to be converted to pyruvate and acetyl-CoA in order to be metabolised (Fig 5.5). For each sugar, six replicate fermentations were performed. Pre-cultures were set up in media containing the same carbon source to be used in the fermentation with a view to decreasing any lag phase, as the appropriate transporters and enzymes will be actively expressed. As above, samples were collected over 21 days and the OD₆₀₀, butanol and ethanol levels were measured.

In terms of cell density, the butanol production strain attains an OD₆₀₀ value of ~0.5 for glucose or mannose early in the fermentation, this then decreases gradually over time. A similar profile was obtained for sucrose but with higher OD₆₀₀ values throughout. Interestingly, the OD₆₀₀ values for glycerol, maltose and galactose increased gradually over time (Fig 5.6.A). However, measuring the OD₆₀₀ may not necessarily reflect genuine cell growth because yeast cells can swell when not growing

leading to artificially high OD₆₀₀ values (Haase and Reed 2002). A better measure of proliferation would have been obtained from cell counts. Furthermore, the level of ethanol production might provide a better measure of the cells capacity to ferment each sugar under semi-anaerobic conditions. Interestingly, ethanol levels were almost zero when maltose or glycerol was used, while ethanol levels were increased over time up to a peak level of 0.6% when galactose was used. For glucose and sucrose more standard levels of ethanol were obtained \approx (0.3%). However, the highest ethanol levels were obtained from mannose fermentation Fig 5.6.B.

In terms of butanol yields, no detectable butanol was obtained when glycerol, maltose or galactose were used as carbon sources Fig 5.6.C. It seems that the butanol production strain B^R *adh1Δ ALD6 ACS2+5g* doesn't ferment maltose under semi-anaerobic conditions as neither ethanol nor butanol were obtained from these fermentations (Fig. 5.6.C). These results are consistent with previous studies where the limiting factor in maltose metabolism seems to be transporters and the activity of the maltase enzyme, which breaks maltose down into two molecules of glucose (Drewke and Ciriacy 1988; Day, Rogers *et al.* 2002). Similarly, the butanol production strain doesn't produce ethanol when glycerol was used under semi-anaerobic conditions. Glycerol needs to be phosphorylated to glycerol-3-phosphate in the cytosol and then oxidised to di-hydroxy-acetone-phosphate in mitochondria then can enter the glycolytic pathway. It seems likely that this mitochondrial reaction would be deficient under semi-anaerobic conditions. In terms of galactose, *S. cerevisiae* uses the Leloir pathway ultimately converting it to the glycolytic intermediate glucose-6-phosphate (Sellick, Campbell *et al.* 2008). Previous chemostat studies have found that during glucose to galactose transitions under anaerobic conditions, galactose is not consumed possibly because the energy status of the cell is reduced to such an extent that production of the Leloir proteins is prohibited (Van den Brink, 2009).

In contrast, our data revealed that the butanol production strain ferments mannose to large amounts of ethanol and moderate levels of butanol. This is consistent with previous studies where mannose was found to be a highly fermentable carbon source, being converted to fructose-6-phosphate to enter glycolysis (Hashimoto, Sakakibara *et al.* 1997). Interestingly, sucrose is a good carbon source for butanol and

ethanol production, as it is fermented quite efficiently via secreted invertase. The enzyme that hydrolyses sucrose outside the cell to glucose and fructose which pass the cells and are converted to glucose-6-phosphate and fructose-6-phosphate respectively that enter glycolysis directly (Koschwanez, Foster *et al.* 2011).

In conclusion, glucose and sucrose are ideal carbon sources for ethanol and butanol production and moderate amounts of butanol can be obtained when mannose was used. Glycerol and maltose were not fermented by the butanol production strain under semi-anaerobic conditions, whereas galactose was fermented but this only led to ethanol not butanol production. From these results it is clear that if butanol is to be commercially produced by *S. cerevisiae* there will have to be substantial extra engineering to allow use of a range of other carbon sources.

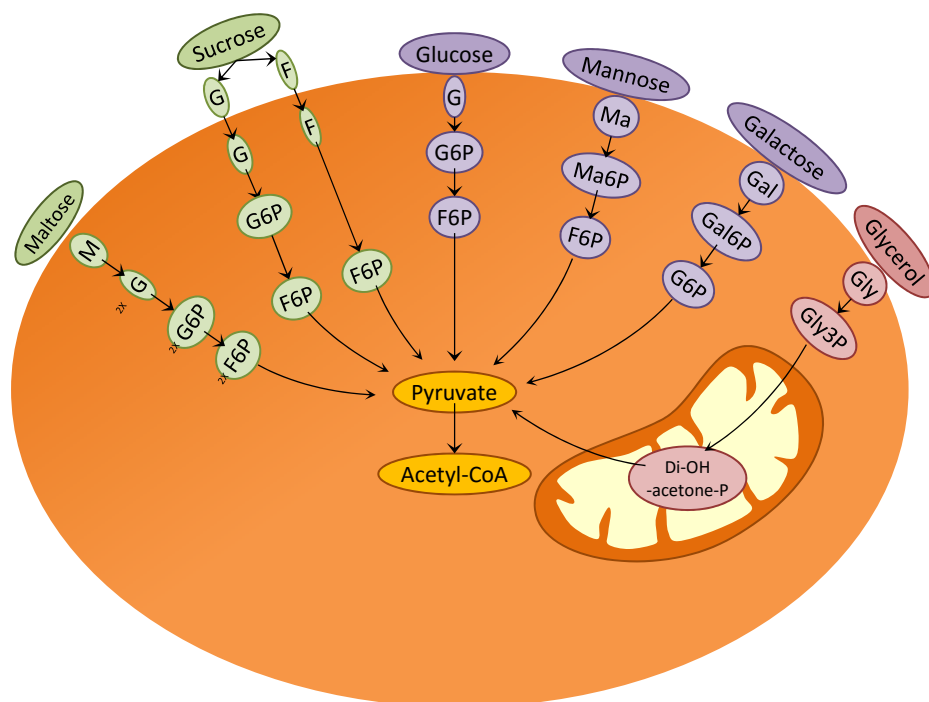


Figure 5.5 Metabolism of disaccharide and monosaccharide sugars in yeast. Figure shows the glycolytic pathway for: the disaccharide sugars, sucrose and maltose (in green); the monosaccharide sugars, glucose, mannose and galactose (in purple) and the sugar alcohol glycerol (in pink).

M	maltose	G6P	glucos-6-phospate
G	glucose	F6P	fructose-6-phoshfate
F	fructose	Ma6P	mannose-6-phosfate
Ma	mannose	Gal6P	galactose-6-phosphate
Ga	galactose	Gly3P	glycerol-3-phosphate
Gly	glycerol		

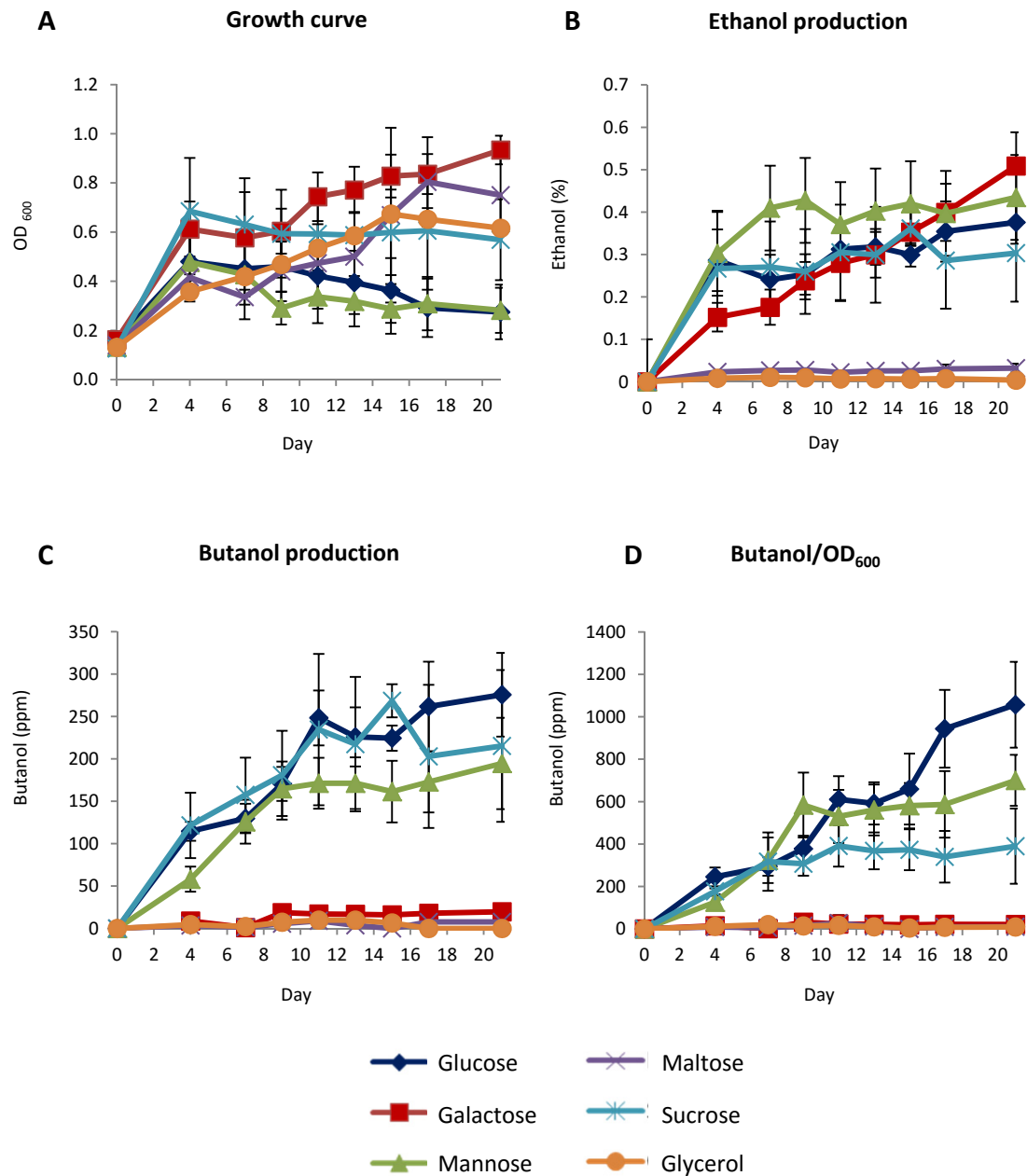


Figure 5.6 The impact of using various feedstock carbon sources on ethanol and butanol production under semi-anaerobic conditions. Plots show the measurement of growth (A), ethanol levels (B), butanol levels (C) and butanol levels normalised to OD₆₀₀ (D) for the butanol production strain (*B^R adh1Δ ALD6 ACS2+5g*) on different carbon sources: the monosaccharide sugars- glucose, galactose and mannose; the disaccharide sugars- sucrose and maltose; and the sugar alcohol- glycerol.

5.6 Detect the influence of using different temperature 25, 30 and 37 °C on butanol and ethanol yield

In order to investigate the impact of using different fermentation temperatures on alcohol production, three different temperatures were assessed across 21 day semi-anaerobic fermentations: 25, 30 and 37°C. Firstly, the OD₆₀₀ of butanol production strain was affected by temperature: the highest OD₆₀₀ reached was at 30°C, while decreasing the fermentation temperature to 25°C reduced this. However, for the 37°C fermentation, the strain only managed to complete the first doubling (Fig. 5.7 A). The ethanol levels were entirely consistent with the growth levels: the highest ethanol levels were obtained at 30°C; intermediate levels at 25°C and the lowest levels at 37°C (Fig. 5.7 B). Overall these results fit with 30°C being the optimum growth temperature for the W303-1A background strain of *S. cerevisiae*, while 37°C and 25°C represent stress conditions requiring expression of chaperones or cold stress proteins (Feder *et al.* 1999). In terms of butanol levels, the highest attained were at 30 and 25°C while at 37°C very little butanol was evident (Fig. 5.7 C). The equal production for the 30°C and 25°C fermentations is perhaps surprising given the lower biomass obtained at 25°C. Indeed, when butanol levels were normalized to the OD₆₀₀, the highest levels of butanol were obtained from the strain that has grown at 25°C compared to 30°C (Fig. 5.7 D). It is unclear why marginally higher butanol levels were obtained at 30°C, it is possible that the explanation lies in the exogenous enzymes activities in the ABE pathway or in the tolerance to alcohols. Expanded temperature studies will be required to explore this phenomenon further.

From the perspective of this thesis, since the butanol concentrations produced were equal at 25°C and 30°C, and all of the other experiments to this point have been conducted at 30°C, a decision was made to conduct the remainder of the experiments at 30°C. Although, it is important to note that 25°C might prove a more optimal temperature under industrial conditions given the high butanol yield and lower ethanol levels obtained.

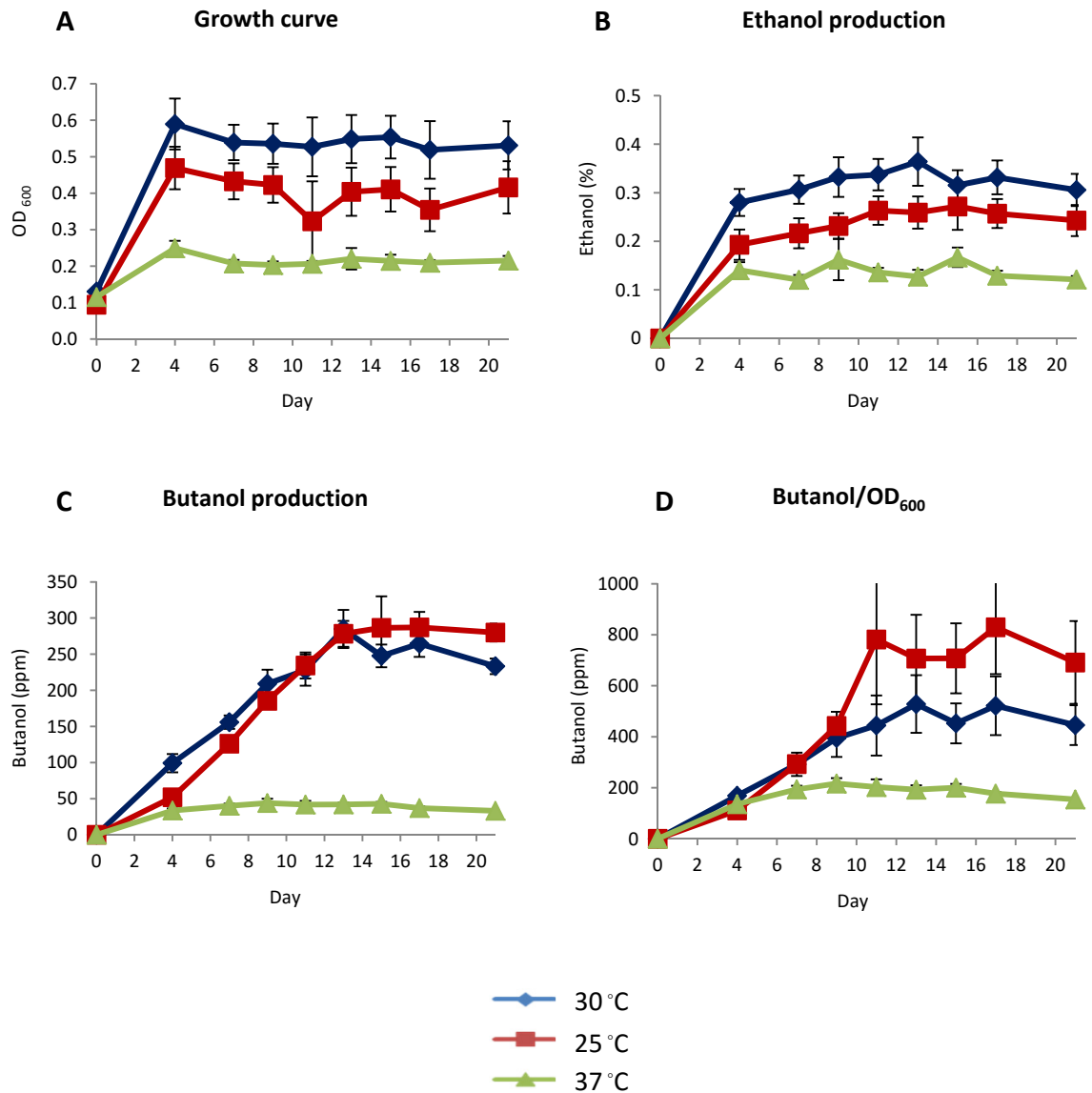


Figure 5.7 The impact of growth at various temperature on butanol and ethanol production under semi-anaerobic conditions. Figure shows measurement of growth (A), ethanol levels (B), butanol levels (C) and butanol levels normalised to OD₆₀₀ (D) for the butanol production strain (*B^R adh1Δ ALD6 ACS2+5g*) grown semi-anaerobically at 25, 30 or 37°C for 21 days.

5.7 The effect of scaling up the volume of the batch culture on production of butanol and ethanol

One of the major limitations associated with butanol production by bacteria is that the bacteria lose the ability to produce the same levels of butanol at industrial scale. Therefore, it was quite interesting at this stage of the project to explore the impact of fermentation scale on butanol production from *S. cerevisiae*. Experiments to date have used small semi-anaerobic fermentation vials with a capacity of 50 ml. A larger scale fermentation experiment using 450 ml was set up in a similar way to mimic the conditions in the small semi-anaerobic vials. Three large bottles were placed in a 15 L chamber under semi-anaerobic conditions at 30°C for 21 days. Interestingly, the butanol production strain B^R *adh1Δ ALD6 ACS2+5g* reached higher OD₆₀₀ values at the larger scale compared to the small scale (Fig. 5.8 A). It is possible that the difficulties in maintaining the semi-anaerobic environment during sample collection at large scale could allow greater biomass accumulation. Consistent with the more robust growth of the strain in the larger scale fermentations, higher levels of ethanol and reduced levels of butanol were obtained (Fig. 5.8 B and C). The same patterns were obtained when levels of butanol were normalized to the OD₆₀₀ (Fig. 5.8 D).

Overall, though even though the butanol levels are somewhat reduced, the butanol production strain *adh1Δ ALD6 ACS2+5g* is able to produce butanol from fermentations at larger scale. The future challenge will be to explore what happens at even higher volumes under conditions that more closely mimic industrial fermentations.

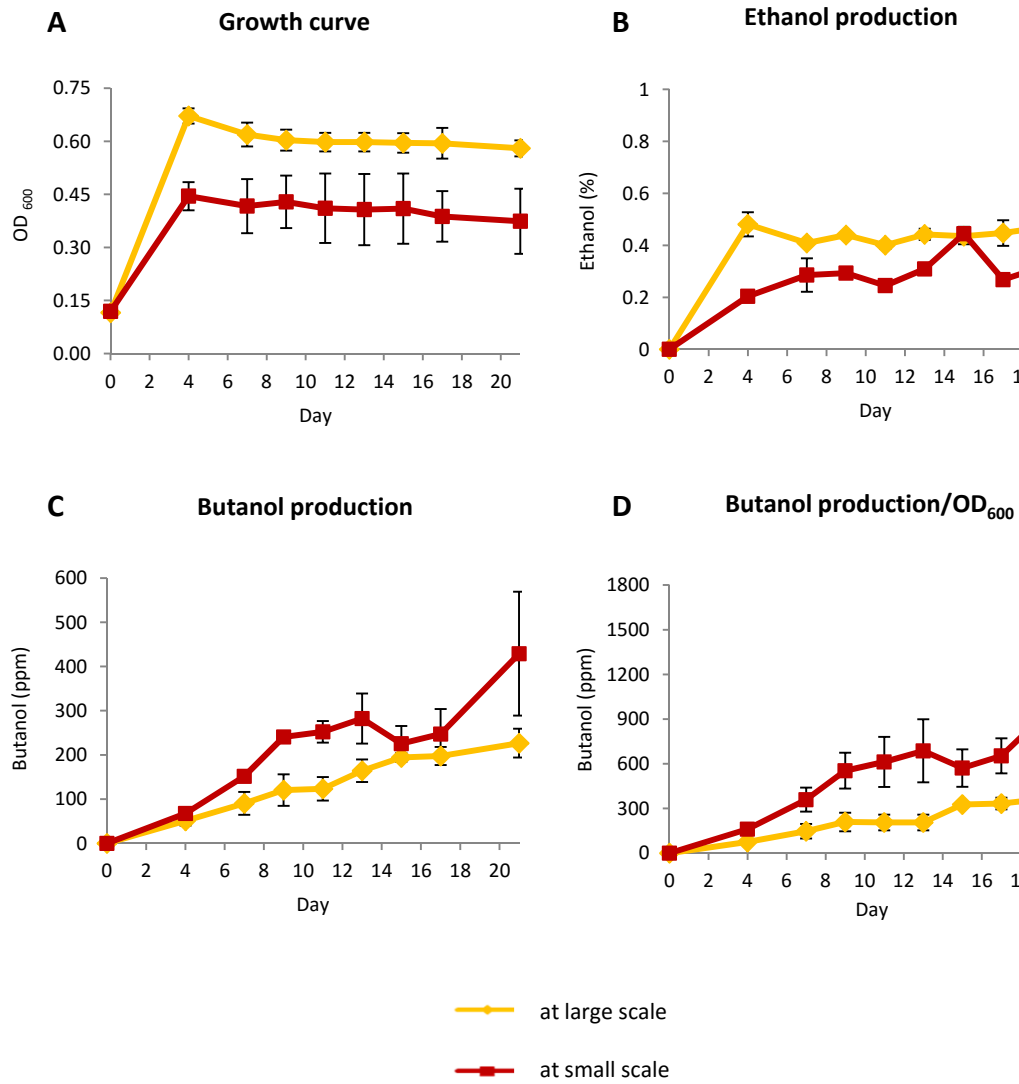


Figure 5.8 The effect of scaling up the volume of the batch culture on butanol and ethanol production under semi-anaerobic conditions. Plots show measurement of growth (A), ethanol levels (B), butanol levels (C) and butanol levels normalised to OD₆₀₀ (D) for the butanol production strain (*B^R adh1Δ ALD6 ACS2+5g*) either at larger scale (450 ml) (yellow) or standard scale (45ml) (red).

5.8 Discussion

In this chapter we have started to explore some of the fermentation and feedstock parameters in order to estimate the optimal conditions for butanol production from the strain *adh1Δ ALD6 ACS2+5g*. Firstly, semi-anaerobic conditions are essential for butanol production; it seems likely that in the presence of oxygen, the strain respire the majority of the carbon source and generates high biomass instead of the desired products. Secondly, using a slightly higher inoculum (0.1 OD₆₀₀ as opposed to 0.05) led to greater biomass, ethanol and butanol levels over the course of the fermentation. Perhaps the butanol production strain is somehow more tolerant to the toxicity of the metabolites generated when starting at a higher inoculum level. This result is consistent with other investigators' observations, as they have found that higher yeast cell densities make the strains more tolerant to solvent toxicity (Westman *et al.* 2015)

Our data also reveal that 2% glucose was optimal for butanol production, as increasing the glucose concentration in the fermentation led to increased ethanol levels without altering butanol yield. The increased ethanol production at higher glucose concentrations is consistent with observations where the activities of enzymes involved in the conversion of pyruvate to ethanol are increased at higher glucose levels. For instance, pyruvate decarboxylase activity is 4 times higher at elevated glucose concentrations and this may increase ethanol production (Rodrigues *et al.* 2006). In addition, enzymes that metabolise ethanol and acetaldehyde may be repressed at very high glucose concentrations. For instance, acetaldehyde dehydrogenase activity could be decreased and this may decrease the flux from pyruvate toward acetyl-CoA production and subsequently lead to less butanol production (Rodrigues *et al.* 2006).

Additionally, six different sugars were tested in order to explore the capacity of the strain to produce butanol from alternative carbon sources. Sucrose was efficient for both butanol and ethanol production and the product levels were similar to glucose fermentations. Although sucrose is a preferable sugar to glucose from an industrial perspective due to financial considerations, its use would not necessarily be viewed favourably, as this would place fuel and food production in direct competition.

Moderate levels of butanol and high levels of ethanol were produced from mannose suggesting that the butanol production strain ferments mannose in a similar manner to glucose, although it is unclear why metabolism to ethanol is more favoured for mannose. Noticeably, galactose was a poor carbon source for butanol production where very low yields of butanol were obtained while ethanol levels increased over the fermentation period. Interestingly, the butanol production strain *adh1Δ ALD6 ACS2+5g* doesn't appear to ferment either maltose or glycerol under semi-anaerobic conditions.

Feedstock usage and flexibility is a key consideration if *S. cerevisiae* is to ever be commercially used for butanol production. The limited analysis described above suggests that the butanol production strain is rather restricted in its capacity to use alternative carbon sources. Therefore, if this strain is ever to be used for butanol production, as well as requiring vastly improved butanol yields, much work would be required to expand the strains carbon source capabilities such that lignocellulosic carbon could be metabolised.

Another factor that has been explored in this thesis was the impact of using different incubation temperature on butanol production. Generally, both 25°C and 30°C led to similar concentrations of butanol. However, at the lower temperature 25°C, butanol production strain generates less biomass and eventually produces lower levels of ethanol while maintains similar levels of butanol. It is quite possible that in an industrial setting, were it possible to maintain the lower fermentation temperature without substantial cooling, that this would be favoured. Importantly, though the butanol concentration produced is relatively unaffected by temperature except at 37°C where growth, ethanol and butanol production are all curtailed.

The last factor studied in this chapter was the scale of the fermentation. Our data revealed that a 10-fold increase in scale along with the associated changes in the stringency of semi-anaerobic growth, led to somewhat diminished levels of butanol relative to the smaller scale experiments. Mimicking semi-anaerobic conditions at the larger scale was not really possible, and therefore it is likely that the yeast cells were exposed to higher oxygen levels at the larger volume. It is possible that this would facilitate biomass and ethanol production whilst lowering the yield of butanol.

Therefore, restricting the availability of oxygen in the fermentation media would be a critical factor to increase the efficiency of butanol production strain to ferment glucose into butanol.

Overall, the conditions used for most of the experiments in this thesis: semi-anaerobic/ 30°C/ 2% glucose/ 0.1 OD₆₀₀ inoculum, produce a reasonable quantity of butanol, which can be scaled up at least 10-fold without substantial loss of production. The challenge in the future will be to not only improve butanol yields further but to also explore industrial fermentation conditions.

6. Improve butanol tolerance with a view to higher butanol yields

6.1 Introduction

Previous work from the Ashe lab has identified mutations in the genes encoding the eukaryotic translation initiation factor eIF2B that impact upon the level of resistance to fusel alcohols in *Saccharomyces cerevisiae* (Ashe *et al.* 2001; Taylor *et al.* 2010). For instance, a point mutation in the gene encoding the gamma subunit of eIF2B, which changes the proline at position 180 to a Serine, increases sensitivity to exogenously added 1-butanol (Ashe *et al.* 2001). More specifically, translation initiation is inhibited in the *GCD1-S180* sensitive strain (B^S) after exposure to 1% butanol for 10 min; while, in the *GCD1-P180* resistant strain (B^R), translation initiation remains unaffected. One of the most intriguing observations presented thus far in this thesis is that a butanol resistant strain (B^R *adh1Δ ALD6 ACS2 +5g*) produces more butanol than a butanol sensitive strain (B^S *adh1Δ ALD6 ACS2 +5g*); where the only difference between the two strains is the *GCD1-S180/ GCD1-P180* allele.

Unpublished data from the Ashe lab has identified a number of phosphorylation sites across the different eIF2B subunits using mass spectrometry (Keenan 2013). For instance, a novel phosphorylation site in eIF2B δ at serine 131 was observed. Interestingly, phosphorylation of serine 131 was detected in samples from the butanol sensitive strain *GCD1-S180* either untreated or butanol treated. However, in samples from the butanol resistant strain, serine 131 was dephosphorylated in most cases after exposure to butanol (Keenan 2013). This phosphorylation event was extensively investigated in the Ashe lab in order to detect whether it is involved in the inhibition of translation initiation after exposure to butanol. More specifically, new strains were constructed with the genomic copy of the *GCD2* gene (encoding eIF2B δ) deleted and different versions of *GCD2* supplied by plasmids. More specifically, serine 131 was mutated on the plasmid to encode either an alanine residue (*GCD2-S131A*), which mimics the structure of unphosphorylated serine, or an aspartic acid (*GCD2S131D*) moiety, which mimics phosphorylated serine. Growth analysis revealed that strains with *GCD2-S131A* are more resistant to exogenously added butanol, whereas strains with *GCD2-S131D* exhibit increased sensitivity to butanol. In fact, the

GCD2-S131A strain appears one of the most butanol resistant strains that the Ashe lab has ever generated.

Therefore, in order to further explore the hypothesis that increased butanol tolerance will facilitate higher butanol production rates, a decision was made to test the *GCD2-S131A* and *GCD2-S131D* mutations in the context of the butanol production strain (*B^R adh1Δ ALD6 ACS2 +5g*). Unfortunately, previous strains from the Ashe lab carry these mutations on plasmids, and this system would be virtually impossible to regenerate in the butanol production strain due to marker gene constraints. Furthermore, a strain where plasmid selection was necessary would not be suitable for industrial use. Therefore, a strategy to mutate the genomic copy of *GCD2* was followed and the resulting strains assessed for butanol production.

6.2 Validation of butanol production in *B^R* versus *B^S* strains

The initial goal of this project was to assess whether differences in the sensitivity of a strain towards butanol would have an impact on butanol production. Therefore, as described previously in chapter 4, appropriate butanol production strains were generated and the comparison was made. However, the difference between the levels of butanol for the *B^R adh1Δ ALD6 ACS2 +5g* relative to the *B^S adh1Δ ALD6 ACS2 +5g* strain was quite small, therefore another independent set of fermentation experiments was performed with the same strains to confirm and extend these results. Little difference was noted in the growth and ethanol production, apart from a very minor increase in ethanol levels for the butanol sensitive strain at some time points (Fig. 6.1 A and Fig. 6.1 B). Butanol levels peak at about 350 ppm using the *B^R adh1Δ ALD6 ACS2 +5g* strain compared to about 200 ppm for the *B^S adh1Δ ALD6 ACS2 +5g* strain (Fig. 6.1 C and D). Although, it should be noted that by the end of the experiment the levels of butanol were more normalised across the two strains and the explanation for this is currently unclear. Overall though, it appears that once again the difference in resistance/ sensitivity to butanol leads to differences in the production levels of butanol. A key question is what is the limit of butanol resistance, and if a strain could be developed that was even more resistant, would it go on to produce even higher levels of butanol.

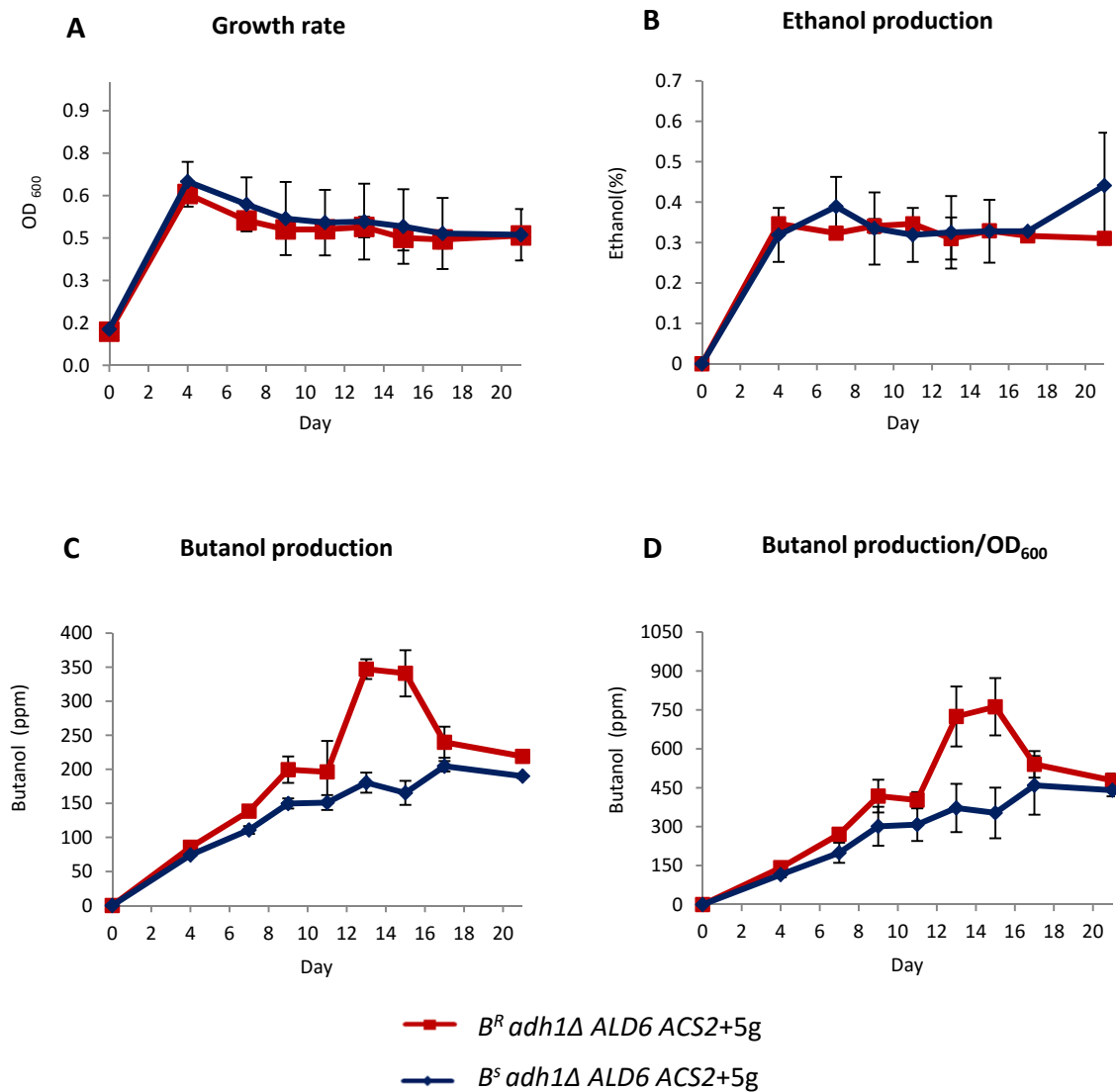


Figure 6.1 Validation of the difference in butanol production between B^R and B^S strains. Plots show the measurement of growth rate (A), ethanol levels (B), butanol levels (C) and butanol levels normalised to OD₆₀₀ (D) for the butanol production strains B^R $adh1\Delta$ ALD6 ACS2+5g (red) and B^S $adh1\Delta$ ALD6 ACS2+5g (blue) over a 21 day semi-anaerobic fermentation. 3 biological replicates were tested for each strain and error bars represent \pm STDEV.

6.3 Construction strategy to generate a ‘super’ resistant strain in the butanol production background.

In order to further investigate the hypothesis that the toxic effect of butanol is important in determining the butanol yield in butanol producing strains, a strategy to generate a ‘super’ butanol resistant yeast strain was taken. Past work in the Ashe lab shows that mutation of serine 131 to alanine in eIF2B δ makes the strain even more resistant to butanol than other butanol resistant mutants. In contrast, an aspartic acid substitution at this site makes the strain much more sensitive to butanol (Keenan 2013). Therefore, mutation of eIF2B δ serine 131 to alanine seemed the obvious route towards the generation a ‘super’ butanol resistant production strain.

Due to difficulties with the number of available markers in the butanol production strain, a decision was made to attempt to generate these mutations on the genomic copy of the gene for eIF2B δ , *GCD2*. The strategy devised to generate the *GCD2* mutants involved two phases: in the first phase the *loxp-natNT2-loxp* cassette would be inserted upstream of the *GCD2* gene in a wild type strain. In the second stage, genomic DNA from this strain would be used to amplify a *GCD2* gene fragment bearing the *loxp-natNT2-loxp* marker using *GCD2* specific primers. Specific mutations could be introduced into this fragment using mutagenic *GCD2* primers. Then both mutagenic and wild type versions of the *GCD2 loxp-natNT2-loxp* cassette could be transformed into the *B^R adh1 Δ ALD6 ACS2+5g* butanol production strain and correct integration at the *GCD2* locus could be confirmed (Fig. 6.2). Finally, the *natNT2* marker could be excised from the genome by expressing the Cre recombinase in order to avoid any deleterious effect of the integrated marker gene: especially in terms of expression of the *GCD2* gene itself or the upstream *MRP13* gene (Partaledis *et al.* 1988) (Fig. 6.2).

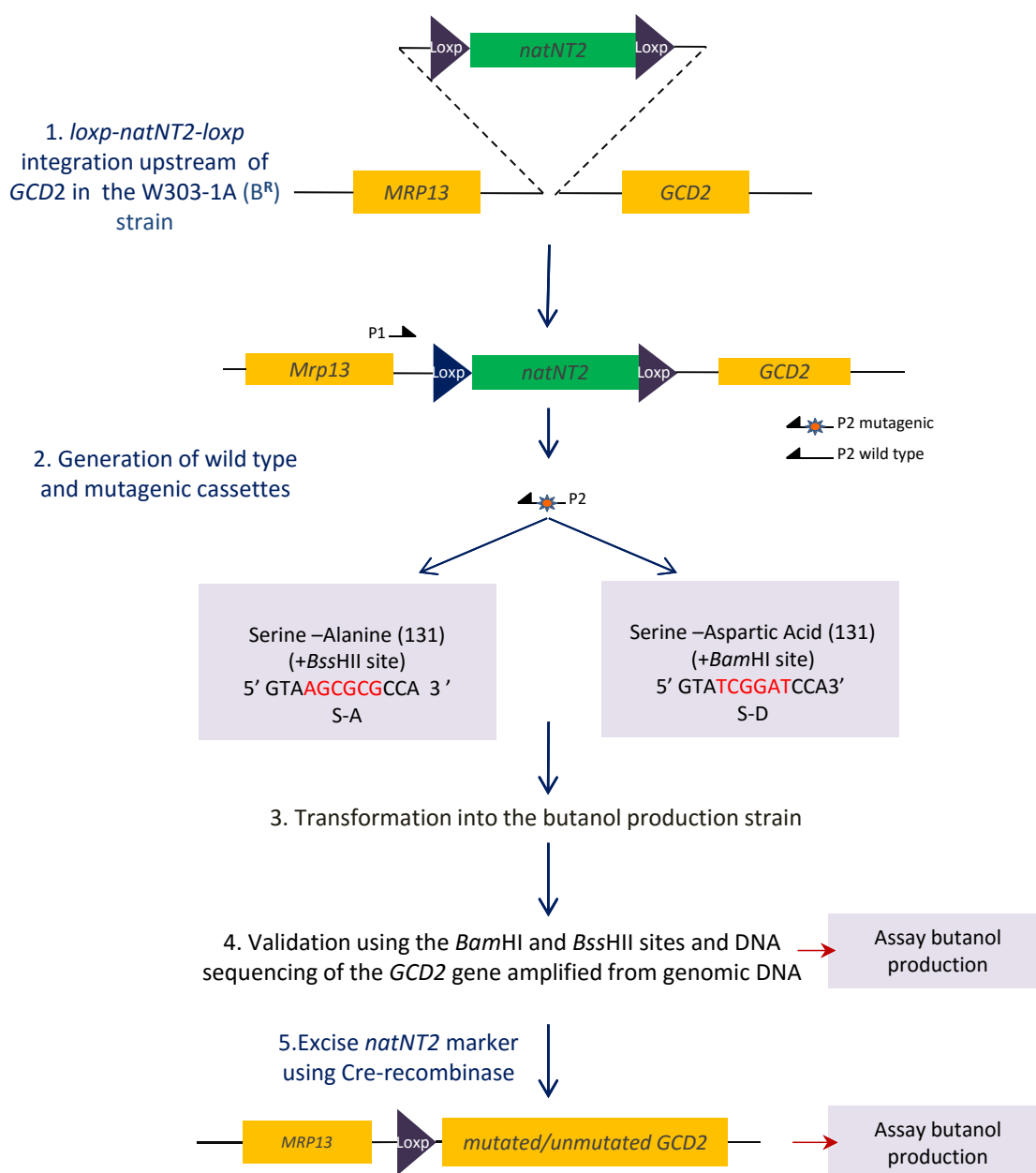


Figure 6.2 Overall strategy used to construct the *GCD2-S131A* and *GCD2-S131D* mutant strains. Figure shows the strategy for *loxp-natNT2-loxp* genomic integration upstream of the *GCD2* gene in a W303-1A (B^R) strain (1). Following the successful integration, the mutagenic cassette was generated using primers listed in Table 2.3. The mutagenic reverse primers contain mutations which introduce restriction sites and alter serine to either alanine or aspartic acid (2). The mutagenic or wild type integration cassettes were transformed into the butanol production strain B^R *adh1Δ* *ALD6 ACS2*+5g (3). Then, the successful mutation of *GCD2* was confirmed by restriction digest/ sequencing of by PCR products (4). Finally, the marker was removed via the Cre-recombinase (5).

6.4 Introducing *loxp-natNT2-loxp* upstream of *GCD2* in WT (B^R)

In order to integrate *loxp-natNT2-loxp* marker upstream of *GCD2*, the marker was PCR amplified from pZC2 vector (Carter and Delneri. 2010) using specific primers: (ORS37 and ORS38 listed in Table 2.3) (Fig. 6.3 A). In order to decrease the likelihood of any negative effects on the expression of either *GCD2* or the upstream *MRP13* gene, the integration site was selected such that it lay as far as possible away from either the poly(A) site of the *MRP13* gene or any potential promoter elements of *GCD2* (Fig. 6.3 B). The resulting cassette was transformed into the yMK23 B^R strain; a W303-1A laboratory strain originally sourced from Alan Sachs lab at UC Berkeley. Appropriate integration was assessed in the resulting transformants using a PCR validation strategy (Fig. 6.3 C). Here three different PCR reactions were performed on genomic DNA prepared from the potential transformants using the verification primers: (ORS39 and ORS40 listed in table 2.1). The first and second PCR reactions have been designed to assess the upstream and downstream chromosomal integration sites, respectively, whereas the third PCR product spans the entire integration cassette. The resulting PCR products closely match the theoretical size and clearly distinguish the positive transformants from the parent strain (Fig. 6.3 D and E). Therefore the first phase in the generation of the desired *GCD2* mutations was successful.

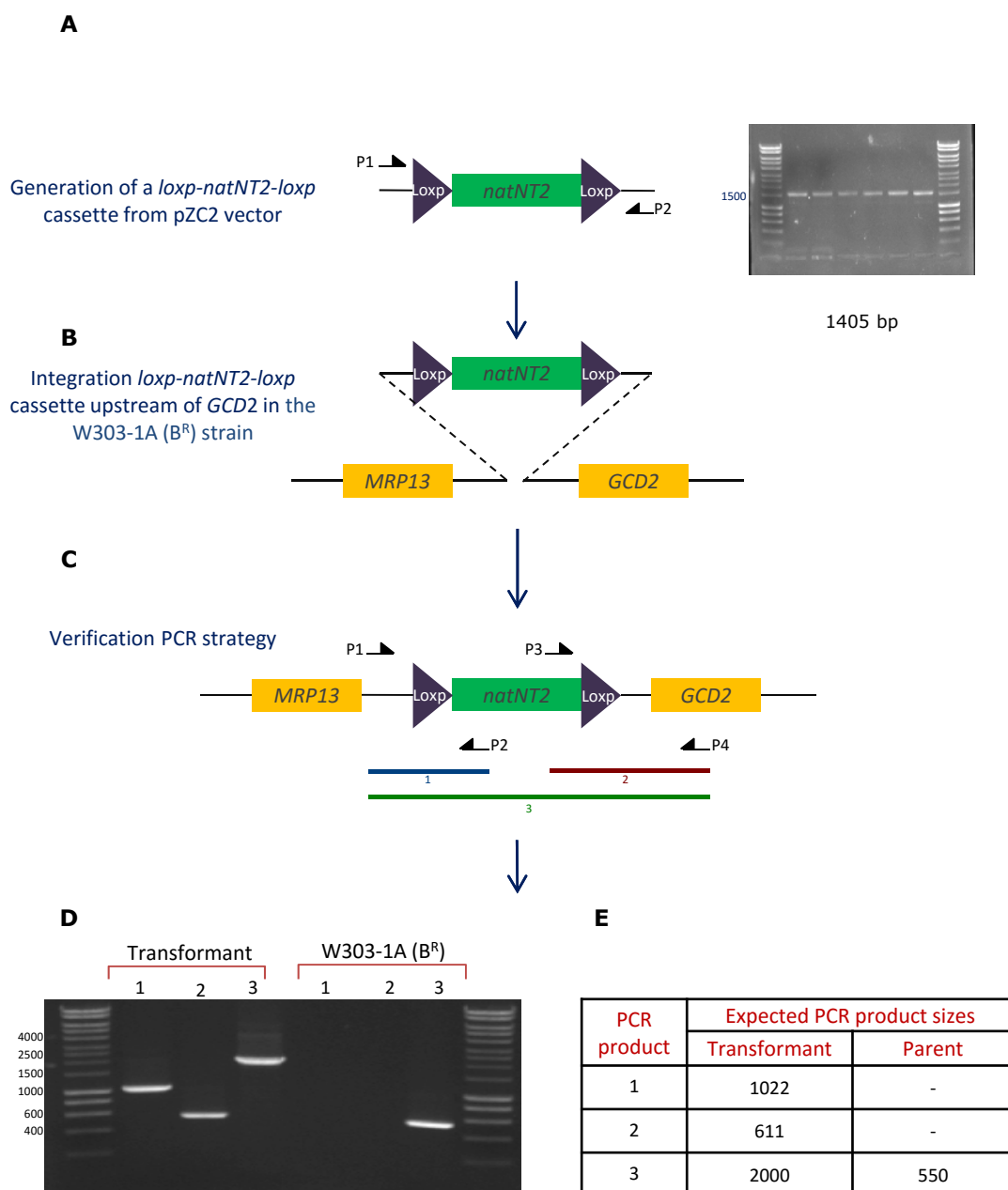


Figure 6.3 Integration of *loxp-natNT2-loxp* upstream of *GCD2*. A) Amplification of the disruption cassette from the pZC2 vector using the amplification primers listed in Table 2.3. B) Integration site of *loxp-natNT2-loxp* upstream of *GCD2* in W303-1A (B^R) strain. C) PCR verification strategy used to confirm the successful genomic integration including three PCR reactions (products depicted in blue, red and green). D) Agarose gel separation of the PCR products from the mutant and parent strains. E) A table depicting the theoretical size of the PCR products .

6.5 Second phase in the mutation of *GCD2-S131* to encode either alanine or aspartic acid.

In the second phase of *GCD2* mutant construction, two mutagenic and one wild type integration cassettes were amplified by PCR from genomic DNA prepared from the yMK23, *loxp-natNT2-loxp::GCD2*, strain using specific amplification primers: (ORS39 with either ORS34, ORS35 or ORS43 listed in Table 2.3). The primers were designed to amplify a region from the mutation site in the *GCD2* gene through to 150 bp upstream of the integrated *loxp-natNT2-loxp* marker cassette. Two different mutagenic reverse primers carrying either the *S131A* or *S131D* mutations as well as specific restriction enzyme sites (either *Bam*HI for *S131D* or *Bss*HII for *S131A*) were used (Fig. 6.4 A). The resulting mutagenic and wild type amplified cassettes (Fig. 6.4 B) were transformed into the butanol production strain (*B^R adh1Δ ALD6 ACS2+5g*) and successful cassette integration was assessed using a PCR based verification strategy (Fig. 6.4 C). In short, a PCR product of 1 kbp was amplified from within the *natNT2* gene to 150 bp downstream of the potential mutation site (Fig 6.4 D) using validation primers: (ORS41 and ORS36 listed in table 2.3). Then the PCR products were digested with the restriction enzymes *Bam*HI and *Bss*HII, respectively, to validate the presence of either the *GCD2-S131A* or *GCD2-S131D* mutations (Fig. 6.4 E and F). The results confirm that relative to the theoretical band sizes (Fig. 6.4 G), the correct products have been obtained suggesting that strains carry the desired mutations. To confirm that the mutations are indeed present, the PCR products were also analysed by DNA sequencing which established that the appropriate mutations were present (Fig. 6.5). Furthermore, the control strain (*B^{*}* control) contained the original sequence of *GCD2* even where the *natNT2* marker was confirmed to be present in the genome upstream of *GCD2*.

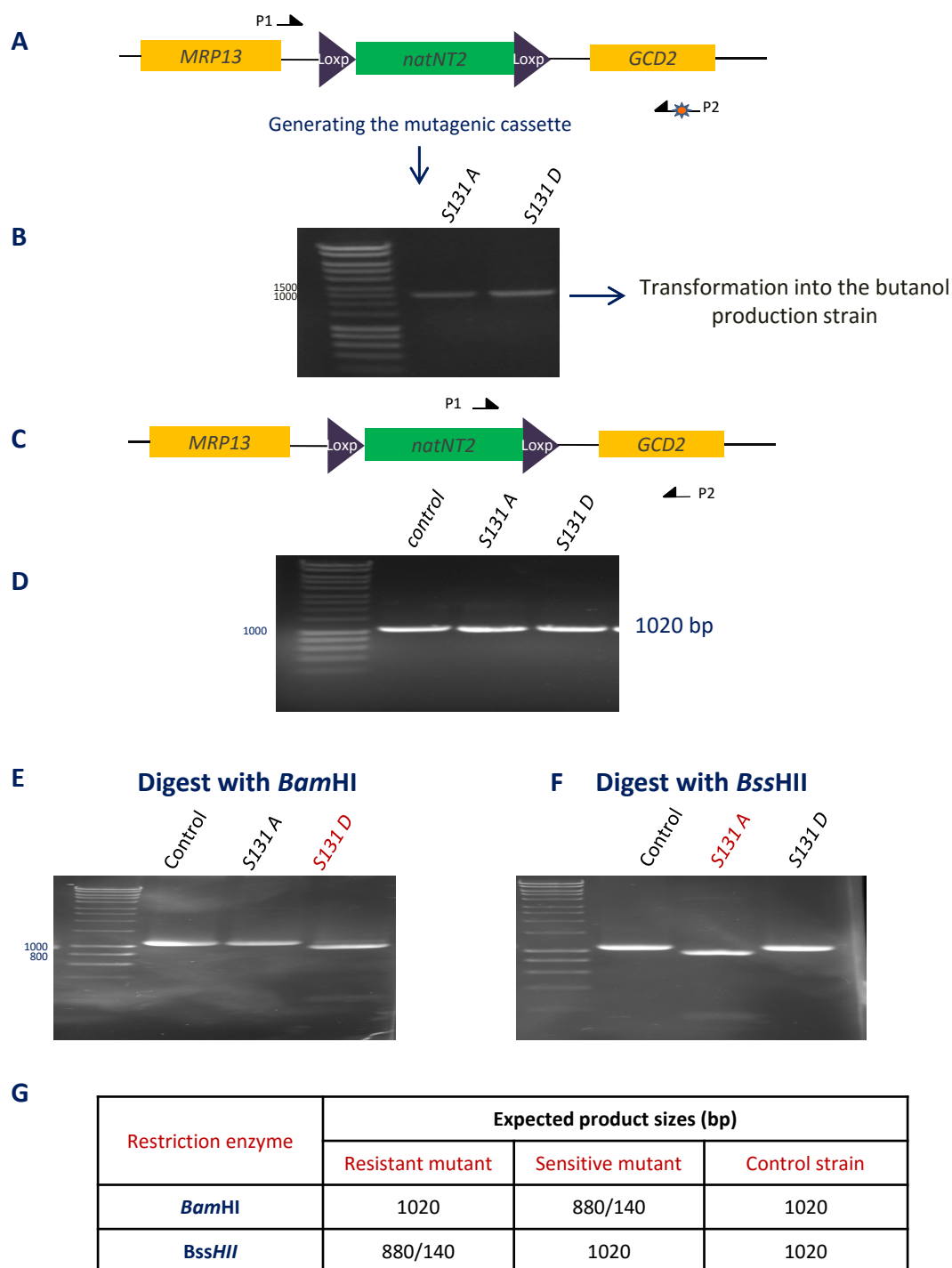


Figure 6.4 Further strategy to generate *GCD2* mutations in the butanol production strain. A) Figure shows the PCR amplification strategy used to generate the disruption cassettes which contain the *S131A* and *S131D* mutations. B) Agarose gel separating the mutagenic PCR products. C) PCR verification strategy to confirm both the successful integration of *natNT2* marker upstream of *GCD2*. D) Agarose gel showing the separation of PCR products for potential transformants. E) Agarose gel of PCR products from D digested with *Bam*HI. F) Agarose gel of PCR products from D digested with *Bss*HII. G) Table depicting the expected fragment sizes for PCR products and *Bss*HII and *Bam*HI digestion products.

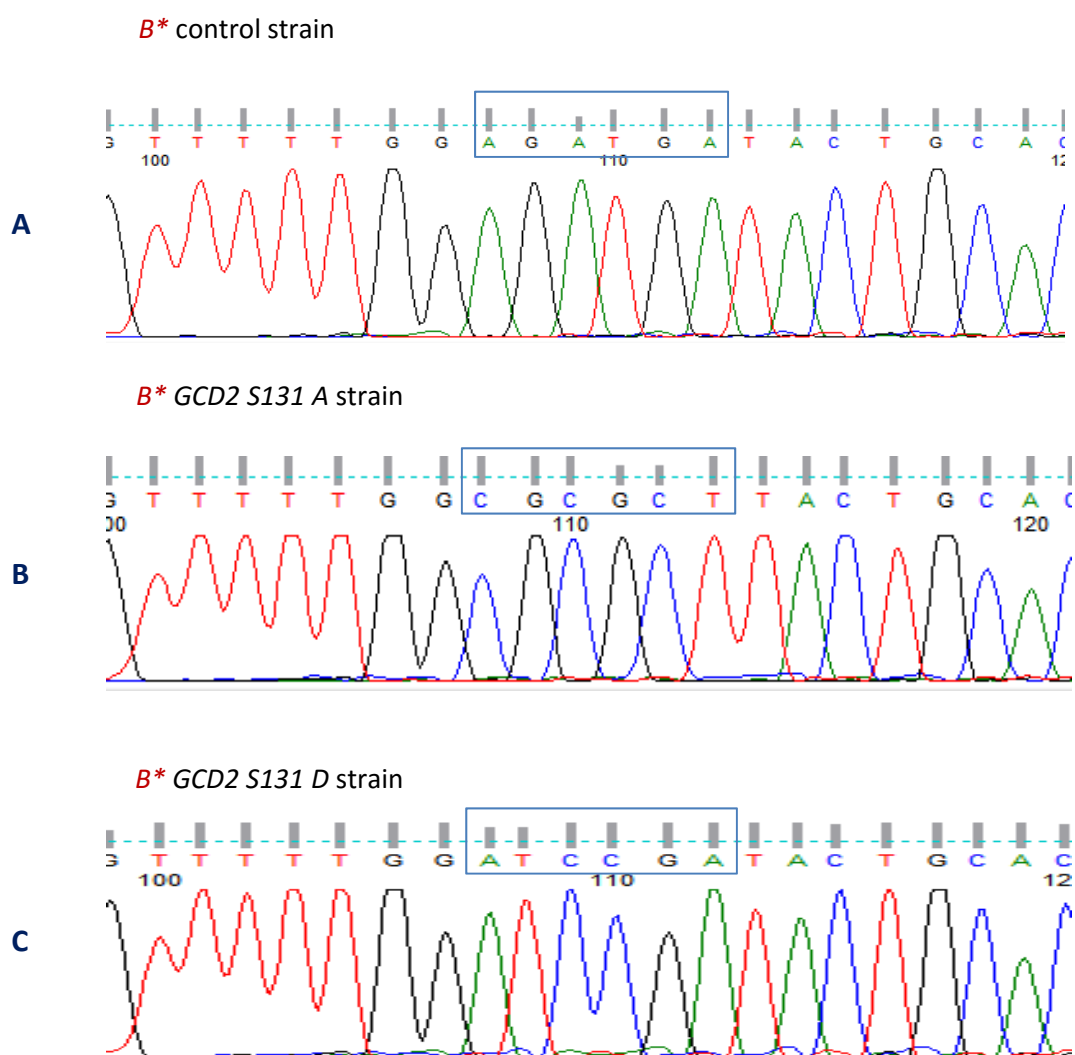


Figure 6.5 DNA sequence analysis of *GCD2* PCR products derived from the potential *GCD2* mutants. PCR products derived from potential transformants were sequenced using an ORS36 primer. Sequences are shown for a control strain harbouring the original amino acid sequence S131, a strain carrying the S131A mutation and a strain carrying the S131D.

B* *B^R adh1Δ ALD6 ACS2 +5g loxp-natNT2-loxp::GCD2*

6.6 Growth analysis of the *GCD2* mutants

Following the successful construction of the *GCD2* mutations in the butanol production strains (with the ABE pathway, *adh1Δ* and *ALD6 ACS2*), growth was assessed on butanol gradient plates. The butanol production strains, *B^R adh1Δ ALD6 ACS2+5g* and *B^S adh1Δ ALD6 ACS2+5g*, exhibited similar differences in growth to those observed previously for the W303-1A (*B^R*) and W303-1A (*B^S*) strains (Ashe *et al.* 2001). Interestingly, the *GCD2* mutant strain *B* GCD2 S131A* exhibits significantly improved growth at high butanol concentrations, whereas the *GCD2 S131D* mutant strain shows much poorer growth across the gradient plate, when compared to the parent strain *B^R adh1Δ ALD6 ACS2+5g* (Fig. 6.6). Noticeably, the *B** control strain that only differs from the parent in the presence of the *loxp-natNT2-loxp* marker upstream of *GCD2* has slightly lower growth levels across the gradient plate compared to the parent strain. This unexpected result suggests that integration of the *natNT2* marker gene upstream of *GCD2* has affected either the expression of *GCD2* or *MPS13*. Further investigation aimed at assessing expression levels would be required to distinguish between these possibilities.

Overall, the gradient plate experiments suggest that the alanine substitution at position 131 within eIF2Bδ has made the strain even more resistant to butanol toxicity than the parental *B^R* strain, while aspartic acid at position 131 has increased sensitivity to butanol.

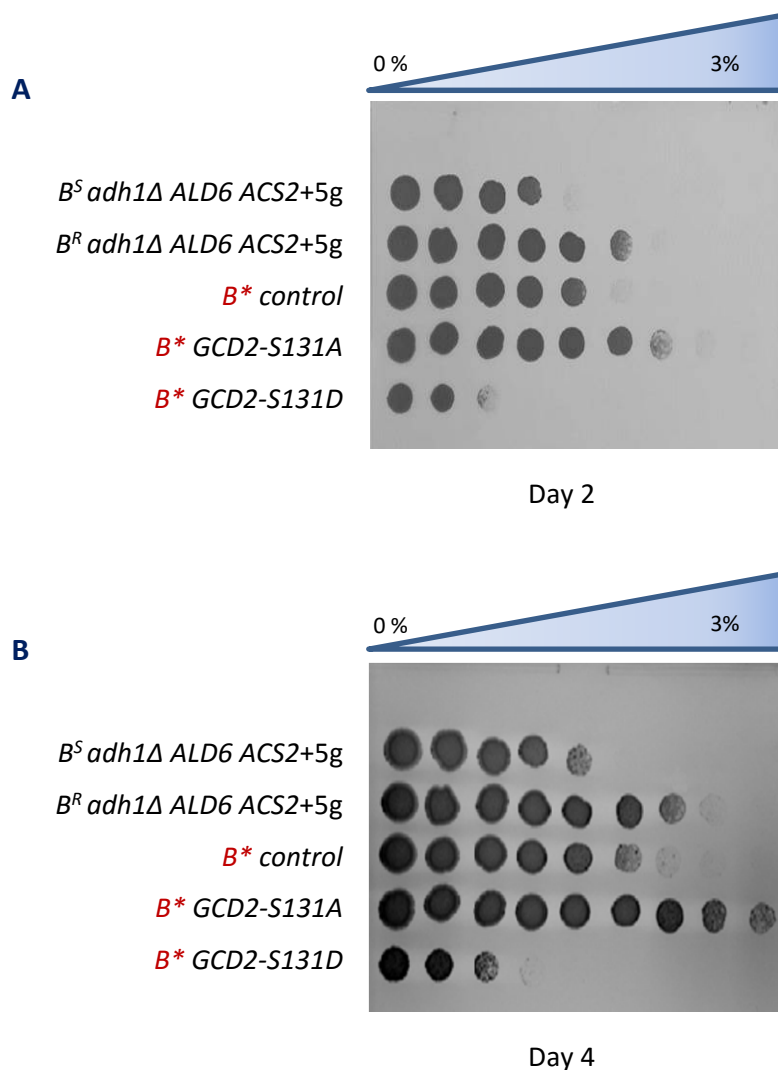


Figure 6.6 Mutation of eIF2B δ serine 131 alters butanol tolerance. The depicted strains were spotted on a butanol gradient plate, where the concentration of butanol was increased from right to left from 0 to 3 % butanol. Plates were incubated for a week and images were taken at days 2 (A) and day 4 (B).

B^{} B^R adh1Δ ALD6 ACS2 +5g loxp-natNT2-loxp::GCD2*

6.7 Polysome analysis of the mutated and unmutated strains

In order to explore whether the *GCD2-S131A* and *S131D* mutants also have an impact on the control of translation initiation, polysome analysis was performed for the constructed strains. Strains were treated with various butanol concentrations (0-1.75% (v/v)) for 10 min, then cycloheximide was added, to freeze the polysomes on the mRNA, and polysome extracts were prepared and analysed. During optimal growth conditions, mRNAs are heavily translated leading to multiple ribosomes on mRNA or 'polysomes' (Warner *et al.* 1963). However, if translation initiation becomes inhibited in response to changing conditions, existing ribosomes on mRNAs complete the elongation and termination process before new ribosomes can initiate leading to a phenomena called 'polysome run-off'. Here the 80S monosomal peak increases dramatically while the polysome peaks decrease (Hutchison *et al.* 1969; Hartwell *et al.* 1969). Previous studies in Ashe lab have shown that strains bearing a butanol sensitive *GCD1-S180* allele of eIF2B γ exhibit an increased 80S monosome peak and reduced polysome peaks after treatment with 1% butanol. In contrast, strains bearing a butanol resistant *GCD1-P180* allele show no significant difference between the untreated and 1% butanol treated samples (Ashe *et al.* 2001). The results in the butanol production strains are entirely consistent with these previous studies: the butanol sensitive strain *B^S adh1 Δ ALD6 ACS2+5g* is inhibited by 1% butanol treatment, whereas the butanol resistant strain *B^R adh1 Δ ALD6 ACS2+5g* is unaffected by this treatment (Fig. 6.7). However at higher concentrations both strains are translationally inhibited. In the strain where only the *loxp-natNT2-loxp* was integrated upstream of *GCD2* (the *B^{*}* control strain) a similar profile of polysomes to the parental *B^R* butanol production strain was noted across the different butanol concentrations. More importantly, for the strain bearing *GCD2-S131A*, the strain exhibits no alteration to the polysome profile unless greater than 1.25% butanol is used, and even at higher butanol concentrations the level of polysomes was greater than any strain previously studied in the Ashe lab. In contrast, for the *B^{*} GCD2 S131D* strain, higher levels of polysome run-off were observed than the parental *B^R adh1 Δ ALD6 ACS2+5g* strain (Fig. 6.7). These data combined with the growth analysis verify and validate the butanol resistant and

sensitive phenotypes observed previously using plasmid derived versions of the different *GCD2* alleles.

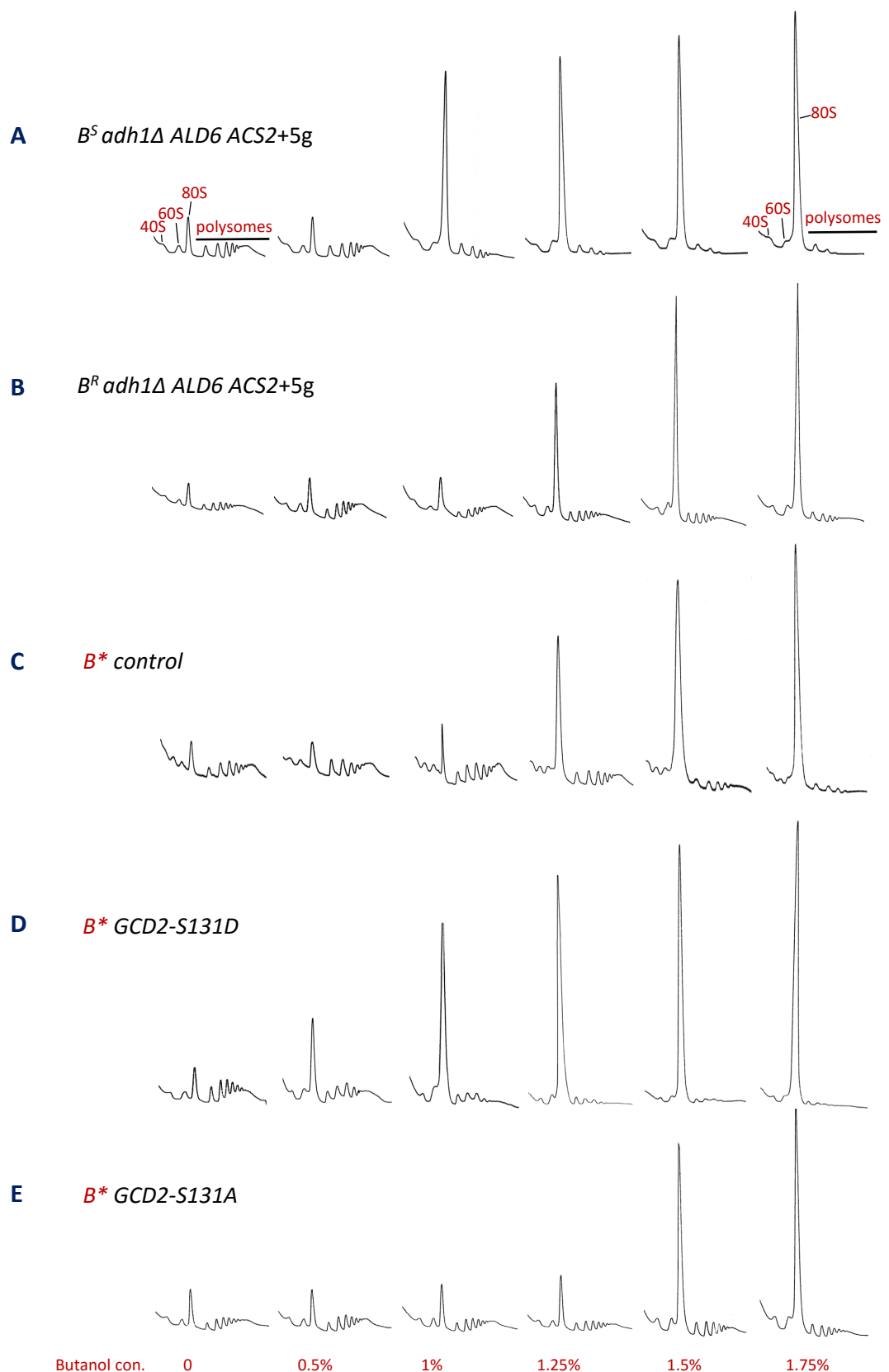


Figure 6.7 Polysome analysis reveals that the *GCD2-S131A* mutant has increased tolerance to butanol, while the *GCD2-S131D* mutant is more sensitive to butanol. Figure shows polysome gradient profiles for the strains depicted. All strains were grown to 0.6 OD₆₀₀ on YPD media. Extracts were prepared from untreated cells and from cells treated with different concentrations of butanol for 10 min. The position of the 40S, 60S, 80S and polysomal peaks across the gradient are depicted on an untreated trace and a trace where significant polysome run-off has occurred.

*B** *B^R adh1Δ ALD6 ACS2 +5g loxp-natNT2-loxp::GCD2*

6.8 The impact of using *loxp-natNT2-loxp::GCD2* mutants on growth, ethanol and butanol production.

Having successfully generated and validated the *GCD2* mutants in the butanol production strain, a decision was made to test these strains for butanol production. Standard semi-anaerobic fermentation experiments were performed and for the strain bearing *GCD2-S131A* small decrease was noted in cell density and ethanol levels relative to the control over a 21 day period (Fig. 6.8 A and B). However, for the strain bearing the *GCD2-S131D* allele a large reduction in the growth and ethanol production was observed (Fig. 6.8 A- purple line). Noticeably, both the *B^R adh1Δ ALD6 ACS2+5g* and *B* control* strains produce similar levels of butanol over the course of the fermentation. The levels of butanol for the resistant *GCD2-S131A* strain are similar to the control strains, whereas the sensitive *GCD2-S131D* strain gave lower levels of butanol (Fig. 6.8 C). When butanol values were normalized to the OD₆₀₀ again all the constructed strains gave similar patterns except the sensitive strain where reduced butanol per cell was observed (Fig. 6.8 D).

Overall, there is no significant difference in terms of cell density, ethanol and butanol production when the eIF2Bδ Serine 131 to alanine mutation was introduced into butanol production strain. In contrast, an aspartic acid substitution at this site caused a large reduction in growth, ethanol and butanol production. However at this stage of project, it is not clear what the impact of introducing the *loxp-natNT2-loxp* cassette upstream of *GCD2* is. It is entirely possible that the cassette affects the physiology of the strains either in the presence or absence of butanol.

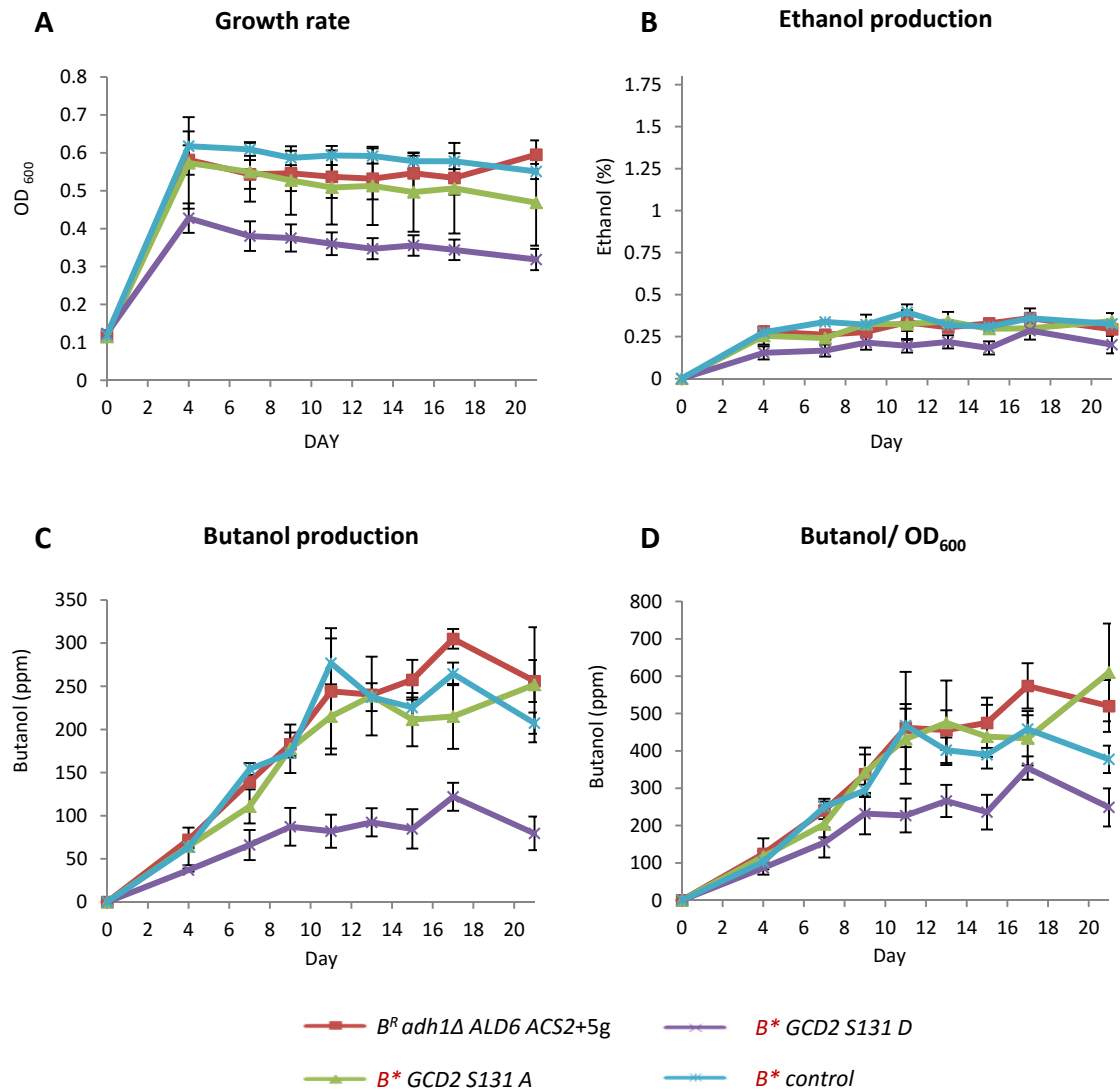
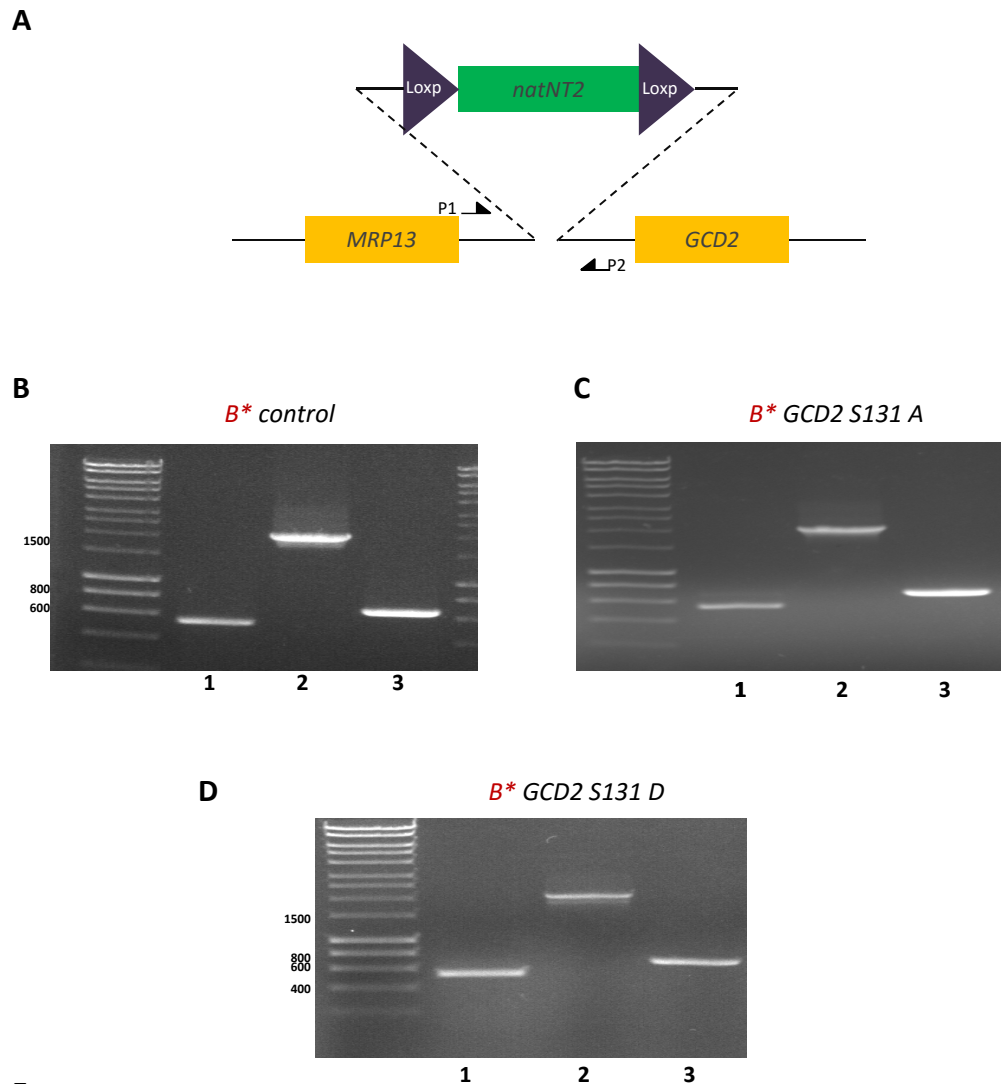


Figure 6.8 Detecting the impact of *GCD2* mutation before marker removal on butanol, ethanol and growth rate. Plots show the measurement of growth rate (A), ethanol levels (B), butanol levels (C) and butanol levels normalised to OD₆₀₀ (D) for the butanol production strain (red) and the *GCD2* mutant or control strains over a 21 day semi-anaerobic fermentation. Three biological replicates were tested for each strain and error bars represent \pm STDEV.

6.9 Excision of the *loxp-natNT2-loxp* marker from the *GCD2* mutants

In order to explore whether the *loxp-natNT2-loxp* upstream of *GCD2* is affecting the physiology of the yeast, a decision was made to remove the marker from the genome taking advantage of *loxp* sites. Both the *GCD2* mutants and the control strain were transformed with a plasmid expressing the Cre recombinase under the control of a galactose inducible promoter. Following induction of the Cre recombinase (see Materials and Methods), colonies were selected that could no longer grow on CloNat containing plates. The successful and precise removal of the *natNT2* marker was confirmed using a PCR verification analysis (Fig. 6.9 A). Here, primers upstream and downstream of the site of integration were used: (ORS39 and ORS40 listed in Table 2.3) on genomic DNA prepared from the relevant strains. Controls show the size of PCR products for the parent strain before and after integration of the *loxp-natNT2-loxp* (Fig. 6.9 B and D, lanes 1 and 2). After Cre recombinase induction, the size of the PCR product was reduced such that it was only just bigger than that generated from the parent strain (Fig. 6.9 B and D, lane 3). All of the PCR products closely match the theoretical sizes (Fig. 6.9 E). Therefore, new *GCD2* mutants and a control strain have been generated which now only carry the small *loxp* 'scar' upstream of *GCD2*.



E

PCR product	Purpose	Size (bp)
1	The parent strain	550
2	After <i>loxp-natNT2-loxp</i> integration	2000
3	After Cre mediated recombination	582

Figure 6.9 Excising strategy to take off *natNT2* from the genome. A) showing the verification PCR analysis used to confirm the successful deletion of *natNT2* from the genome. B) ,C) and D) are photograph gels of three PCR products generated from the strain, at three different stages: before/ after introducing *loxp-natNT2-loxp* and after had been excised from the genome. The identity of each strain is labelled above the image. E) table showing the aim behind generating each PCR product and the theoretical sizes of each band .

6.10 Analysis of Gcd2p expression levels for the *GCD2* mutants.

In order to assess whether the protein expression level of Gcd2p is affected by the mutations in the *GCD2* gene or by the presence of the *loxp-natNT2-loxp* cassette, whole cell protein extracts were prepared from all of the *GCD2* mutants and controls. Immunoblotting using a primary rabbit anti-Gcd2p antibody (a gift from Prof G. Pavitt) revealed a single major band of approximately the right size. The level of this band was largely unaltered in terms of level, relative to a Pab1p loading control, across all of the different mutant strains generated (Fig. 6.10). Therefore, it seems like neither the presence of *natNT2* nor the *GCD2* point mutations alters the level of expression of Gcd2p in the strains. However, this analysis does not show that the mutations or insertion of the marker have no impact on the physiology of the cell. It is still possible that the mutations would impact on basal eIF2B activity as well as its regulation by butanol and that the insertion would affect the upstream *MRP13* gene.

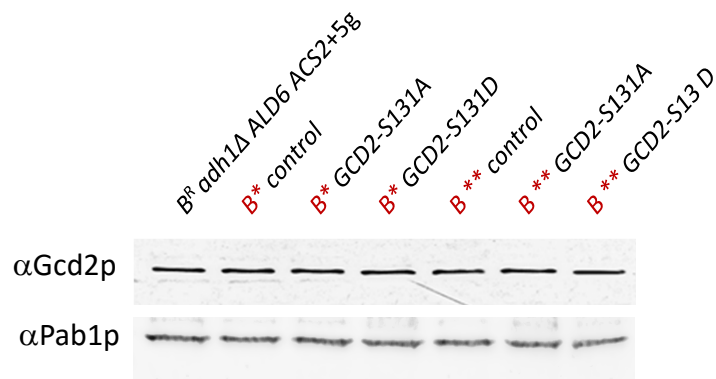


Figure 6.10 Investigation of the expression of Gcd2p in the *GCD2* mutants and control strains. Western blot using protein extracts prepared from the strains listed above each lane, probed with either a rabbit anti-Gcd2p antibody or as a loading control a mouse monoclonal anti-Pab1p antibody.

B^* B^R adh1 Δ ALD6 ACS2 +5g, *loxp-natNT2-loxp::GCD2*

B^{**} B^R adh1 Δ ALD6 ACS2 +5g, *loxp::GCD2*

6.11 Assessment of butanol levels in the *GCD2* mutants lacking the *natNT2* marker.

Following the successful excision of the *natNT2* marker gene, semi-anaerobic fermentations were conducted to measure the level of butanol production in the various butanol resistant and sensitive mutants. In keeping with previous observations (Fig. 6.8 A and B), growth and ethanol levels for the ‘super-sensitive’ strain bearing the *GCD2-S131D* mutation were dramatically reduced compared to the control strains (Fig. 6.11 A and B, cf. purple line relative to red or blue lines). For the ‘super-resistant’ strain bearing the *GCD2-S131A* mutation growth and ethanol levels were also reduced relative to controls but to a lesser extent (Fig. 6.11 A and B, cf. green line relative to red or blue lines). This is different to the results presented in Fig. 6.8 A and B, and this could suggest that the presence of the *natNT2* marker did indeed alter the physiology of the mutant strain, although further experiments would be required to conclude this.

In terms of butanol yield, consistent with growth and ethanol yields and the toxicity of butanol, very low levels of butanol were obtained from the super-sensitive *GCD2-S131D* strain (Fig. 6.11 C), while for the super-resistant *GCD2-S131A* strain the overall yield was not altered relative to control strains (Fig. 6.11 C), the level of butanol produced per cell was increased (Fig. 6.11 D), presumably as the strain had accumulated less biomass.

Overall, increasing butanol tolerance in the butanol production strain has led to an improvement in the butanol yield per unit of biomass but no increase in the overall butanol concentration in the fermentation media. It is entirely possible that, although the *eIF2B δ -S131A* mutation increases tolerance to butanol, it also somehow slightly decreases the level of growth under semi-anaerobic conditions. *eIF2B* mutations commonly lead to reduced growth rates due to their effects on the guanine nucleotide exchange function of *eIF2B* and overall protein synthesis (Niederberger *et al.* 1986; Foiani *et al.* 1991). If this is true, the challenge becomes the identification of a super-resistant mutation in *eIF2B* that does not affect growth rates.

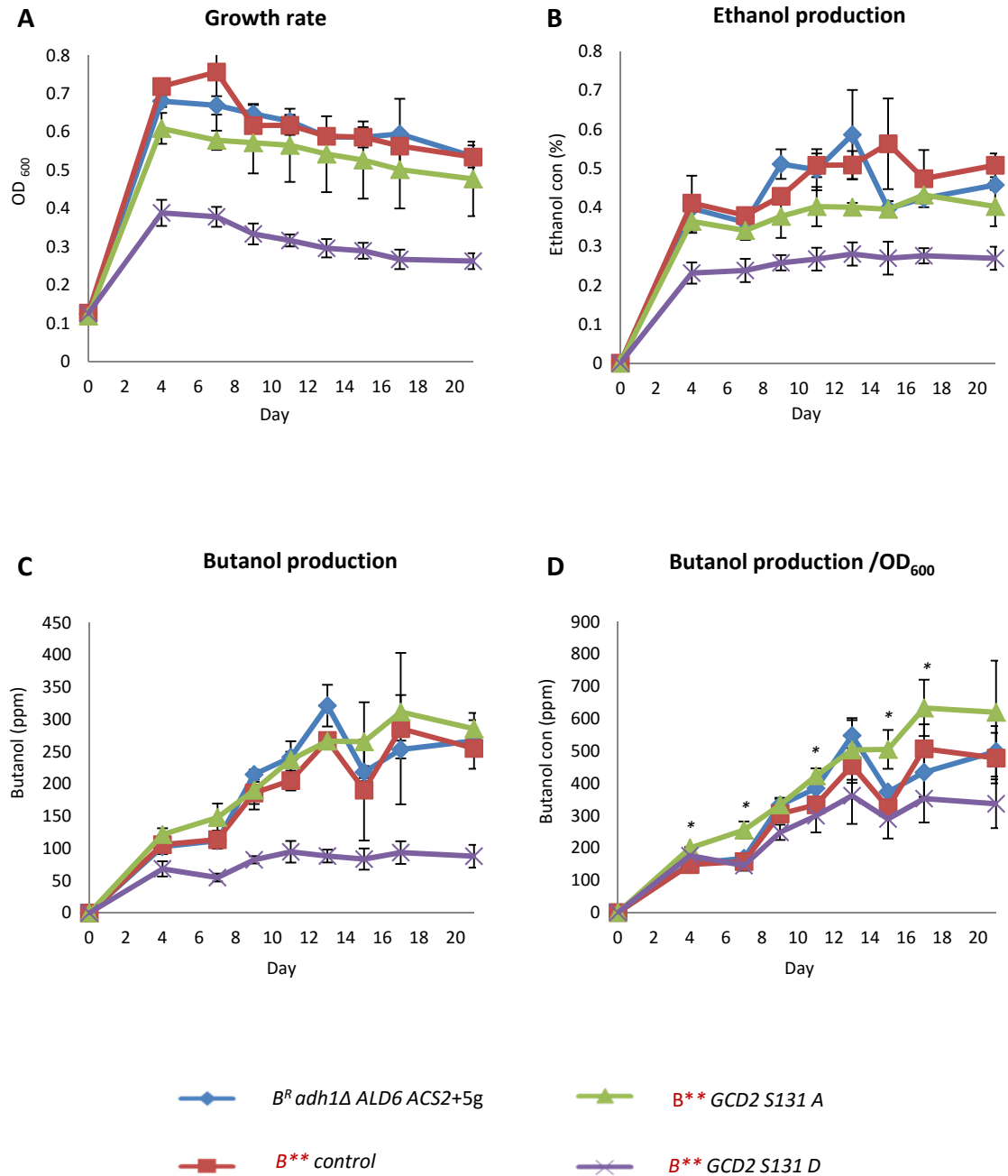


Figure 6.11 Assessing the impact of *GCD2* mutations after marker removal on butanol, ethanol and growth rate. Plots show the measurement of growth rate(A), ethanol levels (B), butanol levels (C) and butanol levels normalised to OD₆₀₀ (D) for the butanol production strain (red) and the *GCD2* mutant or control strains over a 21 day semi-anaerobic fermentation. Three biological replicates were tested for each strain and error bars represent \pm STDEV. * significant difference between *B^{**}* (*B^R adh1Δ ALD6 ACS2 +5g, loxp:: GCD2*) and the control *B^R adh1Δ ALD6 ACS2+5g* strain ($p < 0.05$).

6.12 Discussion

Previous work in *S. cerevisiae* from the Ashe lab has identified a role for the translation initiation factor eIF2B in the response to fusel alcohols in a translation control mechanism (Ashe *et al.* 2001; Taylor *et al.* 2010; Kubota *et al.* 2003). Unpublished work has identified phosphorylation sites within eIF2B via mass spectrometry. In particular, serine 131 on eIF2B δ is phosphorylated in a manner that correlates with butanol resistance and sensitivity. Indeed strains where the serine was replaced with alanine in the eIF2B δ gene, *GCD2*, are highly resistant to butanol. A key question addressed in this thesis is whether the toxic effects of butanol are important in determining the yield from butanol producing strains.

Evidence supporting this hypothesis has been presented in chapter 4 using butanol resistant and sensitive production strains varying in the eIF2B γ gene, *GCD1*. The observed difference between these strains in terms of production was unexpected, as relative to the level of exogenous butanol that is required to inhibit translation initiation (Ashe *et al.* 2001; Taylor *et al.* 2010), a considerably lower concentration of butanol is produced. So given these low production levels, it is difficult to rationalise why the butanol sensitive and resistant strains should exhibit differences in butanol production levels. One possible explanation lies in the capacity of butanol to cross biological membranes. For instance, the intracellular concentration of butanol in a butanol producing strain could be much higher than anticipated if butanol crosses the cell membrane poorly. Previous studies have shown that the degree of butanol toxicity is important for butanol production (Fischer *et al.* 2008) and that butanol tolerance can be improved when specific efflux pumps are expressed in *E.coli* (Dunlop *et al.* 2011). It is entirely possible that by further increasing butanol tolerance, greater improvements in butanol production will be achieved.

On this basis, a decision was made to generate the *GCD2* mutations in the genome of the butanol production strain *B^R adh1 Δ ALD6 ACS2+5g*. These mutations were successfully introduced with a *loxP-natNT2-loxP* cassette to generate three strains: *GCD2-S131A*, *GCD2-S131D* and the control strain. The strains were validated using both growth and polysome analyses: the *GCD2-S131A* mutant proved highly resistant, whereas the *GCD2-S131D* mutant exhibited high sensitivity to butanol.

Interestingly, the growth of the control strain (with the *loxp-natNT2-loxp* marker integrated upstream of wild type *GCD2*) was decreased slightly compared to the parent. Given that the level of Gcd2p remains the same for all of the constructed strains (either with or without the *loxp-natNT2-loxp* marker), it is possible that integration of the marker somehow causes altered expression of the adjacent *MPS13* gene, which is involved in respiratory growth (Partaledis *et al.* 1988). Overall, the toxicity results from the mutants support a model where eIF2B δ Ser131 phosphorylation within eIF2B increases butanol sensitivity and dephosphorylation increases butanol tolerance. It is not clear whether eIF2B phosphorylation is regulated as a result of controls at the level of the protein kinases or phosphatases that are involved in the phosphorylation, or even which kinases and phosphatases play a role. In mammalian cells, four protein kinases are involved in eIF2B phosphorylation: casein kinase 1(CK1), casein kinase 2(CK2), dual-specificity tyrosine phosphorylated and regulated kinase (DYRK) and glycogen synthase kinase (GSK) (Wang *et al.* 2001; Woods *et al.* 2001). In contrast, studies in yeast have not focussed upon eIF2B phosphorylation. More detailed investigation would be required in order to explore which kinases/ phosphatases are involved and what their role might be in the regulation of translation initiation in response to alcohols.

Having shown that the *GCD2-S131A* gives a 'super-resistant' phenotype, the obvious question is whether this improves butanol production. For the strain bearing the *loxp-natNT2-loxp* cassette little difference in butanol yield was noted relative to the control strain. However, for the strain where the marker cassette had been removed, two effects were noted. Firstly, the mutant grew to lower cell densities during the course of the fermentation and secondly even though the biomass accumulation was reduced the level of butanol produced is maintained. Thus in this strain the butanol production per cell is likely improved. Mutations to eIF2B commonly lead to both reductions in growth rate and to effects on the cell's capacity to respond to stresses such as alcohol accumulation (Foiani *et al.* 1991; Niederberger *et al.* 1986; Ashe *et al.* 2001). A key goal in the future will be to identify super-resistant mutants, which don't impact upon biomass accumulation.

The *GCD2-S131D* mutant leads to significantly reduced growth, ethanol and butanol production in semi-anaerobic conditions. Again, the mutation appears to be having two effects reducing cellular growth and increasing the sensitivity to alcohols. Overall these results highlight that for eIF2B, the impact of mutations on growth and stress tolerance are critical parameters to evaluate in terms of their use in the improvement of butanol yields from production strains.

7. General Discussion

Butanol is an alternative source of energy to gasoline, which can be produced from renewable resources as a second or third generation biofuel (Peralta-Yahya *et al.* 2012). In addition, n-butanol is arguably superior to ethanol and biodiesel because of a wide range of preferable properties. For instance, compared to the current major player in the biofuel area, ethanol; butanol is less hygroscopic, it is less corrosive, it has a higher energy content and it can be used at any ratio with gasoline, including directly as a fuel without modification to existing car engines and infrastructure (Cascone 2008). In the past, butanol was produced extensively from *Clostridia* species. However, bacterial production can be associated with a range of difficulties, including product toxicity, bacteriophage contamination, complicated two phase (acidogenesis and solventogenesis) fermentations, sporulation during solventogenesis, high levels of by-products and decreased yields at large scale (Zheng *et al.* 2009; Xue *et al.* 2013; Hong *et al.* 2012; Huffer *et al.* 2012). Therefore, in this thesis a decision was made to investigate whether the use of yeast as an alternative host for butanol production could overcome some of the problems associated with bacterial production.

A major goal of this project was to produce butanol using *S. cerevisiae* and explore the efficiency of this production. In order to achieve this goal, strains of *S. cerevisiae* were constructed bearing the *Clostridia* ABE pathway including 5 butanol synthetic genes. In addition, various metabolic engineering strategies were specifically designed to increase the carbon flux towards the butanol production pathway. As a result yields of 308 mg/L were obtained as the maximal output.

Given the previously published work from the Ashe lab on the impact of butanol on protein synthesis (Ashe *et al.* 2001), a second goal was to explore the hypothesis that increased butanol tolerance in a butanol production strain would lead to increased butanol production. Two strategies were taken to explore this hypothesis. Firstly previously characterised butanol resistant and sensitive strains were used and higher butanol levels were consistently observed for the resistant strain. In a second strategy, a super butanol resistant strain carrying a specific mutation in eIF2B δ was generated and although the butanol yield was not increased, it did appear that the strain produced more butanol per cell than controls.

7.1 The ABE pathway and butanol production in *S. cerevisiae*.

In keeping with previous studies (Steen *et al.* 2008), introduction of a codon optimised ABE pathway into yeast did not yield appreciable levels of butanol. All indications suggested that the proteins were expressed, although it is clearly possible that some aspect of their production such as their folding or the presence of the C-terminal epitope tag could inhibit enzyme activity. Alternative explanations for the lack of butanol production could come from yeast metabolism itself. For instance, redox imbalance could be generated within cells due to the high NADH requirements of the butanol synthetic pathway. Furthermore, it is entirely possible that a lack of cytosolic acetyl-CoA, the precursor for butanol production, could account for the low yields.

In order to explore whether the setup of the yeast metabolism was responsible for the low butanol yields, we deleted the major alcohol dehydrogenase gene *ADH1*. The Adh1p enzyme accounts for the major part of ethanol production and is a key player in redox control where it recycles the NADH generated in glycolysis back to NAD⁺. Therefore a deletion of this gene should decrease ethanol production, which would compete with butanol synthesis; the deletion would also increase the pool of cytosolic NADH and potentially increase the level of cytosolic acetyl-CoA. A disadvantage of this strategy was immediately apparent, the deletion (even by itself without the ABE pathway) led to a large reduction in growth rate compared to the wild type strains.

While our studies were in progress an added complication to the interpretation of experiments using the *adh1* mutant became apparent. A single deletion of *ADH1* in *S. cerevisiae* was shown to generate 120 mg/L butanol via the activation of an endogenous pathway of butanol production based on threonine catabolism in the mitochondria (Si *et al.* 2014). Consistent with this, our *adh1* mutant strain also produced approximately 40 mg/L of butanol.

Interestingly, strains bearing the five ABE pathway enzymes in an *adh1* mutant background, generate approximately four times higher butanol levels than the *adh1Δ* mutant strain alone. Our interpretation of these data is currently that the exogenous and endogenous pathways of butanol production are both activated by the *adh1*

deletion. Hence, synergistic effects are observed for strains bearing both the ABE pathway and the *ADH1* deletion. However, we cannot formally rule out the possibility that elements of the ABE pathway activate the endogenous pathway of butanol production.

Intriguingly, gas chromatography–mass spectroscopy (GC-MS) studies performed by Dr. Hui Wang in the Ashe lab reveal that the *ADH1* deletion also leads to the accumulation of acetaldehyde and other end-product metabolites such as 2,3-butanediol. Further evidence for the activity of the exogenous ABE pathway when in an *adh1* deletion strain also stems from these GC-MS studies: crotonal accumulates in this strain and it is likely that this metabolite derives from crotonyl-CoA an intermediate in the butanol synthetic pathway (Swidah *et al.* 2015).

7.2 Improved carbon flux toward acetyl-CoA production promotes butanol production.

The accumulation of intermediates and end product metabolites like acetaldehyde, acetate and 2,3-butanediol in strains bearing both the ABE pathway and the *adh1* deletion suggests that carbon flux toward butanol production is not optimal in this strain. Therefore, a decision was made to overexpress the enzymes involved in the conversion of acetaldehyde to acetyl-CoA. Ald6p, a cytosolic aldehyde dehydrogenase, and Acs2p, the acetyl-CoA synthase, are endogenous enzymes that are involved in this conversion. Usually, these enzymes are maximally expressed under stress conditions or when non-fermentable sugars are being metabolised as a sole carbon source (Aranda *et al.* 2003). Therefore, the *ALD6 ACS2* cassette was designed and integrated such that the genes were placed in a high expression context. Interestingly, overexpression of *ALD6 ACS2* gives a small improvement in terms of butanol yields for the *adh1* mutant bearing the ABE pathway (360 ppm, 308 mg/L). These results are consistent with previous studies where the accumulation of cytosolic acetyl-CoA improves butanol production in yeast (Krivoruchko *et al.* 2013) and are again consistent with the interpretation that the exogenous ABE pathway is active in these strains.

The Ald6p enzyme was selected as it is thought to be the major cytosolic acetaldehyde dehydrogenase. However, Ald6p generates NADPH and for butanol synthesis it might be more advantageous to use an enzyme that generates NADH. Therefore, the *ALD6* gene in the cassette was replaced with *ALD2*, as the Ald2p enzyme is NAD⁺/NADH specific. Nevertheless, overexpression of Ald2p as part of an *ALD2 ACS2* cassette does not improve butanol levels. Possible explanations for this relatively unexpected result could be that the activity of the Ald2p enzyme might be lower than that of Ald6p; or equally one of the butanol synthetic enzymes might be more dependent on NADPH than previously realised. However, further investigation would be required to address this, and as the level of improvement, even with the *ALD6 ACS2* cassette, is only 2-fold, the strategy was not pursued further.

7.3 Targeted deletion of redox active enzymes in competing pathways

Another metabolic engineering strategy that was explored towards improving butanol production was the deletion of competing pathways, such as the glycerol biosynthesis pathway. Gpd1p and Gpd2p are NADH dependent glycerol-3-phosphate dehydrogenases that are involved in glycerol production. The genes encoding these enzymes, *GPD1* and *GPD2*, were deleted individually from the butanol production strain. Deletion of the *GPD1* gene did not give any improvement in butanol yield, while almost no butanol was obtained when *GPD2* was deleted. Intriguingly, in this mutant (which also carries the *ADH1* deletion) growth and ethanol production are restored to the level normally associated with strains bearing a functional *ADH1* gene. One possible explanation for this could be that the *GPD2* deletion activates other alcohol dehydrogenases and this rescues ethanol production. Other labs have taken similar strategies in yeast strains bearing the ABE pathway. For instance, the deletion of *ADH1*, *ADH4*, *GPD1* and *GPD2* as well as the overexpression of a pyruvate dehydrogenase bypass system generated around 100 mg/L butanol (Lian *et al.* 2014). Therefore, one possible future direction to complete this work would be to generate the double deletion of both *GPD1* and *GPD2* then explore the impact on butanol production in the context of the butanol production strain.

7.4 The best conditions for butanol production were detected

Another goal in this project was to identify the best fermentation conditions for efficient butanol production. The strain that produces the highest butanol levels was selected for these optimisation experiments (B^R *adh1Δ* *ALD6* *ACS2*+5g). Our data revealed that semi-anaerobic conditions are significantly better than aerobic conditions; highly fermentable carbon sources give the best yields of butanol but are not particularly relevant to industrial production; higher inoculums are better than lower; and temperatures of 37°C or higher disfavour butanol production. However, these experiments were conducted in small semi-anaerobic jars and are very far removed from the types of conditions used in industrial fermentations. A possible future direction for this project is to apply a host of industrial conditions to the yeast strain in order to assess performance. This could be achieved using scalable process development in bioreactors.

7.5 A butanol resistant strain generates higher levels of butanol

The initial goal of the butanol project was to assess whether improved resistance to butanol toxicity would have any impact on butanol yield in strain that produces butanol. Previous work in the Ashe lab identified a point mutation in the gamma subunit of translation initiation factor eIF2B (the *GCD1* gene), which alters the butanol tolerance phenotype of the strain (Ashe *et al.* 2001; Taylor *et al.* 2010). Proline at position 180 confers a resistant phenotype, while serine at this position increases sensitivity to exogenously added butanol. In order to assess whether resistant strains produce more butanol, we generated *GCD1-P180* or *GCD1-S180* strains bearing the ABE pathway, an *ADH1* deletion and overexpressed *ALD6* *ACS2* genes. The butanol resistant strain was found to produce 1.5-2 fold higher levels of butanol relative to the butanol sensitive strain.

Given the promising result above, a strategy was devised to generate strains that are even more resistant to butanol with the goal of improving yields further. Two specific mutations were introduced within the *GCD2* gene encoding the delta subunit of eIF2B in the genome of the butanol production strain (B^R *adh1Δ* *ALD6* *ACS2*+5g). The

mutations were designed to mimic the phosphorylated or non-phosphorylated state at serine 131. So serine 131 was replaced with alanine *GCD2-S131A* or aspartic acids *GCD2-S131D*. For the *GCD2-S131A* strain, which is significantly more resistant to butanol than controls, butanol production seemed to be improved if measured relative to biomass. However, the level of biomass generated was reduced. Overall the combined effect of these two outcomes was that little difference was found in the butanol concentration produced. However, these results do fit the hypothesis that increasing butanol tolerance promotes higher butanol production. Unfortunately, as for many eIF2B gene mutations (Vazquez de Aldana *et al.* 1994; Niederberger *et al.* 1986), the growth rate was reduced in the *GCD2-S131A* strain. If growth could be improved in this strain, it may represent a viable approach to improving butanol yields.

The results above where butanol resistant strains generate more butanol were somewhat unexpected because the butanol levels produced in the media (~0.3 g/L) are significantly lower than levels required to inhibit growth and protein synthesis (1%, 10 g/L). It seems possible that this discrepancy could be explained if butanol does not get transported efficiently across the plasma membrane either into or out of the cell. As such even though cells are exposed to 1% butanol exogenously, the intracellular concentration would remain low. Equally the intracellular butanol level produced inside a butanol production strain would accumulate inside the cell. As a result, the toxic level of intracellular butanol required to inhibit growth and translation initiation could be much lower than the concentration of butanol added exogenously.

Studies from other labs have actually targeted butanol transport in an attempt to increase butanol tolerance in *E. coli*. Expression of specific efflux pumps which recognise intracellular toxic compounds and pump them out against a concentration gradient have been investigated (Dunlop 2011). Interestingly, expression of a particular efflux pump called *acrAB-tolC* pump restores growth on all other biofuels apart from n-butanol and isopentanol. This suggests that the effected pumps work efficiently with long chain alcohols like hexane, heptane, octane and nonane but they were not so useful for short chain alcohols like butanol. Another bacterial study has found that overexpression of fatty acid biosynthesis genes, an iron uptake gene and the introduction of the flux pump gene *SrpABC* led to increased butanol tolerance in *E.coli*.

The level of butanol accumulating inside the cell was reduced by the efflux pump and this pump served as a strong exporter facilitating butanol transit to the media (Bui le *et al.* 2015).

Other investigators have generated *S. cerevisiae* strains that are tolerant to 3% sec-butanol (2-butanol) by up-regulating the *GPP2* gene (Ghiaci *et al.* 2013). This gene is involved in the last step of glycerol biosynthesis (Pahlman *et al.* 2001) and the authors speculate that tolerance may stem from subtle changes in fatty acids present on lipids in the plasma membrane (Ghiaci *et al.* 2013). However, even though the constructed strain becomes more tolerant to butanol, the authors of the study do not feel it would lead to increased butanol yields, as carbon would be diverted from butanol synthesis towards glycerol production and respiration.

Other studies have screened various backgrounds of *S. cerevisiae* for tolerance to butanol (Zaki *et al.* 2014; Gonzalez-Ramos *et al.* 2013). Mutations to either the *RPN4* or *RTG1* gene were identified as conferring a tolerant phenotype (Zaki *et al.* 2014). *RPN4* and *RTG1* encode transcription factors controlling the proteasome genes and inter-organelle communication respectively (Xie *et al.* 2001). Furthermore, a range of strains with increased butanol tolerance were found to exhibit higher *RPN4* gene expression (Zaki *et al.* 2014).

Overall while many mutations have been identified to increase butanol tolerance, it is largely unclear at the molecular level how these mutations lead to butanol resistance.

7.6 Overall Summary

In this thesis, a strategy has been devised to integrate a butanol synthetic pathway into specific loci in the yeast genome. The resulting strain bearing the ABE pathway produces a very low yield of butanol. Therefore, various alternative metabolic strategies were taken with a view to improving butanol production. As such a strain was engineered that produced ~0.3 g/L. This strain was subsequently used to test the hypothesis that increased tolerance to butanol would give greater butanol yields. Evidence supporting this hypothesis was generated, although the impact of mutations on strain growth complicated the interpretation and the improvements in butanol production were quite small. A key question for future work is how can butanol production be optimised to a point where it is of interest to the commercial sector. An estimate based on what is possible using *Clostridial* systems would suggest that at least a ten-fold improvement in butanol yield would be required. Some of this increase may come from process engineering considerations, but it is still envisaged that further improvements and modifications to the strain will be necessary.

8. Bibliography

- Aguilera, J., and J. A. Prieto. 2004. 'Yeast cells display a regulatory mechanism in response to methylglyoxal', *FEMS Yeast Res*, 4: 633-41.
- Albertyn, J., S. Hohmann, J. M. Thevelein, and B. A. Prior. 1994. 'GPD1, which encodes glycerol-3-phosphate dehydrogenase, is essential for growth under osmotic stress in *Saccharomyces cerevisiae*, and its expression is regulated by the high-osmolarity glycerol response pathway', *Mol Cell Biol*, 14: 4135-44.
- Alper, H., J. Moxley, E. Nevoigt, G. R. Fink, and G. Stephanopoulos. 2006. 'Engineering yeast transcription machinery for improved ethanol tolerance and production', *Science*, 314: 1565-8.
- 'Alternative Fuels Data Center'. 2014. http://www.afdc.energy.gov/fuels/ethanol_production.html.
- Antoni, D., V. V. Zverlov, and W. H. Schwarz. 2007. 'Biofuels from microbes', *Appl Microbiol Biotechnol*, 77: 23-35.
- Aranda, A., and M. I. del Olmo. 2003. 'Response to acetaldehyde stress in the yeast *Saccharomyces cerevisiae* involves a strain-dependent regulation of several *ALD* genes and is mediated by the general stress response pathway', *Yeast*, 20: 747-59.
- Asano, K., J. Clayton, A. Shalev, and A. G. Hinnebusch. 2000. 'A multifactor complex of eukaryotic initiation factors, eIF1, eIF2, eIF3, eIF5, and initiator tRNA(Met) is an important translation initiation intermediate in vivo', *Genes Dev*, 14: 2534-46.
- Ashe, M. P., J. W. Slaven, S. K. De Long, S. Ibrahim, and A. B. Sachs. 2001. 'A novel eIF2B-dependent mechanism of translational control in yeast as a response to fusel alcohols', *EMBO J*, 20: 6464-74.
- Atsumi, S., and J. C. Liao. 2008. 'Metabolic engineering for advanced biofuels production from *Escherichia coli*', *Curr Opin Biotechnol*, 19: 414-9.
- Atsumi, S., T. Y. Wu, I. M. Machado, W. C. Huang, P. Y. Chen, M. Pellegrini, and J. C. Liao. 2010. 'Evolution, genomic analysis, and reconstruction of isobutanol tolerance in *Escherichia coli*', *Mol Syst Biol*, 6: 449.
- Bakker, B. M., K. M. Overkamp, A. J. van Maris, P. Kotter, M. A. Luttik, J. P. van Dijken, and J. T. Pronk. 2001. 'Stoichiometry and compartmentation of NADH metabolism in *Saccharomyces cerevisiae*', *FEMS Microbiol Rev*, 25: 15-37.
- Balat, M., and H. Balat. 2009. 'Recent trends in global production and utilization of bio-ethanol fuel', *Appl Energ*, 86: 2273-82.
- Behera, S., R. Singh, R. Arora, N. K. Sharma, M. Shukla, and S. Kumar. 2014. 'Scope of algae as third generation biofuels', *Front Bioeng Biotechnol*, 2: 90-180.
- Belotserkovskaya, R., D. E. Sterner, M. Deng, M. H. Sayre, P. M. Lieberman, and S. L. Berger. 2000. 'Inhibition of TATA-binding protein function by SAGA subunits Spt3 and Spt8 at Gcn4-activated promoters', *Mol Cell Biol*, 20: 634-47.
- Bennetzen, J. L., and B. D. Hall. 1982. 'The primary structure of the *Saccharomyces cerevisiae* gene for alcohol dehydrogenase', *J Biol Chem*, 257: 3018-25.
- Blank, L. M., and U. Sauer. 2004. 'TCA cycle activity in *Saccharomyces cerevisiae* is a function of the environmentally determined specific growth and glucose uptake rates', *Microbiology*, 150: 1085-93.
- Boubekeur, S., N. Camougrand, O. Bunoust, M. Rigoulet, and B. Guerin. 2001. 'Participation of acetaldehyde dehydrogenases in ethanol and pyruvate metabolism of the yeast *Saccharomyces cerevisiae*', *Eur J Biochem*, 268: 5057-65.
- Branduardi, P., V. Longo, N. M. Berterame, G. Rossi, and D. Porro. 2013. 'A novel pathway to produce butanol and isobutanol in *Saccharomyces cerevisiae*', *Biotechnol Biofuels*, 6: 68.

- Brannvall, E., and M. E. Lindstrom. 2007. 'The hemicellulose composition of pulp fibers and their ability to endure mechanical treatment', *Tappi J*, 6: 19-24.
- Bro, C., and J. Nielsen. 2004. 'Impact of 'ome' analyses on inverse metabolic engineering', *Metab Eng*, 6: 204-11.
- Bui le, M., J. Y. Lee, A. Geraldi, Z. Rahman, J. H. Lee, and S. C. Kim. 2015. 'Improved n-butanol tolerance in *Escherichia coli* by controlling membrane related functions', *J Biotechnol*, 204: 33-44.
- Campbell, S. G., and M. P. Ashe. 2007. 'An approach to studying the localization and dynamics of eukaryotic translation factors in live yeast cells', *Methods Enzymol*, 431: 33-45.
- Campbell, S. G., N. P. Hoyle, and M. P. Ashe. 2005. 'Dynamic cycling of eIF2 through a large eIF2B-containing cytoplasmic body: implications for translation control', *J Cell Biol*, 170: 925-34.
- Carere, C. R., R. Sparling, N. Cicek, and D. B. Levin. 2008. 'Third generation biofuels via direct cellulose fermentation', *Int J Mol Sci*, 9: 1342-60.
- Carter, Z., and D. Delneri. 2010. 'New generation of loxP-mutated deletion cassettes for the genetic manipulation of yeast natural isolates', *Yeast*, 27: 765-75.
- Cascone, R. 2008. 'Biobutanol - A replacement for bioethanol?', *Che Eng Prog*, 104: S4-S9.
- Causey, T. B., K. T. Shanmugam, L. P. Yomano, and L. O. Ingram. 2004. 'Engineering *Escherichia coli* for efficient conversion of glucose to pyruvate', *Proc Natl Acad Sci U S A*, 101: 2235-40.
- Chen, X., K. F. Nielsen, I. Borodina, M. C. Kielland-Brandt, and K. Karhumaa. 2011. 'Increased isobutanol production in *Saccharomyces cerevisiae* by overexpression of genes in valine metabolism', *Biotechnol Biofuels*, 4: 21.
- Chen, Y., V. Siewers, and J. Nielsen. 2012. 'Profiling of cytosolic and peroxisomal acetyl-CoA metabolism in *Saccharomyces cerevisiae*', *PLoS One*, 7: e42475.
- Ciszak, E. M., L. G. Korotchkina, P. M. Dominiak, S. Sidhu, and M. S. Patel. 2003. 'Structural basis for flip-flop action of thiamin pyrophosphate-dependent enzymes revealed by human pyruvate dehydrogenase', *J Biol Chem*, 278: 21240-6.
- Cobucci-Ponzano, B., A. Strazzulli, R. Iacono, G. Masturzo, R. Giglio, M. Rossi, and M. Moracci. 2015. 'Novel thermophilic hemicellulases for the conversion of lignocellulose for second generation biorefineries', *Enzyme Microb Technol*, 78: 63-73.
- Colon, M., F. Hernandez, K. Lopez, H. Quezada, J. Gonzalez, G. Lopez, C. Aranda, and A. Gonzalez. 2011. '*Saccharomyces cerevisiae* Bat1 and Bat2 aminotransferases have functionally diverged from the ancestral-like *Kluyveromyces lactis* orthologous enzyme', *PLoS One*, 6: e16099.
- Cordell, Dana, Jan-Olof Drangert, and Stuart White. 2009. 'The story of phosphorus: Global food security and food for thought', *Global Environ Change*, 19: 292-305.
- Crabtree, H. G. 1928. 'The carbohydrate metabolism of certain pathological overgrowths', *Biochem J*, 22: 1289-98.
- da Silva, G. P., M. Mack, and J. Contiero. 2009. 'Glycerol: A promising and abundant carbon source for industrial microbiology', *Biotechnol Adv*, 27: 30-39.
- Day, R. E., P. J. Rogers, I. W. Dawes, and V. J. Higgins. 2002. 'Molecular analysis of maltotriose transport and utilization by *Saccharomyces cerevisiae*', *Appl Environ Microbiol*, 68: 5326-35.
- de Jong-Gubbels, P., P. Vanrolleghem, S. Heijnen, J. P. van Dijken, and J. T. Pronk. 1995. 'Regulation of carbon metabolism in chemostat cultures of *Saccharomyces cerevisiae* grown on mixtures of glucose and ethanol', *Yeast*, 11: 407-18.
- de Smidt, O., J. C. du Preez, and J. Albertyn. 2012. 'Molecular and physiological aspects of alcohol dehydrogenases in the ethanol metabolism of *Saccharomyces cerevisiae*', *FEMS Yeast Res*, 12: 33-47.

- de Vries, S., and L. A. Grivell. 1988. 'Purification and characterization of a rotenone-insensitive NADH:Q6 oxidoreductase from mitochondria of *Saccharomyces cerevisiae*', *Eur J Biochem*, 176: 377-84.
- Demirbas, A., and M. F. Demirbas. 2011. 'Importance of algae oil as a source of biodiesel', *Energ Conver Manage*, 52: 163-70.
- Dever, T. E., L. Feng, R. C. Wek, A. M. Cigan, T. F. Donahue, and A. G. Hinnebusch. 1992. 'Phosphorylation of initiation factor 2 alpha by protein kinase GCN2 mediates gene-specific translational control of GCN4 in yeast', *Cell*, 68: 585-96.
- Dickinson, J. R. 1996. 'Fusel' alcohols induce hyphal-like extensions and pseudohyphal formation in yeasts', *Microbiology*, 142: 1391-7.
- Dong, H., C. Zhao, T. Zhang, Z. Lin, Y. Li, and Y. Zhang. 2015. 'Engineering *Escherichia coli* Cell Factories for n-Butanol Production', *Adv Biochem Eng Biotechnol*.
- Dong, J., H. Qiu, M. Garcia-Barrio, J. Anderson, and A. G. Hinnebusch. 2000. 'Uncharged tRNA activates GCN2 by displacing the protein kinase moiety from a bipartite tRNA-binding domain', *Mol Cell*, 6: 269-79.
- Drewke, C., and M. Ciriacy. 1988. 'Overexpression, purification and properties of alcohol dehydrogenase IV from *Saccharomyces cerevisiae*', *Biochim Biophys Acta*, 950: 54-60.
- Dunlop, M. J. 2011. 'Engineering microbes for tolerance to next-generation biofuels', *Biotechnol Biofuels*, 4: 32.
- Dunlop, M. J., Z. Y. Dossani, H. L. Szmidt, H. C. Chu, T. S. Lee, J. D. Keasling, M. Z. Hadi, and A. Mukhopadhyay. 2011. 'Engineering microbial biofuel tolerance and export using efflux pumps', *Mol Syst Biol*, 7: 487.
- Dyer, J. M., D. C. Chapital, J. W. Kuan, R. T. Mullen, and A. B. Pepperman. 2002. 'Metabolic engineering of *Saccharomyces cerevisiae* for production of novel lipid compounds', *Appl Microbiol Biotechnol*, 59: 224-30.
- Egbe, N. E., C. M. Paget, H. Wang, and M. P. Ashe. 2015. 'Alcohols inhibit translation to regulate morphogenesis in *C. albicans*', *Fungal Genet Biol*, 77: 50-60.
- Ezeji, T. C., N. Qureshi, and H. P. Blaschek. 2007. 'Bioproduction of butanol from biomass: from genes to bioreactors', *Curr Opin Biotechnol*, 18: 220-7.
- Feder, M. E., and G. E. Hofmann. 1999. 'Heat-shock proteins, molecular chaperones, and the stress response: evolutionary and ecological physiology', *Annu Rev Physiol*, 61: 243-82.
- Fischer, C. R., D. Klein-Marcuschamer, and G. Stephanopoulos. 2008. 'Selection and optimization of microbial hosts for biofuels production', *Metab Eng*, 10: 295-304.
- Flagfeldt, D. B., V. Siewers, L. Huang, and J. Nielsen. 2009. 'Characterization of chromosomal integration sites for heterologous gene expression in *Saccharomyces cerevisiae*', *Yeast*, 26: 545-51.
- Flores, C. L., C. Rodriguez, T. Petit, and C. Gancedo. 2000. 'Carbohydrate and energy-yielding metabolism in non-conventional yeasts', *Fems Microbiology Reviews*, 24: 507-29.
- Foiani, M., A. M. Cigan, C. J. Paddon, S. Harashima, and A. G. Hinnebusch. 1991. 'GCD2, a translational repressor of the GCN4 gene, has a general function in the initiation of protein synthesis in *Saccharomyces cerevisiae*', *Mol Cell Biol*, 11: 3203-16.
- Formanek, J., R. Mackie, and H. P. Blaschek. 1997. 'Enhanced Butanol Production by *Clostridium beijerinckii* BA101 Grown in Semidefined P2 Medium Containing 6 Percent Maltodextrin or Glucose', *Appl Environ Microbiol*, 63: 2306-10.
- Fortman, J. L., S. Chhabra, A. Mukhopadhyay, H. Chou, T. S. Lee, E. Steen, and J. D. Keasling. 2008. "Biofuel alternatives to ethanol: pumping the microbial well." In *Trends Biotechnol*, 375-81.
- Gabriel, C. L. 1928. 'Butanol fermentation process', *Ind Eng Chem*, 20: 1063-67.
- Gabriel, C. L., and F. M. Crawford. 1930. 'Development of the butyl-acetonic fermentation industry', *Ind Eng Chem*, 22: 1163-65.

- Ghiaci, P., J. Norbeck, and C. Larsson. 2013. 'Physiological adaptations of *Saccharomyces cerevisiae* evolved for improved butanol tolerance', *Biotechnol Biofuels*, 6: 101.
- Gonzalez-Ramos, D., M. van den Broek, A. J. van Maris, J. T. Pronk, and J. M. Daran. 2013. 'Genome-scale analyses of butanol tolerance in *Saccharomyces cerevisiae* reveal an essential role of protein degradation', *Biotechnol Biofuels*, 6: 48.
- Gonzalez Siso, M. I., M. A. Freire Picos, and M. E. Cerdan. 1996. 'Reoxidation of the NADPH produced by the pentose phosphate pathway is necessary for the utilization of glucose by *Kluyveromyces lactis* rag2 mutants', *FEBS Lett*, 387: 7-10.
- Guthrie, C. 1991. 'Messenger RNA splicing in yeast: clues to why the spliceosome is a ribonucleoprotein', *Science*, 253: 157-63.
- Haase, S. B., and S. I. Reed. 2002. 'Improved flow cytometric analysis of the budding yeast cell cycle', *Cell Cycle*, 1: 132-6.
- Hahn-Hagerdal, B., K. Karhumaa, C. Fonseca, I. Spencer-Martins, and M. F. Gorwa-Grauslund. 2007. 'Towards industrial pentose-fermenting yeast strains', *Appl Microbiol Biotechnol*, 74: 937-53.
- Hahn, S., and E. T. Young. 2011. 'Transcriptional regulation in *Saccharomyces cerevisiae*: transcription factor regulation and function, mechanisms of initiation, and roles of activators and coactivators', *Genetics*, 189: 705-36.
- Hartwell, L. H., and C. S. McLaughlin. 1969. 'A mutant of yeast apparently defective in the initiation of protein synthesis', *Proc Natl Acad Sci U S A*, 62: 468-74.
- Hashimoto, H., A. Sakakibara, M. Yamasaki, and K. Yoda. 1997. '*Saccharomyces cerevisiae* VIG9 encodes GDP-mannose pyrophosphorylase, which is essential for protein glycosylation', *J Biol Chem*, 272: 16308-14.
- Hein, L., and R. Leemans. 2012. 'The impact of first-generation biofuels on the depletion of the global phosphorus reserve', *Ambio*, 41: 341-9.
- Hermann, T. 2004. 'Using functional genomics to improve productivity in the manufacture of industrial biochemicals', *Curr Opin Biotechnol*, 15: 444-8.
- Hinnebusch, A. G. 2011. 'Molecular mechanism of scanning and start codon selection in eukaryotes', *Microbiol Mol Biol R*, 75: 434-67, first page of table of contents.
- Hinnebusch, A. G., J. S. Dong, M. Garcia-Barrio, E. Sattlegger, T. Krishnamoorthy, H. F. Qiu, and J. Anderson. 2000. 'Translational control in by phosphorylation of initiation factor 2', *Mol Biol Cell*, 11: 1A-1A.
- Hiser, L., M. E. Basson, and J. Rine. 1994. '*ERG10* from *Saccharomyces cerevisiae* encodes acetoacetyl-CoA thiolase', *J Biol Chem*, 269: 31383-9.
- Hoffman, C. S., and F. Winston. 1987. 'A ten-minute DNA preparation from yeast efficiently releases autonomous plasmids for transformation of *Escherichia coli*', *Gene*, 57: 267-72.
- Hong, K. K., and J. Nielsen. 2012. 'Metabolic engineering of *Saccharomyces cerevisiae*: a key cell factory platform for future biorefineries', *Cell Mol Life Sci*, 69: 2671-90.
- Huang, G. H., F. Chen, D. Wei, X. W. Zhang, and G. Chen. 2010. 'Biodiesel production by microalgal biotechnology', *Appl Energy*, 87: 38-46.
- Huang, H., H. Liu, and Y. R. Gan. 2010. 'Genetic modification of critical enzymes and involved genes in butanol biosynthesis from biomass', *Biotechnol Adv*, 28: 651-7.
- Huffer, S., C. M. Roche, H. W. Blanch, and D. S. Clark. 2012. '*Escherichia coli* for biofuel production: bridging the gap from promise to practice', *Trends Biotechnol*, 30: 538-45.
- Hutchison, H. T., L. H. Hartwell, and C. S. McLaughlin. 1969. 'Temperature-sensitive yeast mutant defective in ribonucleic acid production', *J Bacteriol*, 99: 807-14.
- Jones, D. T., and D. R. Woods. 1986. 'Acetone-butanol fermentation revisited', *Microbiol Rev*, 50: 484-524.

- Jordan, F., I. Baburina, F. Guo, H. Li, and J. Wang. 1997. 'Yeast pyruvate decarboxylase, an enzyme with two highly reactive centers for substrate, catalytic and regulatory.', *FASEB J*, 11: A1152-A52.
- Kapp, L. D., and J. R. Lorsch. 2004. 'GTP-dependent recognition of the methionine moiety on initiator tRNA by translation factor eIF2', *J Mol Biol*, 335: 923-36.
- Keenan, Jemma. 2013. 'An investigation into the proteins responsible for translational inhibition seen in the yeast *Saccharomyces cerevisiae* following fusel alcohol exposure', University of Manchester.
- Keis, S., R. Shaheen, and D. T. Jones. 2001. 'Emended descriptions of *Clostridium acetobutylicum* and *Clostridium beijerinckii*, and descriptions of *Clostridium saccharoperbutylacetonicum* sp. nov. and *Clostridium saccharobutylicum* sp. nov', *Int J Syst Evol Microbiol*, 51: 2095-103.
- Kim, S. R., Y. C. Park, Y. S. Jin, and J. H. Seo. 2013. 'Strain engineering of *Saccharomyces cerevisiae* for enhanced xylose metabolism', *Biotechnol Adv*, 31: 851-61.
- Koschwanetz, J. H., K. R. Foster, and A. W. Murray. 2011. 'Sucrose utilization in budding yeast as a model for the origin of undifferentiated multicellularity', *PLoS Biol*, 9: e1001122.
- Kozak, M. 1999. 'Initiation of translation in prokaryotes and eukaryotes', *Gene*, 234: 187-208.
- Krivoruchko, A., C. Serrano-Amatriain, Y. Chen, V. Siewers, and J. Nielsen. 2013. 'Improving biobutanol production in engineered *Saccharomyces cerevisiae* by manipulation of acetyl-CoA metabolism', *J Ind Microbiol Biotechnol*, 40: 1051-6.
- Krivoruchko, A., V. Siewers, and J. Nielsen. 2011. 'Opportunities for yeast metabolic engineering: Lessons from synthetic biology', *Biotechnol J*, 6: 262-76.
- Krivoruchko, A., Y. Zhang, V. Siewers, Y. Chen, and J. Nielsen. 2015. 'Microbial acetyl-CoA metabolism and metabolic engineering', *Metab Eng*, 28: 28-42.
- Kubota, H., T. Obata, K. Ota, T. Sasaki, and T. Ito. 2003. 'Rapamycin-induced translational derepression of *GCN4* mRNA involves a novel mechanism for activation of the eIF2 alpha kinase *GCN2*', *J Biol Chem*, 278: 20457-60.
- Laemmli, U. K. 1970. 'Cleavage of structural proteins during the assembly of the head of bacteriophage T4', *Nature*, 227: 680-5.
- Lampitt, L. H. 1919. 'Nitrogen metabolism in *Saccharomyces cerevisiae*.', *Biochem J*, 13: 459-86.
- Larsson, C., I. L. Pahlman, R. Ansell, M. Rigoulet, L. Adler, and L. Gustafsson. 1998. 'The importance of the glycerol 3-phosphate shuttle during aerobic growth of *Saccharomyces cerevisiae*', *Yeast*, 14: 347-57.
- Lee, S. Y., J. H. Park, S. H. Jang, L. K. Nielsen, J. Kim, and K. S. Jung. 2008. 'Fermentative butanol production by *Clostridia*', *Biotechnol Bioeng*, 101: 209-28.
- Lee, W. H., S. O. Seo, Y. H. Bae, H. Nan, Y. S. Jin, and J. H. Seo. 2012. 'Isobutanol production in engineered *Saccharomyces cerevisiae* by overexpression of 2-ketoisovalerate decarboxylase and valine biosynthetic enzymes', *Bioprocess Biosyst Eng*, 35: 1467-75.
- LeFebvre, A. K., N. L. Korneeva, M. Trutschl, U. Cvek, R. D. Duzan, C. A. Bradley, J. W. Hershey, and R. E. Rhoads. 2006. 'Translation initiation factor eIF4G-1 binds to eIF3 through the eIF3e subunit', *J Biol Chem*, 281: 22917-32.
- Leskovac, V., S. Trivic, and D. Pericin. 2002. 'The three zinc-containing alcohol dehydrogenases from baker's yeast, *Saccharomyces cerevisiae*', *FEMS Yeast Res*, 2: 481-94.
- Lian, J., T. Si, N. U. Nair, and H. Zhao. 2014. 'Design and construction of acetyl-CoA overproducing *Saccharomyces cerevisiae* strains', *Metab Eng*, 24: 139-49.
- Liu, J. Y., J. Mukherjee, J. J. Hawkes, and S. J. Wilkinson. 2013. 'Optimization of lipid production for algal biodiesel in nitrogen stressed cells of *Dunaliella salina* using FTIR analysis', *J Chem Technol Biotechnol*, 88: 1807-14.
- Liu, X. B., Q. Y. Gu, X. B. Yu, and W. Luo. 2012. 'Enhancement of butanol tolerance and butanol yield in *Clostridium acetobutylicum* mutant NT642 obtained by nitrogen ion beam implantation', *J Microbiol*, 50: 1024-8.

- Luo, M., J. D. Weinstein, and C. J. Walker. 1999. 'Magnesium chelatase subunit D from pea: characterization of the cDNA, heterologous expression of an enzymatically active protein and immunoassay of the native protein', *Plant Mol Biol*, 41: 721-31.
- Luttik, M. A., K. M. Overkamp, P. Kotter, S. de Vries, J. P. van Dijken, and J. T. Pronk. 1998. 'The *Saccharomyces cerevisiae* NDE1 and NDE2 genes encode separate mitochondrial NADH dehydrogenases catalyzing the oxidation of cytosolic NADH', *J Biol Chem*, 273: 24529-34.
- Madsen, M. F., S. Dano, and P. G. Sorensen. 2005. 'On the mechanisms of glycolytic oscillations in yeast', *FEBS J*, 272: 2648-60.
- Malys, N. 2012. 'Shine-Dalgarno sequence of bacteriophage T4: GAGG prevails in early genes', *Mol Biol Rep*, 39: 33-9.
- Marres, C. A., S. de Vries, and L. A. Grivell. 1991. 'Isolation and inactivation of the nuclear gene encoding the rotenone-insensitive internal NADH: ubiquinone oxidoreductase of mitochondria from *Saccharomyces cerevisiae*', *Eur J Biochem*, 195: 857-62.
- Martin, C. H., D. R. Nielsen, K. V. Solomon, and K. L. Prather. 2009. 'Synthetic metabolism: engineering biology at the protein and pathway scales', *Chem Biol*, 16: 277-86.
- McGinn, P. J., K. E. Dickinson, S. Bhatti, J. C. Frigon, S. R. Guiot, and S. J. O'Leary. 2011. 'Integration of microalgae cultivation with industrial waste remediation for biofuel and bioenergy production: opportunities and limitations', *Photosynth Res*, 109: 231-47.
- Meaden, P. G., F. M. Dickinson, A. Mifsud, W. Tessier, J. Westwater, H. Bussey, and M. Midgley. 1997. 'The *ALD6* gene of *Saccharomyces cerevisiae* encodes a cytosolic, Mg(2+)-activated acetaldehyde dehydrogenase', *Yeast*, 13: 1319-27.
- Meher, L. C., D. V. Sagar, and S. N. Naik. 2006. 'Technical aspects of biodiesel production by transesterification - a review', *Renew Sustainable Energy Rev*, 10: 248-68.
- Mirostawa Szczesna Antczak, Aneta Kubiak, Tadeusz Antczak, Stanislaw Bielecki. 2009. "Enzymatic biodiesel synthesis – Key factors affecting efficiency of the process." In *Renew Energy*, 34:1185-1194.
- Mussatto, S. I., M. Fernandes, G. J. Rocha, J. J. Orfao, J. A. Teixeira, and I. C. Roberto. 2010. 'Production, characterization and application of activated carbon from brewer's spent grain lignin', *Bioresour Technol*, 101: 2450-7.
- Naik, S. N., V. V. Goud, P. K. Rout, and A. K. Dalai. 2010. 'Production of first and second generation biofuels: A comprehensive review', *Renew Sustainable Energy Rev*, 14: 578-97.
- Navarro-Avino, J. P., R. Prasad, V. J. Miralles, R. M. Benito, and R. Serrano. 1999. 'A proposal for nomenclature of aldehyde dehydrogenases in *Saccharomyces cerevisiae* and characterization of the stress-inducible *ALD2* and *ALD3* genes', *Yeast*, 15: 829-42.
- Nevoigt, E., and U. Stahl. 1997. 'Osmoregulation and glycerol metabolism in the yeast *Saccharomyces cerevisiae*', *FEMS Microbiol Rev*, 21: 231-41.
- Ng, C. Y., M. Y. Jung, J. Lee, and M. K. Oh. 2012. 'Production of 2,3-butanediol in *Saccharomyces cerevisiae* by in silico aided metabolic engineering', *Microb Cell Fact*, 11: 68.
- Niederberger, P., M. Aebi, and R. Hutter. 1986. 'Identification and characterization of four new *GCD* genes in *Saccharomyces cerevisiae*', *Curr Genet*, 10: 657-64.
- Nielsen, J. 2001. 'Metabolic engineering', *Appl Microbiol Biotechnol*, 55: 263-83.
- Noree, C., B. K. Sato, R. M. Broyer, and J. E. Wilhelm. 2010. 'Identification of novel filament-forming proteins in *Saccharomyces cerevisiae* and *Drosophila melanogaster*', *J Cell Biol*, 190: 541-51.
- Onodera, J., and Y. Ohsumi. 2004. 'Ald6p is a preferred target for autophagy in yeast, *Saccharomyces cerevisiae*', *J Biol Chem*, 279: 16071-6.

- Overkamp, K. M., B. M. Bakker, P. Kotter, A. van Tuijl, S. de Vries, J. P. van Dijken, and J. T. Pronk. 2000. 'In vivo analysis of the mechanisms for oxidation of cytosolic NADH by *Saccharomyces cerevisiae* mitochondria', *J Bacteriol*, 182: 2823-30.
- Pahlman, A. K., K. Granath, R. Ansell, S. Hohmann, and L. Adler. 2001. 'The yeast glycerol 3-phosphatases Gpp1p and Gpp2p are required for glycerol biosynthesis and differentially involved in the cellular responses to osmotic, anaerobic, and oxidative stress', *J Biol Chem*, 276: 3555-63.
- Paquin, C. E., and V. M. Williamson. 1986. 'Ty insertions at two loci account for most of the spontaneous antimycin A resistance mutations during growth at 15 degrees C of *Saccharomyces cerevisiae* strains lacking *ADH1*', *Mol Cell Biol*, 6: 70-9.
- Park, S. H., S. Kim, and J. S. Hahn. 2014. 'Metabolic engineering of *Saccharomyces cerevisiae* for the production of isobutanol and 3-methyl-1-butanol', *Appl Microbiol Biotechnol*, 98: 9139-47.
- Partaledis, J. A., and T. L. Mason. 1988. 'Structure and regulation of a nuclear gene in *Saccharomyces cerevisiae* that specifies *MRP13*, a protein of the small subunit of the mitochondrial ribosome', *Mol Cell Biol*, 8: 3647-60.
- Pavitt, G. D., K. V. Ramaiah, S. R. Kimball, and A. G. Hinnebusch. 1998. 'eIF2 independently binds two distinct eIF2B subcomplexes that catalyze and regulate guanine-nucleotide exchange', *Genes Dev*, 12: 514-26.
- Pavitt, G. D., W. Yang, and A. G. Hinnebusch. 1997. 'Homologous segments in three subunits of the guanine nucleotide exchange factor eIF2B mediate translational regulation by phosphorylation of eIF2', *Mol Cell Biol*, 17: 1298-313.
- Peralta-Yahya, P. P., F. Zhang, S. B. del Cardayre, and J. D. Keasling. 2012. 'Microbial engineering for the production of advanced biofuels', *Nature*, 488: 320-8.
- Petranovic, D., K. Tyo, G. N. Vemuri, and J. Nielsen. 2010. 'Prospects of yeast systems biology for human health: integrating lipid, protein and energy metabolism', *FEMS Yeast Res*, 10: 1046-59.
- Pronk, J. T., H. Yde Steensma, and J. P. Van Dijken. 1996. 'Pyruvate metabolism in *Saccharomyces cerevisiae*', *Yeast*, 12: 1607-33.
- Qureshi, N., and H. P. Blaschek. 1999. 'Production of acetone butanol ethanol (ABE) by a hyper-producing mutant strain of *Clostridium beijerinckii* BA101 and recovery by pervaporation', *Biotechnol Prog*, 15: 594-602.
- Richard, P., R. Verho, M. Putkonen, J. Londesborough, and M. Penttila. 2003. 'Production of ethanol from L-arabinose by *Saccharomyces cerevisiae* containing a fungal L-arabinose pathway', *FEMS Yeast Res*, 3: 185-9.
- Rodrigues, Fernando, Paula Ludovico, and Cecília Leão. 2006. 'Sugar Metabolism in Yeasts: an Overview of Aerobic and Anaerobic Glucose Catabolism.' in Gábor Péter and Carlos Rosa (eds.), *Biodiversity and Ecophysiology of Yeasts* (Springer Berlin Heidelberg).
- Rowlands, A. G., R. Panniers, and E. C. Henshaw. 1988. 'The catalytic mechanism of guanine nucleotide exchange factor action and competitive inhibition by phosphorylated eukaryotic initiation factor 2', *J Biol Chem*, 263: 5526-33.
- Rowlands, T., P. Baumann, and S. P. Jackson. 1994. 'The TATA-binding protein: a general transcription factor in eukaryotes and archaeobacteria', *Science*, 264: 1326-9.
- Ruhal, R., S. Aggarwal, and B. Choudhury. 2011. 'Suitability of crude glycerol obtained from biodiesel waste for the production of trehalose and propionic acid', *Green Chem*, 13: 3492-98.
- Sakuragi, H., H. Morisaka, K. Kuroda, and M. Ueda. 2015. 'Enhanced butanol production by eukaryotic *Saccharomyces cerevisiae* engineered to contain an improved pathway', *Biosci Biotechnol Biochem*, 79: 314-20.
- Schiestl, R. H., and R. D. Gietz. 1989. 'High efficiency transformation of intact yeast cells using single stranded nucleic acids as a carrier', *Curr Genet*, 16: 339-46.

- Sellick, C. A., R. N. Campbell, and R. J. Reece. 2008. 'Galactose metabolism in yeast-structure and regulation of the leloir pathway enzymes and the genes encoding them', *Int Rev Cell Mol Biol*, 269: 111-50.
- Shiba, Y., E. M. Paradise, J. Kirby, D. K. Ro, and J. D. Keasing. 2007. 'Engineering of the pyruvate dehydrogenase bypass in *Saccharomyces cerevisiae* for high-level production of isoprenoids', *Metab Eng*, 9: 160-68.
- Shimada, Y., Y. Watanabe, A. Sugihara, and Y. Tominaga. 2002. 'Enzymatic alcoholysis for biodiesel fuel production and application of the reaction to oil processing', *J Mol Catal B Enzym*, 17: 133-42.
- Si, T., Y. Luo, H. Xiao, and H. Zhao. 2014. 'Utilizing an endogenous pathway for 1-butanol production in *Saccharomyces cerevisiae*', *Metab Eng*, 22: 60-8.
- Simonetti, A., S. Marzi, A. G. Myasnikov, J. F. Menetret, and B. P. Klaholz. 2011. 'Insights into translation initiation and termination complexes and into the polysome architecture', *Ribosomes: Structure, Function, and Dynamics*: 113-28.
- Singhania, R. R., A. K. Patel, R. K. Sukumaran, C. Larroche, and A. Pandey. 2013. 'Role and significance of beta-glucosidases in the hydrolysis of cellulose for bioethanol production', *Bioresour Technol*, 127: 500-7.
- Small, W. C., and L. McAlister-Henn. 1998. 'Identification of a cytosolically directed NADH dehydrogenase in mitochondria of *Saccharomyces cerevisiae*', *J Bacteriol*, 180: 4051-5.
- Snyder, M., and J. E. Gallagher. 2009. 'Systems biology from a yeast omics perspective', *FEBS Lett*, 583: 3895-9.
- Steen, E. J., R. Chan, N. Prasad, S. Myers, C. J. Petzold, A. Redding, M. Ouellet, and J. D. Keasling. 2008. 'Metabolic engineering of *Saccharomyces cerevisiae* for the production of n-butanol', *Microb Cell Fact*, 7: 36.
- Storici, F., L. K. Lewis, and M. A. Resnick. 2001. 'In vivo site-directed mutagenesis using oligonucleotides', *Nat Biotechnol*, 19: 773-6.
- Svitkin, Y. V., A. Pause, A. Haghighat, S. Pyronnet, G. Witherell, G. J. Belsham, and N. Sonenberg. 2001. 'The requirement for eukaryotic initiation factor 4A (eIF4A) in translation is in direct proportion to the degree of mRNA 5' secondary structure', *RNA*, 7: 382-94.
- Swidah, R., H. Wang, P. J. Reid, H. Z. Ahmed, A. M. Pisanelli, K. C. Persaud, C. M. Grant, and M. P. Ashe. 2015. 'Butanol production in *S. cerevisiae* via a synthetic ABE pathway is enhanced by specific metabolic engineering and butanol resistance', *Biotechnol Biofuels*, 8: 97-105.
- Takahashi, H., J. M. McCaffery, R. A. Irizarry, and J. D. Boeke. 2006. 'Nucleocytosolic acetyl-coenzyme a synthetase is required for histone acetylation and global transcription', *Mol Cell*, 23: 207-17.
- Tanaka, K., A. Komiyama, K. Sonomoto, A. Ishizaki, S. J. Hall, and P. F. Stanbury. 2002. 'Two different pathways for D-xylose metabolism and the effect of xylose concentration on the yield coefficient of L-lactate in mixed-acid fermentation by the *lactic acid bacterium Lactococcus lactis* IO-1', *Appl Microbiol Biotechnol*, 60: 160-7.
- Tarun, S. Z., Jr., and A. B. Sachs. 1995. 'A common function for mRNA 5' and 3' ends in translation initiation in yeast', *Genes Dev*, 9: 2997-3007.
- Tarun, S. Z., Jr., and A. B. Sachs. 1996. 'Association of the yeast poly(A) tail binding protein with translation initiation factor eIF-4G', *Embo J*, 15: 7168-77.
- Taylor, E. J., S. G. Campbell, C. D. Griffiths, P. J. Reid, J. W. Slaven, R. J. Harrison, P. F. Sims, G. D. Pavitt, D. Delneri, and M. P. Ashe. 2010. 'Fusel alcohols regulate translation initiation by inhibiting eIF2B to reduce ternary complex in a mechanism that may involve altering the integrity and dynamics of the eIF2B body', *Mol Biol Cell*, 21: 2202-16.
- Tomas, C. A., N. E. Welker, and E. T. Papoutsakis. 2003. 'Overexpression of *groESL* in *Clostridium acetobutylicum* results in increased solvent production and tolerance,

- prolonged metabolism, and changes in the cell's transcriptional program', *Appl Environ Microbiol*, 69: 4951-65.
- Tucci, S., and W. Martin. 2007. 'A novel prokaryotic trans-2-enoyl-CoA reductase from the spirochete *Treponema denticola*', *FEBS Lett*, 581: 1561-6.
- Tummala, S. B., N. E. Welker, and E. T. Papoutsakis. 2003. 'Design of antisense RNA constructs for downregulation of the acetone formation pathway of *Clostridium acetobutylicum*', *J Bacteriol*, 185: 1923-34.
- Tyo, K. E., H. S. Alper, and G. N. Stephanopoulos. 2007. 'Expanding the metabolic engineering toolbox: more options to engineer cells', *Trends Biotechnol*, 25: 132-7.
- Unbehaun, A., S. I. Borukhov, C. U. Hellen, and T. V. Pestova. 2004. 'Release of initiation factors from 48S complexes during ribosomal subunit joining and the link between establishment of codon-anticodon base-pairing and hydrolysis of eIF2-bound GTP', *Genes Dev*, 18: 3078-93.
- Updegraff, D. M. 1969. 'Semimicro determination of cellulose in biological materials', *Anal Biochem*, 32: 420-4.
- van den Berg, M. A., P. de Jong-Gubbels, C. J. Kortland, J. P. van Dijken, J. T. Pronk, and H. Y. Steensma. 1996. 'The two acetyl-coenzyme A synthetases of *Saccharomyces cerevisiae* differ with respect to kinetic properties and transcriptional regulation', *J Biol Chem*, 271: 28953-9.
- van Dijken, J. P., E. van den Bosch, J. J. Hermans, L. R. de Miranda, and W. A. Scheffers. 1986. 'Alcoholic fermentation by 'non-fermentative' yeasts', *Yeast*, 2: 123-7.
- van Dijken, J. P., R. A. Weusthuis, and J. T. Pronk. 1993. 'Kinetics of growth and sugar consumption in yeasts', *Antonie Van Leeuwenhoek*, 63: 343-52.
- van Maris, A. J., D. A. Abbott, E. Bellissimi, J. van den Brink, M. Kuyper, M. A. Luttik, H. W. Wisselink, W. A. Scheffers, J. P. van Dijken, and J. T. Pronk. 2006. 'Alcoholic fermentation of carbon sources in biomass hydrolysates by *Saccharomyces cerevisiae*: current status', *Antonie Van Leeuwenhoek*, 90: 391-418.
- Vaseghi, Sam, Anja Baumeister, Manfred Rizzi, and Matthias Reuss. 1999. 'In VivoDynamics of the Pentose Phosphate Pathway in *Saccharomyces cerevisiae*', *Metab Eng*, 1: 128-40.
- Vazquez de Aldana, C. R., and A. G. Hinnebusch. 1994. 'Mutations in the *GCD7* subunit of yeast guanine nucleotide exchange factor eIF-2B overcome the inhibitory effects of phosphorylated eIF-2 on translation initiation', *Mol Cell Biol*, 14: 3208-22.
- Verónica García, Johanna Pääkilä, Heikki Ojamo, Esa Muurinen, Riitta L. Keiski. 2011. "Challenges in biobutanol production: How to improve the efficiency?" In *Renew Sustainable Energy Rev*, 15: 964–80.
- Vinciguerra, P., and F. Stutz. 2004. 'mRNA export: an assembly line from genes to nuclear pores', *Curr Opin Cell Biol*, 16: 285-92.
- Wallner, T., S. A. Miers, and S. McConnell. 2009. 'A Comparison of Ethanol and Butanol as Oxygenates Using a Direct-Injection, Spark-Ignition Engine', *Journal of Engineering for Gas Turbines and Power-Transactions of the Asme*, 131.
- Wang, X., C. J. Mann, Y. Bai, L. Ni, and H. Weiner. 1998. 'Molecular cloning, characterization, and potential roles of cytosolic and mitochondrial aldehyde dehydrogenases in ethanol metabolism in *Saccharomyces cerevisiae*', *J Bacteriol*, 180: 822-30.
- Wang, X., F. E. Paulin, L. E. Campbell, E. Gomez, K. O'Brien, N. Morrice, and C. G. Proud. 2001. 'Eukaryotic initiation factor 2B: identification of multiple phosphorylation sites in the epsilon-subunit and their functions in vivo', *EMBO J*, 20: 4349-59.
- Wang, X., and C. G. Proud. 2008. 'A novel mechanism for the control of translation initiation by amino acids, mediated by phosphorylation of eukaryotic initiation factor 2B', *Mol Cell Biol*, 28: 1429-42.
- Warner, J. R., P. M. Knopf, and A. Rich. 1963. 'A multiple ribosomal structure in protein synthesis', *Proc Natl Acad Sci U S A*, 49: 122-9.

- Wells, S. E., P. E. Hillner, R. D. Vale, and A. B. Sachs. 1998. 'Circularization of mRNA by eukaryotic translation initiation factors', *Mol Cell*, 2: 135-40.
- Werner-Washburne, M., E. Braun, G. C. Johnston, and R. A. Singer. 1993. 'Stationary phase in the yeast *Saccharomyces cerevisiae*', *Microbiol Rev*, 57: 383-401.
- Westman, J. O., and C. J. Franzen. 2015. 'Current progress in high cell density yeast bioprocesses for bioethanol production', *Biotechnol J*, 10: 1185-95.
- Wheals, A. E., L. C. Basso, D. M. Alves, and H. V. Amorim. 1999. 'Fuel ethanol after 25 years', *Trends Biotechnol*, 17: 482-7.
- White, J., and E. Stelzer. 1999. 'Photobleaching GFP reveals protein dynamics inside live cells', *Trends Cell Biol*, 9: 61-5.
- Woods, Y. L., P. Cohen, W. Becker, R. Jakes, M. Goedert, X. Wang, and C. G. Proud. 2001. 'The kinase DYRK phosphorylates protein-synthesis initiation factor eIF2Bepsilon at Ser539 and the microtubule-associated protein tau at Thr212: potential role for DYRK as a glycogen synthase kinase 3-priming kinase', *Biochem J*, 355: 609-15.
- Wotton, D., K. Freeman, and D. Shore. 1996. 'Multimerization of Hsp42p, a novel heat shock protein of *Saccharomyces cerevisiae*, is dependent on a conserved carboxyl-terminal sequence', *J Biol Chem*, 271: 2717-23.
- Wu, J., N. Zhang, A. Hayes, K. Panoutsopoulou, and S. G. Oliver. 2004. 'Global analysis of nutrient control of gene expression in *Saccharomyces cerevisiae* during growth and starvation', *Proc Natl Acad Sci U S A*, 101: 3148-53.
- Xie, Y., and A. Varshavsky. 2001. 'RPN4 is a ligand, substrate, and transcriptional regulator of the 26S proteasome: a negative feedback circuit', *Proc Natl Acad Sci U S A*, 98: 3056-61.
- Xue, C., X. Q. Zhao, C. G. Liu, L. J. Chen, and F. W. Bai. 2013. 'Prospective and development of butanol as an advanced biofuel', *Biotechnol Adv*, 31: 1575-84.
- Yoshida, T., Y. Tashiro, and K. Sonomoto. 2012. 'Novel high butanol production from lactic acid and pentose by *Clostridium saccharoperbutylacetonicum*', *J Biosci Bioeng*, 114: 526-30.
- Young, E. T., and D. Pilgrim. 1985. 'Isolation and DNA sequence of *ADH3*, a nuclear gene encoding the mitochondrial isozyme of alcohol dehydrogenase in *Saccharomyces cerevisiae*', *Mol Cell Biol*, 5: 3024-34.
- Zaki, A. M., T. T. Wimalasena, and D. Greetham. 2014. 'Phenotypic characterisation of *Saccharomyces* spp. for tolerance to 1-butanol', *J Ind Microbiol Biotechnol*, 41: 1627-36.
- Zaldivar, J., J. Nielsen, and L. Olsson. 2001. 'Fuel ethanol production from lignocellulose: a challenge for metabolic engineering and process integration', *Appl Microbiol Biotechnol*, 56: 17-34.
- Zheng, Y. N., L. Z. Li, M. Xian, Y. J. Ma, J. M. Yang, X. Xu, and D. Z. He. 2009. 'Problems with the microbial production of butanol', *J Ind Microbiol Biotechnol*, 36: 1127-38.
- Ziegler, A., S. Ghosh, T. D. Dyer, J. Blangero, J. MacCluer, and L. Almasy. 2011. 'Introduction to genetic analysis workshop 17 summaries', *Genetic Epidemiology*, 35: S1-S4.

9. Appendix



RESEARCH ARTICLE

Open Access



Butanol production in *S. cerevisiae* via a synthetic ABE pathway is enhanced by specific metabolic engineering and butanol resistance

R. Swidah^{1†}, H. Wang^{1†}, P.J. Reid¹, H.Z. Ahmed¹, A.M. Pisanelli², K.C. Persaud², C.M. Grant¹ and M.P. Ashe^{1*}

Abstract

Background: The fermentation of sugars to alcohols by microbial systems underpins many biofuel initiatives. Short chain alcohols, like n-butanol, isobutanol and isopropanol, offer significant advantages over ethanol in terms of fuel attributes. However, production of ethanol from resistant *Saccharomyces cerevisiae* strains is significantly less complicated than for these alternative alcohols.

Results: In this study, we have transplanted an n-butanol synthesis pathway largely from *Clostridial* sp. to the genome of an *S. cerevisiae* strain. Production of n-butanol is only observed when additional genetic manipulations are made to restore any redox imbalance and to drive acetyl-CoA production. We have used this butanol production strain to address a key question regarding the sensitivity of cells to short chain alcohols. In the past, we have defined specific point mutations in the translation initiation factor eIF2B based upon phenotypic resistance/sensitivity to high concentrations of exogenously added n-butanol. Here, we show that even during endogenous butanol production, a butanol resistant strain generates more butanol than a butanol sensitive strain.

Conclusion: These studies demonstrate that appreciable levels of n-butanol can be achieved in *S. cerevisiae* but that significant metabolic manipulation is required outside of the pathway converting acetyl-CoA to butanol. Furthermore, this work shows that the regulation of protein synthesis by short chain alcohols in yeast is a critical consideration if higher yields of these alcohols are to be attained.

Keywords: Biobutanol, *Saccharomyces cerevisiae*, ABE pathway

Background

Since fossil fuels represent a finite resource and their continued use contributes to climate change, alternative sources of energy have been widely sought [1]. Biofuels produced from fermentation of renewable resources are expected to represent an important replacement for gasoline [2]. Commercial bioethanol production from high yielding fermentations of the yeast *Saccharomyces cerevisiae* relies upon the inherent resistance of yeast cells to the damaging properties of ethanol [3]. However, ethanol's low energy content and high hygroscopicity are viewed as disadvantages in terms of its quality as a fuel [4, 5]. n-Butanol (1-butanol) and other short chain

alcohols have a range of physical properties, which make them superior fuels to ethanol [4]. For instance, in comparison to ethanol, n-butanol is less hygroscopic making it less corrosive, and it has a higher energy density and octane value. These characteristics mean that n-butanol can be mixed with gasoline in almost any proportion [4].

Post World War I, n-butanol was produced from acetone-butanol-ethanol (ABE) clostridial fermentations [6]. Butanol production via this route (Fig. 1a) involves the intracellular conversion of acetyl-CoA derived from carbohydrate catabolism through a series of five enzymatic reactions to n-butanol. More specifically, thiolase catalyses a Claisen condensation reaction between two acetyl-CoA molecules producing acetoacetyl-CoA, which is then sequentially reduced through 3-hydroxybutyryl-CoA, crotonyl-CoA and butyryl-CoA to n-butanol [7]. Increasing commercial competition with fossil fuel-derived n-butanol supplanted this technology for largely economic

* Correspondence: mark.p.ashe@manchester.ac.uk

[†]Equal contributors

¹The Faculty of Life Sciences, The Michael Smith Building, The University of Manchester, Oxford Rd., Manchester M13 9PT, UK

Full list of author information is available at the end of the article

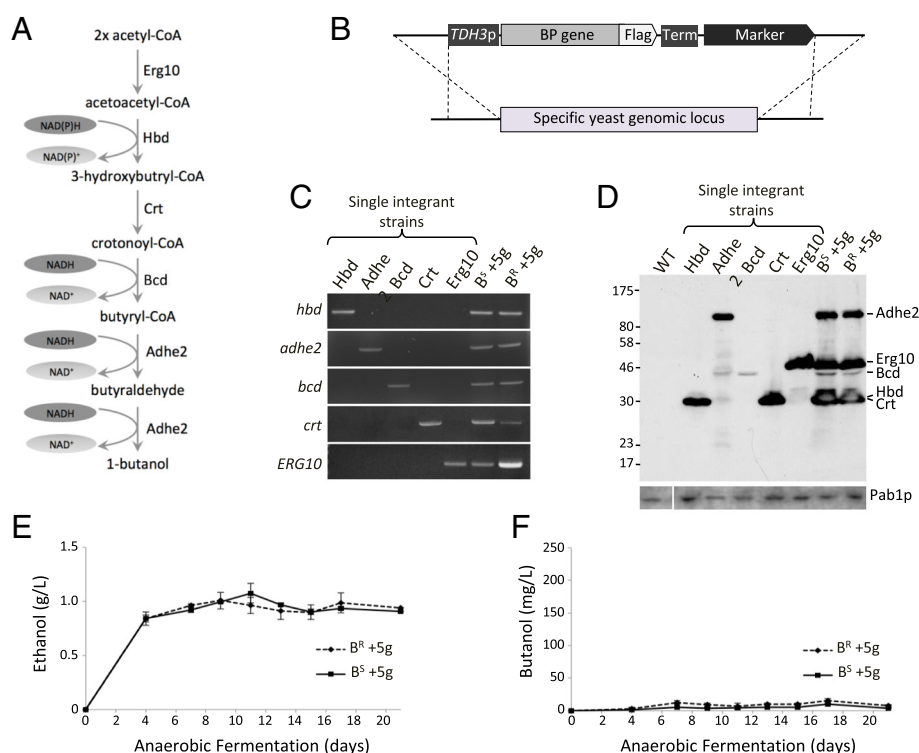


Fig. 1 The ABE butanol pathway does not lead to high levels of butanol production in *S. cerevisiae*. **a** Schematic diagram of a butanol production pathway utilised by a variety of clostridial species as part of ABE fermentation. The Hbd (3-hydroxybutyryl-CoA dehydrogenase), Crt (3-hydroxybutyryl-CoA dehydratase), Bcd (butyryl-CoA dehydrogenase) and Adhe2 (alcohol dehydrogenase) enzyme genes were derived from *Clostridium beijerinckii*, and the Erg10 (thiolase) sequence was taken from *S. cerevisiae*. **b** The strategy for expression of these genes via genomic integration into *S. cerevisiae* is depicted. Codon-optimised cassettes bearing C-terminal Flag epitope tags were expressed from the strong *TDH3* gene promoter and *CYC1* terminator sequences. Each cassette also carries a different marker downstream and was integrated at a precise location associated with high level expression (see Methods). **c** PCR analysis on genomic DNAs derived from either single integrant strains or a strain that has been back-crossed such that it harbours all five cassettes. The primers used are specific to the genomic integration loci and the cassettes labelled to the left of the gel pictures. **d** Western blotting using an anti-Flag antibody to detect the expressed proteins in either the single integrant strains or the strains bearing all five cassettes. Protein products are labelled to the right of the gel image. A blot probed with an anti-Pab1p antibody provides a loading control (lower panel). **e** and **f** Graphs depicting the level of ethanol or butanol produced from butanol sensitive (*GCD1-S180*) or butanol resistant (*GCD1-P180*) strains bearing the five butanol production genes (B^S + 5g or B^R + 5g) over a 21-day anaerobic fermentation. Error bars are \pm SEM from five biological repeats

reasons, although with respect to biofuel production it has renewed significance [7]. However, there are a number of problems that are associated with this n-butanol production route at the industrial scale. For instance, these can include product inhibition, the potential for bacteriophage contamination, sporulation during solventogenesis, the complicated two-stage multi-temperature fermentation reaction and the mixed fermentation products [5, 8]. Based upon these difficulties, a number of studies have attempted to produce n-butanol in other organisms. For instance, investigators have used both of the biotechnology workhorse model organisms, *Escherichia coli* and *S. cerevisiae* [9, 10].

Engineered *E. coli* bearing the ABE pathway have been generated in a number of different ways and have been shown to produce high levels of butanol [11, 12]. However, as for *Clostridia*, some problems still exist in the use

of engineered *E. coli* for butanol production, including the potential for phage infection/fermentation spoilage and product/degradation product toxicity [13]. As *S. cerevisiae* is currently widely used for the production of bioethanol, it holds significant advantages in terms of scalable industrial fermentation for the production of butanol [14]. However, initial attempts at introducing the ABE pathway into *S. cerevisiae* produced very low yields of 2.5 mg/L [15]. Subsequent studies have generated improved yields by targeting specific metabolic pathways or utilising specific starting substrates [16, 17]. In addition, alternative pathways for butanol production have been sought with varying degrees of success [18, 19]. Recurrent issues associated with these butanol fermentations are relatively low yields and the potential for end-product toxicity.

Previously, we have studied, at the molecular level, mechanisms underlying the toxic effects of n-butanol

and other alcohols in yeast [20–23]. We have found that these alcohols specifically inhibit protein synthesis at the translation initiation step by perturbing the guanine nucleotide exchange factor, eukaryotic initiation factor (eIF)2B [20, 21]. This factor recycles, eIF2, a key G-protein involved in translation initiation. eIF2 in the GTP bound form recruits the initiator methionyl tRNA to the ribosome [24]. As a consequence of translation initiation, GTP is hydrolysed on eIF2 generating eIF2-GDP, which requires eIF2B-dependent recycling before further rounds of translation initiation are possible.

In this study, we explore the hypothesis that yeast strains, which are more resistant to the toxic effects of n-butanol and other alcohols, are capable of producing more alcohol. In order to assess this question, we generated strains bearing the entire ABE pathway, as well as specific metabolic mutations designed to increase carbon flux towards the ABE pathway. As a result, we obtained a strain of yeast that is capable of producing up to 300 mg/L n-butanol. Overall, even though this level of n-butanol does not begin to approach the level required to inhibit eIF2B and generate toxicity, we observe a significant difference in the level of n-butanol produced in strains that only vary in their sensitivity/resistance to alcohols. Therefore, the toxicity of alcohols on cells is a significant factor when considering biofuel production and strategies aimed at overcoming this toxicity hold significant promise in the quest towards commercially economic biofuel yields.

Results and discussion

Addition of the ABE pathway to *S. cerevisiae* results in very low levels of n-butanol

The goal of this project at the outset was to determine whether the toxic effects of alcohols such as n-butanol are important in determining the yield from producing strains. We started with two parent strains that are isogenic apart from a point mutation in a gene encoding a translation initiation factor; *GCD1*. *GCD1-P180* (denoted B^R throughout) is resistant to 1 % butanol, whereas *GCD1-S180* (denoted B^S throughout) is sensitive to this level of exogenously added butanol. In order to evaluate this question, we generated B^S and B^R strains of yeast expressing four *Clostridia beijerinckii* genes and one yeast gene that together encode the enzymes of an ABE pathway. Previous studies had shown that yeast strains harbouring the genes for these enzymes on extremely high copy plasmids produced n-butanol at quite low levels of ~2.5 mg/L [15]. Therefore, we decided to integrate codon-optimised genes directly into specific sites associated with high expression on the genome [25] under the control of a highly efficient ubiquitous yeast *TDH3* gene promoter with a

CYC1 3' end formation sequence downstream. Each open reading frame (ORF) was also tagged with Flag epitopes to aid protein detection (Fig. 1b).

Individual genes were integrated into opposing mating type haploid yeast strains, such that via a combination of genetic crosses (see Methods), strains were constructed bearing all five genes (Fig. 1c). Western blotting using an anti-Flag monoclonal antibody confirmed that proteins of an appropriate size were expressed (Fig. 1d). However, when butanol was quantified from the strains under a variety of conditions, including anaerobic fermentation, very little butanol was recovered in the media (<10 mg/L) and levels of ethanol production were equivalent to the parent strains (Fig. 1e, f). The low butanol production observed in this strain was entirely consistent with previous attempts to produce n-butanol in *S. cerevisiae* [15].

Deletion of the *ADH1* gene improves the n-butanol yield significantly

A number of factors could be contributing to the poor butanol yields and we explored these in the B^R strain background. For instance, it is likely that a redox imbalance exists due to the high NADH requirements of the butanol production pathway, plus it is possible that the substrate for the butanol production pathway, cytosolic acetyl-CoA, is limiting. In an attempt to overcome these problems, we deleted the major yeast alcohol dehydrogenase gene *ADH1*. We reasoned that this deletion should improve the levels of NADH, as the enzyme is the primary route in yeast for balancing the NAD⁺ consumed by the glyceraldehyde 3-phosphate dehydrogenase step of glycolysis. In addition, deletion of *ADH1* could potentially increase cytosolic acetyl-CoA by causing the accumulation of acetaldehyde (Fig. 2a).

Therefore, a strategy was designed whereby the *ADH1* gene was deleted (Fig. 2b) to give strains with the previously described [26] actinomycin A sensitive phenotype (Fig. 2c). The *ADH1* deletion was subsequently confirmed by PCR on genomic DNA from the selected transformants (Fig. 2d).

Consistent with the deletion of a major alcohol dehydrogenase, growth and the levels of ethanol produced by the *adh1Δ* strain were very low compared to the wild type strain under anaerobic conditions (Fig. 2d and Additional file 1: Figure S1). In addition, glucose present at the outset was not entirely consumed during the fermentation (Additional file 1: Figure S1). Interestingly, for the strain bearing the butanol production pathway (B^R +5 g), *adh1Δ* still reduced ethanol levels dramatically but not to the same extent as an *adh1Δ* strain lacking the butanol pathway (Fig. 2d). Furthermore, the impact of deleting the *ADH1* gene in this strain was less pronounced in terms of growth and glucose consumption

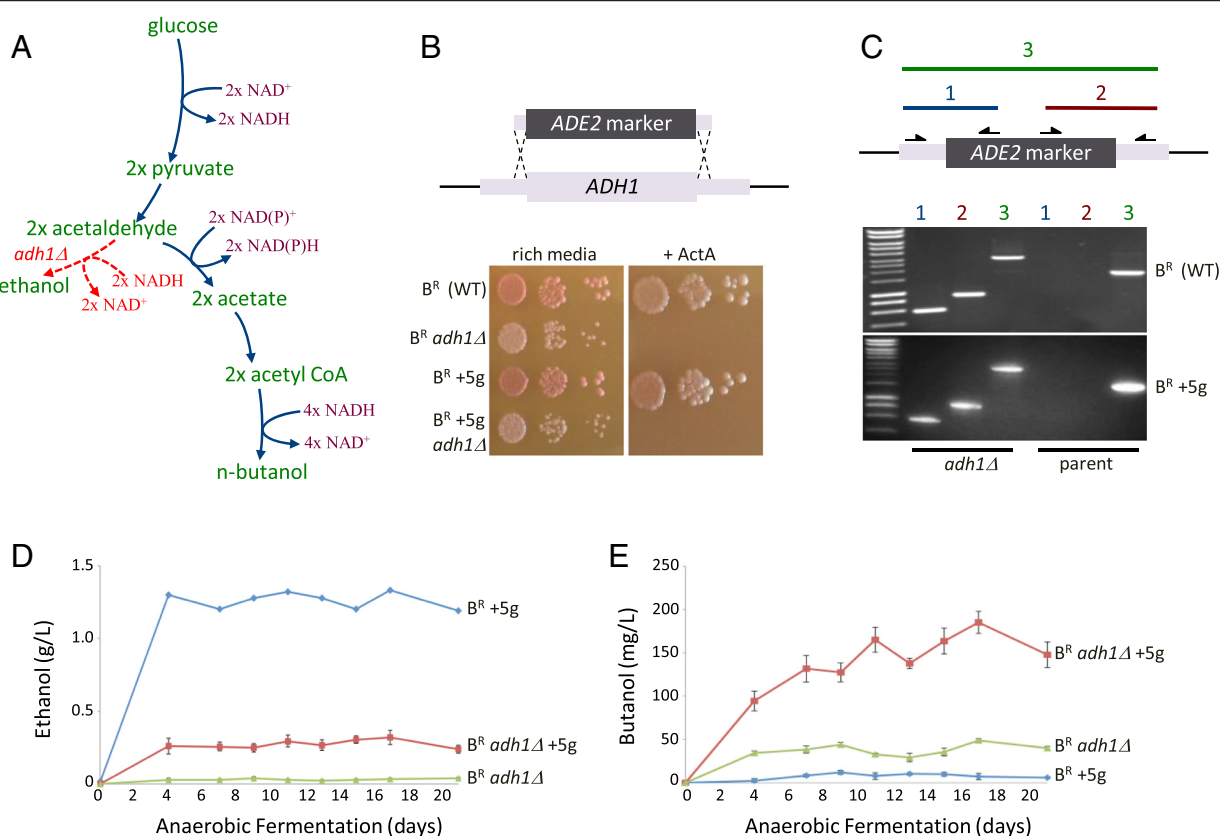


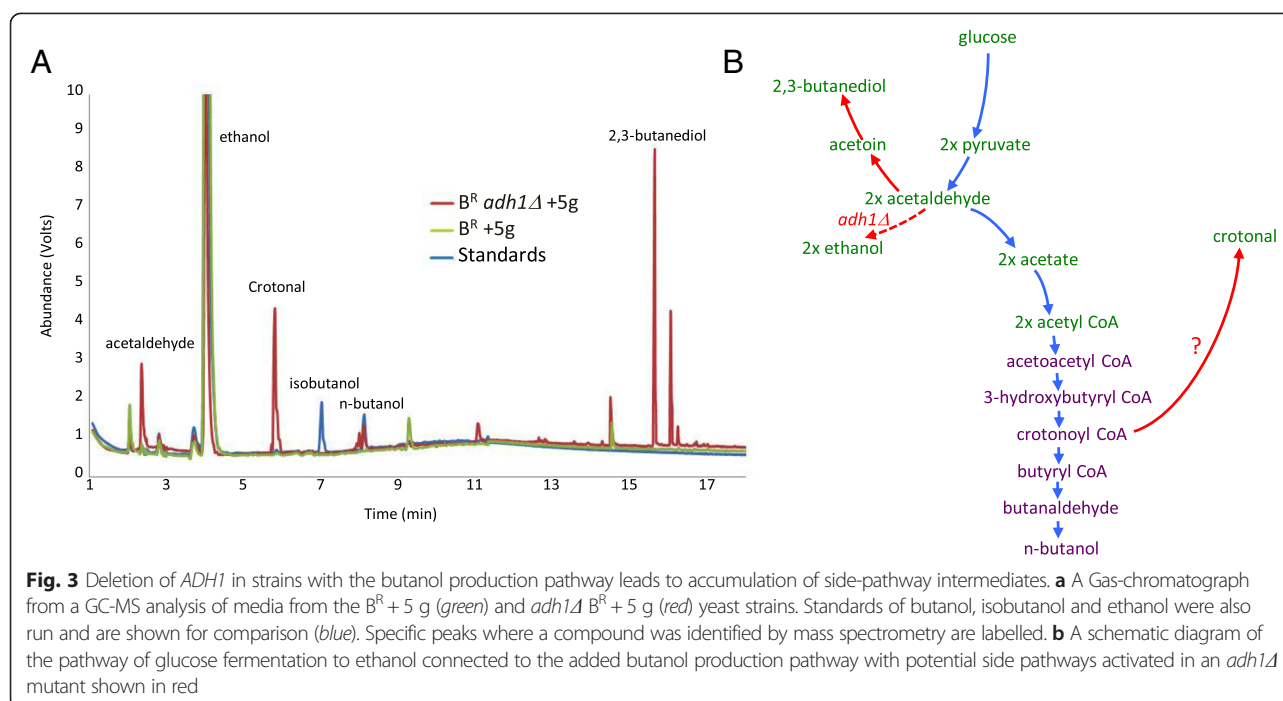
Fig. 2 Deletion of the *ADH1* gene improves butanol production in *S. cerevisiae*. **a** A schematic diagram of how the pathway of glucose fermentation to ethanol is connected to the added butanol production pathway. The step affected by the *ADH1* deletion is highlighted and the balance of reducing equivalent in the form of NADH or NADPH through the pathway is detailed. **b** The strategy for *ADH1* deletion and screening of candidates on Actinomycin A plates. **c** PCR analysis on genomic DNAs derived from either the *adh1Δ* strains or their parent. The primers used and resulting PCR products are detailed above the gels. **d** and **e** Graphs depicting the level of ethanol or butanol produced from the *adh1Δ* strain or from strains bearing the five butanol production genes either alone (*B^R +5g*) or in combination with *adh1Δ* (*B^R adh1Δ +5g*) over a 21-day anaerobic fermentation. Error bars are \pm SEM from five biological repeats

(Additional file 1: Figure S1). It is possible these minor fermentation improvements stem from the fact that the clostridial Adhe2 alcohol dehydrogenase is expressed as part of the butanol pathway, and this enzyme might to a small extent rescue production of ethanol from acetaldehyde.

Intriguingly, deletion of *ADH1* also leads to the production of n-butanol. Recent studies suggest that in the absence of *ADH1*, an endogenous pathway of n-butanol production can be activated [18]. This pathway likely stems from threonine catabolism [18] and appears to be responsible for the production of roughly 40 mg/L n-butanol from our strain (Fig. 2e). However, when an *adh1Δ* mutant is generated in the context of the strain harbouring the butanol production pathway (*B^R adh1Δ +5g*), approximately 150 mg/L n-butanol is generated (Fig. 2e).

In order to explore the profile of chemicals produced by these strains of yeast, a gas chromatography-mass spectrometry (GC-MS) analysis was undertaken (Fig. 3a). This revealed that for strains bearing the butanol production

enzymes, deletion of *ADH1* led to the appearance of a number of new peaks on the gas chromatograph. Mass spectrometry revealed likely identities for many of these peaks, which were explicable in terms of the metabolism of yeast. For instance, the accumulation of a peak corresponding to acetaldehyde and reduced levels of ethanol is entirely consistent with the removal of a major alcohol dehydrogenase. Furthermore, the production of 2,3-butanediol from acetaldehyde likely represents a means to restore the redox imbalance caused by removal of this major alcohol dehydrogenase. Finally, the accumulation of a peak identified as crotonal is intriguing. It is entirely possible that this derives from crotonyl-CoA via the action of a broad specificity aldehyde reductase in yeast. Overall, our interpretation of these data is that the result of the *adh1Δ* is an accumulation of acetaldehyde, which results in increased levels of 2,3-butanediol. Hence, the production of acetyl-CoA from acetaldehyde is not a favoured route as would be required for maximal butanol production. However, improved levels of butanol are being



attained and it appears that intermediates in the butanol pathway or derivatives of them such as crotonal may be accumulating (Fig. 3b).

Replacement of the Bcd gene with Ter does not significantly improve butanol yields

On the basis of the GC-MS data above, a number of discrete strategies were attempted to improve butanol yields further. The first strategy revolved around the accumulation of crotonal as a possible derivative of crotonyl-CoA. This suggests that the Bcd enzyme in the butanol production pathway maybe be somehow deficient. Intriguingly, the levels of the Bcd protein were the lowest of the five added proteins when assessed by western blotting (Fig. 1d). During studies on butanol synthesis in *E. coli* [11, 12], an alternative non-flavin dependent enzyme has been described as a more effective alternative to Bcd: a *trans*-enoyl-CoA reductase (Ter) enzyme from *Treponema denticola* (Fig. 4a). Therefore, a strategy was undertaken to test whether the replacement of Bcd with Ter led to improvements in butanol levels.

A codon-optimised ORF for the Ter gene was used to precisely supplant the Bcd ORF in the integration cassette, and therefore, a directly comparable Ter containing strain was obtained (Fig. 4). In contrast to what has been observed in *E. coli* [11, 12] and even though the levels of Ter were as high as the other integrated genes of the butanol pathway (Fig. 4b), the presence of the Ter gene did not alter the level of ethanol (Fig. 4c) or lead to significant improvements in the butanol titre (Fig. 4d).

Improved flux of carbon to acetyl CoA generates higher butanol levels

The accumulation of acetaldehyde, acetate and 2,3-butanediol in the GC-MS analysis for the *adh1Δ* strains bearing the butanol production pathway is suggestive that the flux towards the butanol pathway is not in any way maximal. The enzymes involved in the conversion of acetaldehyde to acetyl-CoA are the Ald6p cytosolic aldehyde dehydrogenase and the acetyl-CoA synthase Acs2p. The expression of these genes is carefully controlled and predominantly induced where non-fermentable carbon sources are being metabolised or under stress conditions [27]. Therefore, to obviate this regulation, we decided to express the *ALD6* and *ACS2* genes from highly active constitutive promoters in the *adh1Δ* mutant bearing the ABE pathway. An integration cassette was designed (Fig. 5a) where the expression of *ALD6* was placed under the control of the *TDH3* promoter with a *CYC1* 3' end formation sequence, while *ACS2* was expressed from the *TEF1* promoter with *ADH1* 3' end processing signals. Both ORFs were codon-optimised and Flag-tagged at the C-terminus to allow expression to be monitored relative to the other enzymes of the butanol production pathway. Here, expression of all seven transgenes in the strain was found to be roughly comparable (Fig. 5b). Even though expression of both Ald6p and Ald2p was observed, little difference was noted in the levels of acetaldehyde and crotonal produced on GC-MS traces (Additional file 2: Figure S2). However, evaluation of

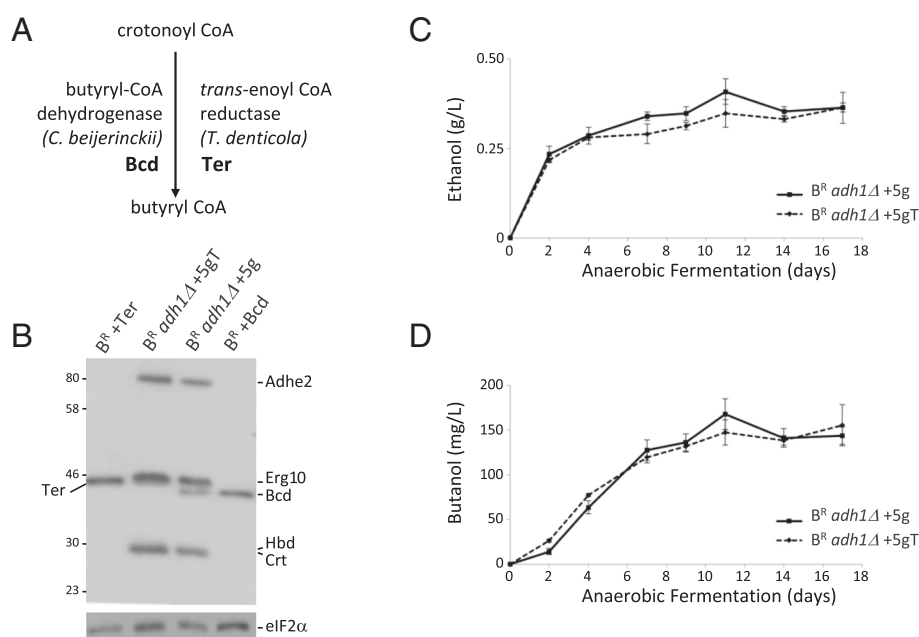


Fig. 4 Replacement of butyryl-CoA dehydrogenase (Bcd) with *trans*-enoyl-CoA reductase (Ter) does not substantially improve butanol levels. **a** A schematic showing the reaction involved and the replacement strategy. **b** Western blotting using an anti-Flag antibody to detect the expressed proteins in extracts from *adh1* mutant strains bearing the butanol production pathway with Bcd (B^R *adh1Δ* +5g) or with Ter (B^R *adh1Δ* +5gT) relative to extracts from control strains bearing just Bcd (B^R + Bcd) or Ter (B^R + Ter). Protein products are labelled to the right and left of the gel image. A blot probed with an anti-eIF2α antibody provides a loading control (lower panel). **c** and **d** Graphs depicting the level of ethanol or butanol produced from *adh1Δ* mutant strains bearing five butanol production genes with either Bcd (B^R *adh1Δ* +5g) or Ter (B^R *adh1Δ* +5gT) over a 21-day anaerobic fermentation. Error bars are \pm SEM from five biological repeats

the resulting strain in terms of butanol and ethanol production showed that expression of Ald6p and Acs2p gave a small improvement in peak butanol levels from 150–175 mg/L (Figs. 2d and 3d) to 250–300 mg/L (Fig. 5d). This is consistent with other studies where improvements in cytosolic acetyl-CoA availability gave small increases in butanol yields [17].

Butanol resistant strains generate higher levels of butanol

Having generated a strain that yields a reasonable level of butanol, we assessed the impact of butanol resistance/sensitivity at the level of translation initiation. Previous work from the lab has defined specific butanol resistance and sensitive mutations in the genes for eIF2B. In this case, we generated strains, which harboured allelic variation at the *GCD1* locus, which encodes the γ subunit of eIF2B. A proline at residue 180 gives a resistant phenotype, whereas a Serine at this position increases sensitivity to butanol.

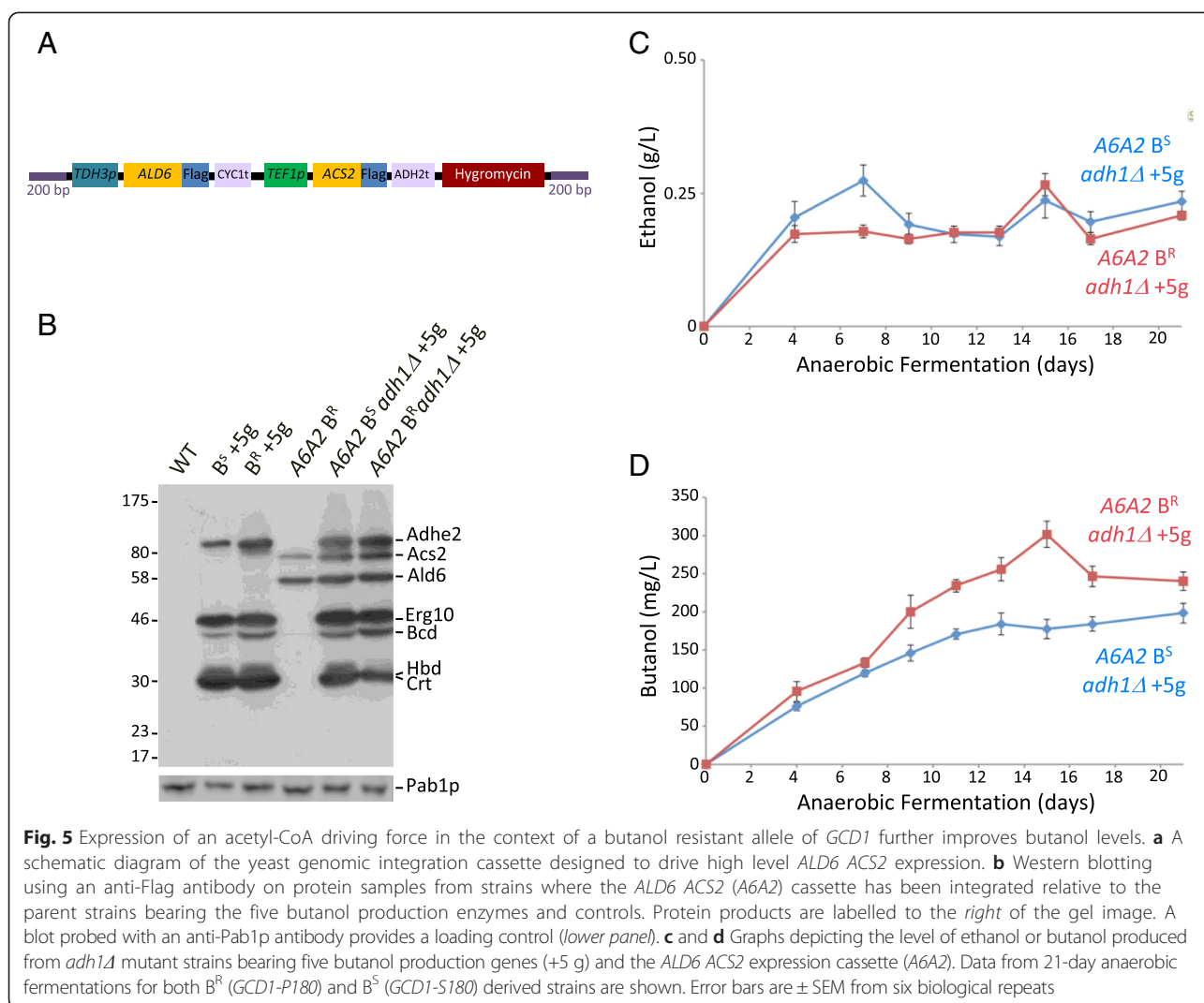
The resulting strains were tested for alcohol production using our standard assay system, and the butanol resistant strain reproducibly generated up to 1.5–2-fold higher peak levels of butanol (Fig. 5d). These results were unforeseen, as the level of butanol generated by these strains is significantly lower than the level added exogenously during the tolerance studies [20, 21]. In addition, the level of ethanol

production was slightly reduced at early time points in the butanol resistant strain (Fig. 5c). This is suggestive that in the butanol resistant strain, a higher flux is attained towards butanol and away from ethanol than in the butanol sensitive strain. These results provide proof of principle that strains that are more resistant to the effects of butanol (and other fusel alcohols) have improved yields of these alcohols from production pathways.

Conclusions

In this study, we show that an exogenous ABE pathway only generates substantial levels of butanol in yeast when a number of metabolic alterations are made. Deletion of the major alcohol dehydrogenase *ADH1* not only leads to butanol production via a previously described endogenous pathway but also promotes much higher levels of butanol where an exogenous butanol production pathway has been added. These data support a view that both the endogenous and exogenous pathways are active in the cells.

Our GC-MS studies highlight a number of potential bottlenecks particularly with regard to the exogenous pathway. Accumulation of crotonal led us to take an approach previously validated in *E. coli*: the replacement of the Bcd enzyme with Ter [11, 12]. However in our studies in yeast, Ter gives little improvement in butanol levels. It seems possible that neither of these enzymes is



particularly efficient in the context of the yeast cytoplasm, and this could represent an area where substantial further improvements in yield are possible. The GC-MS data also show that acetaldehyde, acetate and 2,3-butanediol accumulate in an *adh1Δ* mutant bearing the ABE pathway. The accumulation of these compounds suggests that production of cytosolic acetyl-CoA from acetaldehyde occurs inefficiently. Therefore, a high expression strategy was applied to the *ALD6* and *ACS2* genes involved in this process. In strains, this metabolic alteration generated a moderate improvement in the levels of butanol from the strain; peak levels increase from ~175 to ~300 mg/L. Therefore, while stimulating cytosolic acetyl-CoA production does lead to an improvement in butanol production, a deficiency in this area is not a major limitation. This begs the question what is the major limitation that prevents greater butanol production. Possible answers lie in an imbalance in redox potential or in

sensitivity of the cells to butanol itself or intermediates in the pathway.

The initial goal of this project was to assess whether differences in the sensitivity of strains to butanol prompted equivalent changes in the yield of butanol. Here, we use previously characterised strains bearing butanol sensitive and butanol resistant alleles of the *GCD1* gene to provide proof of principle that the inherent sensitivity of yeast strains to butanol impacts upon butanol production. Given that the concentrations of butanol that are required to inhibit protein synthesis and growth (1–2 %, 10–20 g/L) are very different to the levels that are produced in our yeast strains (0.3 g/L), it is inherently quite startling that greater levels of butanol are produced in a butanol resistant strain. Our current working hypothesis to explain this discrepancy is that butanol transport across the yeast cell membrane is inefficient. Thus, if extracellular butanol does not pass into

a cell and intracellular butanol does not pass out of a cell particularly well, it is possible that the level of extracellular butanol required to inhibit growth and translation would be high, whereas the level of endogenous butanol required to elicit the same effect could be much lower. Indeed, a role for specific efflux pumps in increasing the tolerance of *E. coli* to exogenously added short chain alcohols has been described [28]. This opens up the possibility of an integrated approach towards improved tolerance to, and hence, improved production of, short chain alcohols in *S. cerevisiae*, where both intracellular resistance at the level of proteins synthesis and the cells capacity to export alcohols are enhanced.

Methods

Yeast growth and strain construction/validation

Strains used in this study were grown at 30 °C on either standard yeast extract/peptone/dextrose media (YPD) or synthetic complete dextrose media (SCD) both supplemented with 2 % glucose [29]. Individual genomic integration and deletion cassettes were generated and transformed into yeast using standard PCR-based integration methods to target the integration cassettes to specific high expression sites in the yeast genome [25] and validated using PCR, western blotting and phenotypic analysis. The individual cassettes carried yeast codon-optimised sequences Ter (from *T. denticola*), Cct, Adhe2, Bcd and Hbd (from *Clostridium Beijerinckii*) with a C-terminal Flag tag (two Flag peptide epitopes) and the *CYC1* terminator sequences downstream. Each gene was first inserted into a specific pRS vector with a *TDH3* promoter inserted upstream and the auxotrophic marker gene immediately downstream of the cassette. Integration primers were then designed to isolate the cassette upstream of the *TDH3* promoter to downstream of the auxotrophic marker (Fig. 1b). The sites of integration were selected based on previous studies analysing the efficiency of gene expression from various sites across the yeast genome. The *ADH1* gene was deleted using the *ADE2* marker using standard yeast PCR-based gene disruption methods. The codon-optimised *ERG10* yeast gene was synthesised downstream of the *TDH3* gene promoter and upstream of the *CYC1* terminator sequence, and flag epitope tags were placed at the C-terminus. The cassette was sub-cloned into the pFa6-KanMX4 plasmid upstream of the *KanMX4* gene. Integration primers were designed to amplify the entire fragment prior to transformation into yeast. Codon-optimised versions of the yeast *ALD6* and *ACS2* genes were synthesised downstream of the *TDH3* and *TEF1* gene promoters and upstream of the *CYC1* and *ADH2* terminator sequences, respectively. Flag epitope tags were placed at the C-terminus of each cassette and a hygromycin marker gene was added (Fig. 5a). The whole cassette was bounded by 200 n sequences

directing it to the *TRP1* locus in the yeast genome. Finally, the cassette was flanked by sites for the type IIS restriction enzyme, *BspQI*, such that the whole fragment could be released and transformed into yeast. All commercial DNA synthesis was carried out by either Mr Gene GmbH (Regensburg, Germany) or GenScript (Piscataway, NJ).

Measurements of butanol and ethanol

Strains were grown in liquid YPD media from a starting OD₆₀₀ of 0.1 using semi-anaerobic 50 ml vials over a 21-day period. On specific days, 2 ml samples were taken, passed through a 0.22 µ filter into gas chromatography (GC) vials and analysed by GC-FID using an Agilent 6850A GC system with an Agilent 4513A automatic injector, sampler and controller (Agilent technologies Ltd., Stockport, UK). A J&W DB-WAX capillary column (30 m × 0.25 mm, 0.25 µM) (Agilent technologies Ltd.) was used for separation. Samples were quantified relative to standards of ethanol and butanol.

GC-MS was carried out using media from anaerobic cultures grown in YPD for 5 days. Using a 6890 N GC system coupled to a 5973 Mass Selective Detector (MSD) (Agilent technologies Ltd.), 2 ml samples were collected and analysed. Data was analysed and processed using the MSD ChemStation software (Agilent technologies Ltd.).

Western blot analysis of Flag-tagged proteins

Yeast culture (5 ml) were grown to an OD₆₀₀ of 0.7 in YPD, pelleted; then protein samples were prepared and processed for electrophoresis and immunoblot analysis as described previously [30]. A monoclonal anti-Flag antibody (Sigma-Aldrich, Dorset, UK) was used as the primary antibody for the detection.

Additional files

Additional file 1: Figure S1. Growth (OD₆₀₀) and glucose consumption (%) for the strains indicated over 21 day anaerobic fermentations. Error bars are ± SEM from 3 biological repeats.

Additional file 2: Figure S2. A Gas chromatograph from a GC-MS analysis of media from the A6A2 B^R *adh1Δ* 5 g (blue) yeast strains relative to standards of butanol, isobutanol and ethanol (red). Specific peaks where a compound was identified by mass spectrometry are labelled.

Competing interests

The authors declare that they have no competing interests.

Authors' contributions

RS generated/designed strains and performed the experiments in Figs. 1, 2, 5 and Additional file 1. HW generated/designed strains, set up the alcohol quantification and performed experiments in Figs. 3 and 4 and Additional file 2. PJR generated and designed strains. AMP helped with GC analysis. HZA helped with strain validation and Additional file 1. MPA, KCP and CMG led the project and were responsible for the design of the study, data analysis and interpretation. MPA oversaw the design of the figures and wrote the manuscript. All authors were involved in the intellectual aspects of the study, and they edited and approved the final manuscript.

Acknowledgements

This work was supported by a University of Manchester Intellectual Property-Proof of Principle (UMIP-PoP) award and a Biotechnology and Biological Sciences Research Council (BBSRC) grant (BB/K002767/1). RS was initially supported by a Syria Ministry of Higher Education Capacity Building Project studentship, then subsequently by funds from the British Council and HZA was supported by a BBSRC DTP studentship.

Author details

¹The Faculty of Life Sciences, The Michael Smith Building, The University of Manchester, Oxford Rd., Manchester M13 9PT, UK. ²School of Chemical engineering and Analytical Science, The Mill, The University of Manchester, Sackville St., Manchester M139PL, UK.

Received: 31 March 2015 Accepted: 29 June 2015

Published online: 08 July 2015

References

- Kerr RA. Climate change. Global warming is changing the world. *Science*. 2007;316:188–90.
- Peralta-Yahya PP, Zhang F, del Cardayre SB, Keasling JD. Microbial engineering for the production of advanced biofuels. *Nature*. 2012;488:320–8.
- Laluce C, Schenberger AC, Gallardo JC, Coradello LF, Pombeiro-Sponchiado SR. Advances and developments in strategies to improve strains of *Saccharomyces cerevisiae* and processes to obtain the lignocellulosic ethanol—a review. *Appl Biochem Biotechnol*. 2012;166:1908–26.
- Cascone R. Biobutanol—a replacement for bioethanol? *Chem Eng Prog*. 2008;104:54–9.
- Zheng YN, Li LZ, Xian M, Ma YJ, Yang JM, Xu X, et al. Problems with the microbial production of butanol. *J Ind Microbiol Biotechnol*. 2009;36:1127–38.
- Bud R. The uses of life: a history of biotechnology. Cambridge: Cambridge University Press; 1993.
- Jang YS, Lee J, Malaviya A, Seung do Y, Cho JH, Lee SY. Butanol production from renewable biomass: rediscovery of metabolic pathways and metabolic engineering. *Biotechnol J*. 2012;7:186–98.
- Xue C, Zhao XQ, Liu CG, Chen LJ, Bai FW. Prospective and development of butanol as an advanced biofuel. *Biotechnol Adv*. 2013;31:1575–84.
- Hong KK, Nielsen J. Metabolic engineering of *Saccharomyces cerevisiae*: a key cell factory platform for future biorefineries. *Cell Mol Life Sci*. 2012;69:2671–90.
- Lan EI, Liao JC. Microbial synthesis of n-butanol, isobutanol, and other higher alcohols from diverse resources. *Bioresour Technol*. 2013;135:339–49.
- Bond-Watts BB, Bellerose RJ, Chang MC. Enzyme mechanism as a kinetic control element for designing synthetic biofuel pathways. *Nat Chem Biol*. 2011;7:222–7.
- Shen CR, Lan EI, Dekishima Y, Baez A, Cho KM, Liao JC. Driving forces enable high-titer anaerobic 1-butanol synthesis in *Escherichia coli*. *Appl Environ Microbiol*. 2011;77:2905–15.
- Huffer S, Roche CM, Blanch HW, Clark DS. *Escherichia coli* for biofuel production: bridging the gap from promise to practice. *Trends Biotechnol*. 2012;30:538–45.
- Generoso WC, Schadowew V, Oreb M, Boles E. Metabolic engineering of *Saccharomyces cerevisiae* for production of butanol isomers. *Curr Opin Biotechnol*. 2014;33C:1–7.
- Steen EJ, Chan R, Prasad N, Myers S, Petzold CJ, Redding A, et al. Metabolic engineering of *Saccharomyces cerevisiae* for the production of n-butanol. *Microb Cell Fact*. 2008;7:36.
- Sakuragi H, Morisaka H, Kuroda K, Ueda M. Enhanced butanol production by eukaryotic *Saccharomyces cerevisiae* engineered to contain an improved pathway. *Biosci Biotechnol Biochem*. 2015;79:314–20.
- Krivoruchko A, Serrano-Amatriain C, Chen Y, Siewers V, Nielsen J. Improving biobutanol production in engineered *Saccharomyces cerevisiae* by manipulation of acetyl-CoA metabolism. *J Ind Microbiol Biotechnol*. 2013;40:1051–6.
- Si T, Luo Y, Xiao H, Zhao H. Utilizing an endogenous pathway for 1-butanol production in *Saccharomyces cerevisiae*. *Metab Eng*. 2014;22:60–8.
- Branduardi P, Longo V, Berterame NM, Rossi G, Porro D. A novel pathway to produce butanol and isobutanol in *Saccharomyces cerevisiae*. *Biotechnol Biofuels*. 2013;6:68.
- Ashe MP, Slaven JW, De Long SK, Ibrahim S, Sachs AB. A novel eIF2B-dependent mechanism of translational control in yeast as a response to fusel alcohols. *Embo J*. 2001;20:6464–74.
- Taylor EJ, Campbell SG, Griffiths CD, Reid PJ, Slaven JW, Harrison RJ, et al. Fusel alcohols regulate translation initiation by inhibiting eIF2B to reduce ternary complex in a mechanism that may involve altering the integrity and dynamics of the eIF2B body. *Mol Biol Cell*. 2010;21:2202–16.
- Smirnova JB, Selley JN, Sanchez-Cabo F, Carroll K, Eddy AA, McCarthy JE, et al. Global gene expression profiling reveals widespread yet distinctive translational responses to different eukaryotic translation initiation factor 2B-targeting stress pathways. *Mol Cell Biol*. 2005;25:9340–9.
- Egbe NE, Paget CM, Wang H, Ashe MP. Alcohols inhibit translation to regulate morphogenesis in *C. albicans*. *Fungal Genet Biol*. 2015;77:50–60.
- Pavitt GD. eIF2B, a mediator of general and gene-specific translational control. *Biochem Soc Trans*. 2005;33:1487–92.
- Flagfeldt DB, Siewers V, Huang L, Nielsen J. Characterization of chromosomal integration sites for heterologous gene expression in *Saccharomyces cerevisiae*. *Yeast*. 2009;26:545–51.
- Paquin CE, Williamson VM. Ty insertions at two loci account for most of the spontaneous antimycin A resistance mutations during growth at 15 degrees C of *Saccharomyces cerevisiae* strains lacking *ADH1*. *Mol Cell Biol*. 1986;6:70–9.
- Slavov N, Botstein D. Coupling among growth rate response, metabolic cycle, and cell division cycle in yeast. *Mol Biol Cell*. 2011;22:1997–2009.
- Dunlop MJ, Dossani ZY, Szmidt HL, Chu HC, Lee TS, Keasling JD, et al. Engineering microbial biofuel tolerance and export using efflux pumps. *Mol Syst Biol*. 2011;7:487.
- Guthrie C, Fink GR. Guide to yeast genetics and molecular biology. San Diego, California: Academic; 1991.
- Ashe MP, De Long SK, Sachs AB. Glucose depletion rapidly inhibits translation initiation in yeast. *Mol Biol Cell*. 2000;11:833–48.

Submit your next manuscript to BioMed Central and take full advantage of:

- Convenient online submission
- Thorough peer review
- No space constraints or color figure charges
- Immediate publication on acceptance
- Inclusion in PubMed, CAS, Scopus and Google Scholar
- Research which is freely available for redistribution

Submit your manuscript at
www.biomedcentral.com/submit

